# The mounded nature of the Balder Field area

# The Mounded Nature of the Balder Field area

Simon Patrick Morris 2013

## Declaration

The content of this thesis is the original work of the author and has not previously been submitted for a degree at this or any other university. Other people´s work is acknowledged by reference.

Simon Patrick Morris

June 2013
School of Earth Sciences
Birkbeck College, The University of London

## Abstract

The Balder, Grane and Ringhorne oil fields locate on the north-western flank of the Utsira High in the Norwegian sector of the North Sea. Reservoir sandstones deposited by gravity flows during the Palaeocene and Eocene Epochs originate from the East Shetland platform, to the West. The post-deposition effects of remobilization and injection are known to distort deposited sandstones creating irregular reservoir characteristics. It is also known that post-depositional processes are non-uniform, affecting sedimentary bodies variably. Low magnitude remobilization will cause minor geometrical distortion, whereas high magnitude deformation connects non-contemporaneous sands, destroying depositional geometries and potentially complicating hydrocarbon extraction.

Cored section, wireline logs and 3D seismic data allow description of the reservoir interval. Wireline logs do not facilitate identification of post-depositional processes, as remobilized and injected sandstone posses a non-unique signature. Cored section, however, allows direct identification of remobilized and injected sandstones. Seismic data, when calibrated by cored section can identify remobilized and injected sandstones. However, injected sandstones observed in cored section in Balder and Ringhorne Fields is seismically unresolvable.

Eighteen steep sided mounds are identified in the study area. Seismic geometries tentatively suggest Balder Field as having experience higher magnitude soft sediment deformation than Grane Field, which is of a higher magnitude than Ringhorne Field. Crosscutting seismic reflections emanate from crests and flanks of mounds in Balder Field and Grane Fields. Injected sandstones are identified in cored section in each of the field areas.

# Table of contents



## Chapter 1: Introduction



## Chapter 2: Literature review

## Chapter 3: Methodology and data



## Chapter 4: Sequence stratigraphic scheme



## Chapter 5: Facies schemes

## Chapter 6: Facies interpretation



## Chapter 7: Synthesis and conclusions

# List of Figures

## Chapter 1: Introduction



## Chapter 2: Literature review

## Chapter 3: Methodology



## Chapter 4: Sequence stratigraphic scheme

## Chapter 5: Facies schemes



## Chapter 6: Facies interpretation

## Chapter 7: Synthesis and conclusions

## List of Tables

### Chapter 2: Literature review



### Chapter 3: Methodology and datasets



### Chapter 4: Sequence stratigraphic scheme



### Chapter 5: Facies schemes

## List of appendices

# Chapter 1: Introduction

## 1.1 Background

Sandstone injections defy the concepts of stratigraphy (Posamentier et al. 2009) falling between the subjects of sedimentology and structural geology (Hurst and Cartwright, 2007). In the North Sea the presence of sandstone remobilization and injection in sandstones of Tertiary age is common. Recently, Cartwright (2010) and Huuse et al. (2010) suggested that, in excess of 40,000km$^2$ of the North Sea basin contained remobilised and injected sediments. Sandstone remobilization and injection is known to alter the depositional characteristics of sandstones. Accurate assessment of sandstone reservoirs that have been post-depositionally altered is important when exploring for, and producing hydrocarbons. An understanding of the conditions leading to soft sediment deformation, the processes during deformation and the sedimentary products of deformation are key in characterising these sediments.

The economic value of remobilization and injection has also been recognised. Hurst et al. (2005) believed that sandstone intrusions within the North Sea basin contained in excess of 2.4 billion barrels of oil equivalent. Targeted exploration for injected sandstone hydrocarbon reservoirs is at an early stage. The first exploration wellbore with the objective to test hydrocarbons trapped in injected sandstones was undertaken in 2004 (de Boer et al. 2007) proving more than a 100m oil column.

In a Field development context, reservoir properties (Hurst et al. 2011), vertical and lateral reservoir connectivity (Briedis et al. 2007) and reservoir volumetrics (Lonergan et al. 2000) can each be affected by remobilization and injection. Early identification of remobilization and injection is important as Exemplified in Templeton et al. (2009) from Gryphon Field, UK North Sea, where an additional 16 million barrels of oil equivalent have been produced from injected sandstones (Figure 1.1).

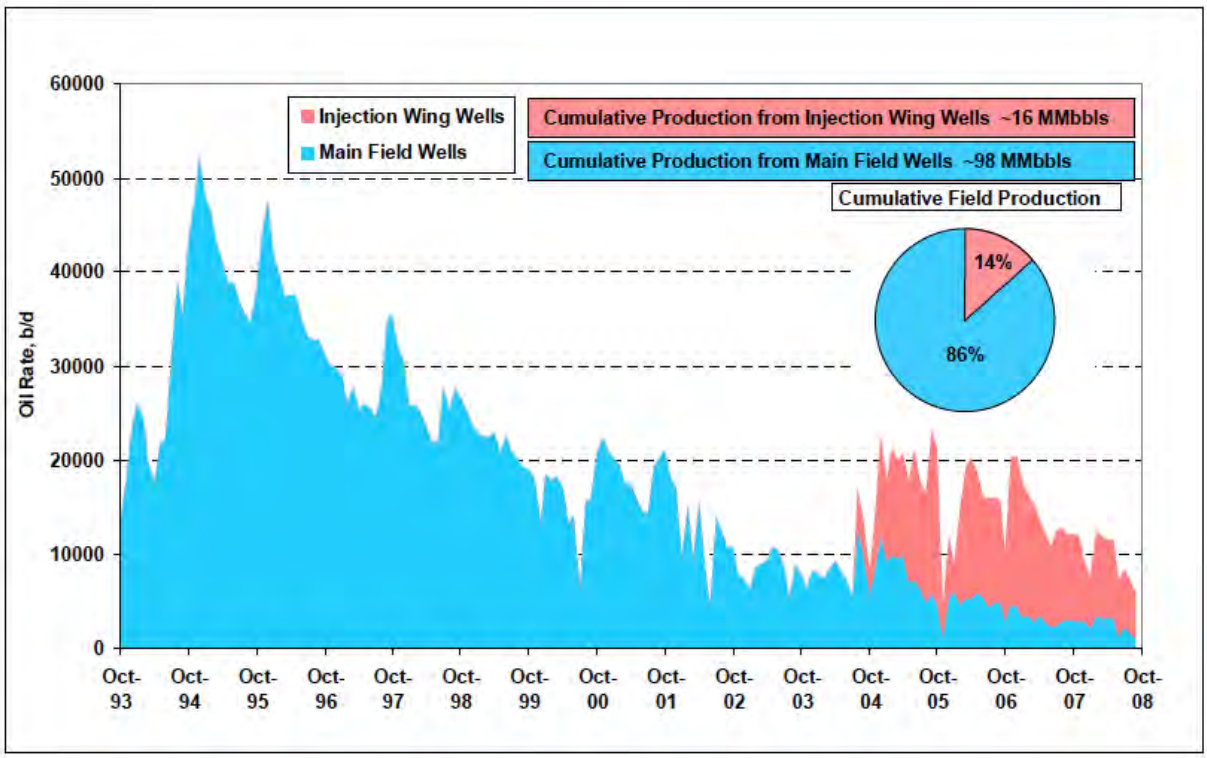


Figure 1.1: Uplift of hydrocarbon production from injected sandstones Gryphon Field, United Kingdom, North Sea in Templeton et al. (2009)

## 1.2 Project rationale

The study area is located on the North Western Flank of the Utsira High a prominent basement high situated within the Viking Graben of the North Sea (Figure 1.2a). Hydrocarbons are present in Paleocene and Eocene aged sandstones and comprise three separate field developments namely, Balder, Grane and Ringhorne Fields (Figure 1.2b). Hydrocarbons are also present in Jurassic aged Statfjord Formation sandstones beneath Ringhorne Field, which are not considered in this study.

The focus of this project is Tertiary aged sediments that display steep mounded geometries and seismically resolvable injection features in Balder, Grane and Ringhorne Fields. Evidence for remobilization is seen on 3D seismic data as high relief mounded features and discordant sandstone injection features (Wild and Briedis, 2010), in cored section sandstones display discordant bedding contacts against encasing mudstones with soft sediment deformation structures (Jenssen et al. 1993).

Twenty years ago Jenssen et al. (1993) suggested that a possible cause of unusually high flank angle mounds in the Balder Field area maybe attributed to remobilization and injection. This was a clear step away from previous published models for the Balder Field, which aimed to explain steep-sided geometries through depositional processes. The Jenssen et al. (1993) paper was not revolutionary, as injected sandstones had been observed nearly 200 years previously (Murchison, 1827). But it did mark one of the first 'modern' published explanations. Sandstone injection has been much studied over the last two decades (e.g. Dixon et al. 1995, Lonergan et al. 2000, Huuse et al. 2004, Hurst et al. 2011) and is now understood to be a common process, especially in Tertiary aged sediments of the North Sea (Cartwright et al. 2010).

More recently, Briedis et al. (2007), Wild and Briedis (2010) published revised models for the Balder Field based on 3D seismic data reprocessed in 2005. In Wild and Briedis

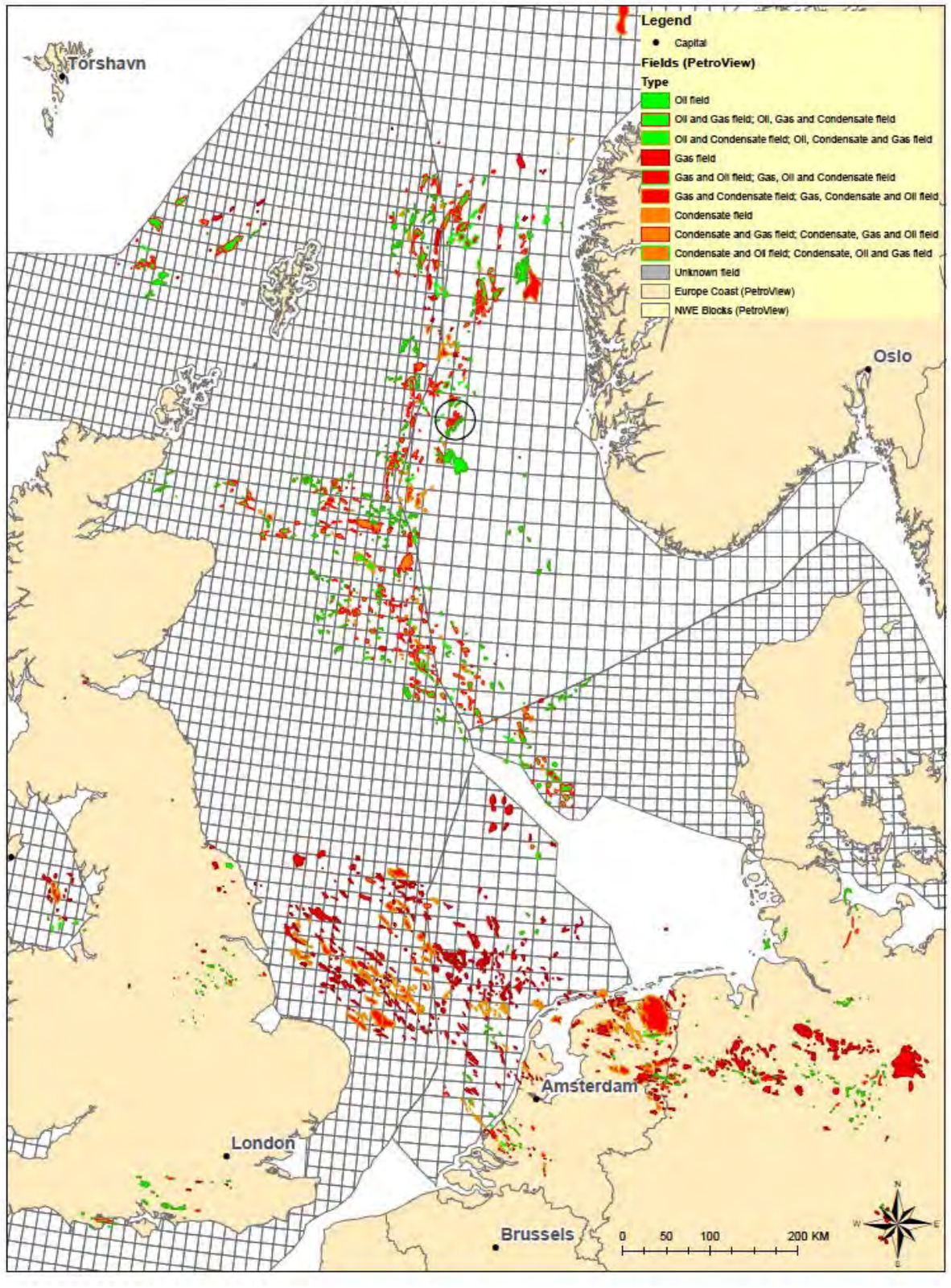


Figure 1.2 (a): Regional location map, showing division of the North Sea area for hydrocarbon exploration and production. Study area highlighted by black circle within the Viking Graben, Norwegian sector North Sea.

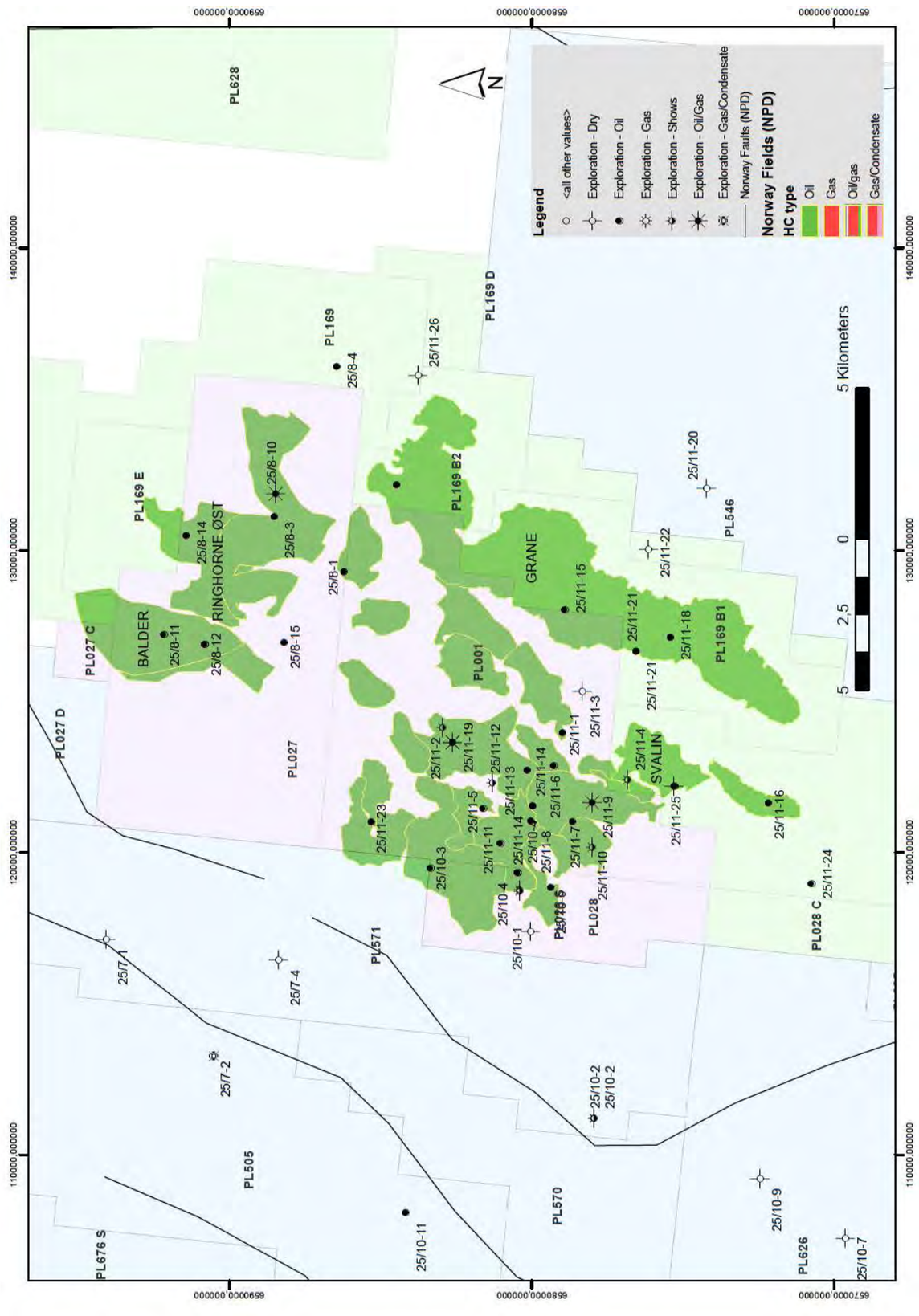


Figure 1.2 (b): Study area location map, showing Ringhorne, Balder and Grane hydrocarbon fields. Background shaded polygons indicate hydrocarbon exploration permits. Superimposed green polygons indicate discovered hydrocarbon outline. All information obtained from Norwegian Petroleum Directorate (NPD).

(2010) it is suggested that instead of three sand prone intervals (Heimdal, Hermod and Balder Members) much if not most of the sandstones observed in Hermod and Balder Members is infact emplaced by injection, probably from Heimdal Member. Wild and Briedis (2010) argue that overpressure required for injection originated from beneath Cretaceous aged Limestones. The authors support their arguments with observations of discontinuities in the chalk surface that appear to represent 'pop-up' structures where deeper fluid may have fractured Limestone during escape, unweathered chalk clasts present 100m into Paleocene stratigraphy and high amplitude vertical sutures which may represent fluid conduits.

Much of the most recent geological model for the Balder Field stems from 2005 reprocessed seismic data. This 3D seismic data is owned under proprietary licence by ExxonMobil and is not available for use. Currently, Grane Field is only briefly described in several publications (Haaland et al. 1999, Martinsen et al. 2005, Huuse et al. 2007) and Wild and Briedis (2010) do not discuss the Grane Field. Therefore, one objective of this project is to compare and contrast Balder, Grane and Ringhorne Fields. Little evidence of remobilization and injection from cored section correlated to wireline logs and seismic data is presented in Briedis et al. (2007) or Wild and Briedis (2010). Seven mounds are identified in the Balder Field (Wild and Briedis, 2010), figure 1.3 (a), although evidence from cored section of post depositional processes is shown from just one mound (Briedis et al. 2007). Initial seismic mapping for this project indicated 18 mounded structures at Top Paleocene interval Figure 1.3 (b) over Balder, Ringhorne and Grane Fields.

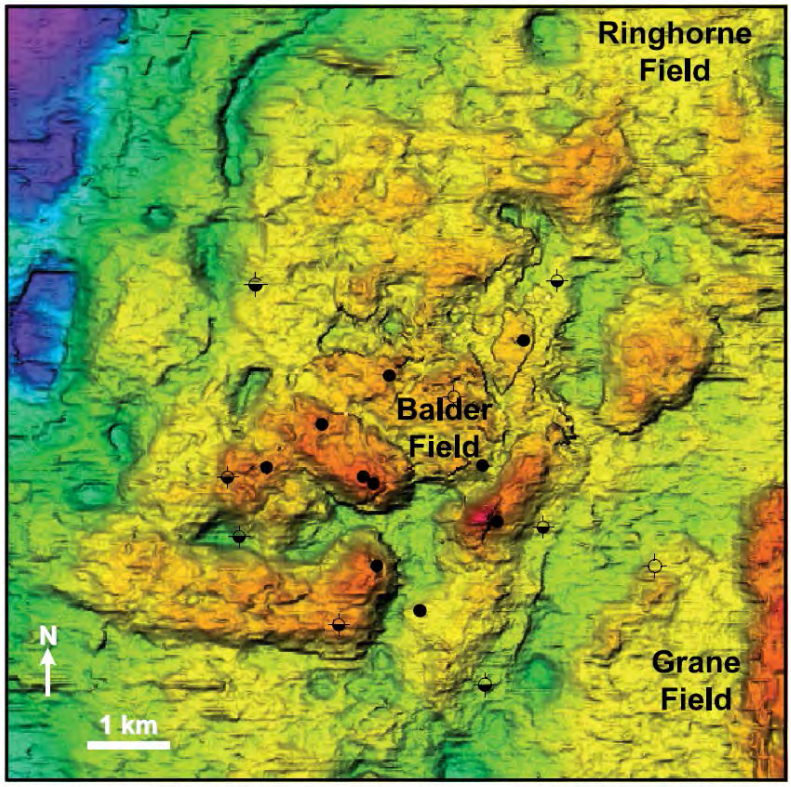


Figure 1.3 (a): Near Top Paleocene depth structure map from Briedis et al. (2007). Mounded structures are highlighted by yellow-red colour scaling with present day flank angles in excess of 20°. Red colours are 1700m depth from seabed and purple colours 2100m depth from seabed.

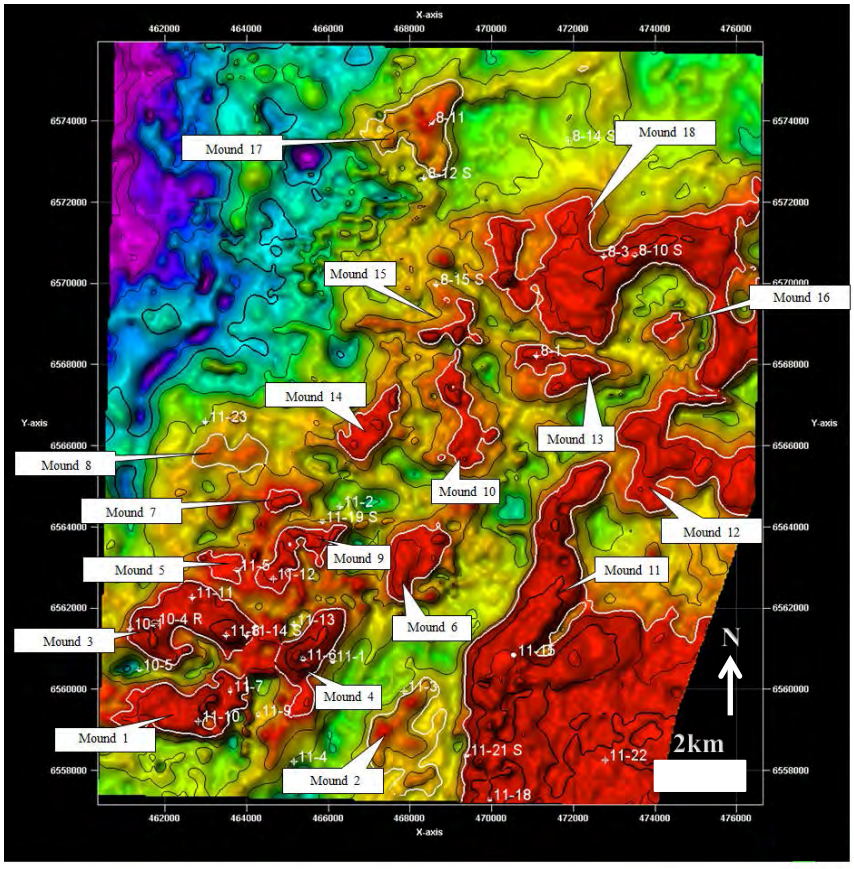


Figure 1.3 (b): Sele sequence Two-Way-Time structure map. Red colour scaling indicates 1730ms, purple colour scaling indicates 1850ms, 20ms contours are shown. Eighteen mounds (white polygons) are highlighted and numbering is based on geographical location.

## 1.3 Primary and Secondary sedimentation

The term Primary sedimentation is used in this study to describe sediments unaltered substantially during burial (Duranti and Hurst, 2004). Mudstones and sandstones deposited in marine environments undergo considerable volume reduction during burial (Jennette et al. 2000). However certain types of sedimentary structures, bedding contacts, mineralogical composition and ichnofacies, must remain broadly intact for a primary classification to be applied.

Secondary sedimentation as used here, is for soft sediment deformation within approximately 1000m of burial (Maltman and Bolton, 2003). A range of characteristic structures and bed contacts are produced and composition of sandstone intervals can be altered. At a small-scale (1-10cm) loading structures are produced and indicate low magnitude secondary deformation (Owen, 1987). At a larger scale injection structures (10cm-1000m) are formed and represent complete destruction of primary sedimentation (Lowe, 1975).

Some sedimentary structures offer clear diagnostic indication of sedimentary process (e.g. trough cross bedding or dish structures). A ‘grey area’ between primary structures and secondary structures exists, where it is unclear if sediments have retained primary character or affected by secondary processes e.g. massive sandstones (Stow and Johansson, 1999).

## 1.4 Aims & objectives

The aim of this project is to distinguish between sediments that have been deposited by primary processes and remained largely unchanged during burial and sediments that have been post-depositionally altered (Gamberi, 2010) during burial. In order to achieve this the characteristics of remobilized and injected sandstones must be identified, from literature review, therefore:

1. Processes leading to remobilization and injection must be understood including depositional emplacement processes.
2. The products of soft-sediment deformation must be understood in order to identify soft-sediment deformation structures in the sub-surface.

The subsequent aims of this study are concerned with the investigation of the Balder Field area and how, if at all Balder, Grane and Ringhore Fields differ. A sequence stratigraphic scheme will be used to allow comparison, therefore:

3. To assess cored section and produce a facies scheme.
4. To assess wireline logs and produce a facies scheme.
5. To assess 3D seismic data and produce a facies scheme.
6. To synthesis observations and make comparisons between the 3 hydrocarbon field areas.

## 1.5 Thesis organisation

Background reasoning and regional geology of the study area is described along with aims and objectives in Chapter 1. The focus of Chapter 2 is to document current published examples of primary and secondary sedimentation. Information from literature review will be used to interpret observations in Chapter 6. Relevant sequence stratigraphic and facies concepts are described along with recent publications from the study area. Methodology and data studied is contained within Chapter 3.

Chapter 4 hosts a description of results from sequence stratigraphic interpretation using both wireline log and 3D seismic data (Figure 1.4, a). Chapters 5 and 6 present and subsequently interpret facies schemes for cored section, wireline log and 3D seismic datasets from Balder, Ringhorne and Grane Fields (Figure 1.4, b). A synthesis of interpretation is presented and discussed in Chapter 7 (Figure 1.4, b), followed by conclusions and suggestions for further work.

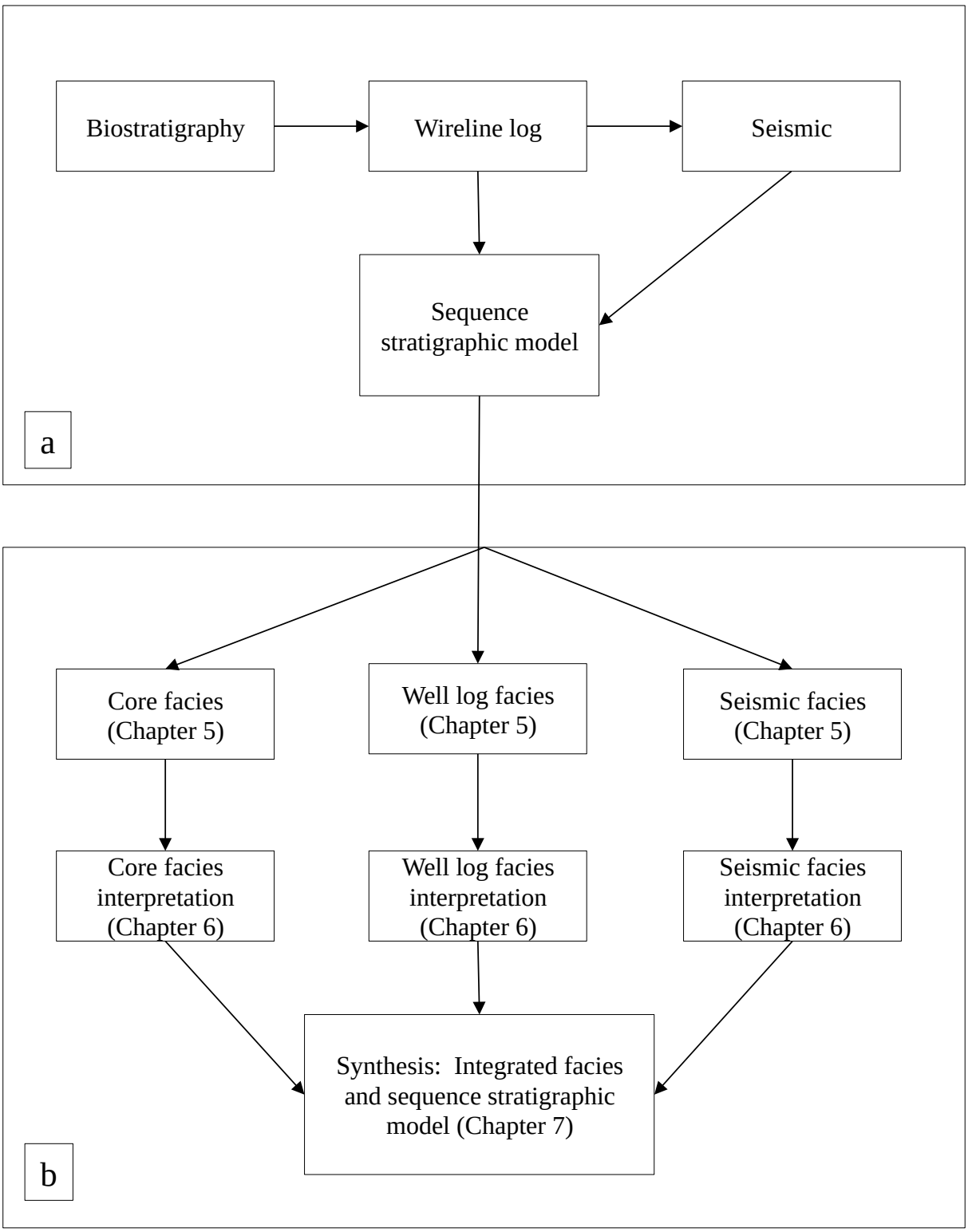


Figure 1.4: Workflow describing thesis organisation. Sequence stratigraphic interpretation (a, Chapter 4), followed by facies identification, interpretation and synthesis (b).

## 1.6 Structural setting

The tectonic evolution of the Northern North Sea is described in Ziegler (1986, 1990) and Coward et al. (2003).

The North Sea is situated in the area of a triple plate collision, which occurred during the Late Ordovician to Caledonian Silurian orogeny (Zanella et al. 2003). Laurentia and Eastern Avalonia plates converged causing large scale thrusting. To the south Eastern Avalonia and Baltica plates reorganised with strike slip movement (Lyngsie and Thybo, 2007).

Rifting during Devonian times was followed by sag and subsidence phases through Carboniferous (Ziegler et al. 1986) producing a proto-Viking Graben with a dominant East-West strike slip component (Coward et al. 1993). Structural elements formed during Devonian times were probably reactivated during later Mesozoic rifting (Zanella and Coward, 2003).

Break up of the Pangean supercontinent before the end of Triassic (Glennie, 1995) initiated rifting episodes within the North Sea Basin during Permian and Triassic times. During late Permian to Early Triassic periods, structural lineaments of the Northern North Sea basin began to transition from East-West (Devonian) strike direction to north-south orientated rifting (Coward et al. 2003), followed by subsidence and progradation of continental and deltaic sediments southward (Goldsmith et al. 2003). Figure 1.5 depicts orientation of Mesozoic rift basins, location of the Viking Graben and the position of the Utsira High.

A second Mesozoic rifting event occurred in the Jurassic between Bathonian to late Volgian times (Ziegler, 1990) associated with the opening of the Atlantic margin (Zanella and Coward, 2003). Sediments deposited in the Northern North Sea basin were predominantly comprised of shallow marine deltaic succession (Husmo et al. 2003), forming the Brent Group reservoir unit. A regional unconformity extends through the North Sea of Toarcian-Aalenian

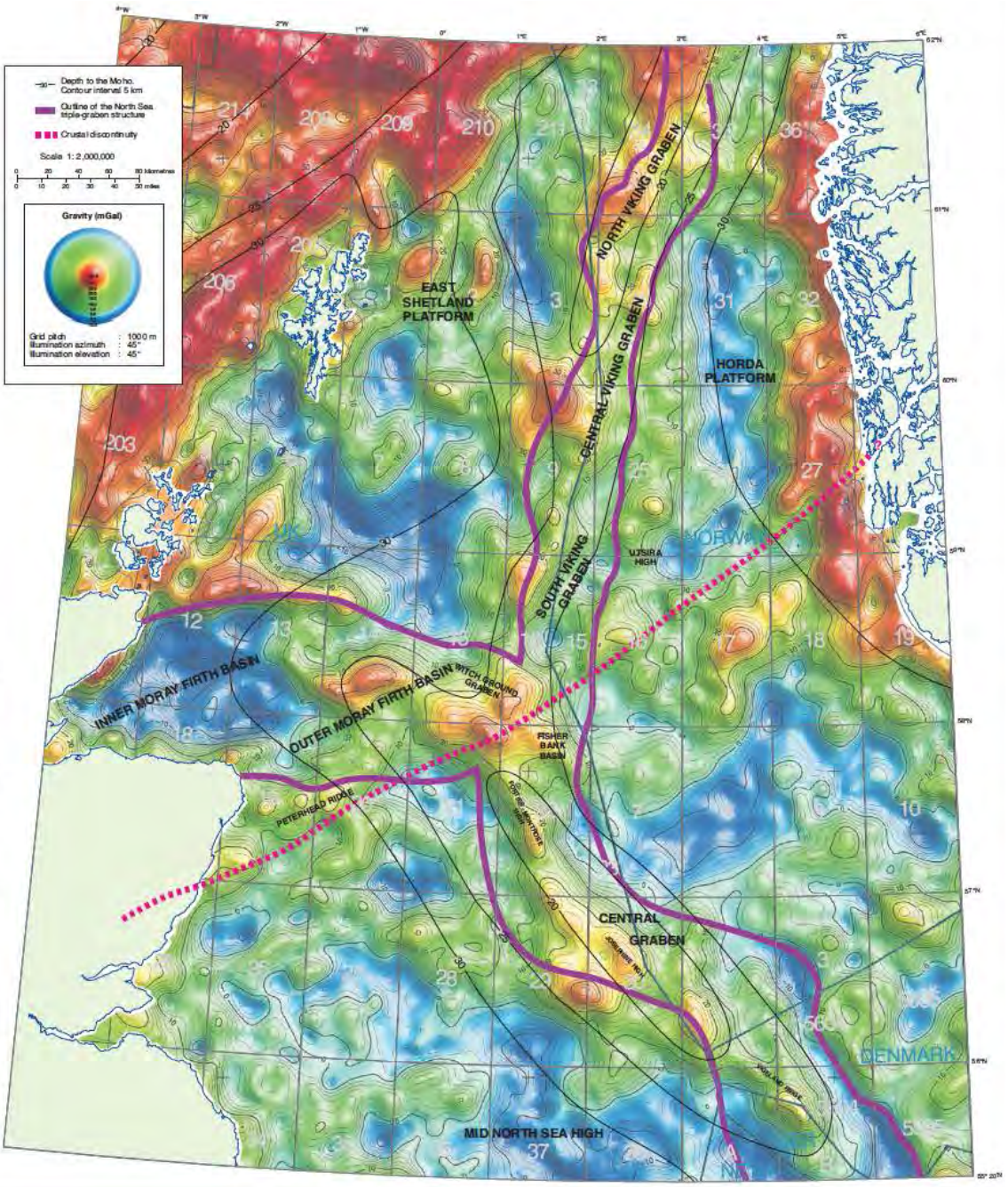


Figure 1.5: Bouger gravity anomaly and depth to the Moho map. The gravity data is based on free-air gravity data from Sandwell (1990). The graben areas contain gravity anomalies (colour scaling) due to elevation of the Moho and denser upper mantle beneath the rift sites. The Utsira High and South Viking Graben are highlighted. Map from Zanella, Coward and McGrandle (2003).

age (Underhill and Partington, 1993) formed by active doming of a mantle driven thermal doming (Underhill and Partington, 1993). The magnitude of rifting increased in the Late Jurassic (Zanella and Coward, 2003), palaeowater depth increased and a thick (50-300m) organic rich mudstone was deposited across the North Sea basin (Isaksen and Tonstad, 1989). Locally on the Utsira High during the early Mesozoic a series of small (100m deep) minibasins evolved. Triassic basins developed in response to passive diapirism of Permian aged evaporites. A series of subsequent secondary basins formed during the Jurassic as a result of Permian aged salt wall collapse (Jackson et al. 2010). Cretaceous sedimentation is characterised by post-rift subsidence and mixed, clastic and limestone deposition in a marine setting (Gabrielsen et al. 2001).

McKenzie (1978) describes the North Sea basin during Cenozoic time as a thermally subsiding passive basin and any tectonic activity was associated with the development of the Iceland plume, described in Ahmadi et al. (2003). Development of the Icelandic plume was caused by the break up of the Pangean supercontinent and the opening of the North East Atlantic (Faleide et al. 2002; Lundin and Dore, 2005). The Scottish Highlands and the East Shetland Platform to the west of the Viking Graben was uplifted, as was the Norwegian landmass (Ahmadi et al. 2003). Sediment input into the North Sea was dominantly sourced from East Shetland Platform during Paleocene and Eocene time (Huuse, 2002) with some input from the Norwegian margin (Dmitrieva et al. 2012, Ahmadi et al. 2003). Maximum sedimentation rates were seen in Late Paleocene time (Huuse, 2002) and correspond to maximum uplift estimations (Joy et al. 1993; Jones et al. 2002).

## 1.7 Depositional setting

Deposition within the Paleocene section is broadly characterised by clastic marine deposition (Milton et al. 1990), although shallow marine depositional environments are described near to basin margins (Kjeilen-Eilertsen et al. 2009). Analysis of garnet minerals

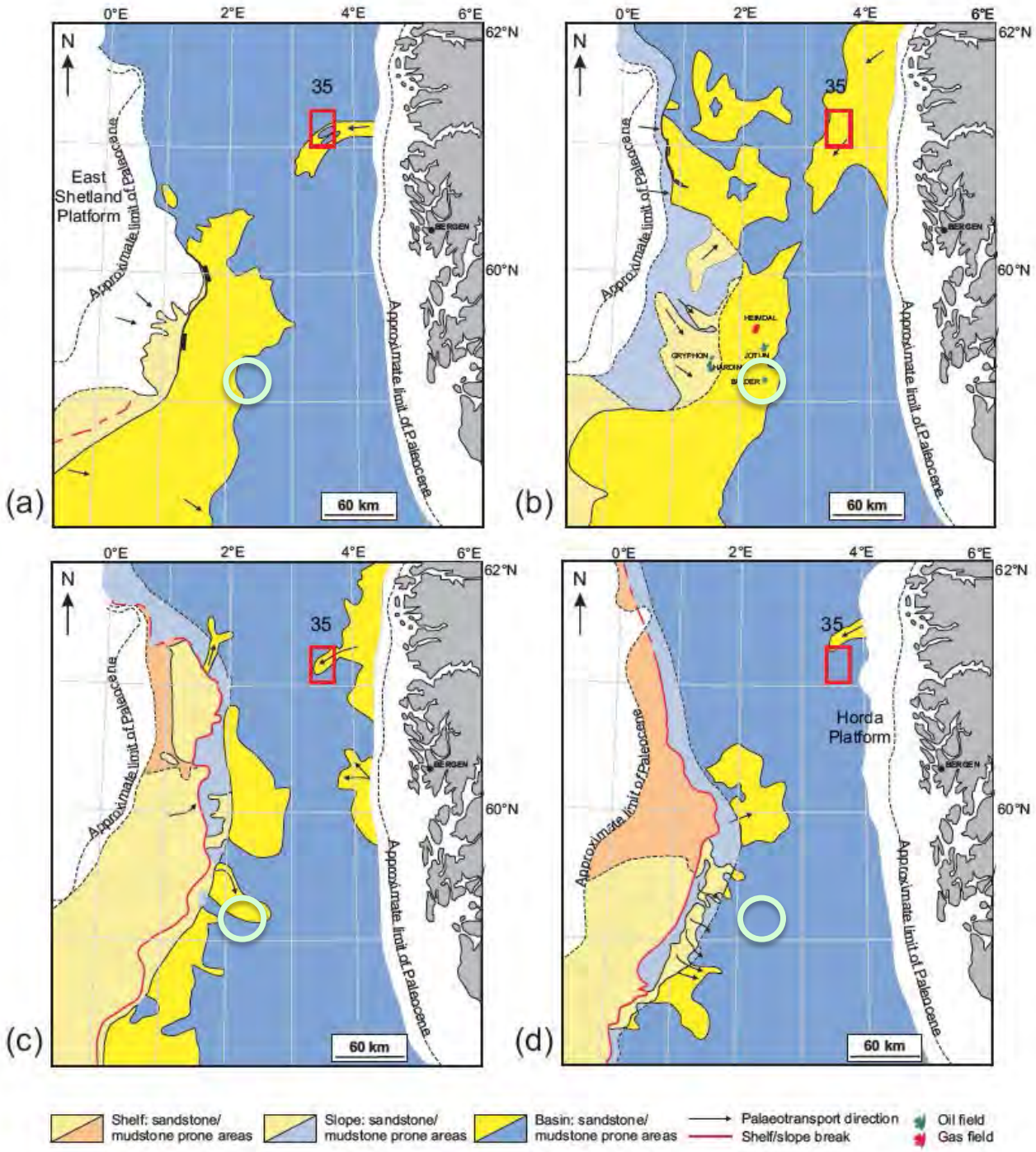


Figure 1.6: Paleogeographic maps for geological periods in the Paleogene evolution of the North Sea Basin, from Dmitrieva et al. (2012) after Ahmadi et al. (2003): (a) Våle (Danian-early Selandian; (b) Lista (late Selandian-Thanetian); (c) Sele (early Ypresian) and (d) Balder (late Ypresian. Red box highlights study area of Dmitrieva et al. (2012), green circles indicate study area of this project.

has linked Paleocene sediments deposited in the North Sea with the East Shetland Platform source terrain (Morton et al. 1993). Jordt et al. (2000) use detrital and authigenic clay mineralogy, wireline logs and seismic data to identify 10 sequences from base Paleocene to Plio-pleistocene. Their work suggests that sediment input into the Tertiary North Sea basin from the East Shetland Platform lasted until early Miocene times. Sediment has been sourced from the Norwegian margin since mid Paleocene with the exception of a hiatus during Eocence (Jordt et al. 2000).

Lithostratigraphic subdivision of the Paleocene and Eocene is described in Deegan and Scull (1977), Isaksen and Tonstad (1989) and Knox and Holloway (1992). A chronostratigraphic scheme is described in Mudge and Copestake (1992 a, b) Mudge and Bujak (1996) for the Eocene interval and Mudge and Bujak (1994) for Paleocene interval. Biostratigraphic zonation of six regionally correlatable dinocyst zones within the Paleocene (Mudge and Bujak, 1996) and 30 bioevents within the Eocene interval (Mudge and Bujak, 1994) act as temporal framework which coincide with nine regionally correlatable sequence stratigraphic sequences throughout the Paleocene and Eocene of the North Sea (Mudge and Bujak 1994, 1996). Dmitrieva et al. (2012) present four palaeogeographic maps from the North Sea basin, modified from Ahmadi et al. (2003) Figure 1.6. These maps offer a simple overview of lithology observed from wireline log profiles. Figure 1.7 correlates mapped intervals with Haq et al. (1988) relative regional sea-level curve and regional stratigraphy. Kjennerud and Gilmore (2003), describe palaeo-waterdepths increasing from around 100m at the onset of the Paleocene up to 500m during mid Eocene times in the Viking Graben of the North Sea.

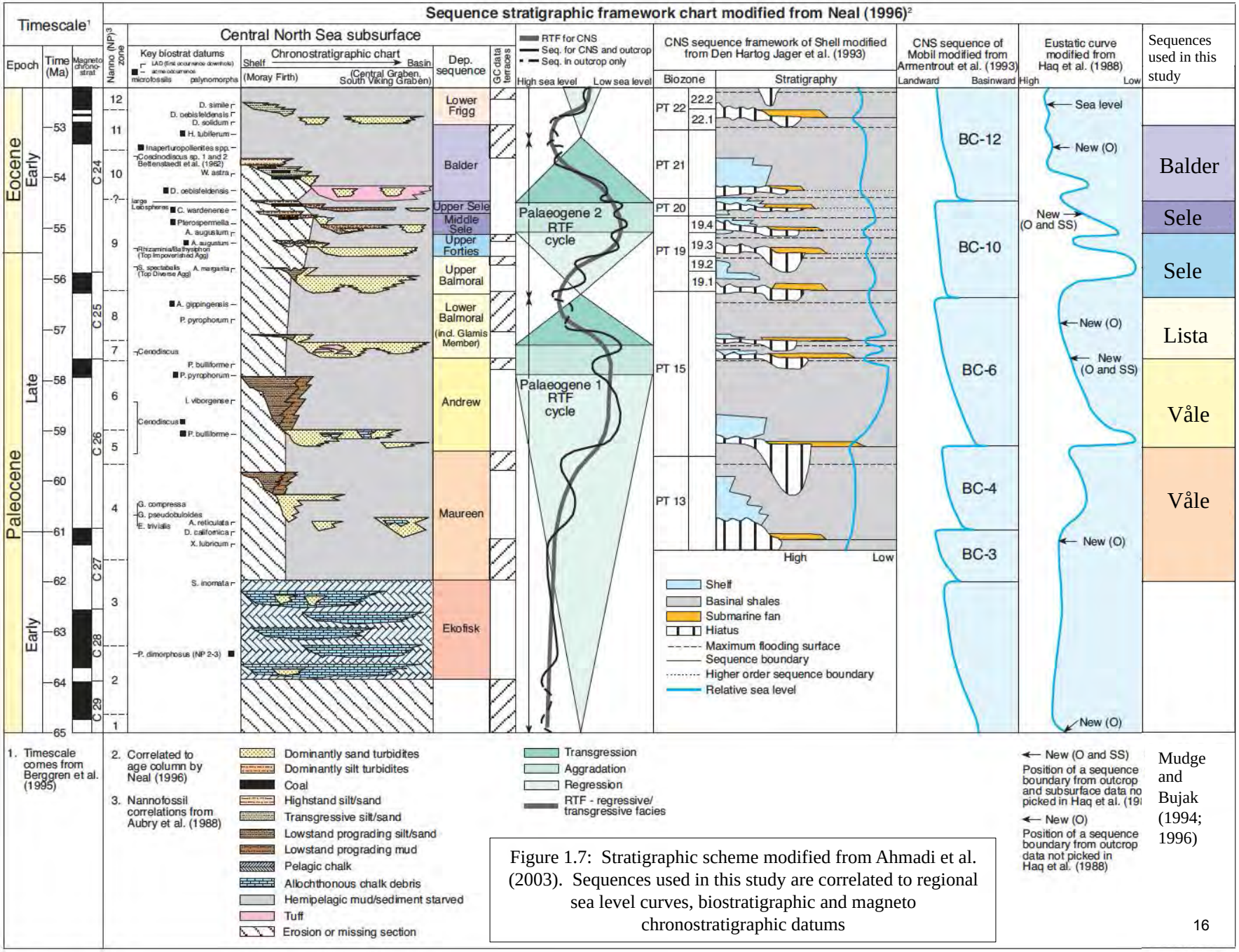


Figure 1.7: Stratigraphic scheme modified from Ahmadi et al. (2003). Sequences used in this study are correlated to regional sea level curves, biostratigraphic and magneto chronostratigraphic datums

# Chapter 2: literature review

## 2.1 Primary sedimentation

One current theme of sedimentary research is to understand, and therefore predict the distribution through time of sedimentation patterns (Flint et al. 2010). Four main controls affect sediment generation and dispersal, these are; tectonics, climate, sea-level and sedimentary characteristics and processes (Bouma, 2004). Allogenic controls have been discussed in Chapter 1. In chapter 2, sediment deposition and burial effects are discussed.

Sediment gravity flows (Talling et al. 2012) transport enormous volumes of sediment from continental shelves to deep-water (below storm wave base or more than 200m, Shanmugam, 2000) marine environments (Leeder, 2011). Gravity flow systems deposit sediment in a range of geometries based on depositional setting (level of confinement), sediment type and flow processes (Lomas and Joseph, 2004) discussed in section 2.1.3.

Confinement is often related to the gradient of the setting (Kneller, 2003). From literature unconfined settings do not have a maximum gradient and confined settings do not appear to have a minimum gradient. Although, unconfined settings do have lower gradients than confined settings (Leeder, 2011).

### 2.1.1 Confined settings

The term confinement is used to describe the state of the depositional setting during through flow of sediment (Lomas and Joseph, 2004). Confined settings are created either through erosion (Mayall et al. 2006) or aggradation (Hadler Jacobsen et al. 2007, Kane and Hodgson, 2010). Confined settings are usually found on slopes (Kneller, 2003) with erosion and bypass common in steeper settings and aggradation in less steep settings. Wyn et al. (2012) describe a modern day example from the Morocco Turbidite system where a gradient of 0.05° is sufficient to cause bypass and erosion and a slope gradient of 0.01° results in deposition.

Containment, however describes a depositional setting where sediment is trapped preventing unidirectional flow (Hiscott and Pickering, 1984; Pickering and Hiscott, 1985). Sinclair and Tomasso (2002) observed high mud to sand ratios at the base of section in a contained setting (Grès d'Annot sandstones, French Alpine foreland basin). Sand to mud ratio was seen to increase upwards through flow stripping (Peakall et al. 2000), as finer grained sediment was held in suspension and transported further than coarse grains.

### 2.1.2 Unconfined settings

Lobe deposits are formed in unconfined settings beyond a transition point where confined slope channels terminate (Posamentier and Kolla, 2003), figure 2.1 (a). Unconfined gravity flow deposition is found at the base of slope and is described in Bouma (1962), Walker (1978). At the core of these models is the concept that broad sheet like deposits (lobes) grade and fine at their margins. Coarsest sediment grain size is encountered within, or near to the axis of the sediment input point. The concepts of flow competence and flow capacity as described by Bouma (1962), drive unconfined deposition and is still relevant today (Amy et al. 2005). However, recently published examples indicate that architectural complexities of unconfined deep-water sandstones exist.

Lobes are not homogenous units but infact comprise channels, splays and distributary channels (Hadler Jacobsen et al. 2007). he details of lobe architecture has been revealed from outcrop investigation and modern high-resolution 3D seismic data. ecent research has shown that older methods of predictive stacking patterns are dated and offer a simplified view of sediment dispersal (Prélat and Hodgson, 2013). Coarsening, fining and aggrading trends and the interpretation of waning or increasing sediment influx respectively, maybe an oversimplification. Instead, five styles of bed stacking patterns were associated with internal stacking and channel avulsion observed at the Laingsburg depocentre, SW Karoo Basin, South Africa (Prélat and Hodgson, 2013).

Unconfined and confined settings display differing aspect ratios (width/thickness). Figure 2.1 (b) from Prélat et al. (2011) shows confined settings commonly have aspect ratios of 10:1 and unconfined settings of 1000:1. The process of remobilization and injection can reduce aspect ratios to less than 1:1 (Sherry et al. 2012).

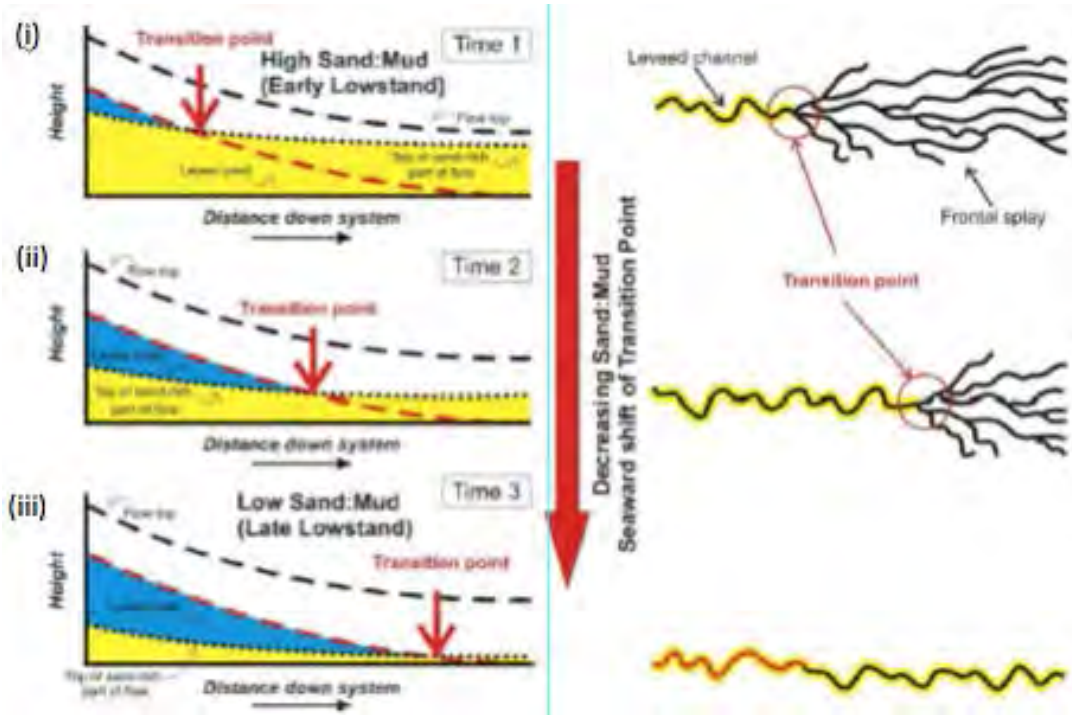


Figure 2.1 (a): Transition point response to differences in sand-to-mud ratio in gravity flows. (i) high sand-to-mud ratio therefore transition point located landward of (ii and iii) from Posamentier and Walker (2006).

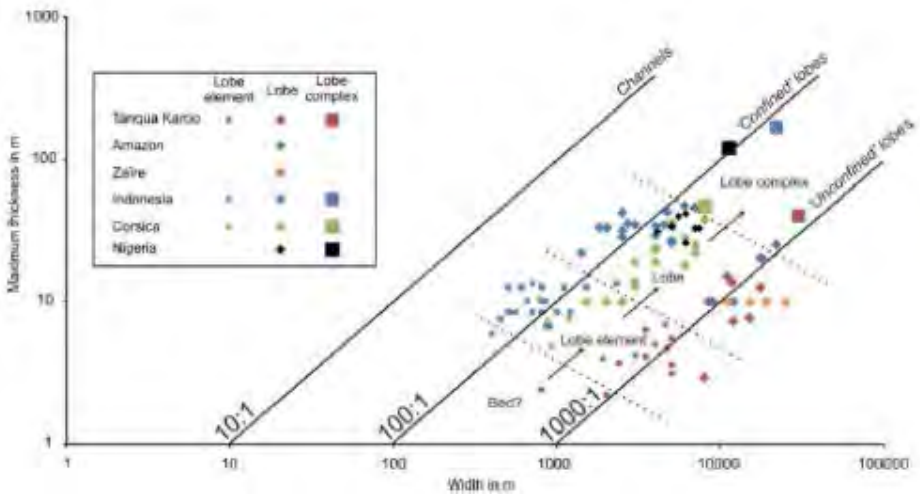


Figure 2.1 (b): Width versus thickness for channel and lobe systems from six basin worldwide from Prélat et al. (2009)

### 2.1.3 Gravity flows

From cored section Paleocene and Eocene structureless sandstones deposited within the North Sea basin have been identified as turbidites (Martinsen et al. 2005), high density turbidites (Fitzsimmons et al. 2004; Davis et al. 2009) and sandy Debris flows (Shanmugan, 2006). It is problematic to name visually similar deposits with differing depositional processes as laminar and turbulent flows are known to produce laterally and vertically distinguishable products (Amy, 2005).

#### 2.1.3.1 Turbulent flows

A Turbidite is a sub-aqueous gravity flow in which sediments are supported by turbulence and cannot exceed 9% sediment concentration (Middleton and Hampton, 1973) or 1.1-1.2g/cm3 density of mass (Reading, 1996). Turbulent flows can be divided into a head, neck, body and tail (Stow, 2007). Sediment travels fastest in the head area producing a reduced buoyancy zone between head and neck. Coarsest sediments are dropped from suspension at this point, finer grained material is transported towards the body and tail areas until grain weight is no longer supported and falls back into suspension (Leeder, 2011) producing graded deposits (Bouma, 1962). The deposits of these flows are described as low-density turbidity currents and produce planar lamination and cross ripple lamination sedimentary structures shown in Figure 2.2 (a) Tb-Te (Talling et al. 2012).

Mulder and Alexander (2001) suggested that gravity flows with between 9% - 46% sediment concentration and reliant upon grain-to-grain interactions and turbulence to transport sediment down slope should be termed high density turbidites. Sediment concentration is higher than in low density turbidites (up to 9%) especially near to the bed which produces an entrained high sediment concentration termed traction carpet (Sohn, 1997). Down slope movement is achieved by grain-to-grain interactions and is driven by the overlying turbulent

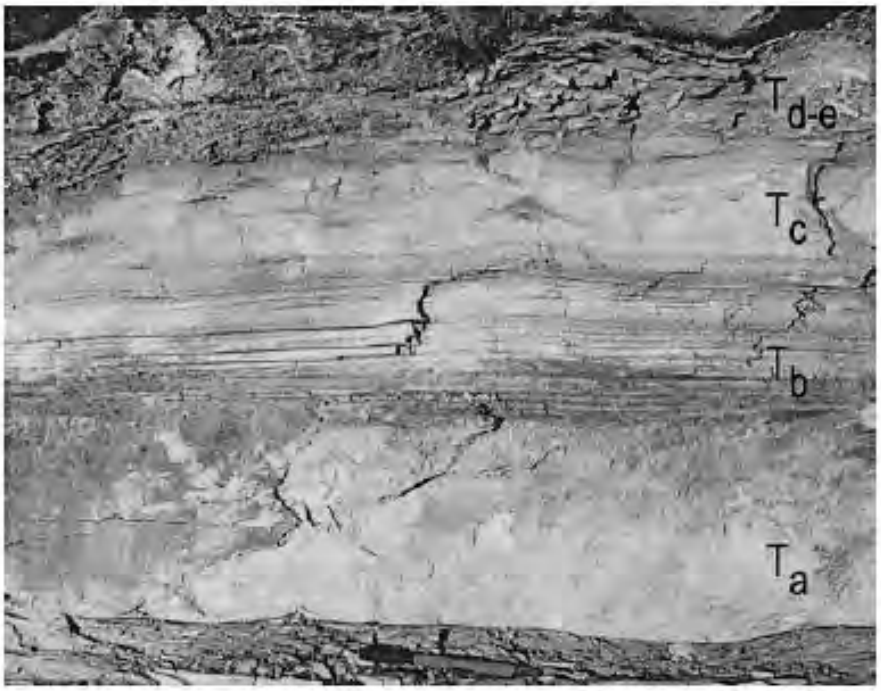


Figure 2.2 (a): An example of normal grading observed at Peira Cava, Oligocene, southern France produced by a turbulent gravity flow as described in Bouma (1962); Talling et al. (2012). From Kneller and McCaffrey (2003)

Figure 2.2 (c): Cs1 facies with ripple cross lamination, interpreted as the deposit of low density turbidity currents. Cs5 Facies structureless sandstones, originating from either high density turbidity currents or from non-cohesive debris flows, Marnoso-arenacea Formation, Italy (Talling et al. 2013).

Figure 2.2 (b): clast supported and inverse to normal graded debris flow conglomerate (stick lower right 90cm long), Cerro Toro Formation, Cretaceous, Southern Chile (Sohn et al. 2002)

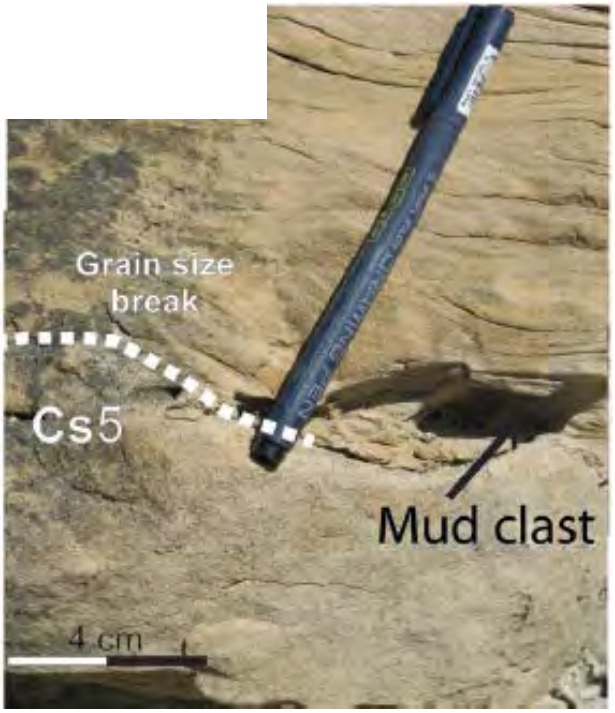

flow (Talling et al. 2013). Deposition is achieved by aggradation and hindered settling (against water rising) Talling et al. (2012) rather than by en masse freezing (Sohn, 1997) characteristic of debris flow deposition.

Shanmugam (1996), proposed reclassification of high density turbidites to sandy debris flows. Mulder and Alexander (2001) argue that the term debris flow implies cohesitivity and laminar flow process, which is not a key driver.

Turbulent flows can be initiated by a single short lived event (surge) or by long lived sustained currents (Johansson et al. 1998). Flow transformation from debris flows (section 2.1.3.3), suspension charged river water and tectonically active settings cause initiation (Leeder, 2011). Secondary structures can be observed and form through dewatering of sediment laiden with water (Allen, 1982).

### 2.1.3.2 Debris flows

Debris flows possess high internal cohesivity through matrix strength (Middleton and Hampton, 1973) and travel downslope with laminar flow rheology often with grain densities of 1.5 to 2.0 g/cm3 (Reading, 1996). High cohesivity is due to at least 20% mud volume (Ilstad et al. 2004) preventing turbulence. Talling et al. (2012) describes a range of cohesive to non-cohesive debris flows that move down slope with laminar flow rheology. One end member of this scheme is sand rich debris flows which can contain as little as 5% mud matrix, are liquefied, non cohesive and move down slope with laminar flow rheology (Dvcs, Talling et al. 2012). In contrast highly cohesive muddy debrites also move down slope with laminar flow rheology and are competent enough to support pebbles, boulder and large clasts (Dm-2, Talling et al. 2012), shown in Figure 2.2 (b).

The deposits of debris flows are commonly ungraded (Figure 2.4) and lack sedimentary structures (Lowe, 1982). Deposition occurs through en masse freezing (Talling et al. 2012) for cohesive flows, in which flows freeze inwardly as applied shear stress drops below the yield strength of the moving material (Lowe, 1982).

Debris flows initiate because of high pore fluid content and subsequent shear strength reduction brought about by earthquakes, rockfall or slumping (Leeder, 2011). Secondary structures can be observed and form through dewatering of sediment laiden with water (Talling et al. 2012).

### 2.1.3.3 Massive or structureless sandstones

Massive, structureless sandstones are the result of no primary structures forming during deposition, or post-depositional removal of primary structures (Stow, 2007). Pickering et al. (1995) suggested that sandy debris flows and high density turbidity currents could form structureless sandstones during deposition and remobilization and injection could lead to the removal of internal sediment structures after deposition during burial. Other examples of ablation of sedimentary structures include, bioturbation (Tonkin et al. 2010) and diagenetic alteration (Stow, 2007).

The presence of massive sandstones in beds a metre or less is common and often represents Ta sequence (Bouma, 1962). It is however, the presence of massive sandstone in excess of 1m and sometimes more than 10m that is unusual (Stow and Johansson, 2000).

According to Talling et al. (2012) debris flows can be differentiated by a patchy or swirly fabric (Figure 2.2 (c) Cs5 facies) with numerous liquefaction and soft sediment deformation structures, chaotically organised clasts and rapid marginal pinch out. Whereas in turbidites if clasts are present they are aligned and banded within a narrow unit and contain grading (Talling et al. 2012).

Amy (2005) compares single beds in terms of lateral geometry from the Miocene aged, Marmoso-arenacea Formation containing debris flows around 1m thick and 2- 10km wide. Turbidite sandstones of around 0.8m thickness and 20-40km were recorded. Therefore in this example debris flow are distinguishable from turbulent flows based on aspect ratio. This is developed in Talling et al. (2013). Graded sandstones deposited by turbidity currents were observed and mud rich sand deposited by cohesive debris flow with ´swirly´ internal fabric and rapid pinchout margins are interpreted as the deposits of liquefied debris flow.

Turbidites and debris flows are not necessarily independent during deposition.

Haughton et al. (2003) describes a linked turbidite, debrite system where a mud rich sediment aqua planes down slope upon liquefied sand recently deposited by turbidites. This is an example of two distinctly different compositional flows where an initial deposit influences subsequent flows. An alternative situation where turbidity currents form from sandy debris flows under laboratory conditions is described in (Felix and Peakall, 2006). Debris flows released from a trap above a slope produced turbidites. A range of mechanisms for transforming debris flows into turbidites were observed, commonly turbidity currents evolved from underlying debris flows (Felix and Peakall, 2006). Highly viscous debris flow mixtures moving down slope were seen to produce low concentration turbidites. Whereas, less dense debris flow mixtures were almost completely transformed to turbidity currents. Field examples of flow transformation are shown in Felix et al. (2009).

These examples are included here to indicate that the products and therefore the inferred processes of deposition may not be relevant for the entirety of sediment transit.

### 2.1.4 Identification of primary sediments from core, wireline and seismic data

A number of core and outcrop facies schemes exist e.g. Pickering et al. (1986), Ghibaudo (1992), Cronin and Kidd (1998). In this study Talling et al. (2012) is favoured because of the described continuum between turbulent and debritic flow processes (figure 2.3). It is acknowledged in Talling et al. (2012 and 2013) that division of these units is sometimes not possible in structureless sandstones.

Slatt et al. (1992), Hurst et al. (1990), Emery and Myers (1996), Rider (2004) and Prélat and Hodgson (2013) describe methodology for interpretation of logs, which can be used to infer depositional setting. Rider (2004) also describes, in detail, acquisition and processing techniques for wireline logs.

Davies et al. (2007) and references therein describe a range of seismic geomorphological examples from deep-water settings. Seismic acquisition techniques and interpretation of 3D seismic data is described in Brown (2006).

2.3 (a)

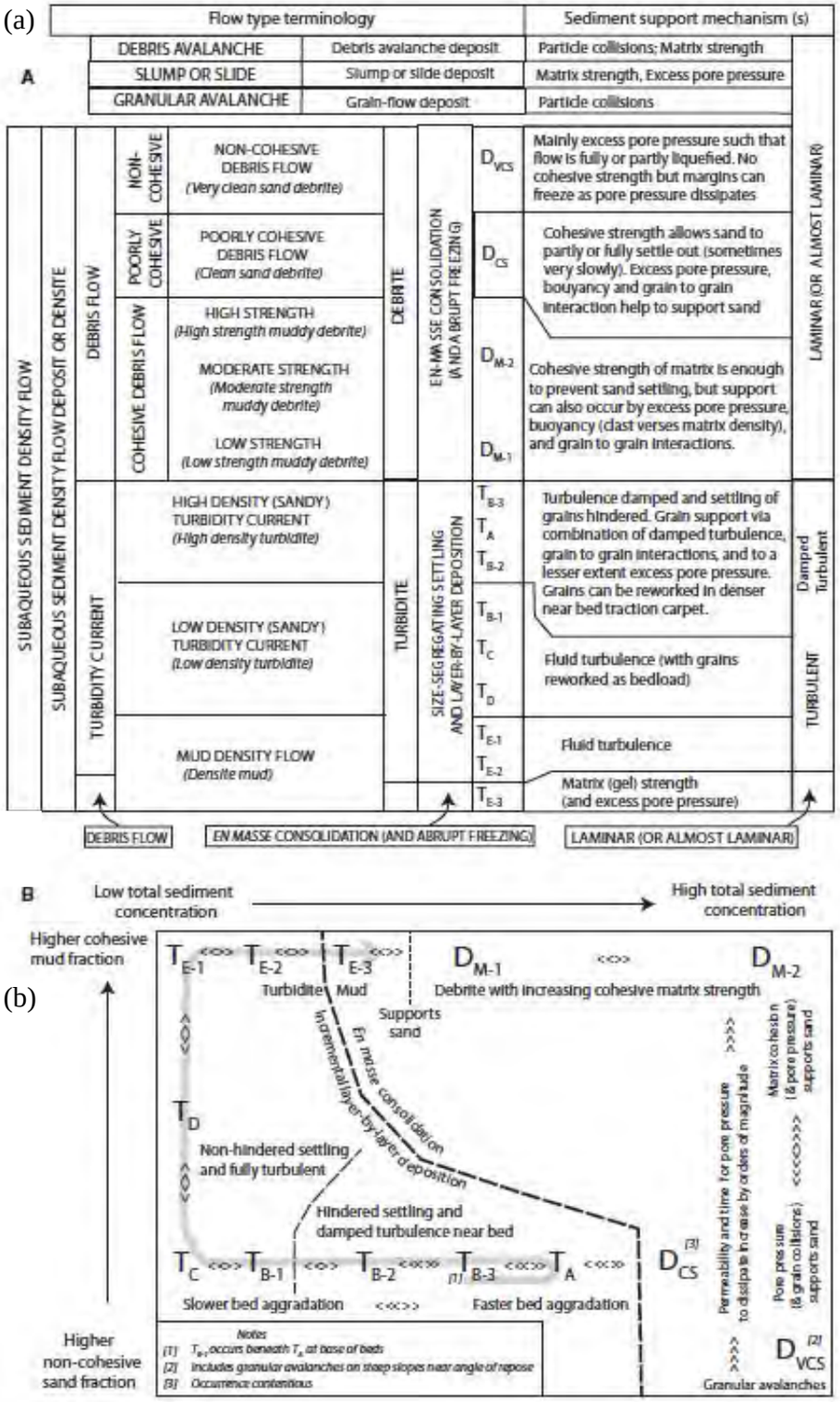


2.3 (b)

2.3 (c)

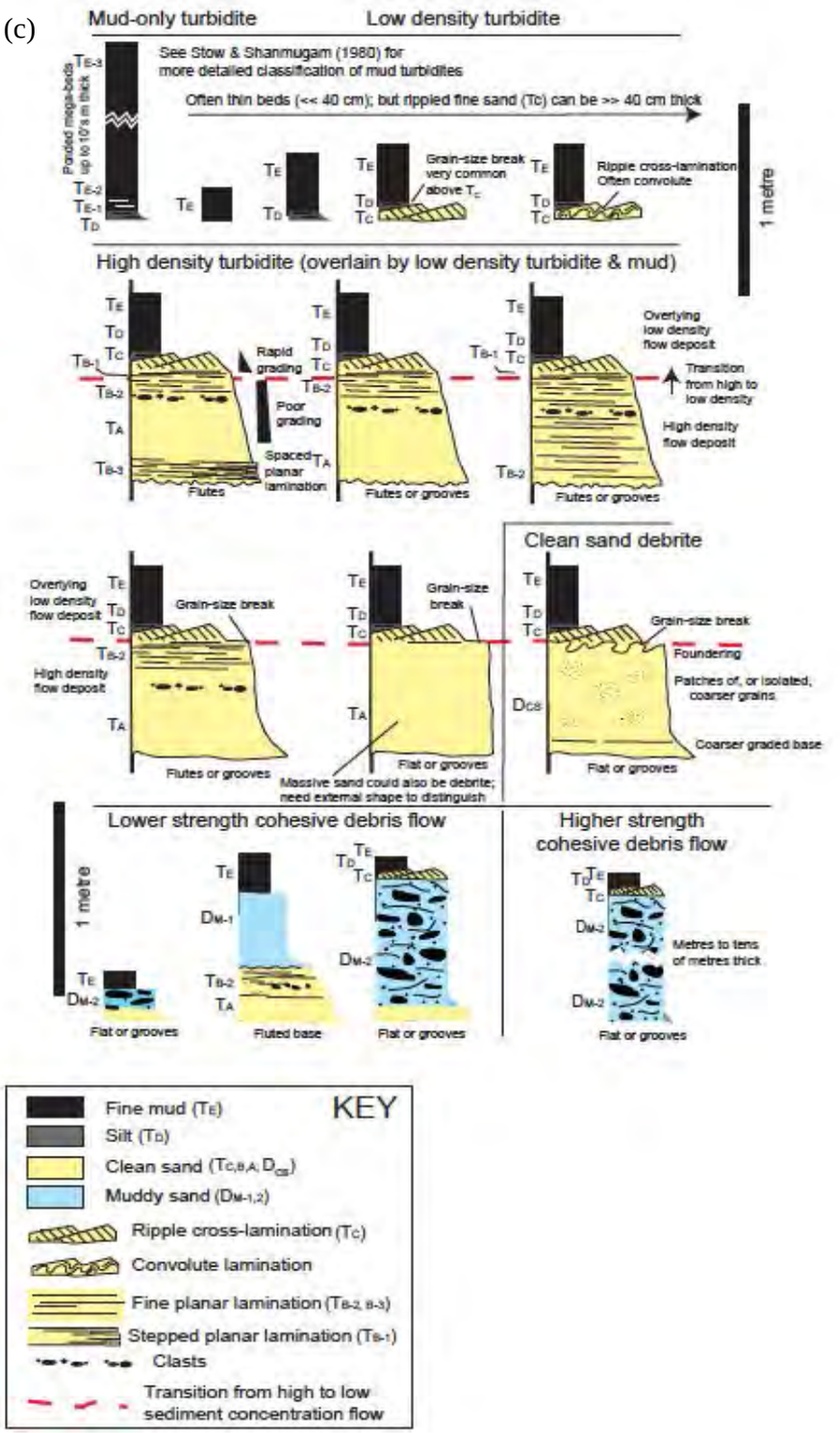


Figure 2.3: Classification scheme from Talling et al. (2012). (a) indicates gravity flow processes and sediment support mechanisms during transport (b) continuum between gravity flow processes influenced by amount of cohesion. (c) Schematic vertical sections of gravity flows deposits

## 2.2 Secondary sedimentation

Sand deposited upon the seafloor is altered chemically and mechanically during burial (Van Rensbergen et al. 2003). Soft sediment deformation causes alteration within 1km of burial (Maltman and Bolton 2003; Jonk 2010) during early lithification (Løseth et al. 2003). Gamberi (2010) subdivides soft sediment defomation into in-situ deformation and post-depositional deformation.

In-situ deformation occurs within the first 400m of burial producing characteristic loading structures (Lonergan et al. 2000). Beyond 400m and up to 1000m burial, post-depositional deformation is active producing a suite of diagnostic sedimentary structures Nichols (1995). Deformation beyond 1km burial results in ductile rock deformation producing folding and boudinage structures (Maltman and Bolton, 2003).

### 2.2.1 Soft sediment deformation

Liquefaction and fluidization are the principle mechanisms responsible for cohesionless deformation (Lowe 1975; Owen 1987). Liquefaction is defined as:

"A loss of strength related to an increase in pore fluid pressure to a level which equals the overburden pressure. Particles become temporarily dispersed in the pore fluid, the strength of the system is reduced virtually to zero and behaves as a viscous fluid." Owen (p. 13, 1987).

Therefore sediments temporally loose frictional strength and become supported by pore fluid stress. Fluidization is defined by Lowe (1975) as:

"Fluidization occurs when the drag exerted by moving pore fluids exceeds the effective weight of the grains; the particles are lifted, the grain framework destroyed, and the sediment strength reduced to nearly zero." Lowe (p. 157, 1975).

Fluidization and liquefaction differ due to sustained net movement upward which destroys grain framework during fluidization, although both processes alter the state of the sediments from solid to fluid. Furthermore, in order for liquidization (encapsulating both liquefaction and fluidization) to be recorded a driving force (Gamberi, 2010) in the form of a principal stress must act whilst liquidization is in effect (Owen, 1987).

For post-depositional deformation to occur the following pathway is observed (Braccini et al. 2008). Unconsolidated sandstones must be encased by a low permeability mudstone. Overpressure must be induced usually through addition of an external fluid (Gamberi, 2010). A trigger mechanism causes fluidization of sand, which leads to hydraulic fracture when pore pressure exceeds fracture gradient (Jolly and Lonergan, 2002).

### 2.2.2 Loading structures

Loading structures are produced within unconsolidated cohesive (mud rich) and non-cohesive (sand rich) materials and represent folding of the sediment interface (Owen, 2003) occurring either at time of deposition (syn-deposition) or relatively soon after deposition (Gamberi, 2010).

Liquefaction processes dominantly lead to loading structures (Owen 1987; Nichols 1995). Examples of loading structures are shown in Figure 2.4 and include simple load casts, flame structures and pseudonodules. The latter entirely detaching from their parent body (Owen, 1987). Loading structures form by density inversion when a less dense fluid is located beneath a more dense fluid (Leeder, 2011) causing instability.

Figure 2.4 (a): Load casts and flame structures in Silurian turbidites, Aberystwyth Grits, central Wales from Owen (2003).

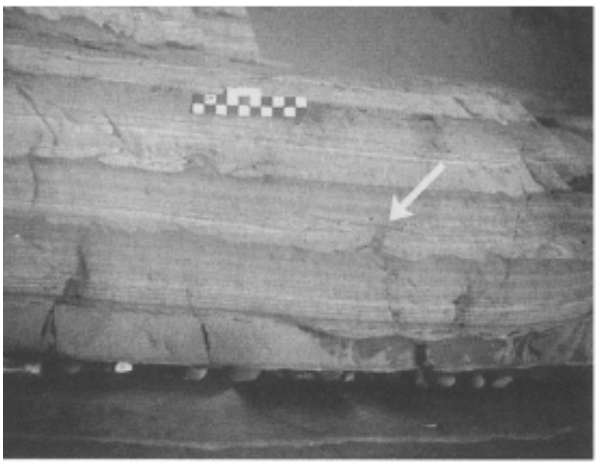

Figure 2.4 (b): Flame structures and mud diapir (arrowed) in Carboniferous Bude Formation, Bude, Cornwall from Owen (2003).

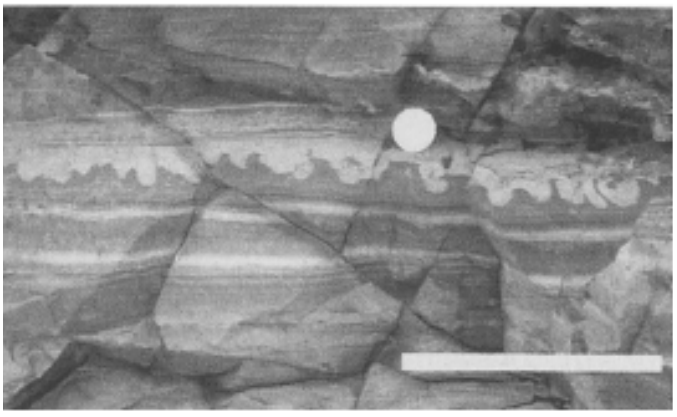

Figure 2.4 (c): Simple and pendulous load casts in Ordovician water-lain tuffs, Ramsey Island, South-West, Wales. Figure 2.4 a,b and c from Owen (2003).

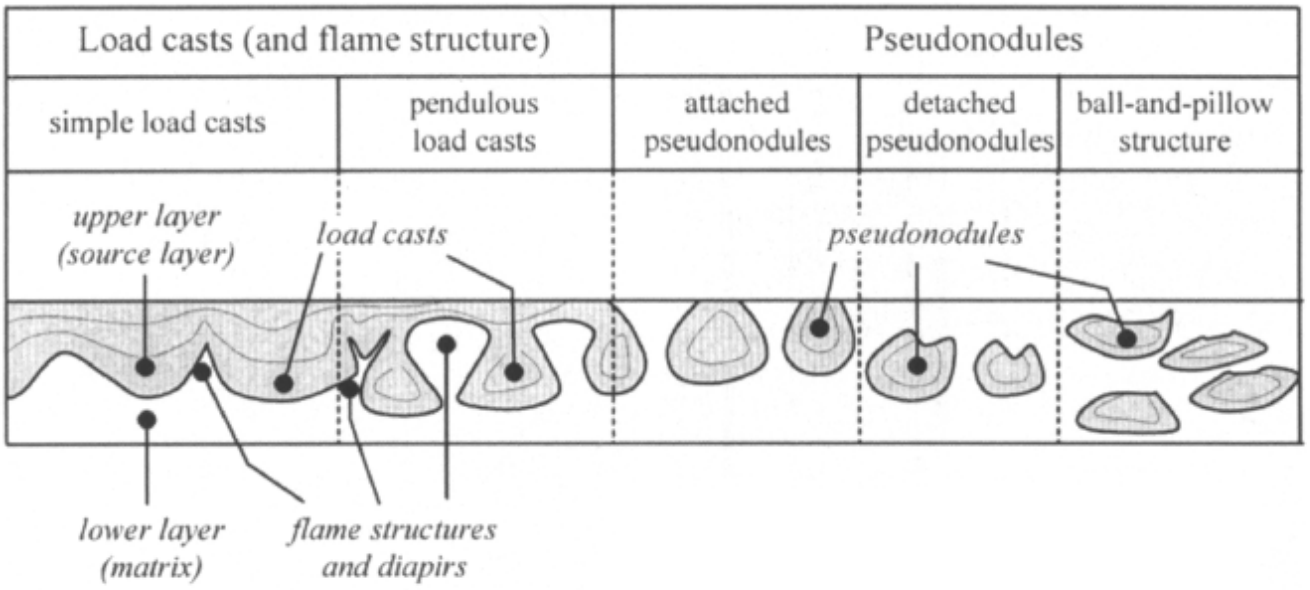


Figure 2.4 (d): Definition diagram for loading structures from Owen (2003).

### 2.2.3 Post-depositional deformation

Post-depositional deformation is distinguished from in-situ deformation as primary sedimentary structures are cross cut (Leeder, 2011). Post-depositional deformation products include clastic dykes and sills, dish and pillar structures, sand/mud volcanoes and slump sheets observed from outcrop (Owen, 2003) and are larger in scale than loading structures (figure 2.5). Figure 2.6 describes the relationship between loading and post-depositional structures. The effects are shown in Figure 2.7

Inference from cored section and outcrop is limited in that preserved sedimentary structures may only record the highest magnitude, latest stage deformation event. Laboratory experiments to replicate post-depositional deformation (Nichols, 1994; Nichols, 1995; Owen, 1996) suggest the process of fluidization is responsible for remobilization and injection (Rodrigues et al. 2009). This maybe an oversimplification as Ross et al. (2011) describes a continuum between fluidization and liquefaction observed from laboratory experiments especially within feeder conduits (described in section 2.2.4.2).

Figure 2.5: (a) Vertical section through fine-grained sandstone with small dish structures (image 3.5cm across). Jackfork Group, Carboniferous, southeast Oklahoma, USA. Photograph from D.R. Lowe in Allen (1982).

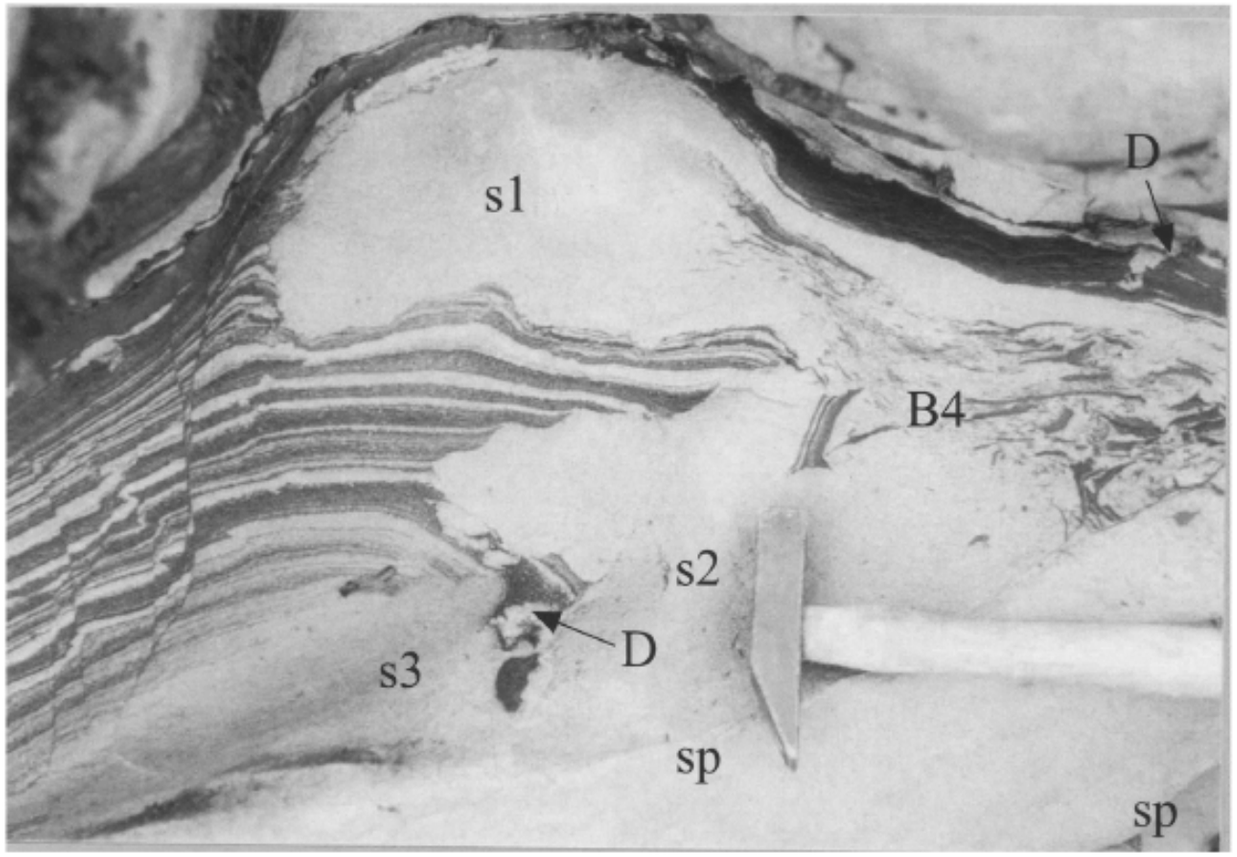


Figure 2.5: (b) Interbedded, organic rich siltstones and fine grained sandstones are disrupted by sills (s1 and s2) containing fine grained sand. S2 is connected downward to parent depositional bed. Ptygmatically folded dykes (D) and shale clast brecciation are also shown (B4). Hammerhead is 10cm long, Upper Jurassic Helmsdale Boulder Beds North-East Scotland. Photography from of N.H. Trewin in Hurst et al. (2005)

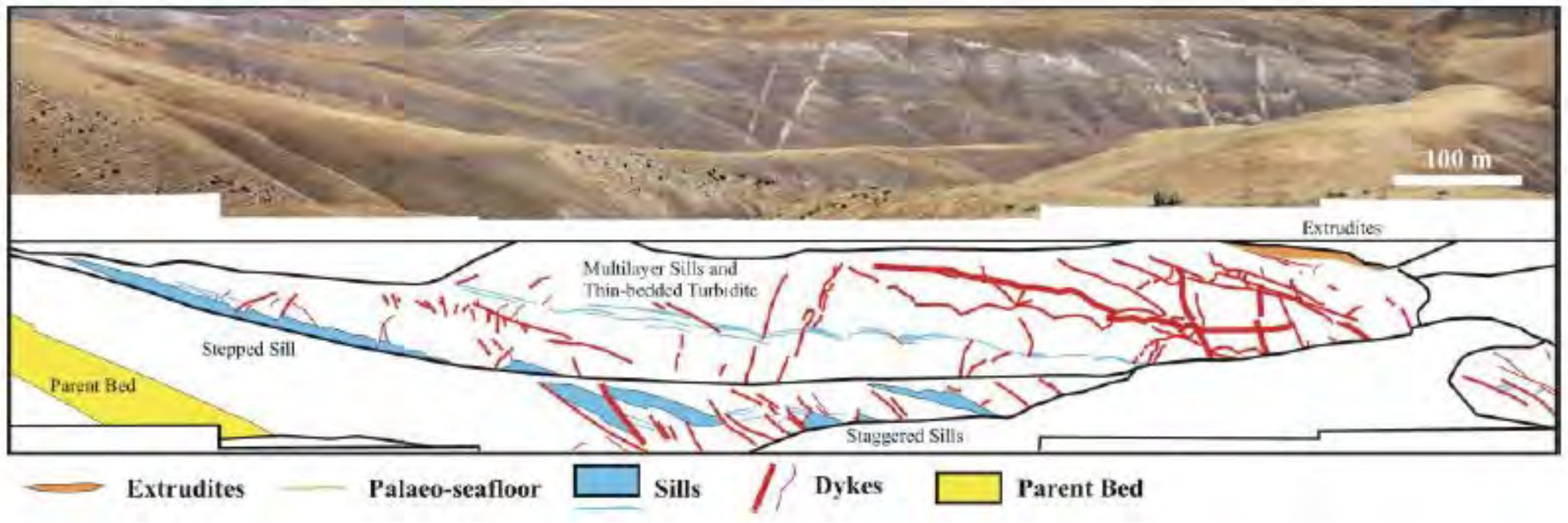


Figure 2.5: (c) Upper photo looking East at Panoche Giant Injection Complex outcrop, Marca canyon, California, USA. Lower image interpretation of photograph from Vigorito et al. (2008). Older bedded strata locate in South-East and intruded sediments, young North-East.

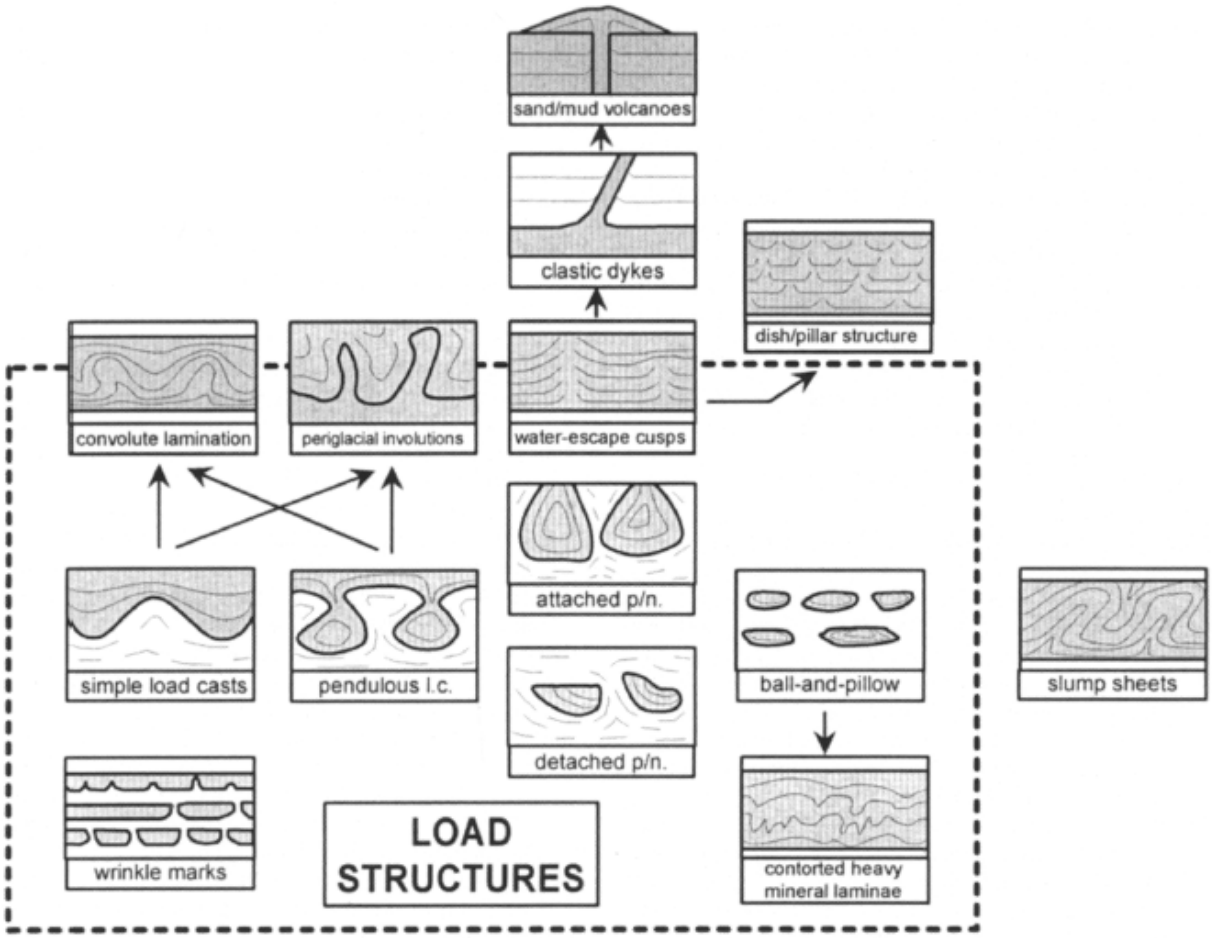


Figure 2.6: Schematic relationships between loading structures and post depositional remobilization and injection, from Owen (2003).

### 2.2.3.1 Overpressure build up

A pore fluid is described as overpressured if its pressure exceeds that of the hydrostatic gradient (Osborne and Swarbrick, 1997). Overpressure can be induced by a reduction in rock matrix or increase in compressive stress due to fluid movement and buoyancy (Osborne and Swarbrick, 1997).

An increase in compressive stress through reduction in rock matrix may be achieved by disequilibrium compaction, a process in which rapid burial of unconsolidated sands and low permeability mudstones inhibits water escape and fluid pressure rises above the hydrostatic gradient (Osborne and Swarbrick, 1997). Hillier and Cosgrove (2000) suggested that most of the injected and remobilised North Sea reservoirs resulted from disequilibrium compaction. Other examples of increase in compressive stress through reduction of rock matrix include salt diapirism (Dixon et al. 1995) and compression in tectonic settings (Hubbard et al. 2007).

Hydrocarbon migration into Tertiary aged sediments in the North Sea basin is an important overpressure generating mechanism (Lonergan et al. 2000). Cartwright (2010) refutes this model due to the regional extent of remobilization and injection (approximately 40, 000km$^2$) and huge quantity of hydrocarbon fluid needed to cause overpressure. Another example of fluid movement leading to overpressure is the release of bound water from silica diagenesis at shallow burial (Davies et al. 2006).

### 2.2.3.2 Triggers

Trigger effects cause the release of overpressure (Braccini et al. 2008) through hydrofracture. Jolly and Lonergan (2002) and Hurst (2011) suggest the difference between build up of overpressure and triggers effects is the fluidization of a solid.

Jolly and Lonergan (2002) describe four principle trigger mechanisms identified from

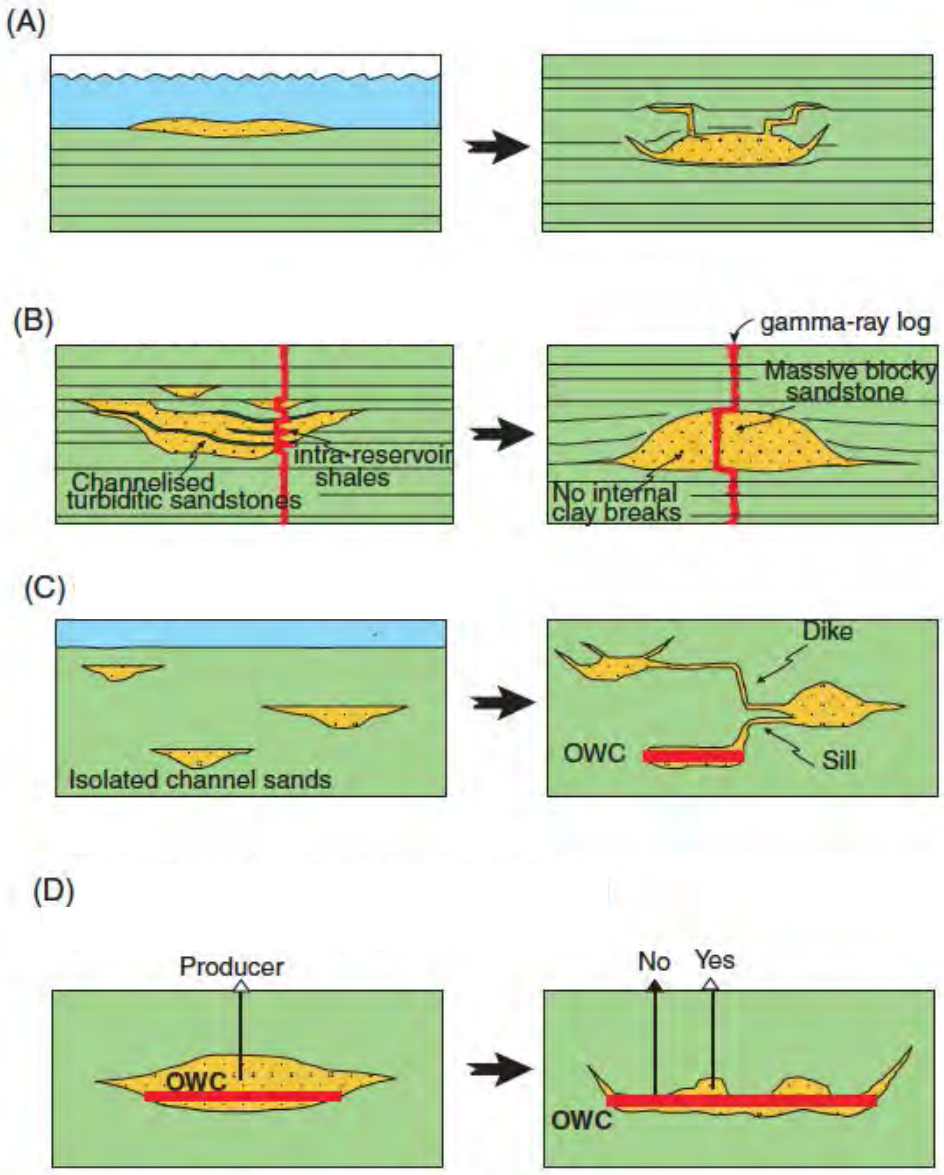


Figure 2.7: Schematic illustration describing the influence of remobilization and injection on depositional sandstones. (A) Winged intrusions and steepening of flank mounds (B) increasing homogeneity (removal of internal baffles). (C) Improved reservoir connectivity, (D) remobilization and injection can cause irregular top reservoir form (from Lonergan et al. 2000)

literature. Seismicity induced liquefaction, tectonic stress, depositional processes and influx of overpressured fluid. Other examples of trigger mechanisms include bolide impacts (Alvarez et al. 1998; Cartwright, 2010) and magmatic intrusion (Moreau et al. 2012). Trigger mechanisms maybe high impact, short duration stress events (e.g. rapid deposition) or cyclical (e.g. current deposition) moderate to high impact, repeated duration events (Gamberi, 2010).

#### 2.2.3.2 Hydrofracture

Hydraulic fracture is initiated by trigger mechanisms and occurs when:

"Pore fluid pressure, is greater or equal to the tensile strength of the rock normal to that plane and the normal stress acting across it." (Hillier and Cosgrove, 2002).

Fracture in this way is responsible for sands injection into surrounding low permeability strata.

### 2.2.4 Architecture of post-depositional deformation

An idealised injectite complex is displayed in Figure 2.8. Sand injectites are formed when clastic sediment is forced into low permeability surrounding strata (Rodrigues et al. 2009). Fluidised sand is unable to resist driving forces and a sufficient pressure differential must then be maintained for clastic intrusions to propagate and develop (Morley 2003; Frey-Martinez 2007).

Intrusion complexes can range in scale from several millimetres to hundreds of metres (Surlyk et al. 2007). At Panoche Giant Injection Complex sandstone injectites extend over 1200m vertically from parent units (Vigorito et al. 2008). Sandstone intrusions are most easily defined by their relationship with host strata (Hurst, 2011). A hypothetical, vertically organised system is described in section 2.2.4, which is large in scale (above 10 m). Basal Parent units offer a source of sediment for injection. Sediment passes through feeder conduits either within parent units or within sandstone injections. Sandstone intrusions consist of both dykes and sills leading upwards or laterally into extrusions where intrusions reach the sea floor.

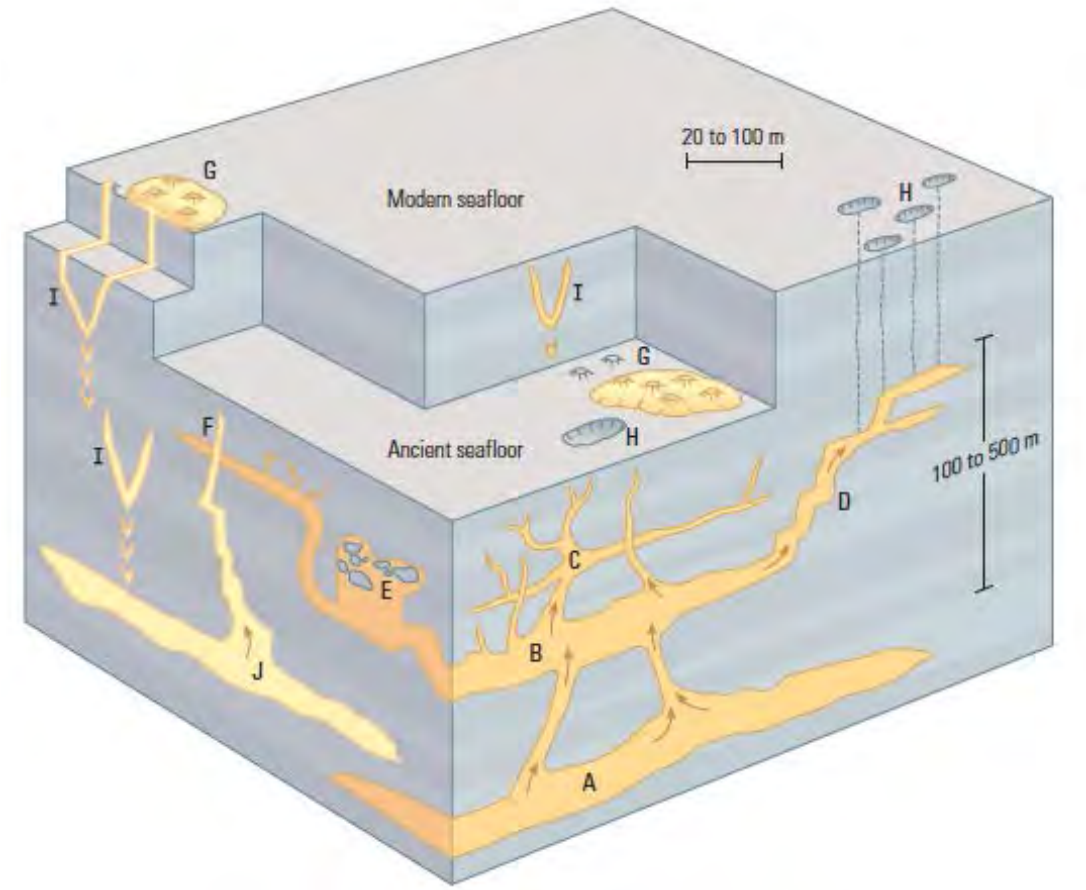


Figure 2.8: Schematic illustration of architectural elements commonly found in sandstone intrusions. (A) Depositional sand body and source of sediment for sandstone intrusion (parent body). (B) A Sill intrusion, (C) a complex of dykes and sills. (D) Stepped dyke and sill network. (E) Irregular intrusive body containing clasts of host rock. (F) Sill from parent body A, crosscut by a dyke from from parent body J. (G) Sandstone extrudites, (H) gas seeps and (I) conicol sand injections (from Braccini et al. 2008).

### 2.2.4.1 Parent units

Sandstone injections emanate from parent units which where deposited by primary depositional processes. However, mounded sandstones with flank angles of between 10-40° are unusual in unconfined settings (Jenssen et al. 1993; Huuse et al. 2004). Sandy debris flows, differential compaction and injection are suggested by Huuse et al. (2004) as possible explanatory mechanisms. Rock falls and slumping can produce steep-sided mounds although it is uncommon to find intact olistostromes beyond base of slope due to disaggregation and erosion during transportation (McArthur et al. 2008).

Parent units can become steep sided or mounded through differential compaction of mudstone and sandstone lithologies although flank angles of more than 15° in unconfined settings is uncommon (Jennette et al. 2000), Figure 2.9. Further steepening of the flanks of parent units beyond 15° can be achieved by post-depositional processes (E.g. Szarawarska, 2010) as fluidized sediment is forced into overlying low permeability strata (Briedis et al. 2007; De Boer et al. 2007) producing thicker, lower aspect ratio features as shown in Figure 2.10 from Cecile Field, Danish North Sea.

Mounded geometries may also be produced entirely by injection. Laccoliths, are fully intruded inflationary structures thought to originate from depositional parent units and potentially can act as parent units (Rodrigues et al. 2009; Kane 2010; Szarawarska et al. 2010).

In several published examples from the North Sea Parent Sandstones have higher porosity and permeability values than injected sandstones e.g., Alba Field (Duranti et al. 2002), Gryphon Field (Lonergan et al. 2007; Templeton et al. 2009). Fluidization does not affect unconsolidated sandstones uniformly (Surlyk, 2007). Fine-grained sandstones are preferentially fluidized over coarser quartz grains (Lowe, 1975), this is because sedimentary features (e.g. mudstones) diagenetic processes (cementation, recrystallization) or burial and

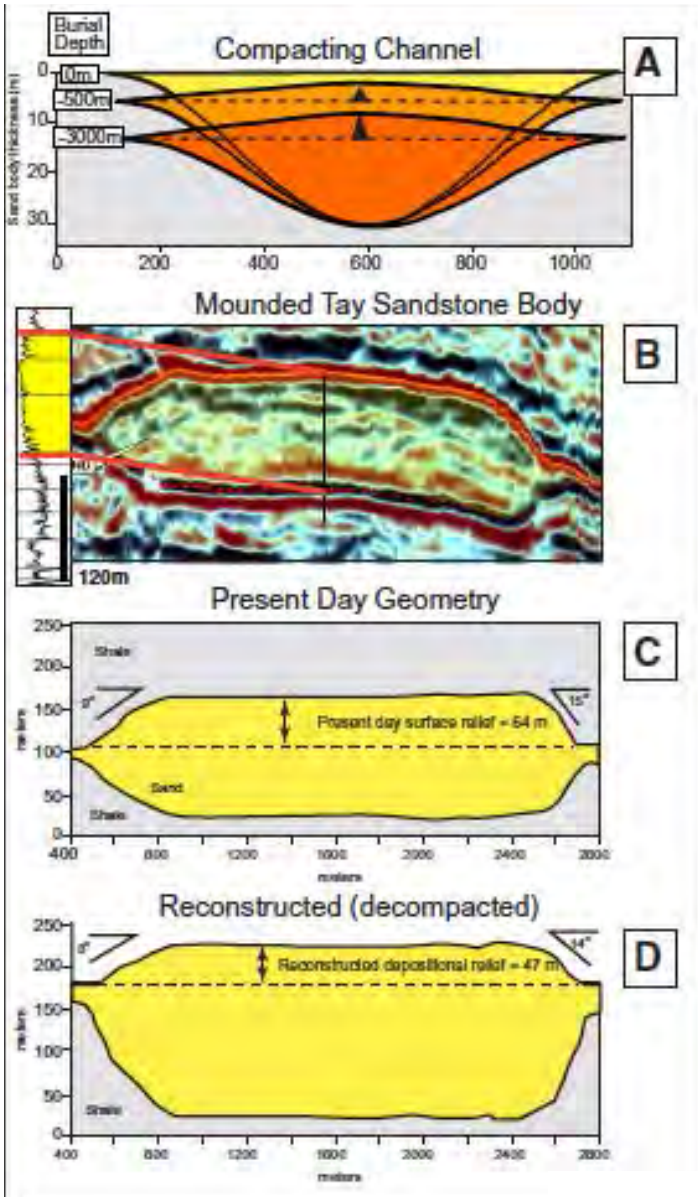


Figure 2.9: Mounded geometries formed through compaction. (A) Channel profile change and development of mounding due to differential compaction of sandstones and mudstones. Black triangles indicate amount of relief above container margins caused by differential compaction. (B) Seismic profile of Paleocene, Tay sandstone, (C) profile of Tay sandstone body after removal of structural deformation. (D) Sandstone bodies decompacted to geometries probable at seafloor (From Jennette et al. 2000).

consolidation (Parnell and Kelly, 2003) may impede fluidization. Parent units often include Feeder conduits and Brecciated intervals (described in section 2.2.4.2).

### 2.2.4.2 Feeder conduits

Feeder conduits originate from Parent units and provide an evacuation route for fluidized sand either redistributing laterally or vertically within the Parent Unit (Diggs, 2007) or facilitating sand exit into injections.

Columnar intrusions or clastic pipes form as overpressured fluid vents (Ross et al. 2011). Pipe morphologies can consist of Tabular feeder conduits (Jolly and Lonergan 2002) to cylindrical and funnel shaped pipes (Moss and Cartwright, 2010). Feeder conduits can range in size from millimetre scale to over ten metres (Gamberi, 2010). Margins of feeder conduits can be marked grey with elutrated clays (Duranti and Hurst, 2004).

Mudstone breccia is observed near the upper terminus of feeder conduits (Hurst et al. 2011) proximal to sandstone intrusions. Mud clasts originate either from primary deposition or host rock included during injection. Scott et al. (2009) build on internal features described in Duranti et al (2002a) and Duranti and Hurst (2004) from the Yellow Bank Creek injectite complex in California, USA. Suggesting that there is sufficient flow velocity to cause mudstone particles to be cut or broken from coherent bedding surfaces by corrosion process usually the result of high velocity turbulent flow conditions.

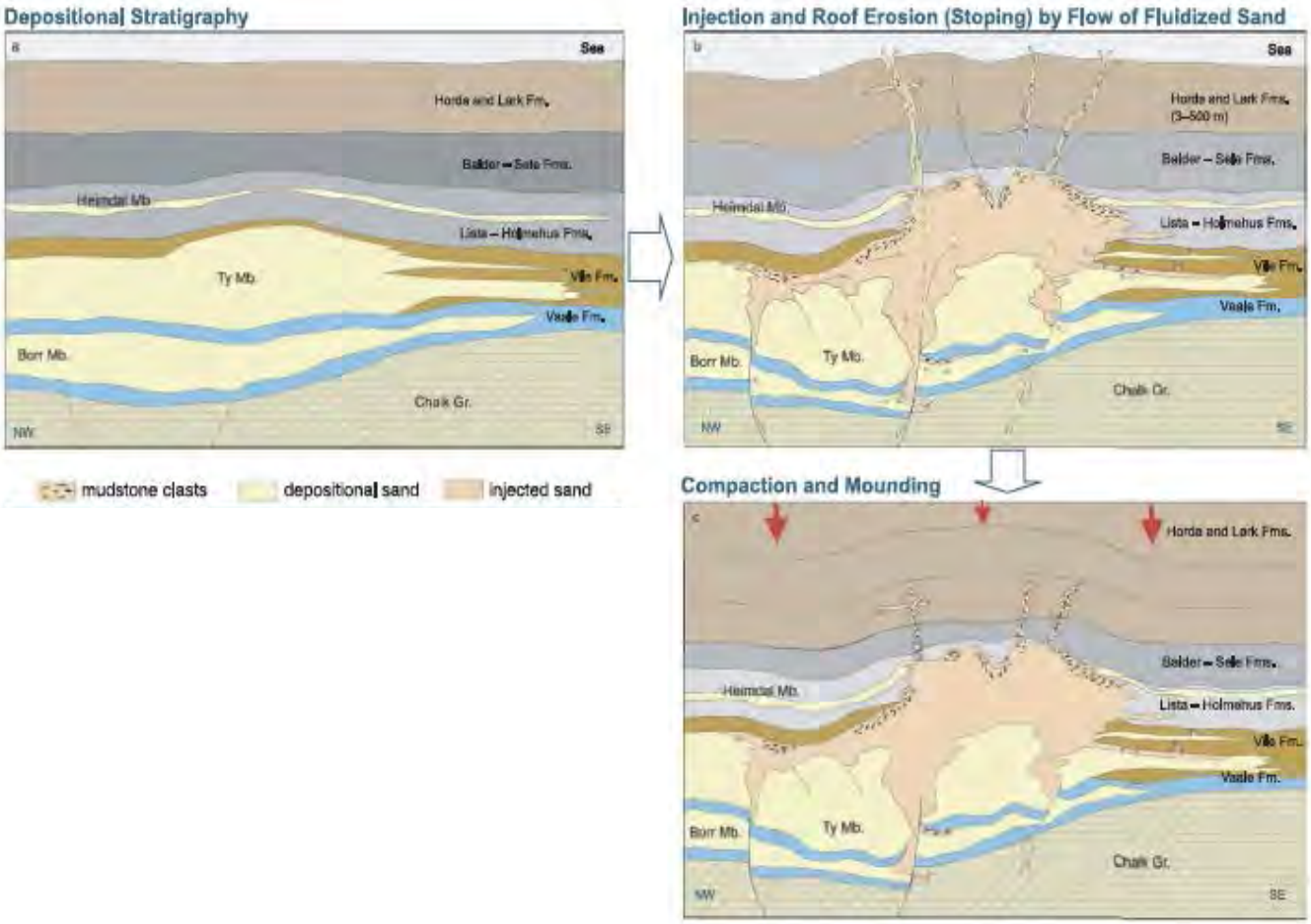


Figure 2.10: Schematic illustration of the formation of the Cecilie mounded injection, deep-water Paleocene, Cecilie Field, Denmark. (a) Before injection, a layer cake stratigraphy is observed with subtle compaction over channelised sandstones of the Ty Member. (b) Tectonic reactivation of Permian faults resulted in propagation of faults though sandstones and overlying mudstones causing fracture of overburden and sandstone injection. (c) Present day geometry enhanced by compaction (from Hamberg et al. 2007)

### 2.2.4.3 Sandstone Intrusions

Sandstone dykes are host rock bedding discordant features (Hurst et al. 2003) that taper away from parent units (Diggs, 2007). Sandstone dykes range from single isolated occurrences to swarms and orientate with unimodal direction through to multiple plane orientations (Taylor, 1982). Commonly dykes are described in literature to intrude vertically upwards, however there are recent examples of downward intrusion (Hamberg et al. (2007); Parize et al. 2007; Kane (2010); Gamberi (2010), Svendsen (2010). External surfaces of dykes may display rill (miniature stream systems, Allen, 1982), flute and groove structures (Diggs, 2007) formed by unidirectional flow (Scott et al. 2009). Dykes may posses grain size grading (Taylor, 1982) with examples of mudstone, sandstone and pebble grading recorded at Cerro Terro Formation, Magallanes Basin, Southern Chile (Hubbard et al. 2007).

Sandstone sills are intrusions that broadly sit in plane with host rock but locally can become discordant (Diggs, 2007) up to 30° (Duranti and Hurst 20004; Vetel and Cartwright, 2010). Two sill types are identified in the Panoche Giant Injection Complex (Staggered and Stepped) based on contact margin to surrounding country rock (Vigorito et al. 2008).

Diggs (2007) offers perhaps a further sub class of asymmetric intrusions – composite concordant and discordant structures where (in 2d cross section) intrusion surfaces maybe perpendicularly orientated, therefore parallel to bedding in one orientation and discordant in the other.

Clastic injections are formed during seal failure (Hurst et al. 2003). In the North Sea Lonergan et al. 2000 observed two styles of intrusion during burial. Small-scale intrusions (cm-m) are described as initiating during early burial. But during greater burial and increased pressure differential the scale of intrusion increases and can reach hundreds of metres in scale (Figure 2.15). Jolly and Lonergan (2002) suggest that sills are formed preferentially over dykes at shallow burial (within 500m) and dykes are more common between 500-1000m Jolly

and Lonergan (2002) in a basins with principle stress vertically. At shallow burial the differential between horizontal and vertical stress is low and bedding anisotropy favours the formation of sills over dykes. During deeper burial seal integrity is greater than at shallow burial and therefore greater overpressures can develop. Dyke propagation will occur once pressure exceeds the lithostatic gradient for a seal rock and will continue until pressure is reduced below the lithostatic gradient, upon which sill propagation will commence (Jolly and Lonergan, 2002).

Sandstone intrusions can lead upwards into extrusions at the sediment fluid interface (Pringle et al. 2007). Sand volcanoes represent the interface between layered sediment and the water bottom (Jonk et al. (2007). Varying between 0.1 to 0.75m for conical features and 0.3 to 3m for elliptical geometries (Hurst et al. 2011). Extrudites (Hurst et al. 2006) can form micro communities. Nutrient rich fluids upwelling through sandstone intrusions created a focal point for seep communities, which existed for around 2Ma at Panoche Giant Injectite Complex (Minisini and Schwartz, 2007). Cold seep communities are also described in Mazzini et al. (2003) from Gryphon Field, United Kingdom, North Sea.

Cohesive muddy remobilization has also been observed (Van Rensbergen et al. 2003). Less literature exists in this subject area than non-cohesive remobilization and injection due to lack of interest from the hydrocarbon industry (Huuse et al. 2010). Cohesive remobilization is largely extrusive (e.g. mud volcanoes, Mazzini et al. 2009) and non-cohesive remobilization commonly intrusive (e.g. sandstone injections). The two mixtures can become remobilized together (Van Rensbergen et al. 2005; Frey-Martinez et al. 2007) although it is unclear whether fluidization propagates mud intrusion during shallow burial or whether fluidization is possible in cohesive sediments during deeper burial (Van Rensbergen et al. 1999, Leon et al. 2010).

### 2.2.4.4 Polygonal faulting

Polygonal fault networks are common in Tertiary aged sediments in the North Sea and Norwegian Sea basins and are often found in mudstone prone intervals although polygonal faulting can extend into sandstone intervals (Stuevold et al. 2003, Jackson, Mahlo and Briggs 2013). Polygonal faulting is a soft sediment deformation feature associated with compaction shrinkage caused by dewatering (Gay, 2007). Polygonal faulting does not form in response to regional tectonic stress as extensional strain is not balanced by compressional strain (Cartwright and Lonergan, 1996). Polygonal fault networks form during early burial (10-500m, Cartwright and Dewhurst, 1998).

Lonergan et al. (2000) and Huuse et al. (2004) suggested that the presence of polygonal faulting in the Alba Field aided both crestal and marginal wing injectites. Huuse et al. (2007) observed that a dip angles between injectites and faults were different. Present day uncompacted dip angles of between 30-50˚ for large-scale intrusions and 35-75˚ for polygonal faults. Whilst dip angles between the two features are not the same Huuse et al. (2007) does suggest that active faulting at the time of sand intrusion would likely be exploited to some degree by sand intrusions.

### 2.2.5 Identification of secondary sediments

Examples of secondary sedimentary features from cored section and outcrop are presented in Table 2.1. Figure 2.7 from Lonergan et al. (2000) describes the effects of remobilization and injection on sandstone intervals. Reservoir geometries are modified with steepened mound flanks and injections, removal of internal (clay) baffles and improved lateral and vertical connectivity (Lonergan et al. 2007). Whilst these are the characteristics of remobilization and injection (Huuse et al. 2005) the appearance of remobilized and injected sandstones in wireline logs and seismic data is not diagnostic of remobilization as the uniqueness of response is low. Cored section, however, does allow confident identification of injected sandstones. A series of flow diagrams are presented in Appendix 1 describing causal depositional process. Figure 2.11 from the Alba Field, United Kingdom, North Sea show remobilized and injected facies in cored section.

According to Parize et al. (2007) and Braccini et al. (2008) post-depositionally remobilized sediments do not possess a unique wireline log signature. A model is presented in Duranti et al. (2000) and Duranti and Hurst (2004) where wireline logs through Eocene aged channel sandstones in the Alba Field, United Kingdom, North Sea were correlated to 3D seismic data, cored section and thin sections. Blocky 100m thick sandstones are identified on wireline logs, Duranti and Hurst (2004) argued that increased wireline Density and Sonic log values near to the top of the sandstone section was created by post-depositional remobilization and injection. Thin sections from corresponding high Density and Sonic log intervals showed tighter grain packing (dominantly quartz) than deeper in section and the authors used this observation to support their interpretation of remobilization and injection, instead of diagenetic cementation or poor results from wireline log tools. Suggesting that the effects of fluidization can be more clearly observed near to upper seal boundary. Jackson and Sømme (2011) present wellbore evidence from an injected sill identified on 3D seismic on the Måløy

slope, Norwegian North Sea. The petrophysical characteristics of this Cretaceous aged turbidite sandstone are similar to other wells in the area with core data. The authors suggest that the presence of regionally similar petrophysical character sandstones and cross-cutting seismic reflections is strong enough evidence to identify either sandstone injection or extrusion and that wireline logs through these sandstones do not have a unique log signature. It seems likely wireline logs will be unable to accurately identify the characteristics of clastic injection as injections produce a non-unique wireline log signature. Although more sophisticated acquisition techniques like well-bore imaging may aid discrimination in the future. Furthermore, Hurst et al. (2011) identified that wireline logs have not been acquired through outcrop. Where secondary sediments are identified by cored section or seismic data observations from corresponding wireline intervals are recorded in Table 2.2.

Examples of secondary features from seismic data are presented in Table 2.3 and figure 2.12. Huuse et al. (2004, 2007) present a series of examples summarised below.

Crestal intrusion complexes (Huuse et al. 2007) are commonly centimetre to metre scale and are characterised by intruded sandstones from a central location. Panoche Giant Injectite Complex is a Crestal intrusion complex with vertical intrusion over hundreds of metres.

Winged sandstone intrusions (Huuse et al. 2004) intrusions range from 10 to 40m thick, 50-250m vertical extent and maybe more or less continuous for 1-5km laterally. Present day wing inclination are often 10-35˚ (dependant upon level of compaction at the time of intrusion), and may have been as much as 60˚ at time of intrusion (Huuse et al. 2007). Similar features are described in Szarawarska et al. (2010), figure 2.12 (a) and Jackson et al. (2011)

Mounded bodies or laccoliths (Frey-Martinez et al. 2007) with steep flank margins above 20°, circular or oval in plan view and ranging from several hundred metres to several

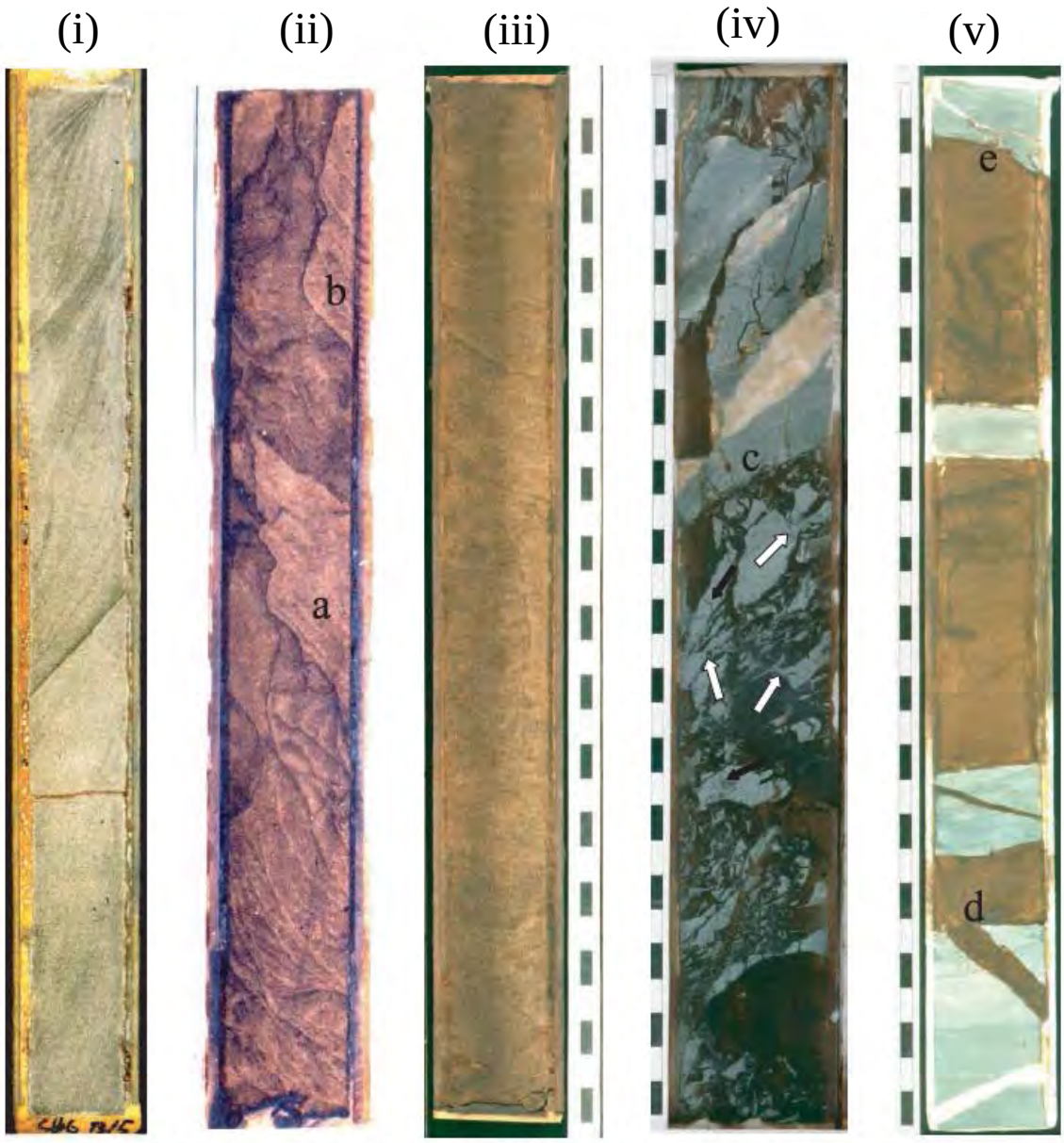


Figure 2.11: Examples of the effects of remobilization and injection (from Duranti and Hurst 2004). (i) Sandstones with oversteepened laminae, (ii) giant pillars (a) cutting through bedded sandstones (b) bedding curved upwards. (iii) Structureless sandstone with little internal character. (iv) Mudstone clast breccia. (v) Intruded sandstones (d) dykes and sills (e) discordant tops (from Duranti and Hurst 2004).

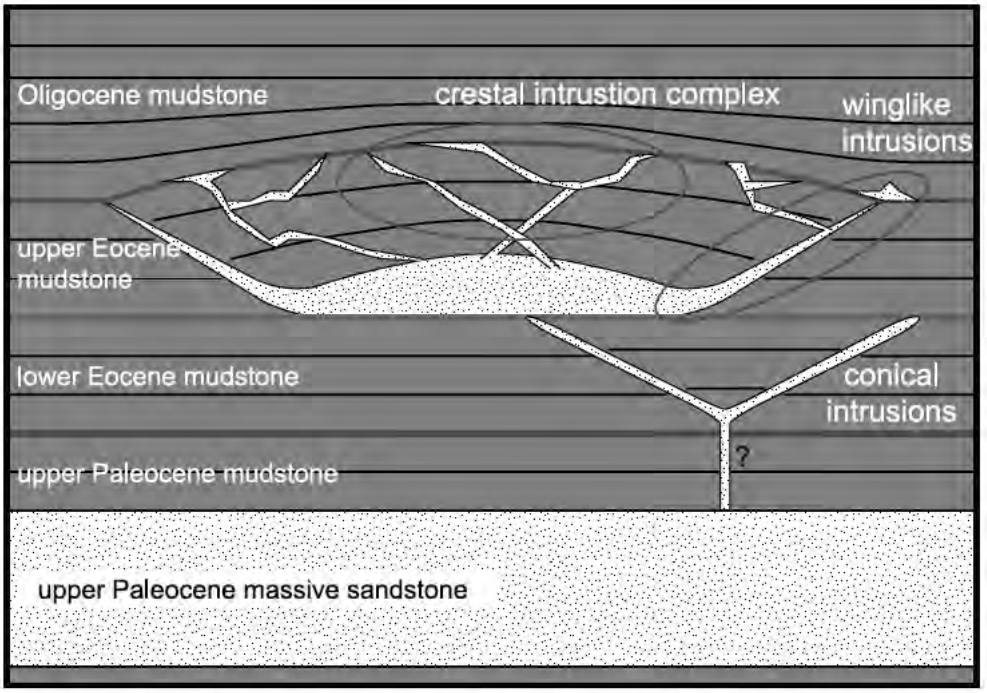


Figure 2.12 (a): Three types of sandstone intrusion described in Huuse et al. (2005) from North Sea, Paleogene sandstones.

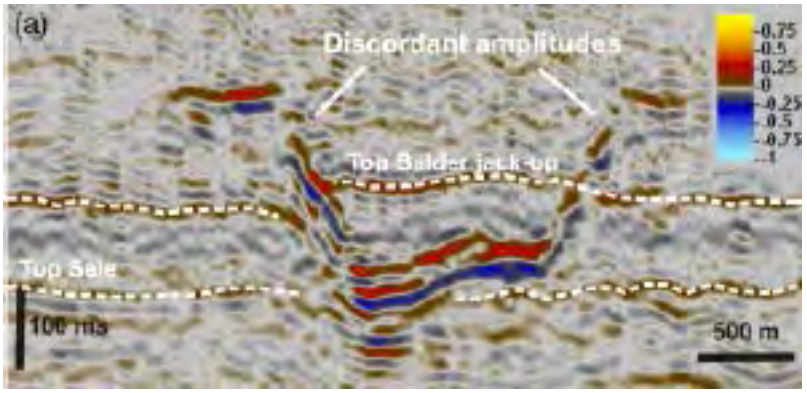


Figure 2.12 (b): A seismic example of a winged sandstone intrusion from Volund discovery, Palaeocene, Norwegian North Sea (from Szarawarska et al. 2010)

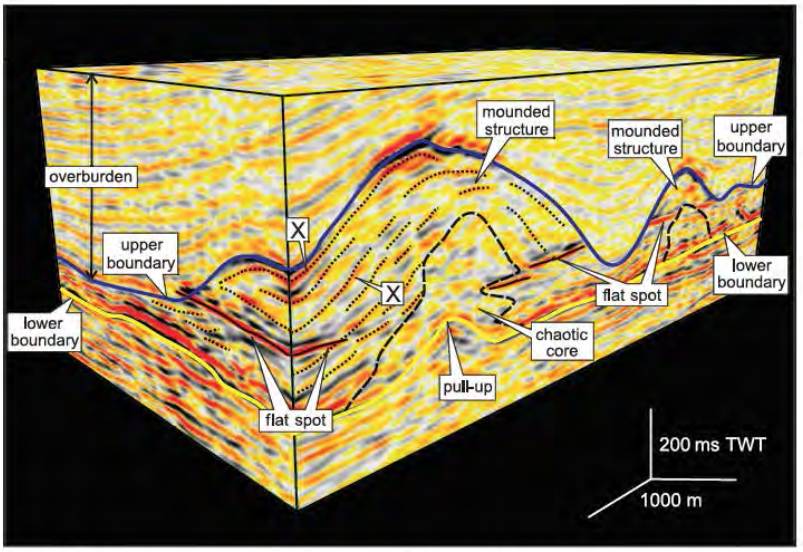


Figure 2.12 (c): A seismic example of mounded sandstones formed by sandstone intrusion from beneath. Oligocene age, offshore Israel from Frey-Martinez et al. (2007)

kilometres at the base of structure (Frey-Martinez et al. 2007) shown in figure 2.12 (b and c).

Conical sandstone intrusions (Cartwright et al. 2008): Intrusions can range from 100 – 2000m in diameter, 50-300m in height and 1-80m in thickness.

| | Feature | Description | Interpretation | Location | Publication |
|---|---|---|---|---|---|
| **In situ water escape structures** | Load casts (flame structures) | Found on the underside of sand overlying mudstones, upward bulging (regular to irregular form) diapiric shapes. There is never detachment. (cm) | Thought to be formed by unequal gravity loading effects due to heterogeneity in overlying sediments, liquefaction | Langdale slates, England (Allen 1982) | Allen (1982); Nichols (1995) |
| | Pseudo-nodules | A structure consisting of a single similar sized laterally repeating sand bodies (typically 0.5m) | Differential loading effects, probably brought about from seismic shaking | United Kingdom | Allen (1982) |
| | Ball and Pillow structures | A sheet of sand bodies of various sizes. Balls are smaller, pillows larger (cm) | Differential loading effects, probably brought about from seismic shaking | United Kingdom | Allen (1982) |
| | Dish structures | More commonly identified in turbidite deposits. Flat to strongly concave upwards 0.2-0.5m. Identified in silts and all grades of sand. | Liquefaction and fluidization (highlighted by filtered fine grained sediments clays) | United Kingdom | Lowe and LoPiccolo (1974); Allen (1982); Nichols (1995) |
| | Pillar structures (Type A and Type B) | Small scale structures (Type A) and large scale (Type B) | Liquefaction and fluidization (highlighted by filtered fine grained sediments clays) | United Kingdom | Lowe and LoPiccolo (1974); Lowe (1975) |
| | Heavy mineral sags | Tear drop downwards (mm-cm) | Form due to density variations when sediments are liquidized | United Kingdom | Allen (1982) |
| | Convolute(d) lamination | Typically identified in fine to very fine sands cross laminated sands. Appear as basin and dome shapes anticline-syncline and range from smooth sided-angular (cm) | Sediment deformation either hydroplastically or liquidized, rare microfracturing observed. | River Ganges, India (Allen 1982) | Lowe (1975); Allen (1982) |
| | | | | | |
| **Post depositional structures (upper Parent unit - mixing zone)** | Giant pillars | Metre scale, sub vertical chutes containing structureless and/or convoluted sandstones. Margins of giant pillars highlighted by dark grey clay. | Large scale sand fluidization features. Margin clay eluttrated during remobilization. | Alba Field, North Sea | Duranti and Hurst (2004) |
| | Breccia | Angular mudstone clasts (mm-cm) held in a matrix of structureless sandstone, microfractured | Remobilized and fractured depositional rip-up clasts and incorporated wall and roof mud clasts. | Alba Field, North Sea | Templeton (2002); Duranti and Hurst (2004) |
| | | | | | |
| **Clastic Injections** | Dykes | Discordant to host bedding, usually 30˚ more than bedding dip. Straight, planar, irregular, bulbous, tapering, bifurcating and carved margin geometries (Hurst et al. 2011). fluidization can lift silt-boulders grade material a range of internal characteristics are identified. | Straight dyke geometry are resultant from intrusion into planar faults. However, non planar geometries result from anisotropy in host lithologies and post intrusion folding. Hydraulic fracture is necessary (fluidization) | Various locations | Hurst et al. (2011) |
| | Sills | Often near to bedding concordant (i.e. with 30˚). A range of geometries exist, including; staggered, stepped, erosive topped and multilayered | Hydraulic fracture is necessary. Sills often form during shallow burial and emanate from dykes (Jolly and Lonergan 2002) (fluidization) | Panoche Giant Injection complex | Vigorito et al. (2008) |
| | | | | | |
| **Internal characteristics of dykes and sills** | Grading in dykes | Clast supported axially, matrix supported at margins | Indicating sorting and grading (Fluidization) | Cerro Torro Formation, Magallanes Basin, Southern Chile | Hubbard et al. (2007) |
| | Laminae | Fine to medium grained sand, wavy, inclined, parallel and folded (0.001-0.005m thick) skirting injectite margin | laminae are deformed into small folds where they cross band contacts | Yellow Creek injection complex California, USA | Hurst and Cronin (2001); Scott et al. (2009) |
| | Grain alignment | Grains and clasts flow aligned | Flow imbrication (Fluidization) | Tesnus Formation, Texas, USA | Diggs (2007); Hubbard (2007) |
| | Raft | Internal bedding, split by intrusions (0.5-1m thick and 5-7m length) | Flow imbricated, eroded from country rocks (Fluidization) | Yellow Creek injection complex California, USA | Scott et al. (2009) |
| | Mushroom structures | Parent beds | | | Surlyk et al. (2007) |
| | Pipes | Fine to medium grained sand. Vertical or steeply inclined, with faint internal laminae (0.02-0.05m diameter and 0.1m in length) | Sand fluidization features. | Yellow Creek injection complex California, USA | Scott et al. (2009) |
| | Scours | Low relief erosional feature incising into country mudstone (0.1 -0.2m length and 0.02 - 0.05 depth) | Erosional feature formed by turbulent flow rheology (corrasion process - Fluidization) | Yellow Creek injection complex California, USA | Scott et al. (2009) |
| | Breccia | | | Yellow Creek injection complex California, USA | Scott et al. (2009) |
| | | | | | |
| **External margin characteristics of dykes and sills** | Erosion and scour, scallop surfaces | In both dykes and sills | indicate of erosive turbulent flow (Fluidization) | Yellow Creek injection complex California, USA | Vigorito et al. (2008); Scott et al. (2009) |
| | Flute and Groove marks | Indentified in sandstone lenses at the margin of the intrusion (near vertical upwards) | indicate of erosive turbulent flow (Fluidization) | Cerro Torro Formation, Magallanes Basin, Southern Chile | Hubbard et al. (2007) |
| | | | | | |
| **Extrusions** | Sand extrusion & palaeoseep structures | Expelling fluid into both sub-aerial and marine environments. May provide sufficient nutrients to support biological communities (palaeoseeps). Small scale features usually under 5m in diameter although huge examples are observed in seismic data (see Andresen et al. 2010) | Represent the uppermost expression of sand fluidization, extrusion. Can be charged by lateral fluid transfer, | County Clare, Ireland; panoche Giant Injection complex | Minisini and Schwartz (2007); Jonk et al. (2007) |
| | | | | | |
| **Other features** | Heavy minerals | Enrichment or decreased concentrations of heavy minerals between injected and parent units | fluidization is known to preferential lift finer grained sands over coarser grains (Lowe 1975) enriching of heavy minerals into placer bands (e.g. Komar, 2007) | Siri Canyon, North Sea | Kazerouni et al. (2011); Hamberg et al. (2007) |
| | Angular, unweathered, extraformational clasts | Unweathered angular chalk clasts in Våle Formation (over 50m above Ekofisk Formation) | Explosive overpressure release from below chalk lithologies included chalk clasts during equilibrium. Angularity, surface texture and proximity from original formation suggest injection | Balder Field, North Sea | Briedis et al. (2007) |

Table 2.1: Characteristics of remobilized and injected sediments observed in cored section and outcrop

| Feature | Description | Interpretation | Location | Publication |
|---|---|---|---|---|
| **Reduced porosity and permeability** | Increased Sonic (DT log values) and Density (Dens) log values in combination with reduced porosity, permeability values and thin section descriptions | Tighter grain packing as result of remobilization. Thin section observation negate the chance of post depositional cementation and diagenetic reservoir quality effects. Cataclastic grain reduction is not representative of remobilization and injection (Hurst et al. 2011). | Alba Field, North Sea | Duranti and Hurst (2002) |
| **Short lived sandstones between closely spaced wells** | Bedding conformant sandstones that do not correlate between closely spaced production wells (sub 1km) | Sansdstones of this type are interpreted as sills | Balder Field, North Sea | Briedis et al. (2007) |
| **Dipmeter measurments** | Sandstones with non-depositional dips (i.e., exceeding 15˚) | Sandstones out of depositional dip are injected sandstones | Alba Field, North Sea | Lonergan et al. (2007) |
| **Thin sandstones overlying massive sandston units** | Presence of thin sandstone units overlying massive sandstones often separated by interstitial shales | Interpreted as injected dykes and sills. Care is made to incorporate other datasets as thin bedded sandstones deposited above massive sandstone units could represent waning depositional phase | Cecile Field, North Sea | Hamberg et al. (2007) |
| **Sandstones out of sequence** | Sandstones appearing in transgressive systems tract and high stand systems tracts (Depositional sequence) | Presence of sandstones in unlikely stratigraphic intervals indicate injections. The authors believe that the depositional sandstones in Balder Field have strong correlation to sequnce stratigraphic scheme (depositional sequence Catuneau et al. 2010) | Balder Field, North Sea | Briedis et al. (2007) |
| **Serrated or spiky log signature** | Serrated or spiky sand shale log signatures | Indicative of injected sandstones. It is important to use this identification method in conjunction with other techniques as log profile like this can indicate waning flow. | Alba Field, North Sea | Lonergan et al. (2007) |
| **Image logs** | Discordant bedding contacts | Similar to observations directly from cored sediments. Braccini et al. (2008) state that discordant bedding contacts are representative of injected sandstones. Image resolution and sections lacking correlation with other datasets reduce confidence. | Not stated | Braccini et al. (2008) |
| **Disconnected sandstones in pressure communication** | Isolated sandstones in regional pressure communication | Isolated sandstones can display non-regional pressures (ref). Isolated sandstones displaying some other features of injected sandstones inline with regional pressures may indicate pressure communication and therefore injection | Terttiary, Norwegian North Sea | Inferred from Bergslien (2002) |

Table 2.2: Characteristics of wireline log responses from remobilized and injected sediment intervals

| | Feature | Description | Interpretation | Alternatives | Location | Publication |
|---|---|---|---|---|---|---|
| **Architectural features** | Winged intrusions | The intrusions range from 10 to 40m thick, 50-250m vertical extent and maybe more or less continous for 1-5km laterally (around parent sandstone body). | Overpressured, fluidised sandstones fracture low permeability surrounding sediments (upwards, laterally and downwards) | Remnants of previously deposited sediments | North Sea basin | Huuse et al. (2004), Jackson (2007) |
| | Crestal intrusion complexes | Intrusions are commonly centimetre to metre scale in thickness although intrusions can intrude vertically hundreds of metres | Overpressured, fluidised sandstones fracture low permeability surrounding sediments (upwards, laterally and downwards) | Faults | North Sea basin | Huuse et al. (2007) |
| | Conicol intrusions | Intrusions can range from 100 – 2000m in diameter, 50-300m in height and 1-80m in thickness. | Overpressured, fluidised sandstones fracture low permeability surrounding sediments (upwards, laterally and downwards) | Very few have been drilled. Therefore could be artefacts in seismic acquisition/processing - gas diffraction effects | North Sea basin | Cartwright et al. (2008) |
| | Mounded bodies or Laccoliths | Steep sided mounds, can appear as part depositional remobilized parent units. Currently poorly described in North Sea literature. | Fully intruded units, that can feed dike and sill complexes | May infact be depositional bodies leading to numerous questions on depositional architecture (or lack there of) | North Sea basin; UK | Huuse et al. (2007); Kane (2010); Szarawarska et al. (2010) |
| | Parent units (steep mounds) | Originally deposited sandstones affected by differential compaction and further post depositional processes | Sandstone bodies become oversteepened through remobilization and injection | Differentially compacted (only) sandstones or mass transport complexes | North Sea basin | Huuse et al. (2004) |
| | Scalloped tops/Listric faulting | Uneven and irregular top surface intricate relationship between intrusion, extension and compaction | Complex relationship between post-depositional compaction, injection enhanced by subsequent compaction. | Faulting | North Sea basin | Hurst et al. (2005) |
| | Fluid flow conduits/Chimneys (chaotic reflector zones) | Can range from several hundred of metres to over a kilometre in width (Løseth et al. 2003). Sub-vertical representing cross stratal fluid flow and several hundred metres deep | Focussed sub-vertical fluid flow | Issues in seismic imaging | Nyegga, Offshore Mid-Norway | Løseth et al. (2003); Hustoft et al. (2010); Moss and Cartwright (2010) |
| | Polygonal faulting | Fault throws range from a few metres to over 100m. Average fault plane dips of 45°. Active during sedimentation and early burial. | Soft sediment deformation features, burial related analogous to shrinkage cracks | | North Sea basin | Lonergan et al. (1998) |
| | Extrudites | Examples are described in literature from the North Sea at many Tertiary unconformity surfaces. An exceptionally large feature 80m and 1400m long is described from Siri Canyon | Focussed fluidised fluid flow upwards (basinal fluids ?) and lateral fluid transfer. | Glacial till, present day depositional or erosion features | North Sea basin | Andresen et al. (2010); Vetel and Cartwright (2010) |
| | Seafloor pockmarks | Craters or eruption surfaces on the seabed, often circular and measure around 150m in diameter | Site of focussed fluid flow sourced from chimey below | Glacial erosion or striations. Bollide impact surfaces | Nyegga, Offshore Mid-Norway | Hustoft et al. (2010) |
| | | | | | | |
| **Basinal features** | Location above bounding faults (basin margins/active tectonism) | Yellow Bank Creek California, locates above fault network | Faults surfaces act as conduits for focussed fluid flows | | Yellow Bank Creek, California, USA | Lonergan et al. (2002) |
| | Gas hydrates | Trapped, frozen gases | | remanants from palaeo-bolide impacts | | |
| | | | | | | |
| **Seismic features** | Flat non-erosional base (Laccolith) | Flat non-erosional base (Laccolith), Volund structure | Evidence for sill like intrusion | Without drilling this feature maybe igneous | North Sea basin | Szarawarska et al. (2010) |
| | Equal mud thickness (non- Laccolith) | Equal mud thickness implies that a laccolith inflation model is not relevant | Evidence for depositional sandstones | Poor seismic imaging of top reservoir | North Sea basin | Szarawarska et al. (2010) |
| | Equal jack-up thickness (Laccolith) | Elevation of the overlying mud thickness equal to intruded sandstone volume | eviden for intrusion and inflation | | North Sea basin | Szarawarska et al. (2010) |
| | Pop-up features (chalk pop up structures) | Elevated chalk blocks above fluid flow conduits | Fracture of chalk below Balder Field due to overpressured fluids (perhaps aided by seismicity and tectonic stresses associated with burial as the field is located upon an intra-basin high | A post depositional feature assumed to indicate fluid flow. In this area chalk rafting is well known | North Sea basin | Briedis et al. (2007) |
| | Amplitude responses | Seismic inversion proved greater imaging of hydrocarbon charged sandstone injection | eviden for intrusion | | North Sea basin | de Boer et al. (2007) |

Table 2.3 : Seismic characteristics of remobilized and injected sediments

## 2.3 North Sea examples

From literature review at least 18 hydrocarbon fields in the North Sea are affected by remobilization and injection, the majority of which are deep-water sandstone reservoirs of Tertiary age.

Table 2.4 summarises 11 published hydrocarbon field examples which display the effects of remobilization and injection, 7 fields are excluded (noted at base of the table 2.4) due to a lack of data. Applying criteria described in Huuse et al. (2007) to published examples of remobilized and injected hydrocarbon fields, winged sandstone intrusions (Huuse et al. 2007) locate in the United Kingdom sector of the North Sea which was a confined slope setting during Paleocene and Eocene times (Timbrell, 1993). From literature review crestal intrusion complexes (Huuse et al. 2007) locate without pattern in both the United Kingdom and Norwegian sectors of the North Sea.

Lonergan et al. (2000) suggests that a transition from sheet geometry sandstones deposited in the Paleocene epoch to more string-like and linear geometries during the Eocene epoch favoured remobilization and injection. Isolated gully sands (Den Hartog Jaeger, 1993; Jennette et al. 2000) and isolated, ponded and sandy mounds were enclosed by low permeability mudstones (Dewhurst et al. 1999; Jordt et al. 2000) allowing overpressure to develop due to a lack of lateral or vertical pressure transfer.

| Hydrocarbon Field | Epoch | Parent Formation | Formation injected sandstones intrude | Classification - after Hurst et al. 2005 & 2007 | Classification - after Huuse et al. (2007) | Polygonal faulting | Depositional process | Depositional setting | Depositional confinement? | Publication |
|---|---|---|---|---|---|---|---|---|---|---|
| **Balder** | Palaocene/ Eocene | Lista/Sele Formation | Lista/Sele/Balder | sills and dykes with a scalloped upper surface | Crestal intrusion complex, conicol sandstone intrusions, steep sided mouonds | Present over Balder Field | High density turbidites and sand rich debris flows | Distal terminus of sand system | Minor relief, base palaeocene within chalk surface | Wild and Briedis (2010), Briedis et al. (2007) |
| **Jotun** | Palaocene/ Eocene | Lista Formation | Lista/Sele/Balder | sills and dykes with a scalloped upper surface | Crestal intrusion complex? | Unclear | High density turbidites and sand rich debris flows | Self confined channel system with compensation stacking near terminus of sand system | Limited relief focussed depo-low | Bergslien (2002) |
| **Gryphon** | Eocene | Balder Fm | Horda Fm | sills and dykes | Crestal intrusion complex / winglike sandstone intrusions | Unclear | High density turbidites and sand rich debris flows | A series of channels within an incised canyon (flow direction west to east) with some ponding and confinement against Crawford Ridge | Yes - incised channel | Newman et al. 1993: Lonergan et al. (2007) |
| **Harding** | Eocene | Palaeocene/Eocene | Balder Fm | sills and dykes | crestal intrusion complex | Unclear | Unclear | Unclear | Unclear | Unpublished |
| **Alba** | Middle/Upper Eocene | Nauchlan Mbr (Alba Fm) | Brioc Mbr (Alba Fm) | sills and dykes | winglike sandstone intrusion | Present | High density turbidites | deposited in a previously incised channel | Yes - incised channel (1-2km wide) | Lonergan and Cartwright (1999); Duranti et al. (2002) |
| **Chesnut** | Upper Eocene | Nauchlan Mbr (Alba Fm) | Brioc Mbr (Alba Fm) | sills and dykes | conicol sandstone intrusions | Present | High density turbidites | deposited in a previously incised channel | Probably, unclear from literature | Huuse et al. (2005) |
| **Hamsun** | Palaocene/ Eocene | Below Balder Fm | Eocene | inclined sill | winglike sandstone intrusion | Unclear | turbidite sandstones | Unclear | Unclear | de Wytze de Boer et al. (2007) |
| **Danica** | Early Eocene | Cromarty sandstone Mbr | Balder Fm | sills and dykes | winglike sandstone intrusion | Present | turbidite sandstones | Confined channel | Probably, unclear from literature | Szarawarska et al. (2010) |
| **Volund** | Late palaeocene/ Early Eocene | Hermod Mbr | Balder Fm | sills and dykes | winglike sandstone intrusion | Present | turbidite sandstones | Confined channel | Probably, unclear from literature | Szarawarska et al. (2010) |
| **Sleipner Øst** | Palaeocence | Ty Mbr | Lista/Sele/Balder | sills and dykes | crestal intrusion complex | Unclear | turbidite sandstones | Confined | Probably, unclear from literature | Satur and Hurst (2007) |
| **Cecile** | Palaeocene | Ty Mbr | Lista/Sele/Balder | sills and dykes, irregular body? | Crestal intrusion complex, steep sided mounds | Unclear | Turbidite sandstones | Slide scar within chalk surface | Confined channel - Siri canyon | Hamberg et al. (2007); Hamberg et al. (2005) |
| **Måloy slope** | Upper Cretaceous | Kyrre Fm | Kyrre Fm | sills and dykes | winglike sandstone intrusion | Present | High density turbidites | Slope channel | Confined incised slope channel | Martinsen et al. 2005; Jackson (2007) |

Table: 2.4 North Sea fields with remobilised and injected sediments. Fields, MacCulloch, Pyne, Grieg, Pilot, Catcher and Bruce-Beryl are not included due to a lack of published data.

## 2.4 Sequence stratigraphy

Sequence stratigraphy is used to provide a chronostratigraphic framework that allows correlation and prediction of sedimentary facies (Emery and Myers, 1996). The use of a chronostratigraphic scheme in a depositional setting where remobilization and injection is present may lead to correlation of non-related packages. But without some form of stratigraphic discrimination, comparison laterally and vertically would not be possible. The sequence stratigraphic scheme used in this study is non-high resolution and correlates with regionally significant biostratigraphic markers and regional maximum flooding surfaces.

A number of different sequence stratigraphic schemes exist, relevant for different allocyclic and allogenic conditions including genetic stratigraphic sequences (Galloway, 1989), depositional sequences (Vail et al. 1977) and transgressive regressive cycles (Embry, 1990). In this study the Galloway (1989) sequence stratigraphic model is used because it has been shown to work well in tectonically quiescent high sediment input settings (Catuneanu, 2006), characteristic of the North Sea basin during Paleocene and Eocene times (Galloway et al. 1993).

Sequences, in the Galloway (1989) sequence stratigraphic scheme require the development of a maximum flooding surface. A maximum flooding surface is defined as a surface that marks the transition from transgression to highstand normal regression manifested in a change in shoreline trajectory (Galloway, 1989). On wireline logs maximum flooding surfaces are identified as peak Gamma-ray values as coarse clastic input is reduced during transgression. This is especially clear at the basin shelf edge and further into deeper water where high Gamma-ray mudstones are deposited. Wireline logs throughout the Tertiary aged section of the North Sea basin possess a repetitive bow shaped log profile (Mudge and Bujak, 1996). Sequence stratigraphy for the Tertiary section as described in Mudge and Bujak (1994 and 1996) correlate consistently with a temporal biostratigraphic framework which provides

chronostratigraphic calibration.

A higher resolution biostratigraphic framework than Mudge and Bujak (1994 and 1996) is described in Mangerud et al. (1999) from Grane Field where Våle, Lista, Sele and Balder sequences are subdivided into 16 sub cycles. These sequences are below the seismic resolution of 3D seismic data obtained for this project and are not considered further.

Catuneanu et al. (2010), compile and review sequence stratigraphic principles. The depositional sequence (Posamentier and Allen, 1999; Van Wagoner et al. 1988) is bounded by sub-aerial unconformities and marine correlative conformity (Mitchum, 1977). When contrasted against the Galloway (1989) genetic sequence the latter does have limitations, with the inclusion of a sub-aerial unconformity within sequences contravening the notion that sequences consist of genetically related packages of strata. However the Galloway (1989) approach is applicable to sedimentation in the North Sea as the sedimentation rate was high during the tectonically quiescent Tertiary age (Den Hartog Jager et al. 1993). This prohibited base level dropping below the shelf edge and therefore incision into previous flooding surfaces is not relevant, a key discriminatory feature when applying the depositional sequence method. The Transgressive-Regressive (T-R) sequence stratigraphic scheme is defined as composite surfaces that include sub-aerial unconformities and the marine portion of the maximum regressive surface (Embry and Johannessen, 1992). Again requiring the identification of a composite (erosional or hiatal) surface making their identification more complex and less applicable.

## 2.5 Facies approach

A facies approach is used in this study similar to that described in Anderton (1995). In Anderton (1995) specific characteristics are recorded and used to catalogue packages with similar properties. Descriptive facies are defined as:

"A certain volume of rock that can be characterized by a set of features, such as grain size, geometry and structure, that distinguish it from other rock units." Anderton (1995)

Descriptive facies can also be used for classifying wireline logs and seismic data. This approach is taken for all datasets and is described in Chapter 5. Once a section is divided into facies classes interpretation is achieved either through comparison with other published examples or by combining facies that appear in association with other facies in vertical organization. Interpretation of facies is defined as:

"A label summarizing the interpretation of the processes and environments of deposition of a certain rock unit." Anderton (1995)

The Bouma sequence (Figure 2.2a) is an example of vertically organised facies associated by the waning of turbulent flow during deposition (Bouma, 1962).

## 2.6 Balder Field area

### 2.6.1 Geological models

For some years published articles on Balder Field described the mounded nature as being formed through depositional processes. E.g. Hanslien (1987) and Sarg and Skjold (1980). However Jenssen et al. (1993) and more recently Briedis et al. (2007) and Wild and Briedis (2010) assign post-depositional remobilization and injection as a potential cause for steep-sided mounds. Skjold (1980) and Sarg and Skjold (1982) both attributed the mounded nature of the Balder Field to submarine channel erosion during emplacement of mass flow sands. Hanslien (1987) interpreted mounding as being depositional in origin enhanced by differential compaction within a channelized setting. Compactional contrast is identifiable in deep-water settings as mudstones compact more than sandstones (Janette et al. 2000).

Improvements in seismic imaging lead Jenssen et al. (1993) to describe channel morphologies west of the Balder Field. Similar features were also identified by Bergslien (2002), who observed channels in Jotun Field (30km north of Balder Field) but not in Balder Field. Jenssen et al. (1993) describe sandstones found in the Balder Field as originating from the East Shetland Platform, transported to the Balder Field area by high density turbidity currents, forming thick high relief mounds. In difference to the earlier models Jenssen et al. (1993) described the mounds as being formed by a mixture of depositional process, syn-depositional processes and post-depositional processes. Describing the post-depositional processes as involving slumping, sliding and sand remobilization. A cross-section through Balder and Grane Fields is presented in Figure 2.13. More recently, Briedis et al. (2007) and Wild and Briedis (2010) suggested that that most of the mounds of the Balder Field have been affected by post-depositional remobilization. Seismic reflectors seen on reprocessed seismic data, cross cut previously biostratigraphically controlled mudstones of the Sele and Balder

Formations, correlated from well data. Therefore indicating that the some if not all of the sandstone originally termed in the Jenssen et al. (1993) model as Hermod and Balder Members may in fact originate from remobilization and injected of sandstones, originally deposited as Heimdal Member. The authors go onto suggest that most of the Paleocene mounds are located above discontinuities in the Late Cretaceous Chalk surface, erroneously interpreted previously (Jenssen et al. 1993) as detached glide blocks sourced from the East. Instead hypothesising that discontinuities in underlying Cretaceous Limestones are related to overlying mounds. Wild and Briedis (2010) suggest that episodic, catastrophic pressure release from deeper buried horizons beneath Balder Field link Mesozoic sediments to Cenozoic sediments through vertical pressure release.

Briedis et al. (2007) presents production pressure data highlighting pressure communication between vertically stacked sandstones of Paleocene to Eocene age, connected by sandstone injection (figure 2.14). This interpretation agrees with Hurst and Cartwright (2007) where sandstone injection can increase reservoir communication through improved vertical permeability. Whilst vertical communication may improve hydrocarbon recovery it may also facilitate “early” water breakthrough during production, which could conversely reduce total recoverable hydrocarbons.

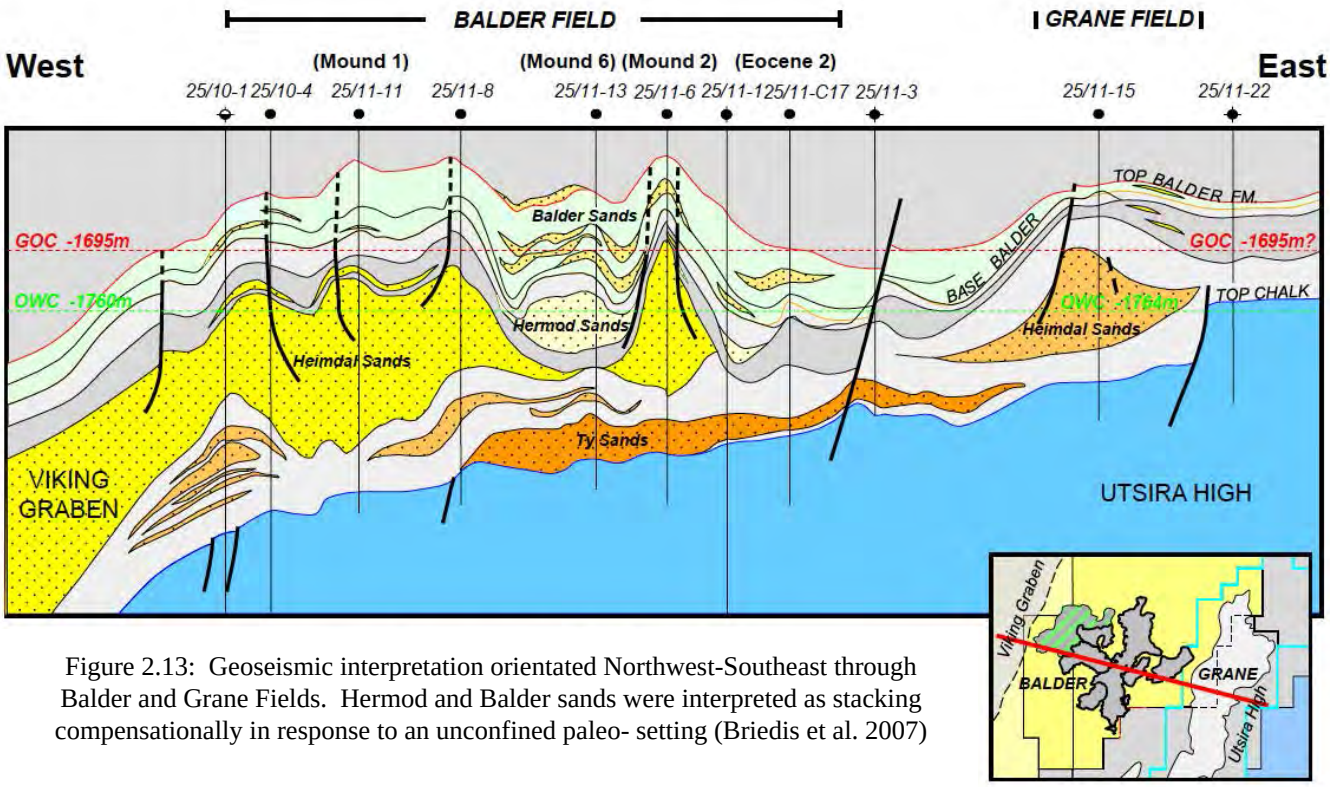


Figure 2.13: Geoseismic interpretation orientated Northwest-Southeast through Balder and Grane Fields. Hermod and Balder sands were interpreted as stacking compensationally in response to an unconfined paleo- setting (Briedis et al. 2007)

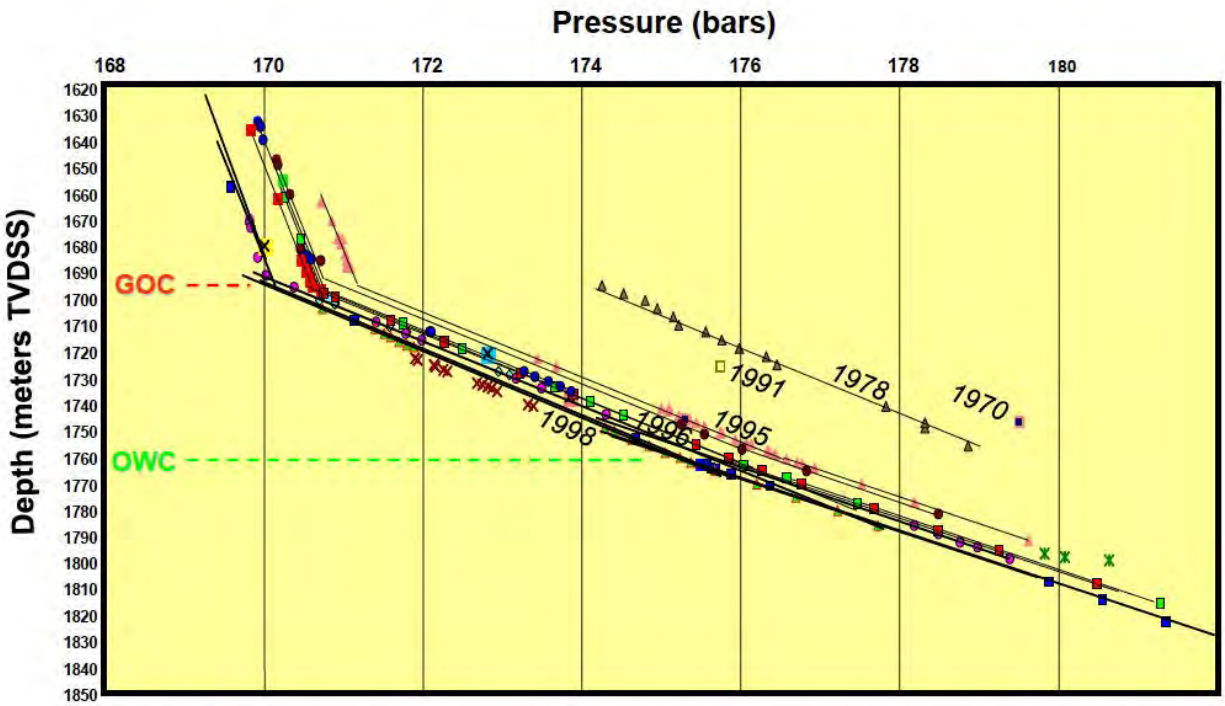


Figure 2.14: Balder Field pre-production pressures. Formation pressure measurments over a 28 year period prior to production indicate a highly connected reservoir interval (Briedis et al. 2007)

## 2.6.2 Exploration and development history:

The Central Balder Field accumulation has been explored and developed under licences PL 001 and PL 028 Balder North (Ringhorne) has been explored and developed under licences PL 027 and PL 028. The Grane Oil Field has been explored and developed under licence PL 169.

Twenty-two exploration well bores have been drilled in the Balder Field. The field has been under ExxonMobil/Esso Exploration AS operatorship since a play was first established in the early-mid 1960's. It took over thirty years from the first wildcat exploration well 11-1 entered on 19th October 1966 under licence 001 (second well drilled on the Norwegian continental shelf), to the commencement of hydrocarbon production. This long delay is attributed to stratigraphic complexities associated with mounded and injected sandstones. The discovery of significant oil (in excess of 25m continuous oil bearing sandstones) in well 25\11-5 in April 1974, was deemed a major success as the six prior appraisal wells only resulted in shows and thin pays (Skjold, 1980; Sarg and Skjold, 1982; Jenssen et al. 1993; Bergslien, 2002—From Briedis et al. 2007).

In 1979 shooting of a 3D seismic survey by Geophysical Services International, formed the basis for a seven well drilling programme from 1980-1981. Poor results lead in 1987 to a high-resolution 3D survey in 1988 by Prakla Seismos, processed by GSI. Advancements in acquisition improved the quality of the data and quelled fears of the prospects potential. The final appraisal well 25\11-19s was drilled in March 1995, initiating a five-month production test before the Plan for Development and Operation (PDO) was accepted in 1995. This consisted of 14 wells drilled from a floating drill rig, tied to a floating production, storage and offloading unit (FPSO). Delivered and installed in 1999, first production commenced on September 30, 1999 (Briedis et al. 2007). Exploration drilling north of Balder and Grane Fields commenced in April 1997. At the time of writing 12

exploration wells have been drilled into Ringhorne Field. A second PDO was submitted at the end of 1999. The field consists of several Paleocene and early Eocene oil accumulations, similar to Balder, plus a deeper Early Jurassic accumulation. Development is achieved through a permanent wellhead platform, with production sent to Balder FPSO (Bergslien, 2002).

Unlike Balder Field, Statoil Hydro's Grane Field took only four years and 4 exploration wells before a PDO was submitted to the Norwegian Petroleum Directorate (NPD). The first well 25\11-15, entered in November 1991, encountered over 45m of heavily oil stained massive sandstones. Well 25\11-18 was drilled three years later to appraise the discovery and to confirm beyond reasonable doubt recoverable oil reserves greater than 30 million cubic metres in the Heimdal Formation. Production started in 2003 and was the first field on the Norwegian continental shelf to produce heavy oil (NPD Fact Pages). Initial recovery was achieved through gas injection, and long-range horizontal production wells at the bottom of the oil zone. Several new wells are planned, most of them as multilateral wells. Water injection to improve recovery performance started in 2009.

# Chapter 3: Methodology and data

Data interpretation and analysis in this study was carried out in four sections. Initially a sequence stratigraphic interpretation (Section 3.1) was carried out using the principles described in Chapter 2. This provided a framework allowing correlation between different sequences and geographic areas. Subsequently facies analysis and interpretation of each dataset was undertaken (Sections 3.2, 3.3 and 3.4). Interpretation of facies between Balder, Grane and Ringhorne Fields were then compared.

The study area is located within Quadrant 25 (Figure 1.2, b). Ringhorne Field is situated entirely within Block 8. Well 8-10, is therefore within block 8 and was the 10$^{th}$ exploration well drilled. Grane Field is situated within block 11 and Balder Field in both blocks 10 and 11.

## 3.1 Sequence stratigraphic scheme

1. Data collection and quality checking including: Checkshot corrections, seismic well tie and wireline log data quality controlling were initially carried out. Workflows used can be found in Petrel Software Manuals (2012).
2. Sequence identification for wells with biostratigraphic information using framework described in Mudge and Bujak, 1994 and 1996.
3. Correlation between wireline logs with biostratigraphic data was achieved using Galloway (1989) correlation method. Five sequences were identified.
4. Interpretation of seismic data utilising methodology described in Galloway (1989) where onlap surfaces, toplap, unconformities are identified and used to identify sequences.

## 3.2 Cored section

In excess of 500m of cored section was viewed. Early cores retrieved from Balder Field are poorly preserved and not possible to core log. Similar poor core preservation for Ringhorne and Grane is not observed as these fields were discovered more than 20 years after Balder Field. 400m of cored section has been logged from the study area. A lithofacies scheme was devised based on observations from cored section.

## 3.3 Wireline logs

In excess of 150 wellbores have been drilled in Balder Field (Briedis et al. 2007). 33 exploration wireline log sets have been used to build a wireline log facies scheme.

## 3.4 Seismic data

One hundred and eighty seven square kilometres of 3D seismic data has been mapped. 11 seismic surfaces have been produced following interpretation techniques described in Brown (2006). A seismic facies scheme was also devised.

## 3.5 Study data

### 3.5.1 Cored section

A list of cored intervals studied is shown in Table 3.1. Core logging was carried out at the Norwegian Petroleum Directorate in Stavanger, Norway in 2007.

### 3.5.2 Wireline logs

Wireline logs available for this project are shown in Table 3.2. Cuttings and biostratigraphic information was obtained from digitised paper prints of well completion reports. Wireline logs were downloaded from Petrobank the Norwegian petroleum data archive.

Well logs are displayed using Schlumberger Petrel (v2011.2) software using scaling described in Rider (1996).

### 3.5.3 Seismic data

Full angle stack 3D seismic data entitled ‘Mega-Merge 2010’ is presented under agreement with TGS-nopec. The data set is displayed using Schlumberger Petrel (v2011.2) software using european polarity (red-blue colour bar). Red seismic response indicates an increase in acoustic impedance, blue seismic response indicates a decrease in acoustic impedance. This data set is a merge of three 3D seismic surveys of varying quality and vintage. Figure 3.1 shows a map of the seabed from the study area, two-way-time scale bar is used to highlight vertical offset between seismic surveys. A 20ms offset is seen across the Balder Field orientated North-East South-West. A similar offset is seen East-West between Ringhorne Field and Balder and Grane Fields. To aid seismic interpretation a median filter has been applied as it is beyond the scope of this project to apply vertical corrections to each seismic survey and produce new angle stacks. Median filters are described in Brown (2006)

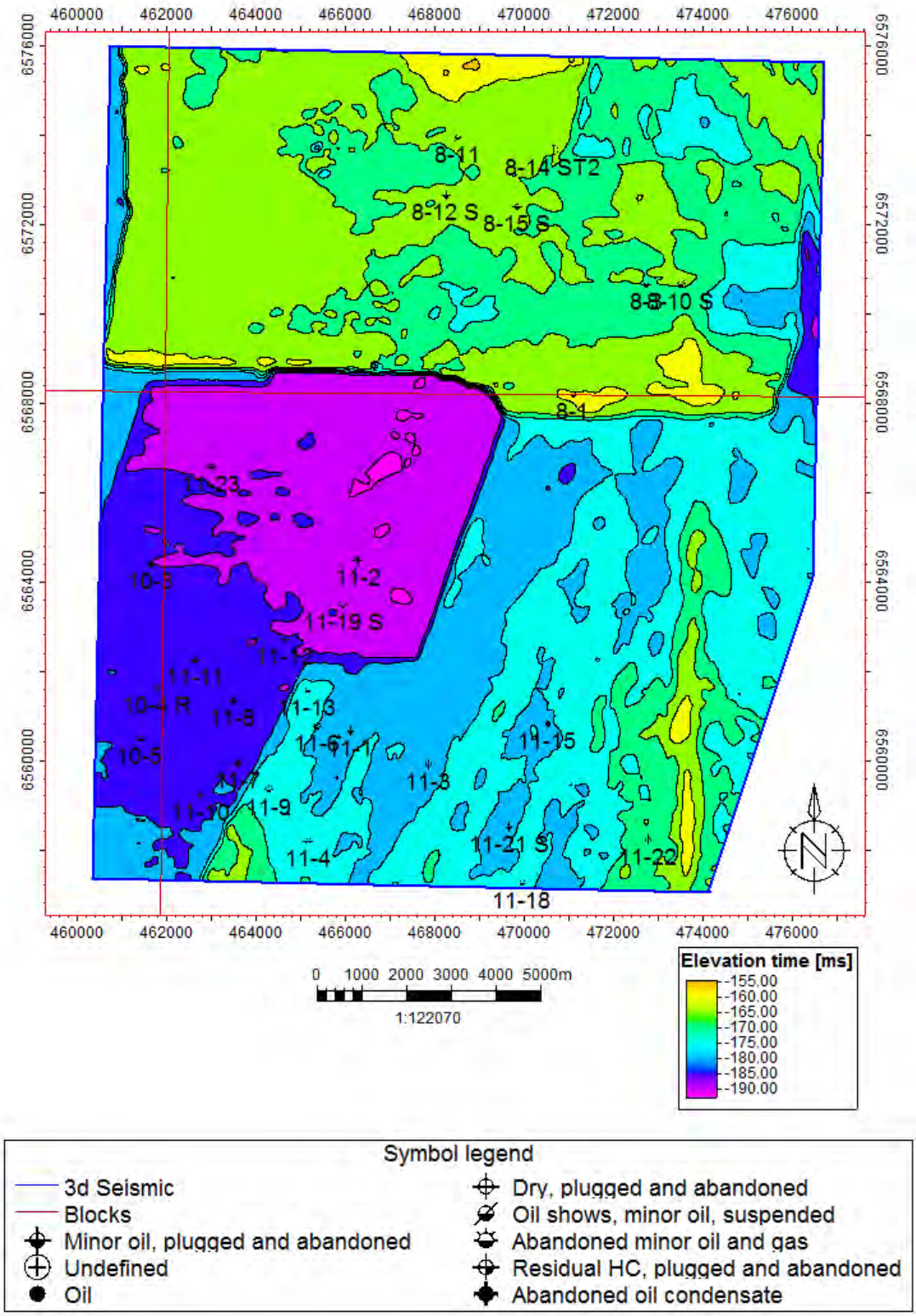


Figure 3.1: A map from seabed reflection (red trough, increase in acoustic impedence). Two-way-time shifts of between 10 to 40 milliseconds are evident indicating inaccuracies in the merge of 3D seismic datasets.

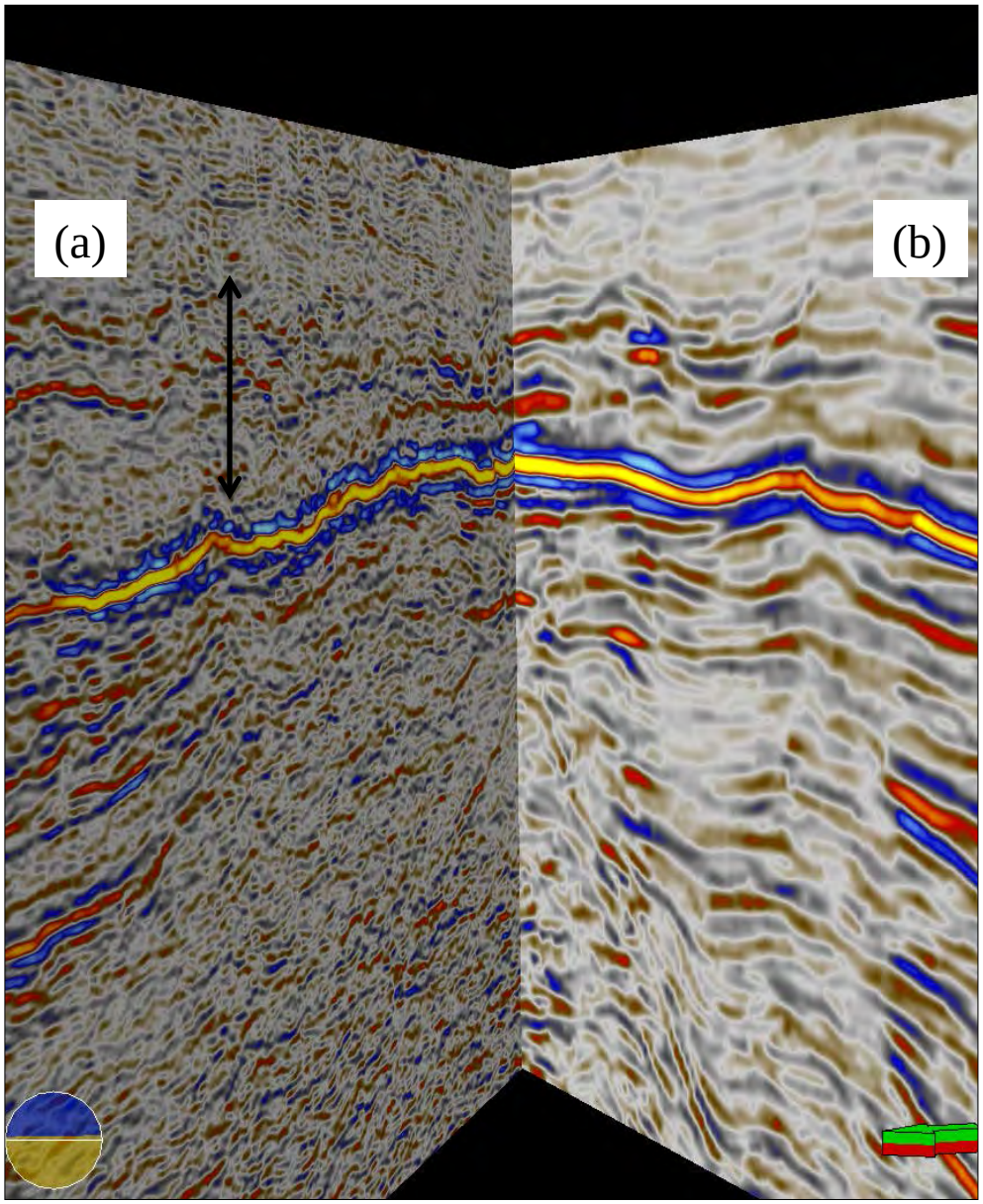


Figure 3.2: Three dimension view looking East into Balder Field. Continous blue-red-blue triple reflection is base Tertiary Limestones. Interval of interest is marked with black vertical arrow. (a) Fullstack 3D seismic data without median filter. Seismic data is noisy and reflector continuity is diminished. (b) Median filter has reduced noise and seismic reflections are more continuous. This process does attenuate some primary reflection.

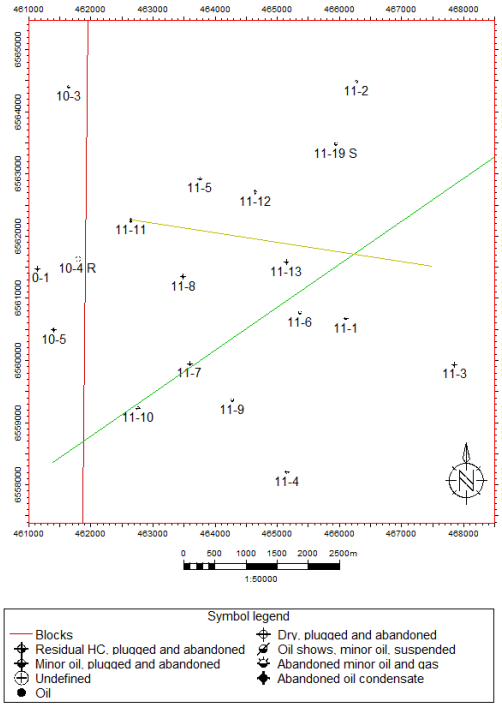

| Well | Core number | Mound name after Briedis et al. (2007) | Sequence | Recovery condition | Top Depth | Base depth | Core logged (m) | Scale logged | Core photos (NPD) | Year drilled | Comments |
|---|---|---|---|---|---|---|---|---|---|---|---|
| 25/8-1 | 2,3,4,5 | Forseti South | Lista | Poor condition | 1771 | 1786 | 15 | 1:25, 1:200 | No | 1970 | Core is poorly preserved (rubble) |
| 25/8-4 | 4,5,6,7,8,9 | Unnamed | Lista | Good condition | 1779 | 1824 | 50 | 1:25, 1:200 | Yes | 1992 | Core is well preserved |
| 25/8-10 S | 1.2 | Forseti | Lista, Sele | Good condition | 1729-1738.5 | 1766-1786 | 24.5 | 1:25, 1:200 | Photos for ST2 not S | 1997 | There are several well bores (S & ST2), S was logged at NPD, but pictures on NPD web site were taken by Weatherford of ST2 |
| 25/8-11 | 1 | Ringhorne | Sele | Good condition | 1765 | 1790 | 25 | 1:25, 1:200 | Yes | 1997 | Good condition (rare example of bedded sediments |
| | | | | | | | | | | | |
| 25/10-1 | 12.13 | M1/Unnamed | Lista | Poor condition | 1767 | 1804 | 36.5 | 1:25, 1:200 | Yes (black and white in Ft) | 1969 | Rubble |
| 25/10-5 | 2,3,4 | M1/Unnamed | Balder | Poor condition | 1738 | 1788 | 8 | 1:25, 1:200 | No | 1981 | Better preservation than 25/10-1 |
| | | | | | | | | | | | |
| 25/11-7 | 1,2,3,4 | Unnamed? | Lista | Poor condition | 1752 | 1772.5 | 20.3 more | 1:25, 1:200 | No | 1978 | Rubble |
| 25/11-8 | 2,3,4,5,6,7,8,9 | Unnamed | Lista | Poor condition | 1773 | 1793 | 25 | 1:25, 1:200 | No | 1979 | Rubble |
| 25/11-15 | 3,4,5,6,7 | Unnamed - Grane | Lista | Moderate condition | 1718 | 1798 | 80 | 1:50, 1:200 | No | 1991 | Moderate condition core has similar apperance to lower section 25/8-4 |
| 25/11-16 | 6,7,8,9,10,11,12 | Unnamed | Lista | Poor condition | 1767 | 1792 | 26 | 1:25, 1:200 | Yes | 1992 | Core is in poor condition, impregnated with a blue coloured wax or plastic during collection/preservation. Making it difficult to identify bedding contacts between lithologies |
| 25/11-19 S | 1,2,3 | Mound 6? | Lista | Good condition | | | 65.7 | | Yes | 1995 | Well preserved core |
| 25/11-23 | 1.2 | Mound 9 | Balder | Good condition | 1733 | 1765.5 | 32 | 1:25, 1:200 | Yes | 1999 | Well preserved core |

Table 3.1: Cored sections viewed at NPD core viewing facility in November 2007. Core recovery is poor for wells old than 1990 vintage. Wax lined core barrels greatly improved coring recovery and preservation after 1991.

this has increased reflector continuity and reduced the abrupt vertical time shift. It is noted that the appliance of a median filter has reduced seismic frequency (Figure 3.2) producing a dominant frequency of 35Hz with a vertical resolution of approximately 30m. The data is approximated to zero phased although inaccuracies in merging this data set complicate this.

| Well | Caliper | Gamma-ray (GR) | Sonic (DT) | Neutron porosity (Neu) | Bulk density (Rhob) | Resistivity (Res) | Synthetic seismogram | Checkshot |
|---|---|---|---|---|---|---|---|---|
| 25/8-1 | X | X | X | - | X | X | - | X |
| 25/8-3 | X | X | X | X | X | X | - | X |
| 25/8-14 ST2 | X | X | | | | | - | X |
| 25/8-11 | X | X | X | X | X | X | - | X |
| 25/8-12 S | X | X | X | X | X | | - | X |
| 25/8-4 | X | X | X | X | X | X | X | X |
| 25/8-10 S (ST2) | X | X | X | X | X | X | - | 8-3 |
| 25/8-15 S | X | - | | - | | | - | - |
| | | | | | | | | |
| 25/10-1 | X | X | X | - | | X | - | - |
| 25/10-3 | X | X | X | - | | X | - | X |
| 25/10-4 | X | X | X | - | X | X | X | X |
| 25/10-5 | X | X | X | X | X | X | - | X |
| | | | | | | | | |
| 25/11-1 | X | X | X | - | | X | - | - |
| 25/11-2 | X | X | X | - | | X | - | - |
| 25/11-3 | X | X | X | - | | X | - | X |
| 25/11-4 | X | X | X | - | | | - | X |
| 25/11-5 | X | X | X | X | X | X | - | X |
| 25/11-6 | X | X | X | X | X | X | - | X |
| 25/11-7 | X | X | X | X | X | X | - | X |
| 25/11-8 | X | - | - | - | | | - | X |
| 25/11-9 | X | X | X | X | X | X | - | X |
| 25/11-10 | X | X | X | X | X | X | - | X |
| 25/11-11 | X | X | X | X | X | X | - | X |
| 25/11-12 | X | X | X | X | X | X | - | X |
| 25/11-13 | X | - | - | - | | | - | - |
| 25/11-14 S | X | - | - | - | | | - | - |
| 25/11-15 | X | X | X | - | | X | X | X |
| 25/11-16 | X | X | X | - | | | - | - |
| 25/11-18 | X | X | X | - | | | - | X |
| 25/11-19 S | X | X | X | - | | | - | X |
| 25/11-21 A | X | X | X | - | | | - | X |
| 25/11-22 | X | X | X | - | | | - | X |
| 25/11-23 | X | X | X | - | | | - | X |

Table 3.2: Wireline log datasets used in this project obtained from Petrobank (NPD). Basic log analysis corrections have been applied including Gamma-ray and Sonic log de-spiking.

# Chapter 4: Sequence stratigraphic scheme

## 4.1 Biostratigraphic framework

Biostratigraphic data for wells 8-4, 11-17, 11-16 and 11-18 was obtained from Petrobank. The interpretation of biostratigraphic data used here is similar to that described in Mudge and Bujak (1994 and 1996), where dinoflagellate cysts, planktonic and benthic foraminifera, radiolarian, diatoms and pollen presence (Mudge and Bujak 1996) are seen regionally in the North Sea to correlate with bow shaped log responses culminating in Gamma-ray peaks, which are interpreted as maximum flooding surfaces (sensu Galloway, 1989). A type well example is shown in Figure 4.1. This scheme is based on last occurrence or last abundance events of one or more taxa or dinocysts as sample material is collected from ditch cuttings (Mudge and Bujak, 1996). Ditch cuttings carry a greater uncertainty range (metres) than samples from cored section or side-wall cores, because of the time delay retrieving samples from drill bit up to the mud shakers on the drill floor. Using this scheme five sequences are identified from Early Paleocene Danian to Early Eocene similar to the sequences identified in Mudge and Bujak (1994 and 1996). Figure 4.2 shows well 8-4 with biostratigraphic interpretation correlated to nearby wells.

## 4.2 Wireline sequence stratigraphic framework

Interpretation of wells without biostratigraphic data was achieved using techniques described in Galloway (1989), described in Chapter 3. Wireline logs were interpreted using a coarsening, aggrading or fining approach described in Emery and Myers (1996). Sequence definitions are defined by Mudge and Bujak (1994 and 1996). A collection of interpreted wireline logs can be found in Appendix 4 and sequence boundary tops in tabulated format can be found in Appendix 2a..

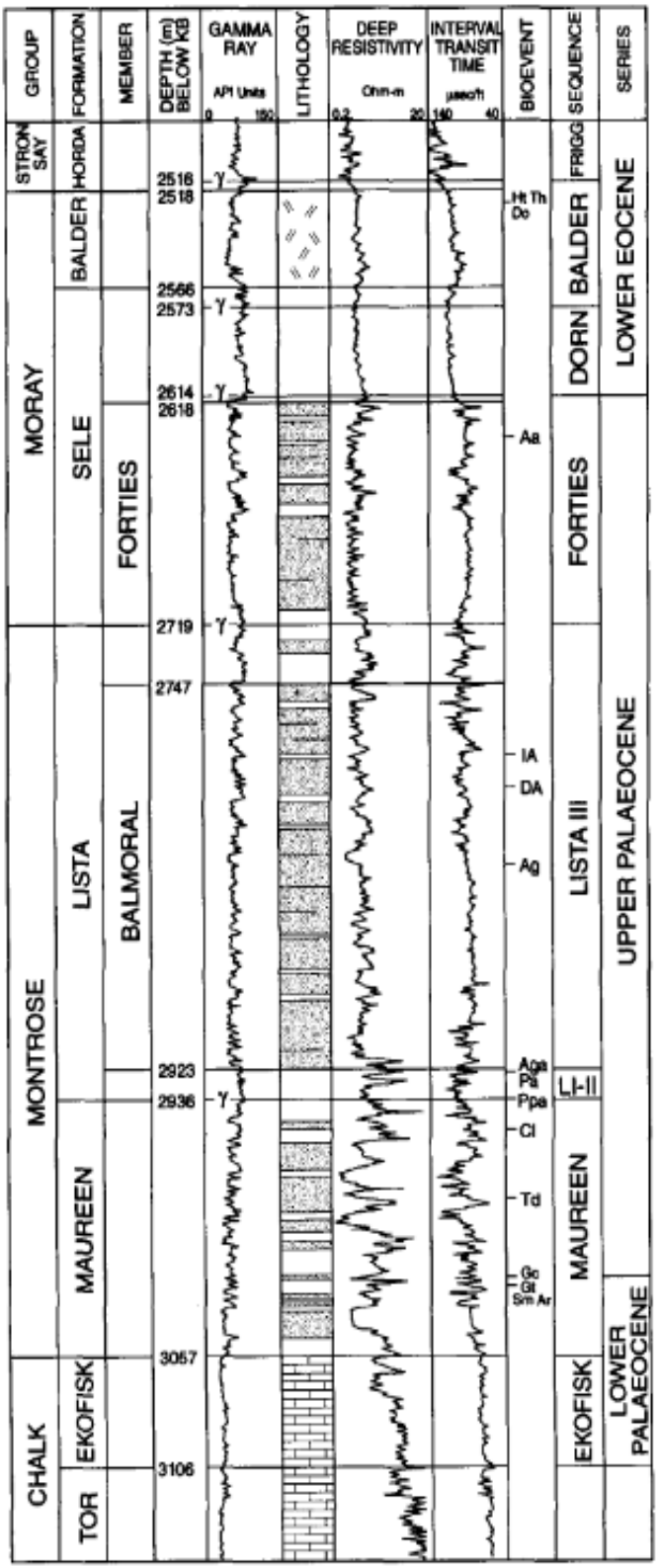


Figure 4.1: Paleocene reference well 22/8a-2 UK sector. Characteristic bow shaped wireline log profile. Maximum flooding surfaces are picked on gamma-ray peaks, which represent sequence boundaries, from Mudge and Bujak, (1996).

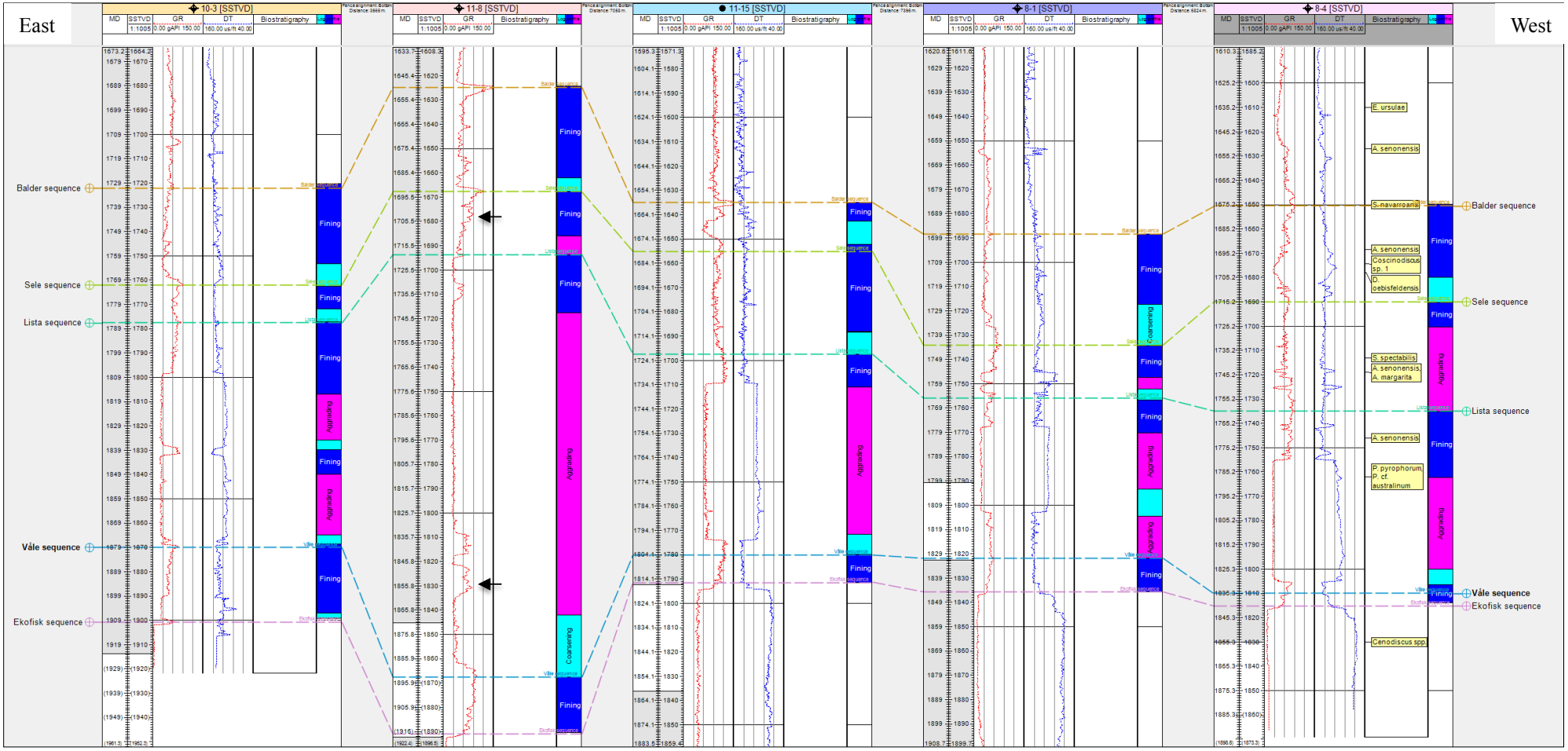


Figure 4.2: Well log correlation East to West from well 25/8-4 with biostratigraphic data. Above Ekofisk sequence four fining upwards cycles are interpreted as sequence boundaries. Identification of Balder and Sele sequence boundaries are usually clearly observable. However, Lista sequence boundary can be ambiguous. Lista sequence in well 25/11-8 could be placed higher (upper black arrow) or lower (lower black arrow) as above both gamma-ray peaks a decrease in gamma-ray log values is observed. The Lista sequence represents a highly aggradational package with weakly defined or short lived fining upwards trends typical of waning turbulent gravity flow.

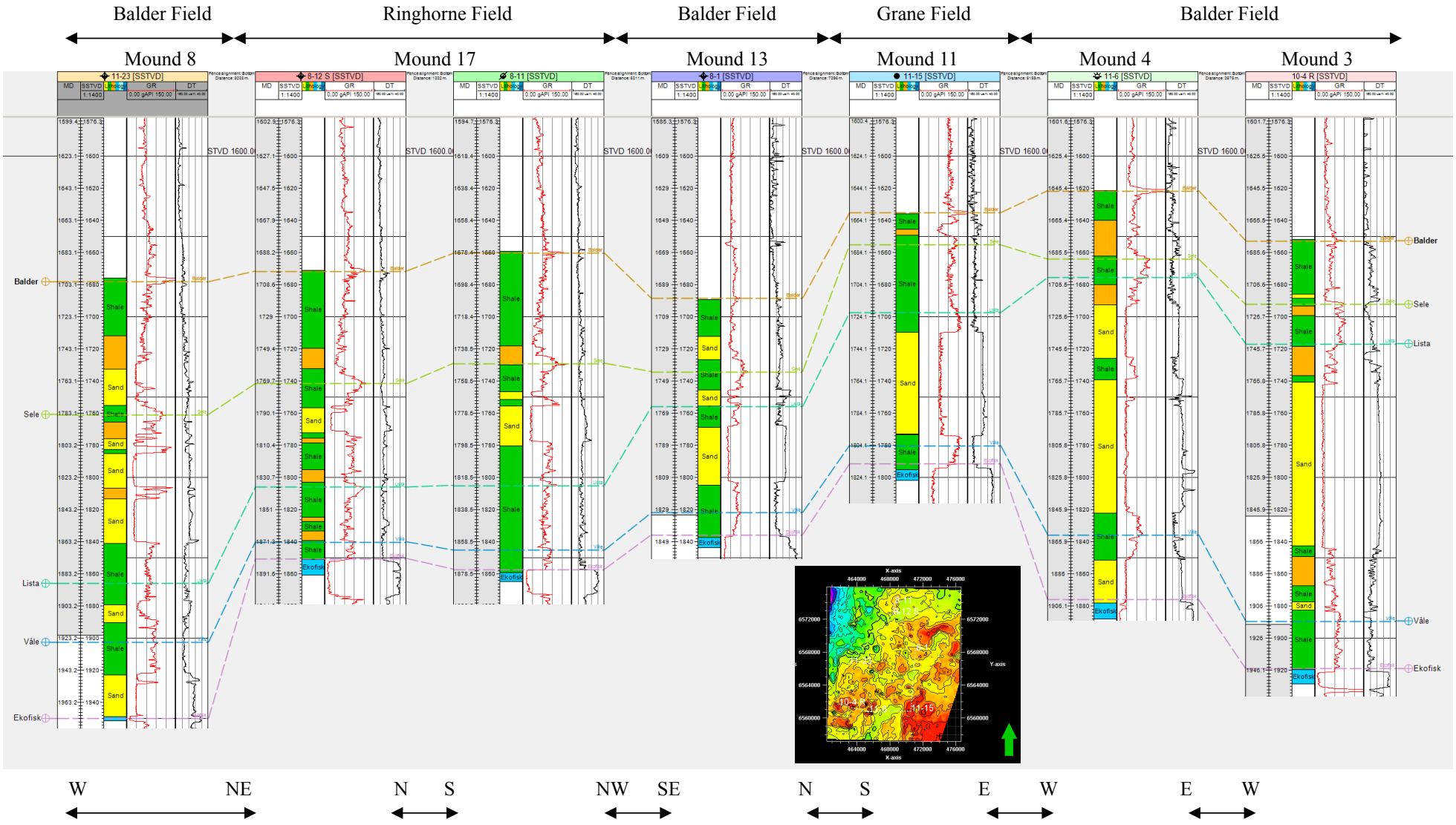


Figure 4.3: Well log correlation from the North western flank of the Balder Field North through Ringhorne Field, South through Grane Field and from East to West across Balder Field. Våle and Balder sequences thin from West to East onto the Utsira High. Sele sequence is thickest (110m) on the Northwestern flank of the Balder Field and in the Ringhorne Field (75m) and thins to less than 10m in central Balder Field. A thick (160m) package of Lista sequence is developed in Balder Field thinning North in Ringhore Field (c.40m).

A regional cross section is shown in Figure 4.3, which describes general sequence thickness trends. Balder and Våle sequences thin from the West of the study area, East onto the Utsira High. Whereas, Lista sequence is thickest and contains most sand in the Balder Field and Sele sequence is thickest in the Ringhorne Field.

Identification of sequences in Ringhorne and Grane Fields was relatively straightforward following the approach described in Mudge and Bujak (1994 and 1996). However, in Balder Field complications arose especially when several sand packages where present or where identification of a maximum flooding surfaces was unclear, an example of this is shown in Figure 4.2. The definition of the Lista sequence boundary states that the maximum flooding surface should be placed at the top of a fining package after Våle sequence. In Well 11-8 Using this criterion the Lista sequence boundary would be placed at the lower black arrow shown in Figure 4.2. This would place the blocky sandstone section between 1690-1830m TVD SS into Sele sequence. The surrounding wells do not contain sandstones of this younger sequence. Therefore, well 11-8 is interpreted based on observations from surrounding well penetrations and observations from 3D seismic data. Caused by either a poorly defined maximum flooding surface, multiple pulses of sandstone deposition or remobilization and injection.

Another example of correlation difficulty in Balder Field is shown in wells 10-1 and 10-4R which are 671m apart and locate in the west of Mound 3 (Figure 4.4). Well 10-4R contains a single 100m thick blocky sandstone within the Lista sequence whereas three 25m thick blocky sandstones are seen in well 10-1 to the South-west. Rapid lateral variation in sandstone thickness is observed between these two wells without indication (from wireline logs) of a change in grain size. As described in Chapter 2 these observations can be caused by depositional architecture (channel and overbank facies), depositional processes (debritic versus turbulent deposition) or post-depositional remobilization (homogenization).

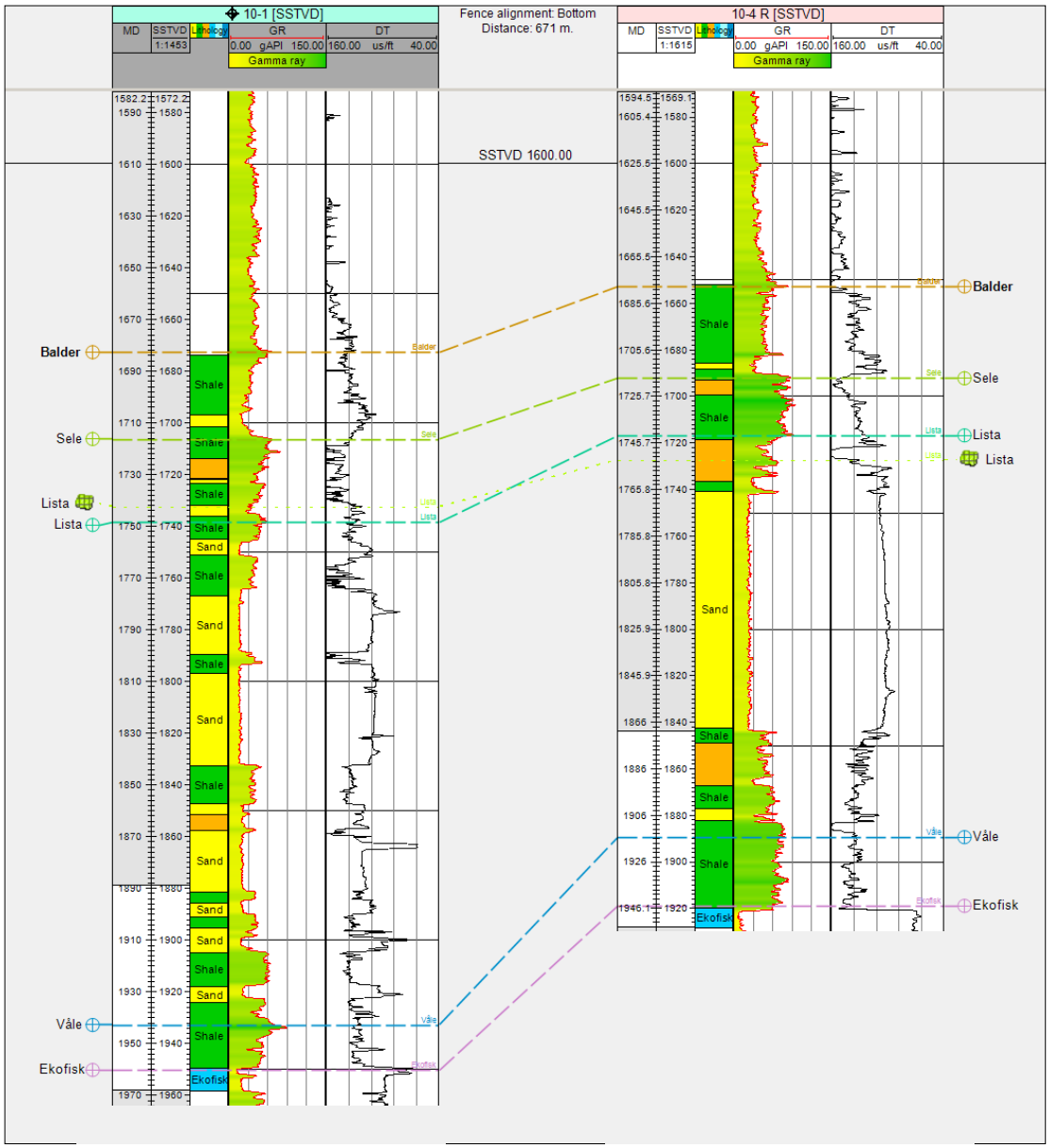


Figure 4.4: Well correlation between wells 10-1 and 10-4R showing lateral variability of Lista sequence sandstones in Mound 3 of the Balder Field area.

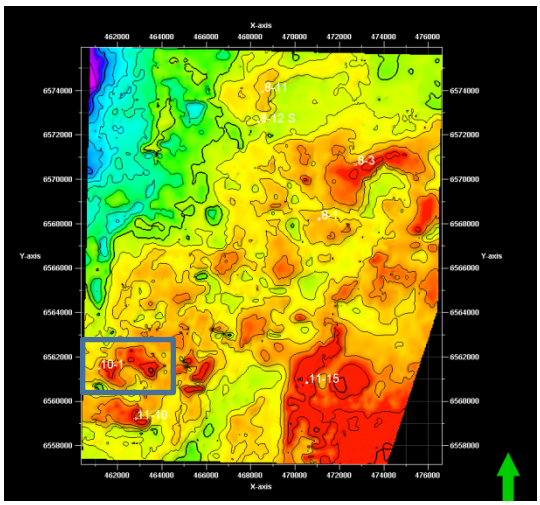

## 4.3 Seismic sequence stratigraphic scheme

Seismic reflections were picked, initially, independently of other datasets. Identification of downlapping reflections, erosional surfaces and onlapping reflections allowed stratigraphic division. The techniques employed are described in Vail et al. 1977, however the interpretation of packages follows Galloway (1989) methodology (Figure 4.5). Two-way-time maps are shown in Appendix 5.

Results showed that whilst the interval of interest is highly mounded and irregular several seismic reflections are prominent and continuous throughout (figure 4.6). Furthermore, once correlated with well log data continuous reflections correlated reasonably with interpreted sequence boundaries from well logs. In total 11 seismic reflections were identified 5 of which correlate to maximum flooding surfaces identified in wireline logs (Table 4.1), this process was unproblematic for Ringhorne Field and a repetitive package of seismic reflections are observed in Grane Field. Within central Balder Field the majority of wireline log to seismic correlation is reasonable although discrepancies do occur. Figure 4.7 shows blocky sandstones interpreted from wireline log correlation to be of Sele sequence, whereas seismic mapping suggests that this sandstone interval is of Lista sequence.

Correlation between seismic (time) and well log (depth) domains was achieved by seismic-well-tie (Petrel Software Manual), Figure 4.8. Hydrocarbons are present in Lista, Sele and Balder sequences, in well 11-15 and from full stack Mega Merge 3D seismic data, hydrocarbon bearing zones do not appear to produce a unique acoustic response. Only Well 11-16 was water bearing at Lista, Sele and Baler levels but Density logs are not available. It is acknowledged that with out modelling hydrocarbon and brine fluid effects for well logs and reflected angle stacks the current seismic interpretation may not accurately represent reservoir geometry.

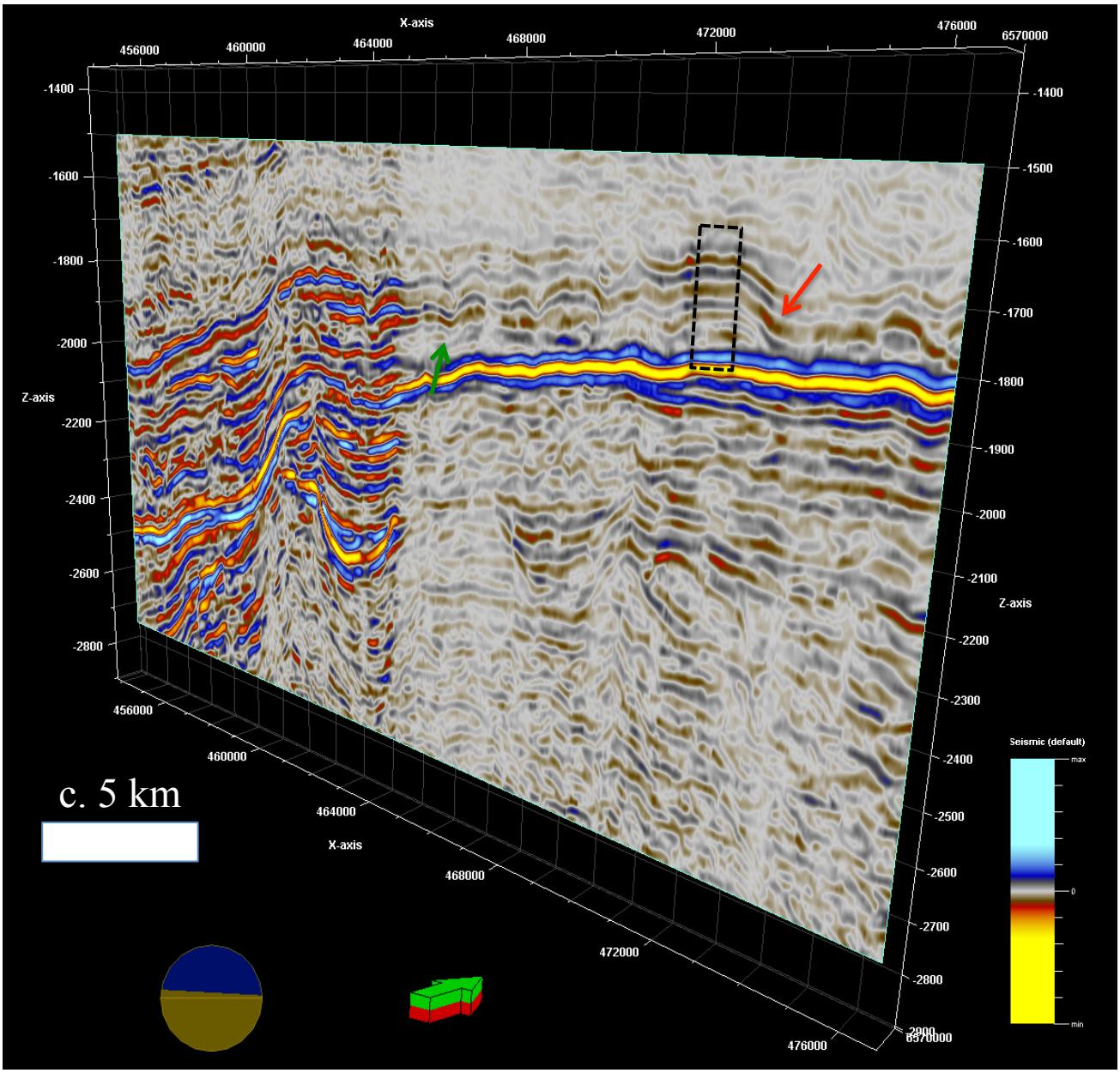


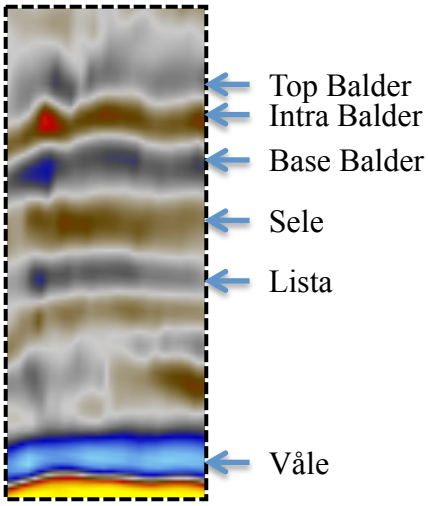


Figure 4.5: Vertical two-way-time section West to East through northern Balder Field (green line inset location map Figure 4.3) looking North- West. Key seismic reflections are readily observable. Red arrow indicates possible downlapping reflections. Formed by either depositional process or remobilization and injection has increased reflector dip angle. Green arrow highlights onlapping reflections within Lista sequence.

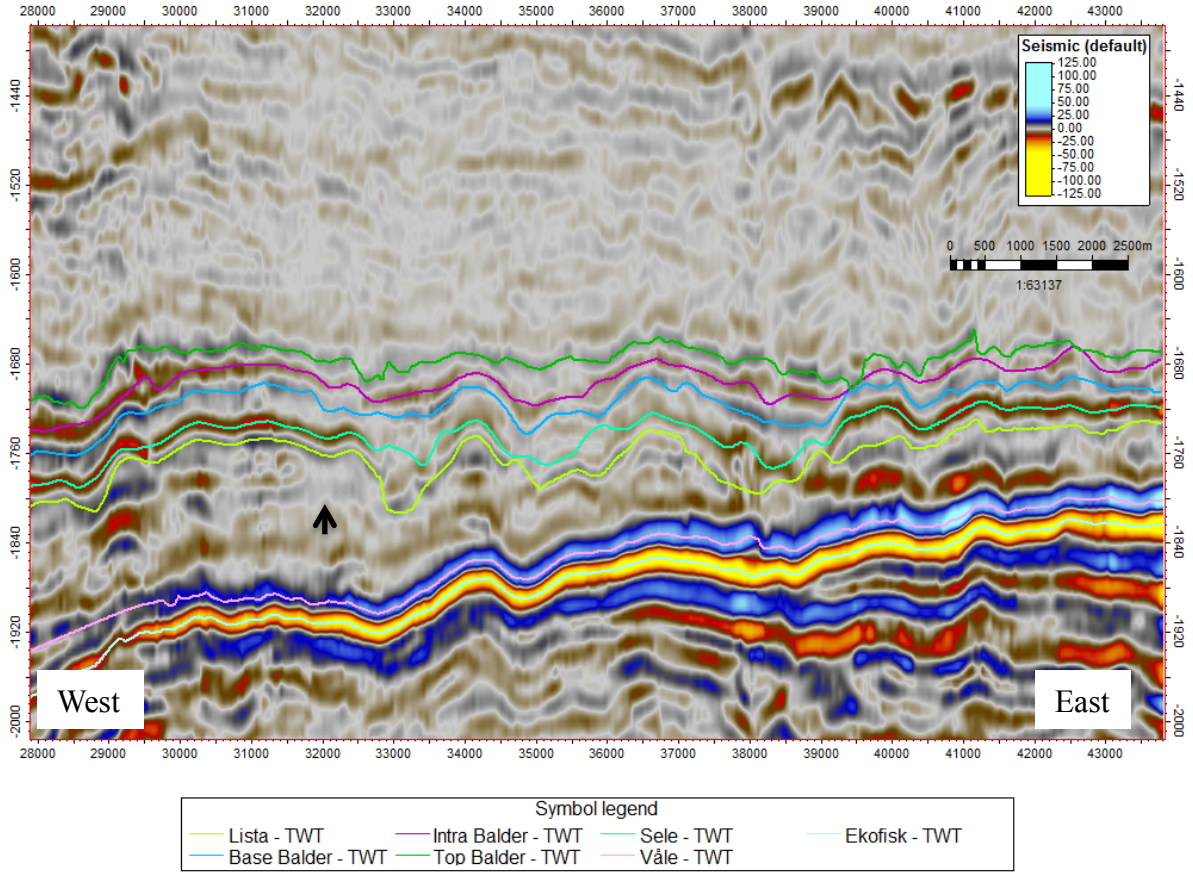


Figure 4.6: Vertical two-way-time section West to East through northern Balder Field (green line inset location map). Seismic chronostratigraphic surfaces are shown (coloured). An irregular mounded upper surface is characteristic of Lista sequence, however a peak seismic response (decrease in acoustic impedence) is identifiable throughout Balder and Ringhorne Fields. In Grane Field this seismic reflection is less clear. Toplapping seismic reflections are identified within upper Lista sequence (black arrow).

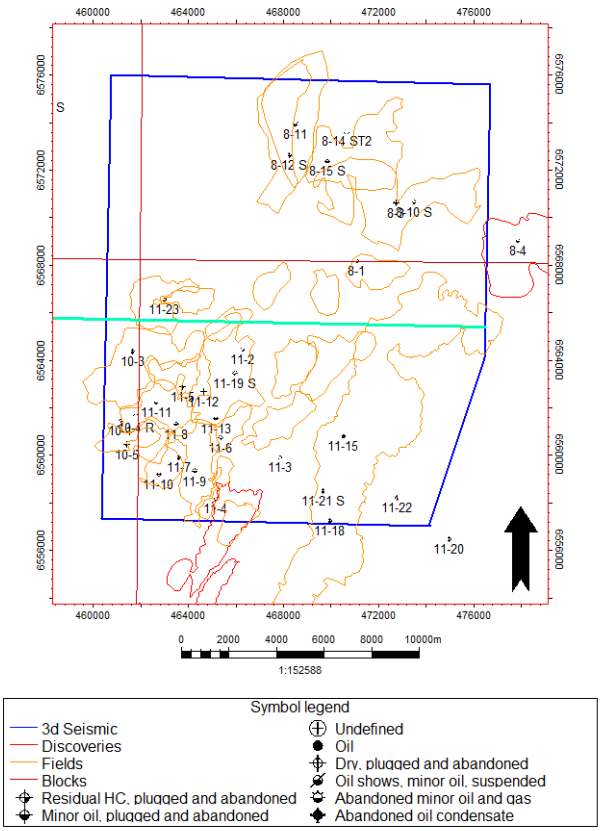

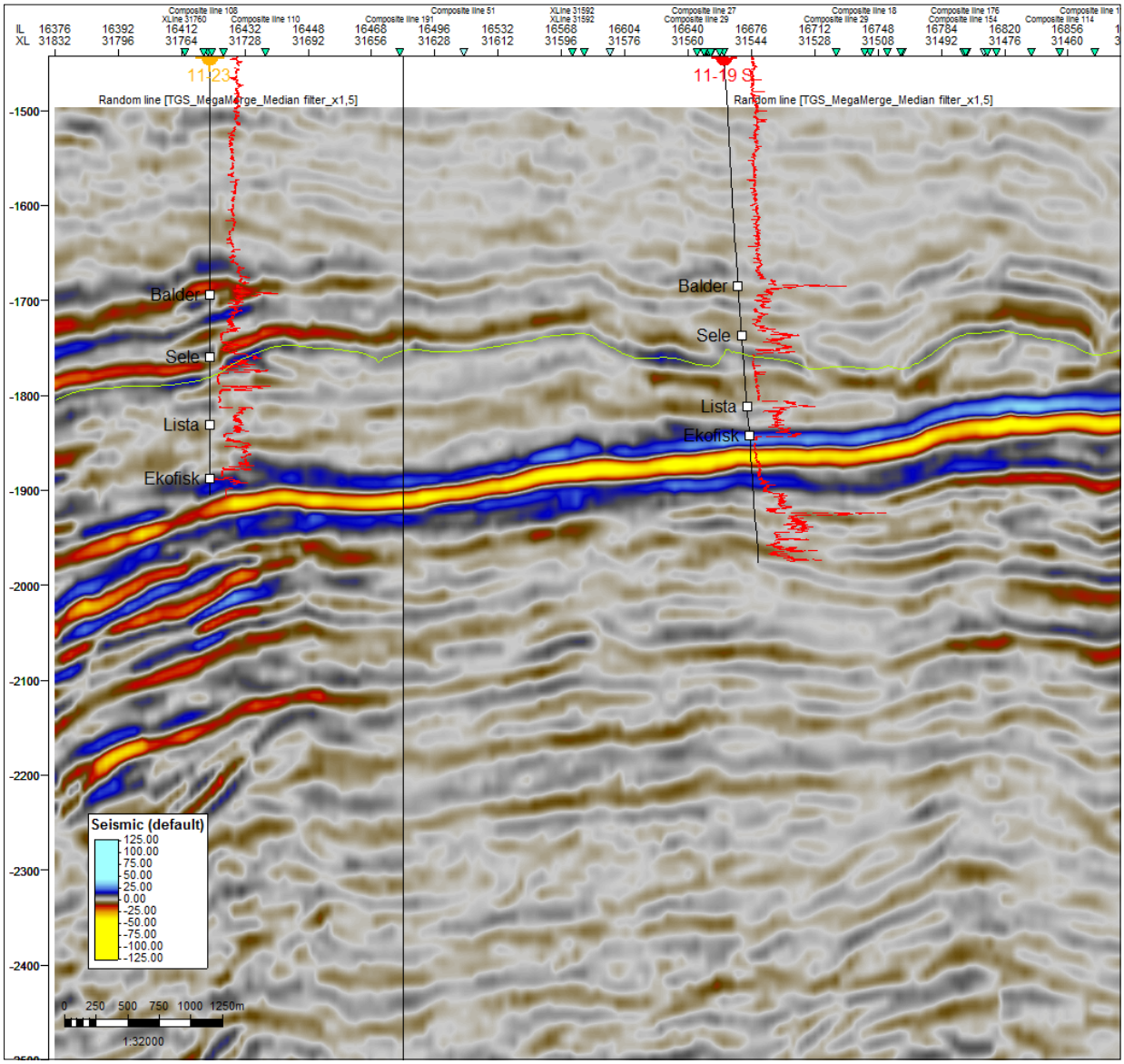


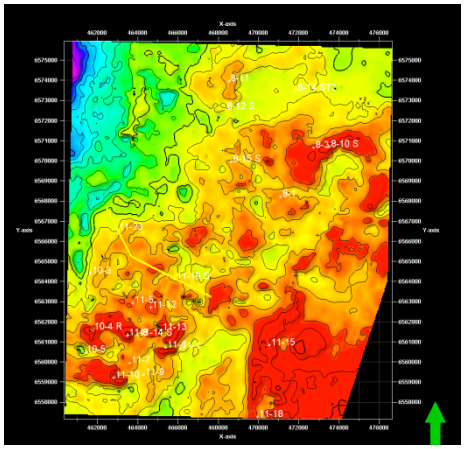

Figure 4.7: Composite seismic section highlighting mis-match between Lista sequence surface in wells 11-23 and 11-19S and interpreted seismic surface.

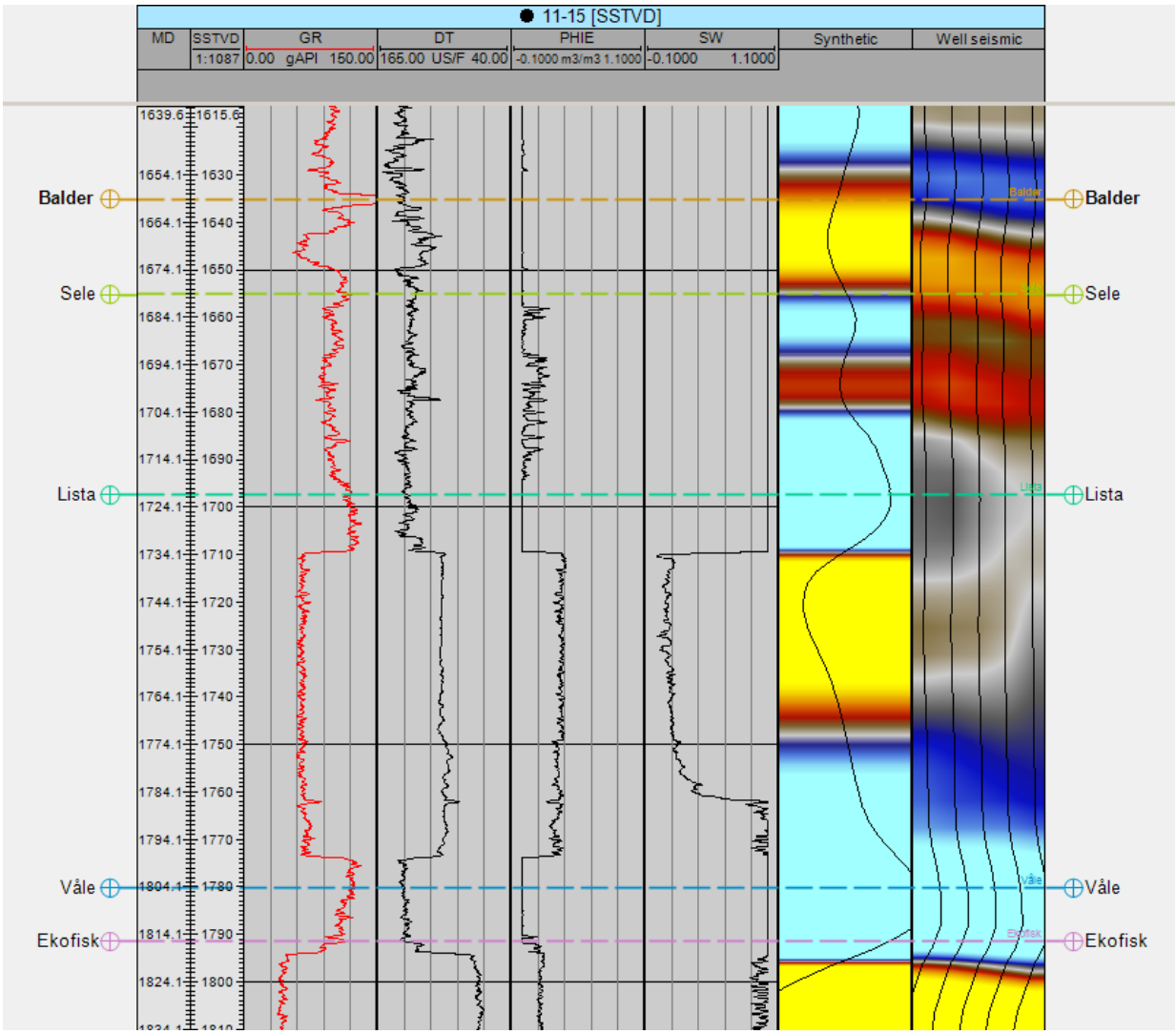


Figure 4.8: Synthetic seismogram of well 11-15 located in Mound 11 in Grane Field. Calculated acoustic response is shown next to actual seismic response at the well location

| Stratigraphic sequence (Mudge and Bujak, 1996) | Seismic sequence (this study) | Pick characteristics | Pick polarity | confidence in pick | Lithology interface | Autotracking |
|---|---|---|---|---|---|---|
| Balder | Top Balder | Decrease in Acoustic impedence | Positive values | Moderate | Mudstone overlying low content sandstone | 2d |
| Balder, Dornoch | Base Balder | Decrease in Acoustic impedence | Positive values | Moderate | Interbedded sandstones and mudstones | 2d |
| Dornoch, Forties, Lista 111b, Lista 111a | Top Sele | Increase in Acoustic impedence | Negative values | Moderate to high (Ringhorne). Low over central Balder and Grane Fields. | Mudstone overlying sandstone | 2d/3d |
| Lista 11, Lista 1b, Lista 1a | Top Lista | Decrease in Acoustic impedence | Positive values | Moderate to high (Ringhorne). Low central Balder and Grane Fields. | Mudstone overlying sandstone | 2d |
| Maureen 11, Maureen 1 | Top Våle | Decrease in acoustic impedence | Positive values | Moderate | Mudstone | 2d |
| Ekofisk | Ekofisk | Increase in Acoustic impedence | Negative values | High | Mudstone overlying chalk | 3d |

Table 4.1: Characteristics of interpreted seismic horizons

# Chapter 5: Facies schemes

## 5.1 Cored section lithofacies

A series of descriptive lithofacies are described based on bedding nature, sedimentary structures, textural attributes and composition (Stow, 2007). A genetic facies interpretation (Anderton, 1995) is achieved by associating observations with other similar published examples. Table 5.1 describes in detail the sedimentological characteristics of identified lithofacies. Sediments are sub-divided into primary and secondary classification as discussed in Chapter 2.

Sub-division of soft-sediment deformation is based on size of deformation structure, either small scale (up to 10cm) or large scale (over 10cm). Or based on mechanism of deformation, producing either Loading structures (L) or Post-depositional structures (P), and require a host lithofacies presence. Sandstone dykes and sills are independent lithofacies in this scheme.

The term lamination refers to sedimentary units of 1cm thickness and under and bedding refers to sedimentary units of 1cm to several metres. Other terms such as planar, sub-planar and so on follow terminology described in Stow (2007). Two examples of corelogs are shown in Figures 5.4 and 5.5 and a complete collection of corelogs are included in appendix 3.

| | Code | Dominant lithofacies | Percentage of Sand (%) | Percentage of Silt (%) | Grain size (sand grains) | Grain roundness | Sorting | Grading (sand grains) | Mudstone clasts | Sedimentary structures | Colour | Beding contacts | Bioturbation Type | Bioturbation intensity | Cementation |
|---|---|---|---|---|---|---|---|---|---|---|---|---|---|---|---|
| **Primary lithofacies** | LM-CS | Laminated mudstones (upto 1cm) | 0-10% | 0-10% | N/A | N/A | N/A | N/A | Absent | Planar to sub-planar lamination | Dark grey, grey green to green and blue | Concordant basal contacts, concordant upper contacts | Zoophycos, Helminthoida, | moderate to high | Ocassional calcite cementation |
| | LSL-CS | Laminated siltstones (upto 1cm) | 0-50% | Over 50% | N/A | N/A | N/A | Normal | Absent | Planar laminated, uncommon wavy lamination | light yellow and brown | Usually sharp lower contact, with gradational upper contact | Zoophycos | high | Calcite cemented horizons |
| | BS-CS | Bedded sandstones (upto 3+m) | Clean (100-80%), silty (80-50%) | Upto 20% | Fine to medium, occasionally coarse | Sub-angular to sub-rounded | Moderately sorted to well sorted. | Normal to scattered. Basal inversion | Lithofacies MB present, basal and near top surface | Planar, wavy, cross, trough cross. | Light grey, grey, light yellow. Brown to dark brown when oil stained | Erosional-irregular sharp basal contact. Sharp to gradual upper contacts | Absent | Absent | Ocassional calcite cementation |
| | MS-CS | Massive sandstones (upto several metres) - without dewatering structures | Clean (100-80%), silty (80-50%) | Upto 20% | Fine to coarse | Sub-angular to Rounded | moderately to well sorted | Normal (basal inversion) | Weak indications of basal breccia clasts, more commonly rounded floating mud clasts | Planar, wavy. Uncommon slump structures | Light grey, grey, yellow, light brown. Brown to dark brown when oil stained | Usually sharp lower and upper contacts | Absent | Absent | Ocassional calcite cementation |
| | | | | | | | | | | | | | | | |
| **Secondary lithofacies** | DTS-CS | Sandstone dykes (mm-m) | variable | Less 10% | Fine to medium | Sub-angular to Rounded | Well sorted to poorly sorted | Normal to inverse and scattered | Normal, inverse and scattered | Dish structures, convoluted laminae, pipe structures | Light grey, grey, yellow, light brown. Brown to dark brown when oil stained | Dykes crosscut bedding surfaces (more than 30˚). | Absent | Absent | Calcite and carbonate cements |
| | SST-CS | Sandstone sills (mm-cm) | variable | Less 10% | Fine to medium | Sub-angular to Rounded | Well sorted to poorly sorted | Normal to inverse and scattered | Normal, inverse and scattered | Dish structures, convoluted laminae, pipe structures | Light grey, grey, yellow, light brown. Brown to dark brown when oil stained | Sills are mostly bedding concordant upto 30˚ | Absent | Absent | Calcite and carbonate cements |
| | MCB-CS | Mudstone-clast breccia (cm-m) | variable | Less 10% | N/A | Matrix Sub-angular to sub-rounded | Matrix moderately to poorly sorted | Clasts aligned normally to inverse | Normal, inverse and scattered | Clast imbrication. Mudstone rip up clasts remobilized rounded. Injected country rock clasts angular. | Dark grey to dark brown | Usually floating within sandstone matrix, although clast support is observed | Absent | Absent | N/A |
| | L-CS | Small scale deformation structures (under 10cm) in massive sandstones | Clean (100-80%), silty (80-50%) | Upto 20% | N/A | Sub-angular to Rounded | Weak (finer grains in axis of structure) | N/A | N/A | Water escape cusps, load casts, ball and pillow, convolute laminations | Outlined by elutrated clays, sandstones often strongly stained brown from oil | Often sharp | Absent | Absent | N/A |
| | P-CS | Large scale deformation structures (over 10cm) in massive sandstones | Clean (100-80%), silty (80-50%) | Upto 20% | N/A | Sub-angular to Rounded | Well sorted to poorly sorted | N/A | N/A | Dish/pillar structures | Outlined by elutrated clays, sandstones often strongly stained brown from oil | Often sharp at high angle (more than 40˚) | Absent | low | N/A |

Table 5.1: Cored section facies characteristics

## 5.1.1 Primary lithofacies

### 5.1.1.1 Laminated mudstone (LM-CS)

Planar and sub-planar laminated mudstones with concordant upper and lower lamination boundaries comprising 80% or more mudstone content throughout. Mudstones vary in colour from light grey, grey, dark grey, light blue, light green and dark green and buff colours. Often fissile, although hard composition is not uncommon especially in blue and green mudstones. Trace fossils Zoophycos and Helminthoida are often common in green to blue grey mudstones. Nodules are also present in the form of Cone-in-cone (5cm to over 15cm) and siderite nodules (1cm to over 8cm)

Laminated mudstone lithofacies are interpreted as Te sequence (Talling et al. 2012) deposited by turbidity currents. No attempt has been made to differentiate hemipelagic and turbiditic mudstones. Trace fossils indicate palaeowater depths of 200-2000m (Stow, 2007). Cone in cone features are typical in organic rich mud rocks and represent calcite cemented nodules (Carstens, 1985). Occasional siderite nodules represent iron reducing conditions. Colours of green and blue to grey and dark grey infer a mudstone with organic content and increasing reduction of iron oxidation state. An example is shown in figure 5.1.

### 5.1.1.2 Laminated siltstone (LSL-CS)

Planar and wavy laminated siltstones. Sharp basal surface contacts grading normally upwards. Grey, yellow brown and brown colours. Commonly hard with indications of cementation (non-calcareous). Fossils are not observed.

Laminated siltstone lithofacies is interpreted as Td sequence (Talling et al. 2012). Sharp basal contacts imply moderate transportation energy. Non calcareous cementation was probably formed during lithification and diagenesis. An example is shown in figure 5.1.


Figure 5.1: Four examples of primary sedimentary facies. (a) Limited to devoid of sedimentary structures. (b) Weakly bedded sandstone with oil stain. (c) Laminted siltstones dark bands are composed of mudstone. (d) Laminated mudstones, minor amounts of siltstones are observed (lighter colours).

### 5.1.1.3 Bedded sandstone (BS-CS)

Planar, wavy and cross laminated structures are observed in sandstones of fine to medium sand grain size that is moderately to well sorted and grade normally upwards. Sandstones are commonly quartz grain dominated. Grey, yellow brown and brown colours are observed. Commonly hard with indications of cementation (non-calcareous). Fossils are not observed.

The presence of bedforms indicates turbulent flow (Baas, 2004) bedded sandstone lithofacies are interpreted as Tb sequence (Talling et al. 2012). Sharp basal contacts and absence of fossils imply moderate transportation energy. Non calcareous cementation was probably formed during lithification and diagenesis. An example is shown in figure 5.1.

### 5.1.1.4 Massive sandstones (MS-CS)

Occasional very weak bedding structures (planar and cross bedding) may be observed in sandstones of fine to coarse grainsize, which are often poorly sorted, containing lithic fragments.

Massive sandstone lithofacies can originate from both turbulent and laminar flow (e.g. Ta and Dvcs sequences, Talling et al. 2012). MS-CS can originate from post-depositional processes such as fluidization (Eggenhuisen et al. 2010), bioturbation (Tonkin et al. 2010) and diagenetic alteration (Stow et al. 2007). No attempt to subdivide these facies has been made. A lack of internal grading promotes poor internal circulations within flows, as well as large intact mudstone fragments. Mud fragments infer a high-energy flow eroding underlying mudstone substrate. An example is shown in figure 5.1.

## 5.1.2 Secondary lithofacies

### 5.1.2.1 Crosscutting sandstones discordant (DTS-CS)

Discordant sandstone to mudstone bedding contacts in excess of 30° are observed in DTS-CS facies. Margin geometries are commonly angular and stepped. Thickness of DTS-CS varies between 1-2cm to over 4m. Internally mudstone clasts are observed and are discussed separately (MCB-CS facies). Sandstones contain weak to clear internal banding, which variably conforms to the orientation of cross cutting margins.

Discordant crosscutting sandstones are readily identified as sandstone dykes where both contacts are observed in cored section and are formed by fluidized sands (Braccini et al. 2008). Identification of DTS-CS is less conclusive when only a single contact is observed either through poor core preservation or a thick oil residue obscuring a contact. Internal banding is probably a feature of fluidization, similar examples are described in Scott et al. (2009). An example is shown in Figure 5.2.

### 5.1.2.2 Crosscutting sandstones concordant (SST-CS)

Sandstones with concordant bedding surfaces less than 30° to surrounding mudstones are seen in SST-CS facies. Margin geometries are commonly angular and stepped and sandstones are 1m thick or less with weak to internal banding.

SST-CS facies are interpreted as sandstone sills after Vigorito et al. (2008), Scott et al. (2009). Concordant crosscutting sandstones can be mistaken for bedded sandstones especially when SST-CS facies is bedding conformant, however sharp irregular contacts, lack of sedimentary structures with characteristic mudstone clasts allow identification. Internal banding is probably a feature of fluidization. An example is shown in Figure 5.2


Figure 5.2: Three examples of post depositional facies. (a) Discordant sandstone-mudstone contacts (white arrows). (b) Largely concordant sandstone-mudstone contacts (white arrows). Breccia facies are contained within sandstone dykes and sill facies, mud clasts are commonly under 5cm and angulr although larger clast are observed (white arrow).

### 5.1.2.3 Breccia (MCB-CS)

MCB-CS facies is only found within sandstone dykes (DTS-CS) or sandstone sills (SST-CS) facies. Mudstone clasts with angular to rounded margins and varying from millimetre scale through to 25cm scale are present. Clasts of MCB-CS facies are often similar to nearby depositional mudstone facies implying inclusion of country rock during injection similar observations and interpretations are presented in Scott et al. 2009. An example is shown in Figures 5.2 and 5.3

### 5.1.2.4 Loading structures (L-CS)

Convolute lamination, water escape structures, and load casts ranging from millimetre scale up to centimetre scale are observed and are interpreted as in-situ loading structures (Owen, 2003) and can be found in MS-CS, BS-CS facies. An example is shown in 5.3.

### 5.1.2.5 Post-depositional structures (P-CS)

Dish and pillar structures usually over 10cm are more commonly identified within fine to medium grained sandstones and can be found within MS-CS, BS-CS, DTS-CS and SST-CS. An example is shown in 5.3.

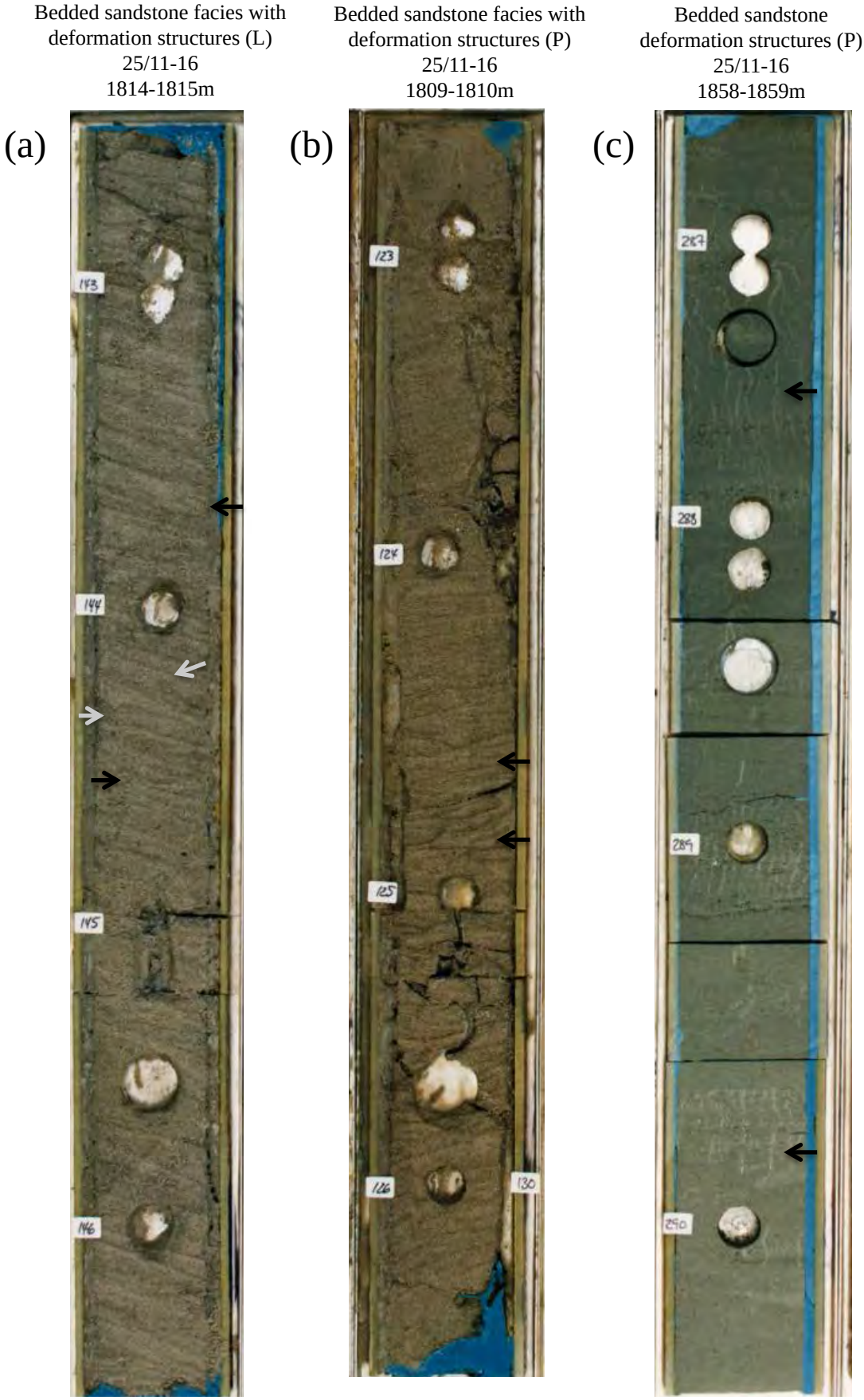


Figure 5.3: Three examples of loading and post depositional sedimentary structures. (a) Water escape cusps black arrows and simple load casts grey arrows (sensu Owen, 2003). (b) Dish structures (black arrows). (c) Pillars or stress pillars (sensu Lowe, 1975).

**SIMON MORRIS** **BIRKBECK COLLEGE** | **WELL: 25\11-23**

**Balder sequence** | **COUNTRY: Norway**

DATE: Autumn 2007 | SCALE: 1:25

AUTHOR: S.Morris | SHEET: 1 of 7

DRILLERS DEPTH METRES | CORE | OIL STAIN | SAMPLE | AGE | GAMMA RAY | GRAIN SIZE AND SEDIMENTARY STRUCTURES | LITHOLOGY | BIOTURBATION | TRENDS | FACIES | COLOUR | DESCRIPTION

CORE: CORE NUMBER; NO RECOVERY; SAMPLE REMOVED; RUBBLE

OIL STAIN: GOOD; MODERATE; POOR; TAR

SAMPLE: T = Thin section; S = SEM; X = XRD; C = Core piece

GAMMA RAY: GR; 0 GAPI 100

GRAIN SIZE: 32mm 16mm 8mm 4mm 2mm 1mm 600µm 250µm 125µm 63µm 20µm; Pebble; Granule; Sand: v. crs. crs. m. f. v.f.; Silty; Clay; Anhydrite / Coal

BIOTURBATION: 25 50 75

1760.5
1761
1762
1763
1764
1765
1765.5

Core Number 2

Balder sequence

| FACIES | DESCRIPTION |
|---|---|
| BS | |
| MS | Massive sandstones with small scale loading structures |
| LSL | Calcite cemented siltstone concretion |
| | Planar lamination |
| MS/DTS? | Mudstone Rip-up clast (in excess of 10cm, note Gamma-ray increase) |
| DTS | Upturned laminae |
| LSL | Calcite cemented siltstone concretion |
| | Pebble horizons |
| DTS | |
| LSL | Occasional grey tuff beds |
| | Planar lamination |
| | Discordant upper and lower contacts mudstone Brecciation |
| SST | Compressional and extensional faults |
| LM | Convolute bedding |
| DTS | Sharp contact to *In situ* claystone and sandstone beds |
| LM | |

Figure 5.5: Core log from well 11-23

## 5.2 Wireline log facies

Table 5.2 describes wireline facies.

### 5.2.1 Thick blocky (BL-WL)

An interval dominated by sandstone with sharp upper and lower contacts. Almost always bounded above and below by mudstones. Lithologies are confirmed from cuttings information. Sandstones of BL-WL facies are more than 25m thick.

Abrupt blocky or cylindrical transition of log response from sandstone to mudstone in a deep-water setting can be indicative of axial sedimentation either in a channelised setting or unconfined lobe (Emery and Myers, 1996), produced by either turbulent or laminar gravity flows. Post-depositional fluidization can lead to homogenization of sand intervals (Lonergan et al. 2000) and the processes of bioturbation (Tonkin et al. 2010) and Diagenesis (Stow, 2007) can modify sediments from their originally deposited form. Blocky wireline log response can also be produced by the processes of remobilization and injection (Lonergan et al. 2000). An example of BL-WL facies is shown in Figure 5.5.

### 5.2.2 Thin blocky (BLI-WL)

Sandstone dominated interval confirmed from cuttings data. Often 10m to 25m in thickness although thin 2m to 5m thick siltstone interbeds exist.

Abrupt blocky or cylindrical transition of log response from sandstone to mudstone in a deep-water setting is indicative of an axial fairway either in channelized setting or unconfined lobe (Emery and Myers, 1996). Other examples of blocky responses in clastic environments can be found in aeolian or braided fluvial settings. Blocky wireline log response can also be produced by remobilization and injection (Lonergan et al. 2000). An example of BL-WL facies is shown in Figure 5.5.

| Wireline log facies | Wireline log facies codes | Gamma Ray log values (API units) | Relative Gamma Ray values (unitless) | Density log values (kg/m3) | Neutron log values (percent porosity) | Acoustic log values (microseconds per metre) | Resistivity log values (Ohm metres) | Minimum thickness of package (m) | Maximum thickness (m) |
|---|---|---|---|---|---|---|---|---|---|
| **Blocky low GR** | **BL-WL** | Below 15 API values | Low | 2.65 | -4 | 53 | High | 25m | - |
| **Blocky low GR with interbeds** | **BLI-WL** | Below 15 API values | Dominatly low with high values | 2.2 - 2.7 | -4 - High | 50 - 150 | Low - High | 10m | 25m |
| **Bell shaped low GR - high GR** | **BS-WL** | Below 15 API values - above 80 API values | Low - High | 2.2 - 2.7 | -4 - High | 50 - 150 | Low - High | 15m | - |
| **Interbedded** | **S-WL** | Between 35 - 125 API values | Moderate | 2.2 - 2.7 | -4 - High | 50 - 150 | Low - High | 2m | - |
| **Shale** | **SH-WL** | Above 80 API values | High | 2.2 - 2.7 | High | 50 - 150 | Low | 1m | - |
| **Limestone** | **L-WL** | Below 5 API values | Low | 2.71 | 0 | 47.5 | High | 1m | - |

Table 5.2: Wireline log facies

| Seismic facies | Seismic facies code | Seismic reflector description | Reflector continuity | Reflection dimensions | Lithology interpretation | Reflector amplitude |
|---|---|---|---|---|---|---|
| **Continous** | **P-S** | Continous flat lying reflections with no reflector discontinuity | Continous | In excess of several kilometers laterally | Shale or Limestone dominated | High amplitude |
| **Mixed** | **MI-S** | Mixed flat lying reflections with reflector discontinuty | Continous to semicontinous | Around one kilometer laterally | Shale with siltstone and occasional sandstone | Moderate to high amplitude |
| **Discontinous** | **D-S** | Occasional parallel reflections exist, all reflectors are short lived events | Discontinous | Above seismic resolution to two hundred metres laterally | siltstone and sandstone occasional shale | Low amplitude |
| **Chaotic** | **C-S** | No parallel reflections exist, all reflectors are short lived events | Discontinous | 30-100m laterally (each event) | Sand and mudstone | Low to moderate amplitude |
| **Crosscutting** | **CR-S** | Seismic reflections are truncated by linear to sub-linear events | Discontinous to semicontinous | 30-500m | Sand and mudstone | High amplitude |
| **Mound** | **M-S** | Flank angles of more than 15° | Discontinous to semicontinous | 750-5000m | Sand and mudstone | Moderate to high amplitude |

Table 5.3: Seismic facies

### 5.2.3 Bell shaped (BS-WL)

Low Gamma-ray log values correlate with sandstones at the base of section, which are overlain by siltstones and mudstones of increasing Gamma-ray log values as lithology becomes more heterolithic. These observations are confirmed by cuttings, in addition ash and tuffaceous material are also observed.

A bell shaped fining upwards log profile is indicative of decreasing grain size vertically (Emery and Myers, 1996). The presence of tuffaceous sediments is widespread across the North Sea basin and is attributed to the opening of the North Atlantic (Haaland et al. 2000). Tuff and ash is non-radioactive and may act to dampen a heterolithic mudstone response. An example of BS-WL facies can be found in Figure 5.5.

### 5.2.4 Interbedded (I-WL)

Thin sandstone and mudstone interbeds of between 1-2m thickness are observed. Log interpretation of lithology is confirmed by cuttings information.

Thinly interbedded heterolithics can be indicative of waning turbulent flow (Emery and Myers, 1996), distal turbulent flow or gravity driven slope deposits. An example of I-WL can be found in Figure 5.5.

### 5.2.5 Mudstone (SH-WL)

Consistently high Gamma-ray log response in conjunction with observations from cuttings information suggest a mudstone dominated lithology. Locally, high Gamma-ray peaks are observed, which could be due to inaccurate data capture and can be checked against the Caliper log. Where hole condition is good, Gamma-ray peaks are probably due to increases in radioactive minerals (Potassium, Uranium and Thorium).

No clear vertical trends are observed. Deposition in deep-water environments is predominantly through turbulent flow although some mudstone may originate from

hemipelagic deposition (Emery and Myers, 1996). An example of SH-WL can be found in Figure 5.5.

### 5.2.6 Limestone (L-WL)

The presence of calcareous material is described in cuttings information in association with a blocky Gamma-ray log response indicates Limestone facies. Ekofisk Formation (Isaksen and Tonstad, 1989) is observed beneath clastic sediments. Shown in Figure 5.5.

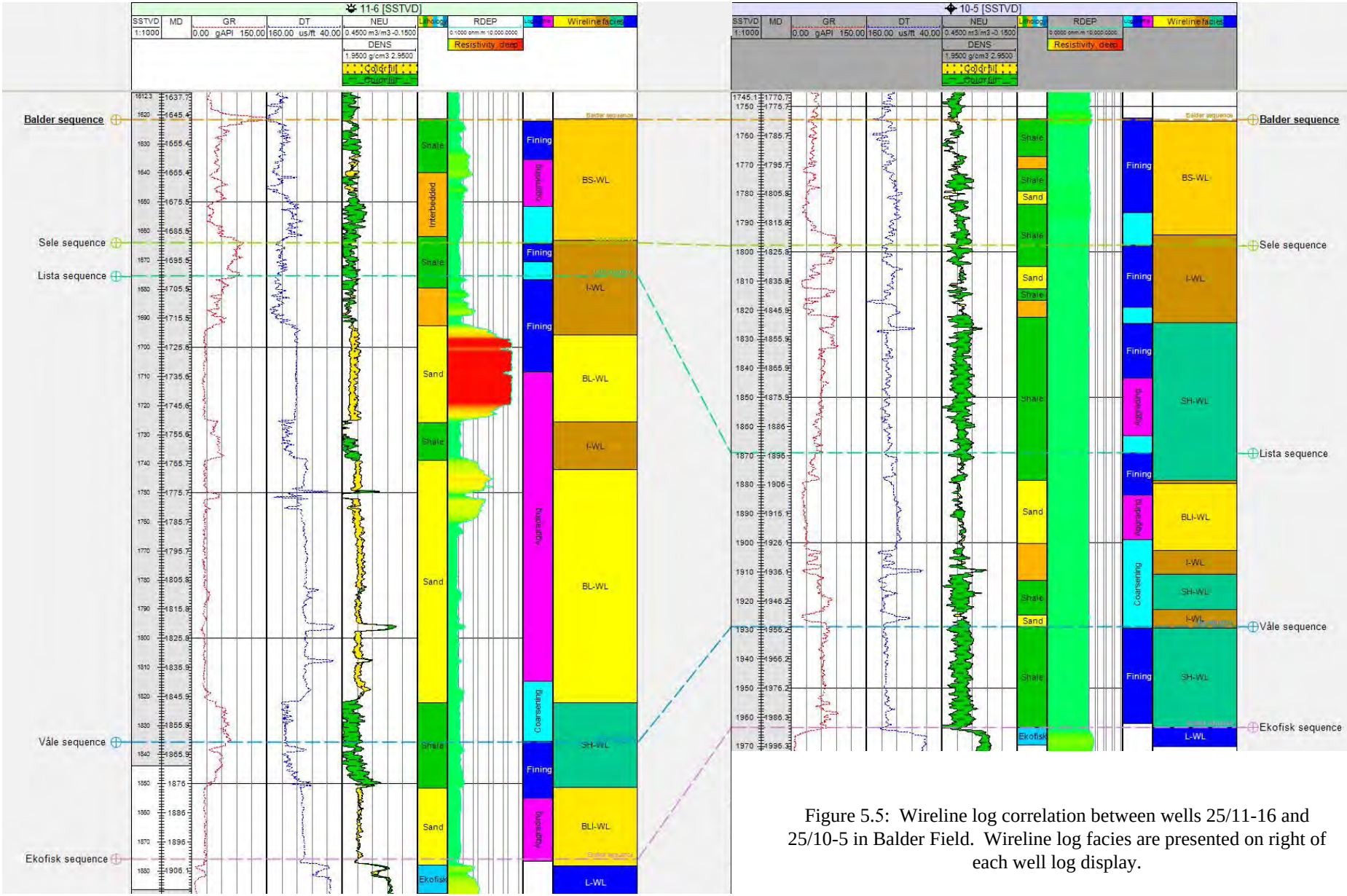


Figure 5.5: Wireline log correlation between wells 25/11-16 and 25/10-5 in Balder Field. Wireline log facies are presented on right of each well log display.

## 5.3 Seismic facies

Amplitude strength and reflector continuity are used as discriminating tools when devising a seismic facies scheme as described by Mitchum et al. 1977. Table 5.3 describes seismic facies.

### 5.3.1 Continuous (P-S)

Continuous flat lying reflections with little to no reflector discontinuity is representative of P-S facies. Seismic reflections are moderate to high amplitude and laterally extensive and extend 100-1000m. Bright amplitudes indicate high acoustic contrast between lithologies, which may represent markedly differing lithologies, hiatal surfaces or unconformities. Parallel reflections indicate vertical aggradation and are common in mudstone or carbonate dominated intervals (Kilhams et al. 2012). An example is shown in Figure 5.6.

### 5.3.2 Semi-continuous (MI-S)

Seismic reflections are commonly continuous, but become semi-continuous. Seismic reflections are of moderate amplitude strength and extend between 100-1000m. Reflections with these properties are common in heterogeneous sandstone and mudstone sections reflector continuity can be affected by diagenetic effects (e.g. cementation), present day fluid effects or Palaeo-fluid effects (Huuse et al. 2004). Post depositional alteration in the form of faulting, remobilization or slumping may also produce MI-S facies. Sandstone and mudstone lithology calibrated from well logs. An example is shown in Figure 5.6.

### 5.3.3 Discontinuous (D-S)

Seismic reflections are less than two hundred metres laterally (discontinuous).

No parallel reflections exist all events are short lived and are generally dull to moderate in amplitude strength. Sandstones with high net to gross can display these reflector characteristics as can present day fluid effects or Palaeo- fluid fill effects (Huuse et al. 2004). Post depositional alteration in the form of faulting remobilization or slumping may also produce this facies. An example is shown in Figure 5.6.

### 5.3.4 Crosscutting (CR-S)

Moderate to high amplitude strength reflections crosscut, mixed, mounded or parallel seismic facies. Seismic reflections can be in excess of 50m length. Whereas, dip of reflection can be shallow (less than 30°) or steep (more than 30°). Seismic reflections with CR-S facies can be caused by sandstone injection (e.g. Szarawarska et al. 2010). Sills are described to be shallow (less than 30°) Dykes have steeper dip angle (more than 30°). An example is shown in Figure 5.6.

### 5.3.5 Mound (M-S)

Moderate to high amplitude reflections with margins less than 15° can be formed by differential compaction especially evident in channel sandstones deposited in deep-water environments (Jennette et al. 2000). M-S facies are moderate to high amplitude reflections with flank margins more than 15° can be formed by remobilization and injection processes (as described in Chapter 2, e.g. Hamberg et al. 2007). Slumping and sliding processes can also produce steep sided bodies (e.g. Jenssen et al. 1993). An example is shown in Figure 5.6.

## 5.4 Summary of possible interpretations for identified facies

Table 5.4 displays possible mechanisms that may have caused facies described in chapter 5. A smaller range of either primary depositional mechanism cause cored

section facies than wireline or seismic facies, further developed in Chapter 7.

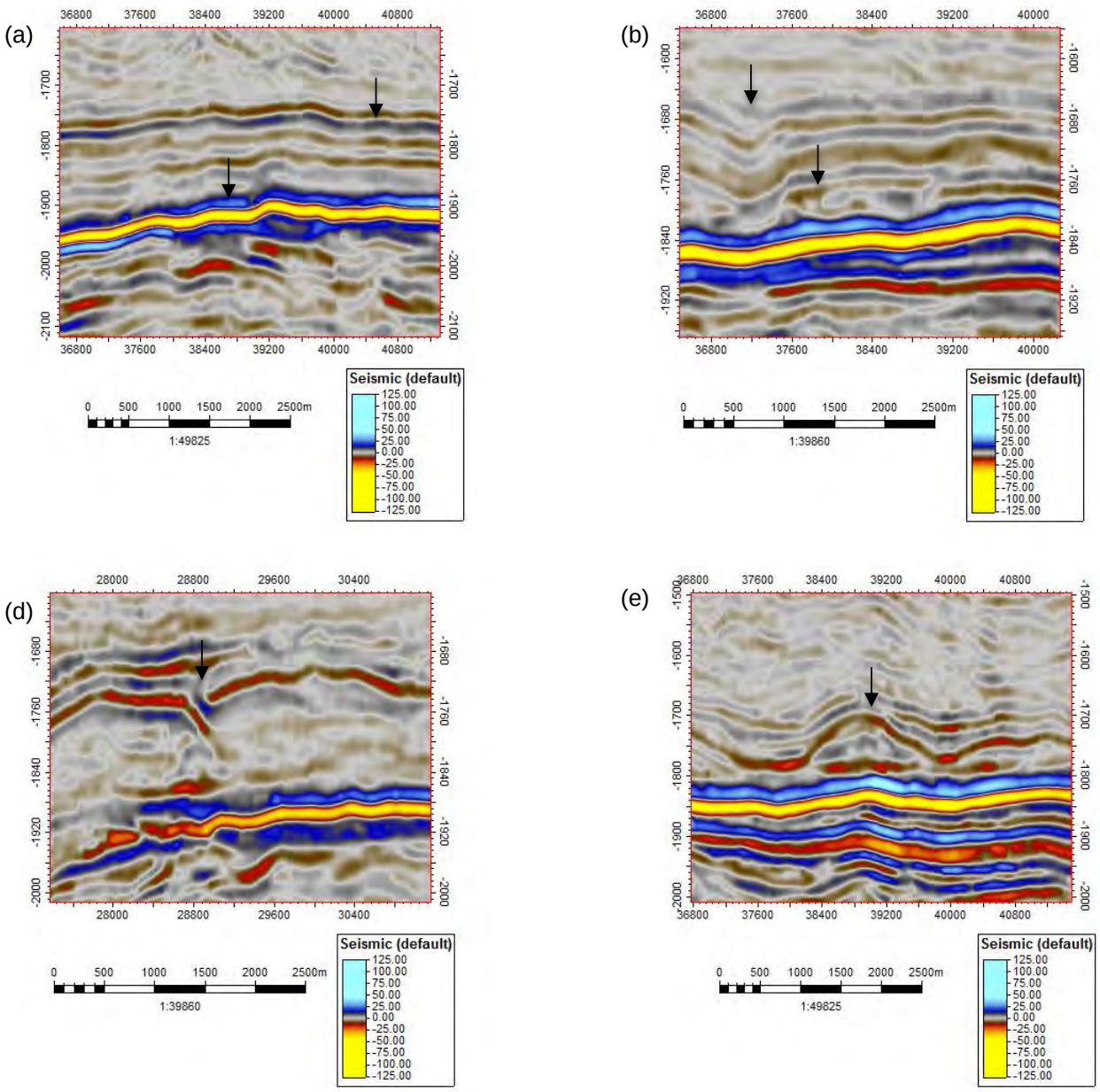


Figure 5.7: Examples of seismic facies. (a) Continous facies (P-S), blue seismic reflections (black arrows) are unbroken and moderate to strong amplitude strength. (b) Semicontinous facies (MI-S), seismic reflections are broken reflector strength is weak to moderate. (c) Discontinous facies (D-S) are completely disconnected and are weak in amplitude strength. (d) Crosscutting facies (CR-S), reflections perpendicular to general amplitude direction disconnect. (e) Mounded facies (M-S).

| | Facies | Possible interpretation |
|---|---|---|
| Cored section facies | LM-CS | Turbulent flow |
| | LSL-CS | Turbulent flow |
| | BS-CS | Turbulent flow |
| | MS-CS | Turbulent and laminar flow, bioturbation, diagenetic alteration, fluidization |
| | DTS-CS | Fluidization |
| | SST-CS | Fluidization |
| | | |
| Wireline log facies | BL-WL | Turbulent and laminar flow, fluidization, diagenetic alteration |
| | BLI-WL | Turbulent and laminar flow, fluidization, diagenetic alteration |
| | BS-WL | Turbulent and laminar flow, diagenetic alteration |
| | I-WL | Turbulent and laminar flow, diagenetic alteration |
| | SH-WL | Turbulent and laminar flow |
| | L-WL | Turbulent and laminar flow |
| | | |
| Seismic facies | P-S | Turbulent and laminar flow, diagenetic alteration, fluid effects |
| | MI-S | Turbulent and laminar flow, diagenetic alteration, fluid effects, structural effects |
| | D-S | Turbulent and laminar flow, diagenetic alteration, fluid effects, structural effects |
| | CR-S | Diagenetic alteration, fluid effects, structural effects, fluidization |
| | M-S | Differential compaction, fluidization, slumping and sliding |

Table 5.4: Possible interpretations based on facies observed

# Chapter 6: Facies interpretation

## 6.1 Cored section

Observations and interpretations from cored section from Balder, Grane and Ringhorne Field are presented in the context of the 5 sequences outlined in (Chapter 4). Lista sequence is the only sequence with cored section from Balder, Ringhorne and Grane Fields. No cored section from Ekofisk sequence was studied.

### 6.1.1 Våle sequence

Core from four wells in the study area have core from Våle sequence. Wells 11-16, 8-1 and 11-22 each contain mudstones only. Well 11-1 is the only well that cored sandstones, 60% recovery was achieved but the core is poorly preserved. Therefore, no core from Våle sequence was logged.

### 6.1.2 Lista sequence

A total of 283m of Lista sequence sediments has been logged. 114m of cored section has been logged in Balder (well 11-16), 89m in Ringhorne (wells 8-10S and 8-4), 80m in Grane Fields (wells 11-15). Interpreted facies are displayed graphically in Figure 6.3 (a) from data displayed in Appendix 3b. This plot is statistically biased and is influenced by factors such as heterogeneity of bedding and other drilling factors (well placement, coring location etc.,). However, Figure 6.3 (a) does highlight the lack of injected sandstones observed in core, with only 3 recorded counts of sandstone dyke facies and no observed occurrence of sandstone sill facies. Only well 8-4 records injected sandstones at Lista interval between depths of 1779-181m (figure 6.1). The causal effect is unclear, either wells have been positioned to avoid CR-S facies, coring targets were planned for deeper intervals or the prospective nature of these levels was not realised.

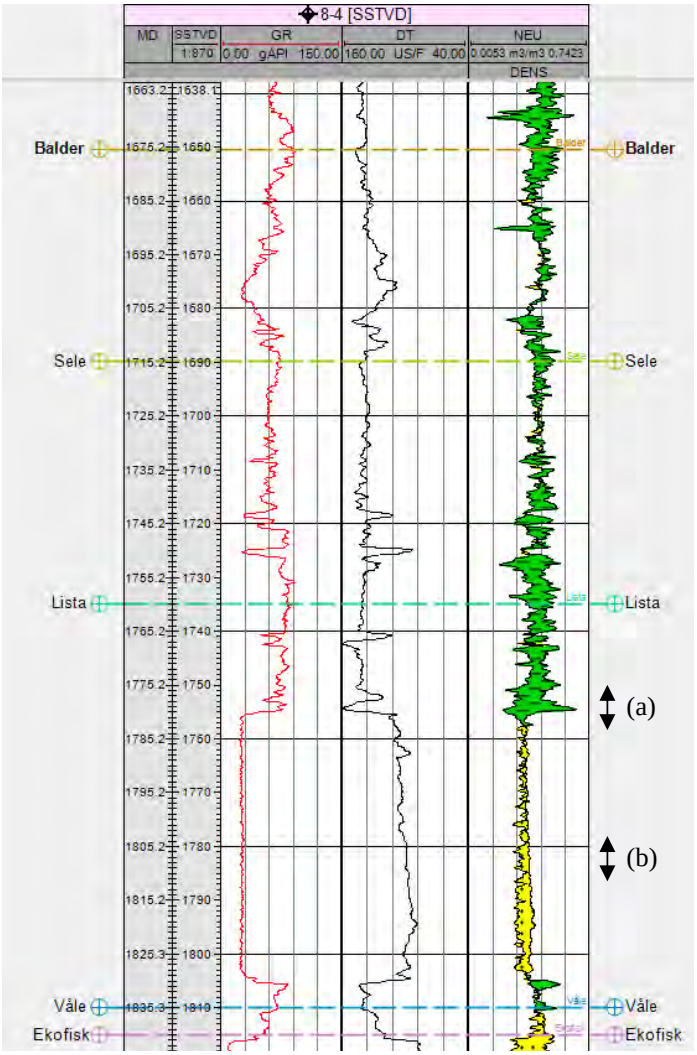


Figure 6.1: An example of cored section correlated to wireline logs from Lista sequence. Well 25/8-4 locates outside of 3D seismic coverage. (a) Remobilized and injected sandstones intruded into overlying mudstones. (b) Structureless sandstones with loading structures.

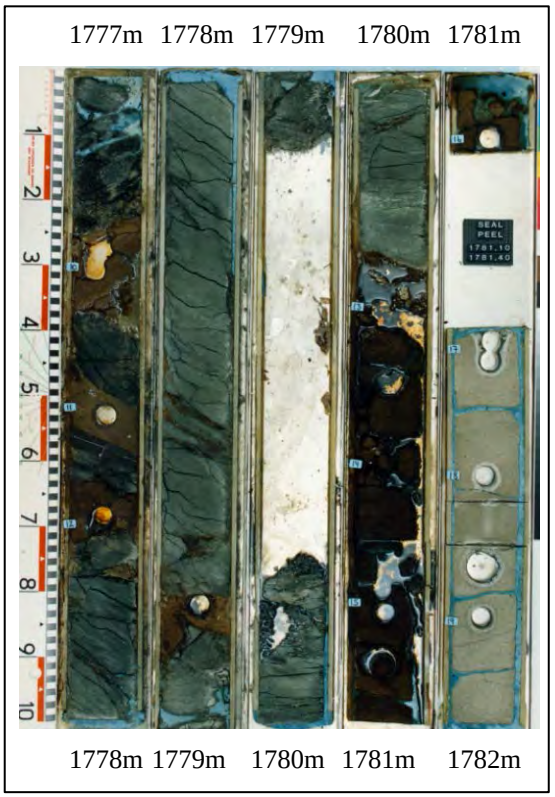


(a) Sandstone dyke intrusion with mudstone clast breccia, sandstones are heavily oil stained (1777m-1778m). 75cm white Limestone clast (1779m-1780m). Sandstone sill intrusion upper contact (1780.30m). Dish structures (1780.5m).

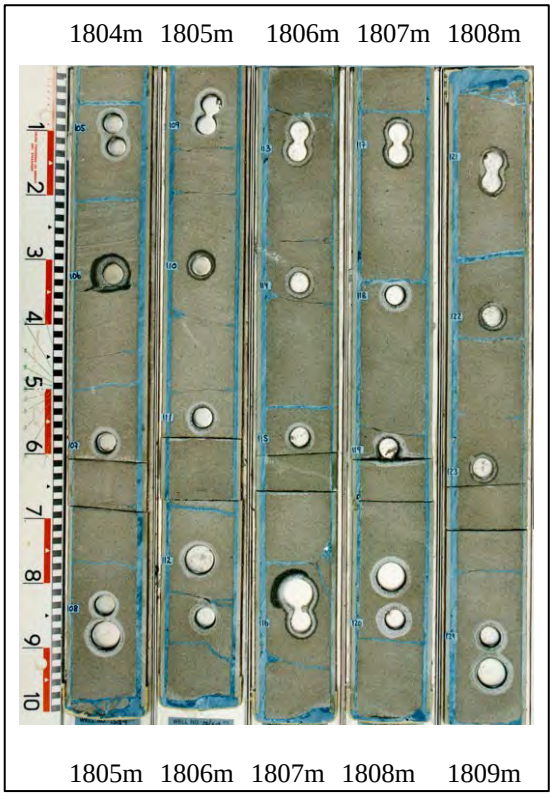


(b) Structureless sandstones with upturned laminae (1804.25m). Weak indication of wavy to paralled bedding (1805.20m). Weak indication of cross-bedding (1807.40m).

Visually, however, Lista sequence is dominated by Massive sandstone lithofacies and fining or coarsening observations are not generally observed. The majority of sandstones were deposited by Ta sequence (Talling et al. 2012) processes although Dvcs sequence (Talling et al. 2012) may also have contributed to some extent. Small-scale loading deformation structures are less common and are located near to the base of the cored Lista sequence. Large-scale deformation structures locate near to the top of the sandstone body. Which implies increased fluidization near to upper contacts of Lista sequence sandstone intervals. Wells 8-10 S, 11-15, 8-4 and 11-16 each have discordant upper contacts with overlying mudstones (figure 6.1).

### 6.1.3 Sele sequence

A total of 94.5m of cored section from three wells has been logged. Core studied in Sele sequence is from the Ringhorne Field (8-10S and 8-11) and Balder Field (11-19S). Massive sandstones, small and large-scale deformation structures are observed in Sele sequence. Generally, massive sandstone intervals (MS-CS) in Sele sequence are thinner (approximately 60-70m) than MS-CS facies in lista sequence. Similar observations are seen from wireline logs and are most likely due to reduced sediment input during Sele sequence times although secondary process may also have affected sediment thickness. Sele sequence contains finer grained bedded heterolithics (well 8-10 S). Laminated and bedded sandstones are seen to grade normally upwards in siltstones and laminated mudstones, interpreted as Tb-d (Talling et al. 2012).

Sandstone dykes and sills are seen to intrude into this heterolithic interval (figure 6.2 ) it is unclear from the gathered data whether there is a geological trend of (e.g. higher concentration of sandstone dykes within Balder field) or data capture bias.

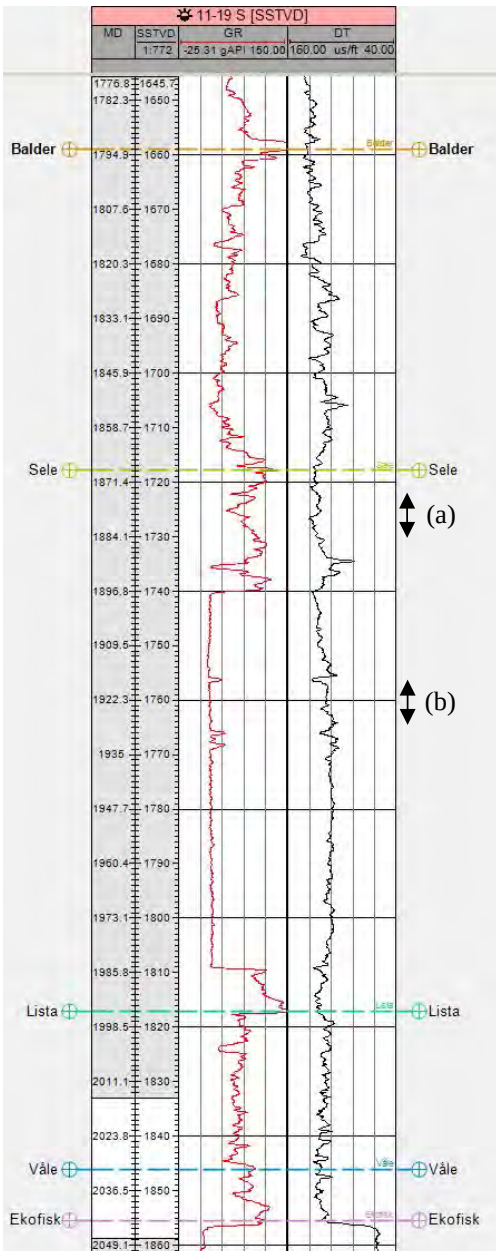


Figure 6.2: An example of cored section correlated to wireline logs from Sele sequence. Well 25/11-19S locates on the northern flank of mound 9. (a) Remobilized and injected sandstones intruded into overlying mudstones. (b) Structureless sandstones with loading structures.

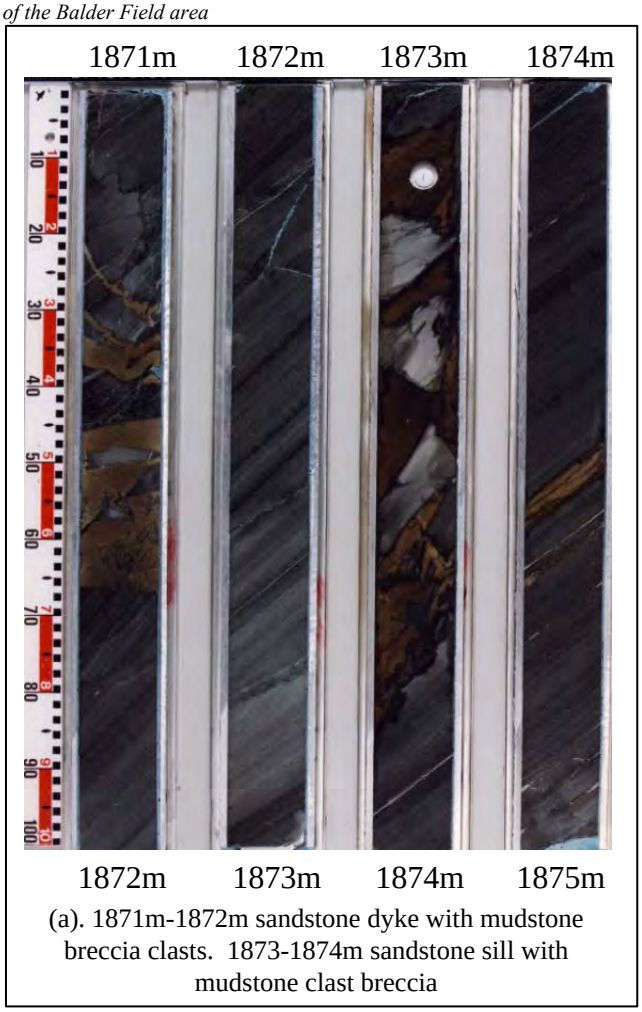


(a). 1871m-1872m sandstone dyke with mudstone breccia clasts. 1873-1874m sandstone sill with mudstone clast breccia

### 6.1.4 Balder sequence

A total of 37.5m of core was logged all core studied in Balder sequence is from Balder Field (wells 10-5 and 11-23). Massive sandstones with small and large-scale deformation structures are observed but are much thinner (15-30m thickness) a range of possibilities for their origin exists.

Finer grained bedded heterolithics are also observed. Laminated and bedded sandstones are seen to grade normally upwards in siltstones and laminated mudstones interpreted as Tb-d (Talling et al. 2012). Sandstone dykes, sills, slumping structures and convolute fabric is observed within this heterolithic interval no pattern in distribution of sandstone injections are seen.

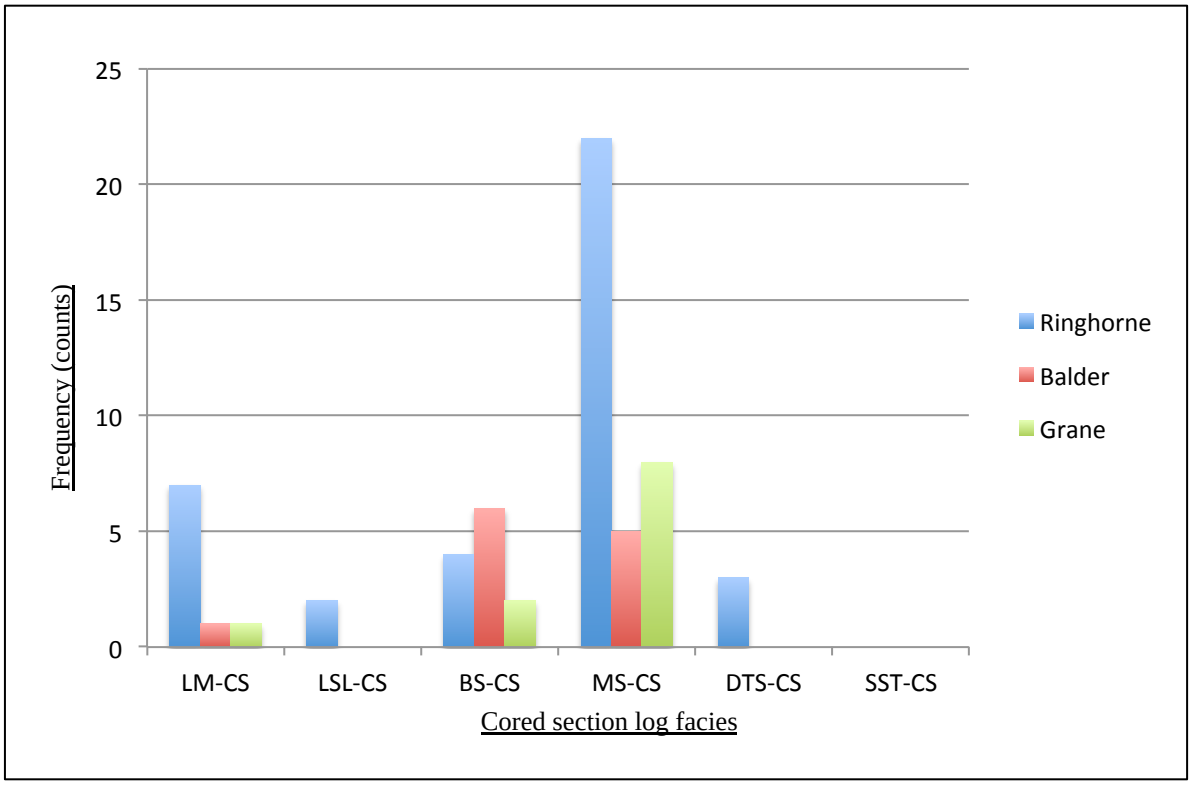


Figure 6.3 (a) showing wireline log lithofacies from Lista sequence only.

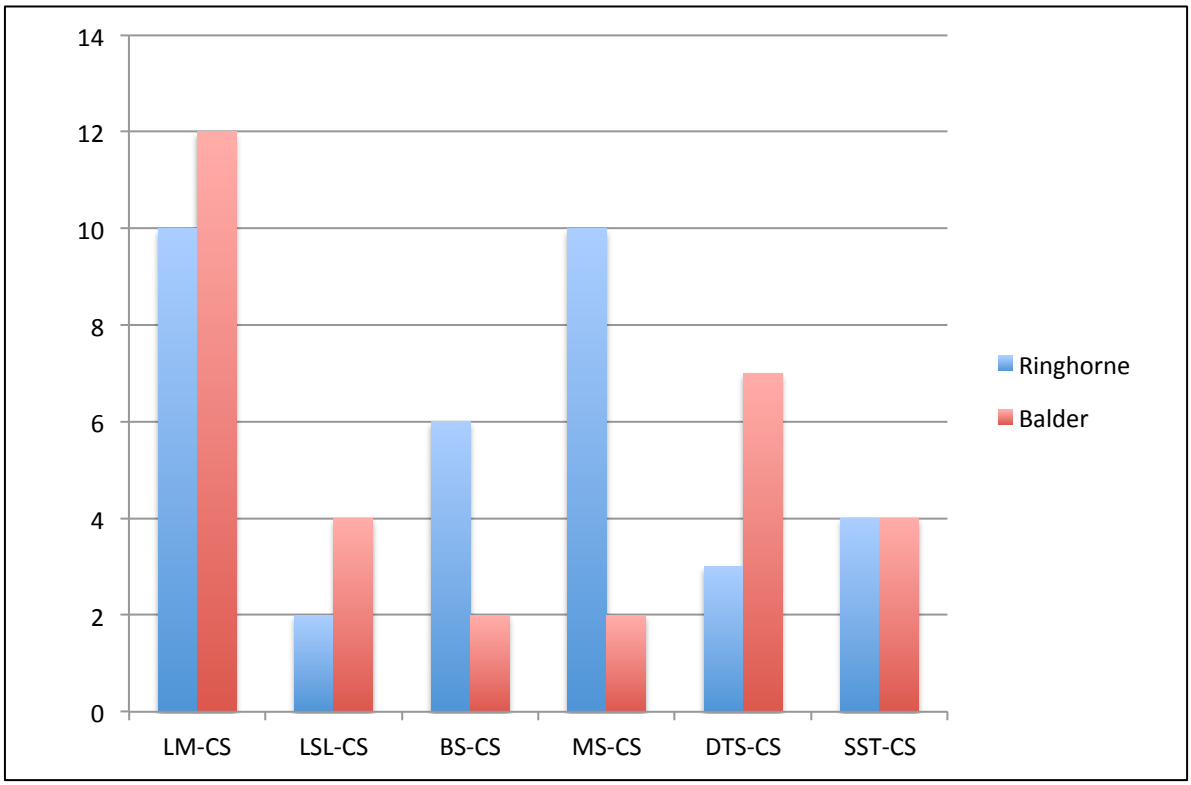


Figure 6.3 (b) showing cored section lithofacies from sele sequence only.

### 6.1.5 Facies association

- Laminated sandstones commonly in Sele and Balder sequences grade normally into laminated siltstones. This observation is in agreement with a fully turbulent flow rheology for these intervals. Similar observations for Lista sequence have not been observed.
- Small scale, Loading structures are often found within massive sandstone facies (MS-CS) no vertical trend is observed. Large-scale deformation structures near to the top of sandstone sections are observed within Lista sequence, Balder Field.
- Dykes and Sills intrude into overlying laminated mudstones for Lista, Sele and Balder sequences. It is unclear if intruded sandstones originated from sandstones beneath.

### 6.1.6 Other observations

White unweathered chalk clasts between 10-25cm are observed in cored section from Lista and Sele sequences. Possible explanations include, erosion of underlying chalk by gravity flows during deposition, or forceful emplacement of fluidized sediment upward during catastrophic remobilization and injection (Wild and Briedis, 2010).

A convolute mud texture is observed in Balder sequence for wells 11-23 and 10-5 in Balder sequence. Similar features in core are not seen in any other wells.

A pervasive heavy oil stain is present on cores of Lista and Sele sequence (e.g. well 11-15) obscuring sedimentary structures. UV photographs are not available for any cored interval in this project.

## 6.2 Wireline logs

Observations and interpretations from wireline logs from Balder, Grane and Ringhorne Fields are presented in the context of the 5 sequences outlined in (Chapter 4).

### 6.2.1 Ekofisk sequence

A blocky log response is identified caused by late Cretaceous and earliest Tertiary Danian Limestones.

### 6.2.2 Våle sequence

A fining upwards log motif from Ekofisk limestones up to a Gamma-ray peak is characteristics of Våle sequence. Våle sequence sandstones are only found in the Balder Field area, which possess a blocky sandstone log response of dubious origin. Sandstones are seen to directly overly limestones of Ekofisk sequence, which may suggest erosion of underlying Våle mudstone during deposition or alternatively injection of sandstone from beneath Ekofisk limestones (Wild and Briedis, 2010), discussed in Chapter 7.

### 6.2.3 Lista sequence

Sandstones with thick (commonly more than 100m) homogenous (no change vertically in Gamma-ray or Sonic log values) and blocky Gamma-ray wireline log responses are characteristic. Sharp contacts define transition between mudstones and sandstones of Lista sequence. Usually composed of a single blocky sandstone unit although in the Balder Field several thinner (10m) basal sandstones are seen, although these units are not laterally extensive. Wells 10-1 and 10-4 locate 670m apart basal sandstones are not observed in well 10-1 (Figure 4.4). Interstitial mudstones within blocky sandstones occur and are commonly only a few metres thick. Blocky sandstones can originate from several processes summarised in Table 5.4. Wireline log facies are shown in Figure 6.4

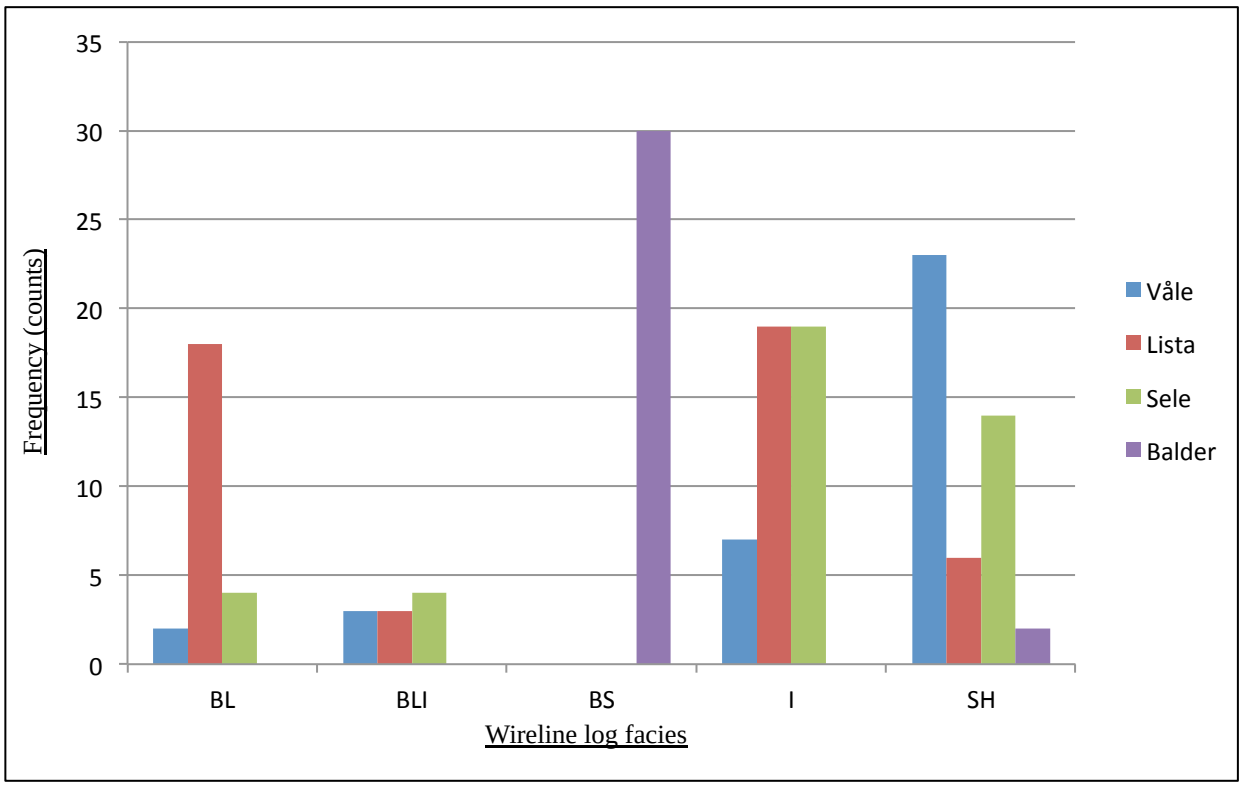


Figure 6.4: Bar chart showing frequency of wireline log facies (x-axis) plotted against frequency (y-axis) of occurence. Våle sequence is dominated by mudstones (SH-WL facies) and interbedded heterolithics (I-WL facies). Blocky sandstone wireline log responses are most common in Lista sequence (BL-WL), whereas Interbedded wireline log facies (I-WL) is common in both Lista and Sele sequences. Balder sequence is charaterised by Bell-shaped (BS-WL) wireline log response.

### 6.2.4 Sele sequence

Sele sequence is present across the Balder Field in varying thicknesses. Thin up to 10m scale sandstones are observed with sharp Gamma-ray and Acoustic log responses. Thicker blocky sandstones over 10m up to 40m are also present with sharp Gamma-ray and Acoustic log responses, these sandstones are found in the East and North of the Balder area. Overall the Sele sequence fines upwards. Ringhorne Field and Balder Field contain similar log responses. Interbedded sandstones of similar thickness are observed predominantly within the East of Ringhorne Field (well 8-4) with blocky sandstones observed in the west of the field area (Well 8-11). Sele sequence over Grane Field contains a mudstone prone fining upwards sequence.

### 6.2.5 Balder sequence

The Balder sequence possesses a characteristic log sequence as described by Mudge and Bujak (1994). Bell shaped Gamma-ray and acoustic DT log response is commonly observed that basally indicates presence of sandstones overlain by mixed heterolithics with higher mudstone and silt content. Some examples of blocky sandstones do occur; well 11-23 contains a 15m thick basal blocky sandstone overlain by mixed heterolithics with a corresponding fining upwards log signature. More commonly however is thin 2m thick sandstones with interbedded siltstone and mudstones overlying. Sandstones are concentrated within the centre of Balder Field and almost no sand is observed in Grane and Ringhorne Fields. In certain wells (e.g. 11-6) picking of top Balder sequence unit is complicated by an internal high Gamma-ray mudstone followed by a second bell shaped log response upwards. Wells with these characteristics locate along the eastern margin of the Balder Field.

### 6.2.6 Other observations

Duranti and Hurst (2004) proposed that remobilized and injected sediments possess reduced porosity and permeability due to tighter grain packing as a result of fluidization when compared to non-fluidized sections (as described in Chapter 2). Wireline logs from the Balder Field do not generally possess similar characteristics. Indications of increased Density and Sonic log values maybe observed in wells 11-6 (Figure 6.5) although core from this interval is poorly preserved and thin sections are not available for study, limiting further investigation. Therefore, a range of explanations for increased Sonic and Density log measurements observed in well 11-6 are relevant which include, diagenetic cementation, inverse grading, or defective wireline log measurements recorded during data capture.

Thin sandstones above massive sandstone intervals are described by Hamberg et al. (2007) as indicating the presence of injected sandstones. In order to apply this interpretation

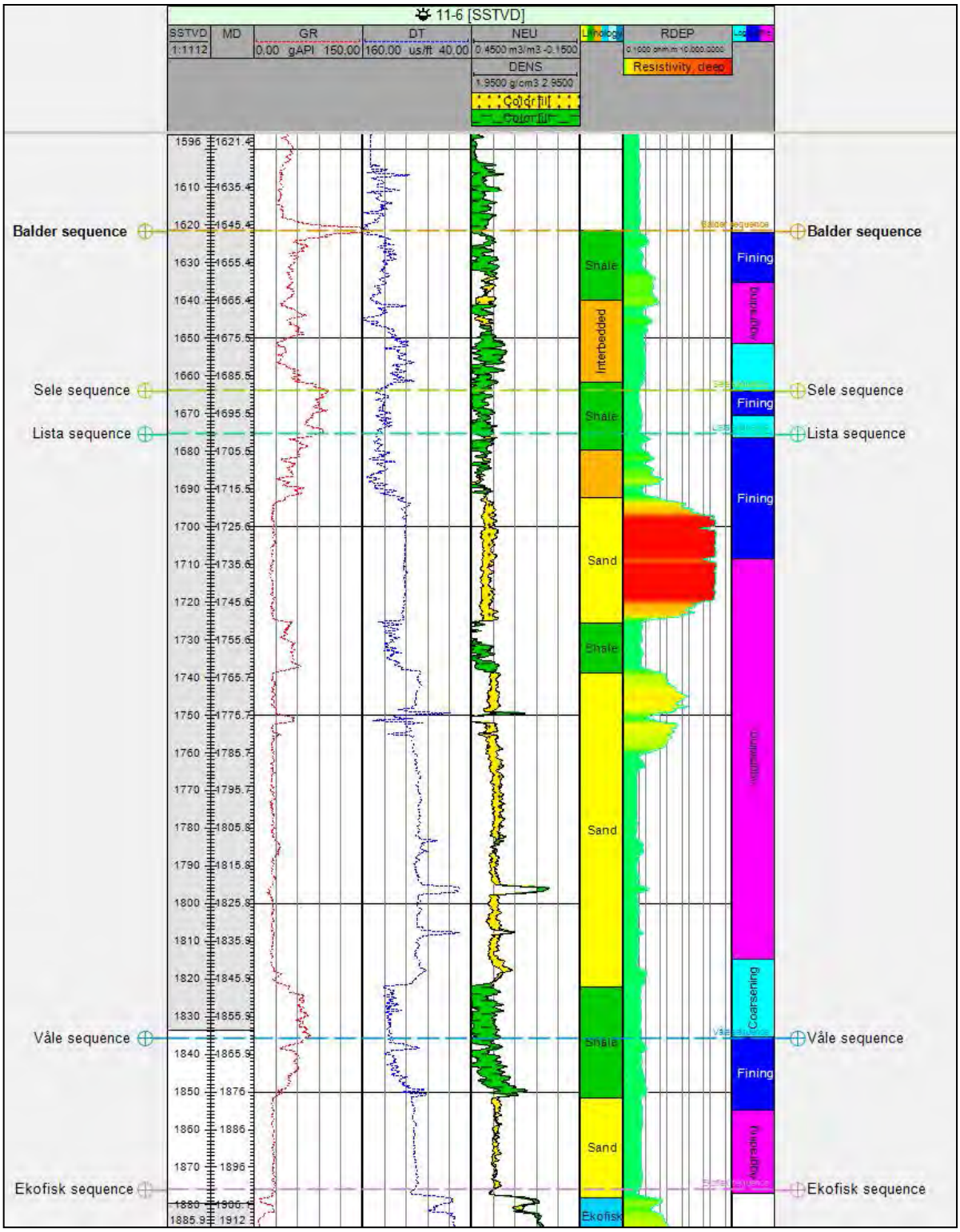


Figure 6.5: indications of increased Acoustic sonic (DT) log values and Density log values are observed between 1776-1800m.

cored section must be present, without cored section thin bedded sandstones maybe formed by a range of primary or secondary processes. Similar observations of serrated or spiky log signature were described by Lonergan et al. (2007) from Gryphon Field, United Kingdom, North Sea.

Other methods for the identification of injected sandstones are described in Chapter 7, further work as they require additional data e.g., dip meter measurements, image logs, wireline logs and cored section from production well bores.

## 6.3 Seismic data

Observations and interpretations from wireline logs from Balder, Grane and Ringhorne Fields are presented in the context of the 5 sequences outlined in Chapter 4.

### 6.3.1 Ekofisk sequence

Dominated by parallel seismic facies, Ekofisk sequence seismic interval is a high amplitude increase in acoustic impedance (seismic amplitude trough). Strong acoustic contrast is due to low acoustic impedance mudstones of Våle sequence overlying high acoustic impedance limestone dominated lithologies of Ekofisk sequence, calibrated by well log data. Limestones of Ekofisk sequence extend throughout the study area. Within the Ekofisk sequence a series of (250-700m wide) discontinuities are present (Figure 6.6). These features are not clearly aligned above underlying Mesozoic aged fault planes or spaced at regular intervals. Erosion during deposition of overlying Våle sequence sediments may have occurred. It is unclear if a rugose or incisional surface is present due to a lack of seismic resolution at this interval (discussed in Chapter 7).

### 6.3.2 Våle sequence

Dominated by Parallel seismic facies. Top Våle sequence is a seismic amplitude peak (decrease in acoustic impedance) that dips to the west. Sandstones of up to 30m thickness are identified on well logs but are not visible on seismic data. Reflector geometries and properties indicate mudstone lithology, which is confirmed by well data.

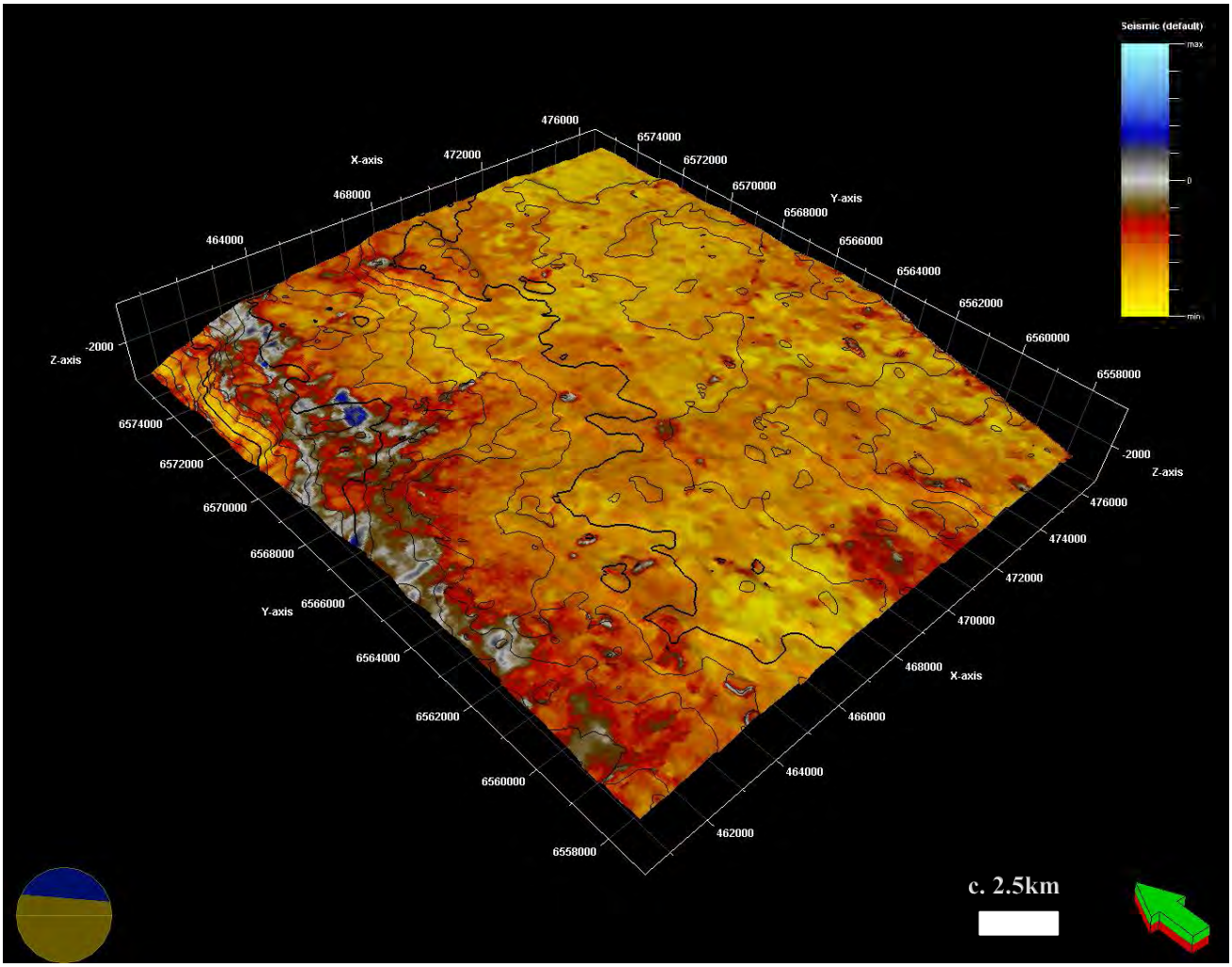


Figure 6.6: Ekofisk surface, looking North-west. Displaying extract value attribute with european polarity colour scaling, blue indicates decrease in acoustic impedence, red indicates increase in acoustic impedence. Grey circular discontinuities are approximately 500m in diameter.

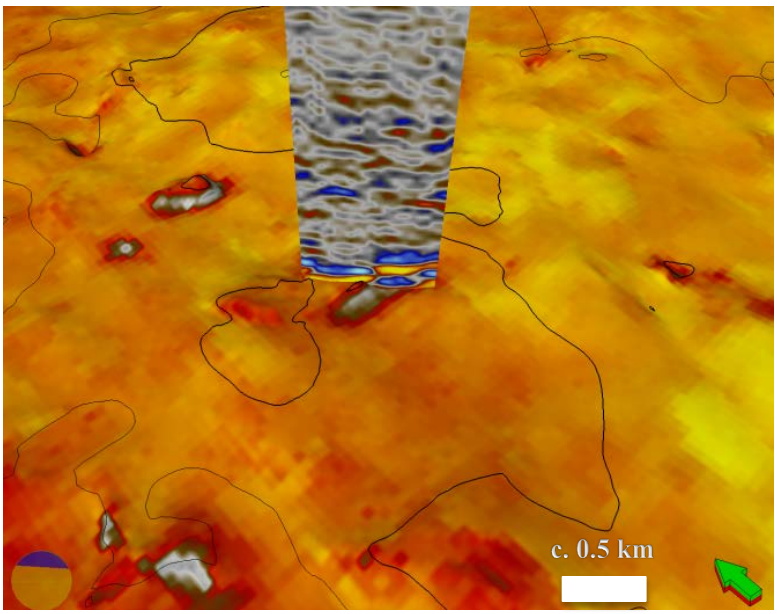


Figure 6.6: Inset image, showing a discontinuity with composite seismic section showing clear juxtaposition.

### 6.3.3 Lista sequence

Seismic geomorphologies for Balder, Grane and Ringhorne fields differ and are therefore described separately for Lista sequence.

#### 6.3.3.1 Balder Field

The Lista sequence seismic horizon is continuous through the western area of the Balder Field (Mounds 8, 5, 3 and 1). The Lista package of sediments thins considerably onto the western flank of the Utsira High. Approximately 7 seismic reflections are identified in the west (near to well 11-23), decreasing to approximately 3 seismic reflections in the east (near to well 11-6). Broadly equalling a reduction of sediment thickness of approximately 90m. Within central and eastern areas reflector continuity and amplitude strength decrease, shown in Figure 6.8 using extract value amplitude attribute. The cause of amplitude strength decrease is not clear, figure 4.8 (synthetic seismogram from Grane Field well 11-15) suggests calculated acoustic response should be of high magnitude. Possible causes for lower amplitude seismic reflectors include hydrocarbon composition variance between Ringhorne and Grane Fields. Balder Field contains oil of 23˚ gravity American Petroleum Institute (API), whilst Grane Field contains 18˚API (NPD). A reduction in hydrocarbon density may reduce the strength of amplitude response. In addition, Sele sequence sandstones are not observed East of Mounds 10, 6 and 2. A lack of acoustic contrast between Sele sequence sandstones and mudstones may also reduce the total reflected response near to the top of the Lista sequence reflection.

Figure 6.7 shows dip angle amplitude attribute steep dip angles along the eastern flank of the Balder Field are observed. This map highlights mounding in the study area but as it is displayed in TWT domain it is not an accurate representation of the subsurface.

Cross cutting seismic reflections are angular and vertical to sub-vertical and usually

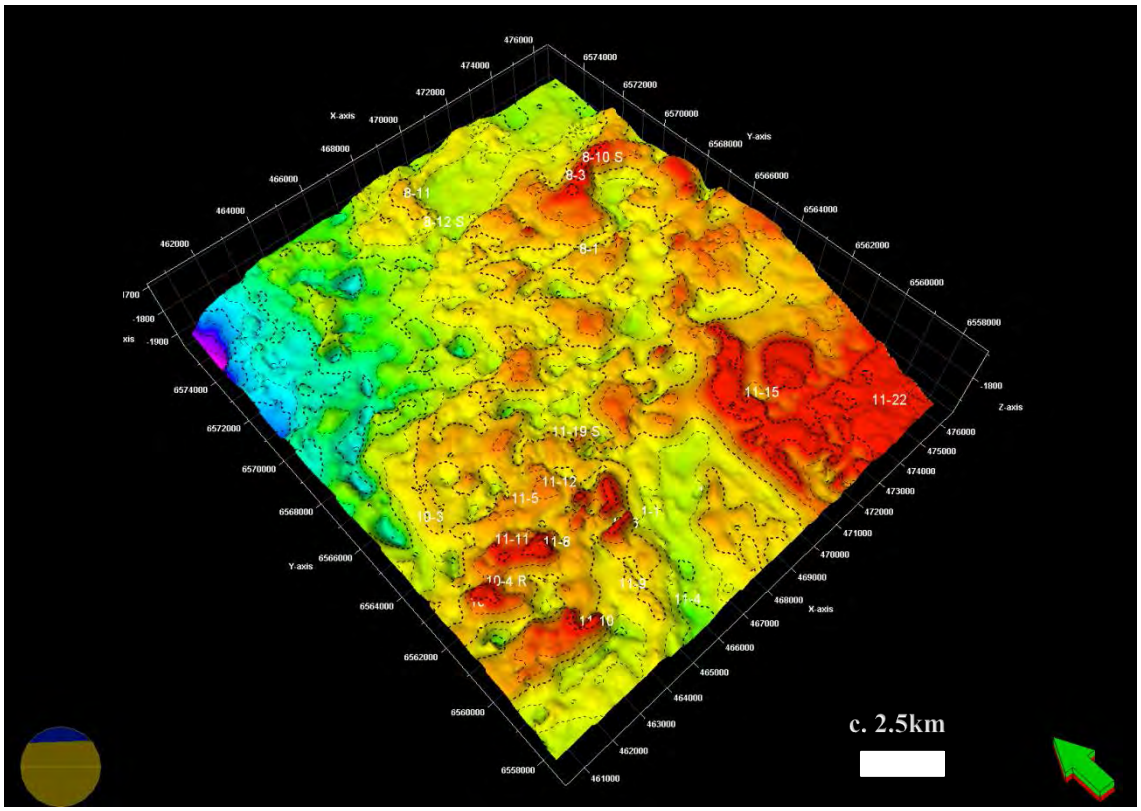


Figure 6.7 (a): Top Lista seismic surface (TWT), looking North-west. Red colours 1730ms, Purple colours 1850ms with 20ms contours.

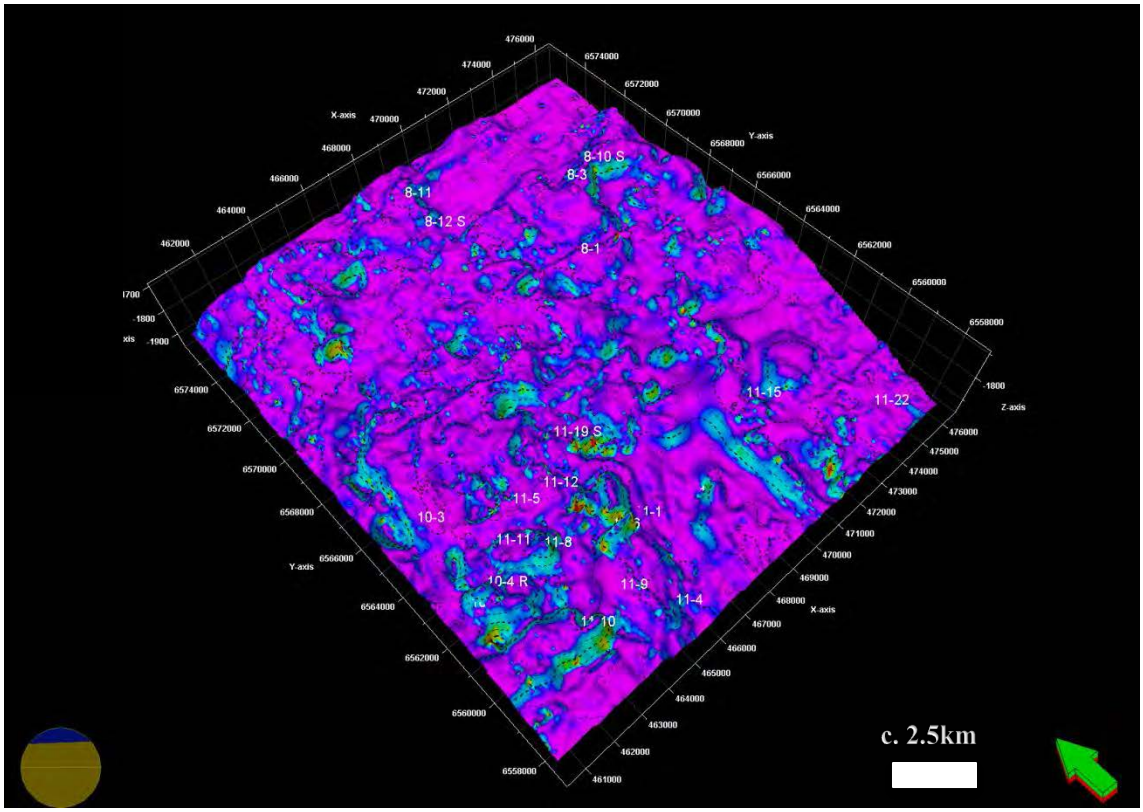


Figure 6.7 (b): Top Lista seismic surface (as above). Dip angles are displayed as surface attribute. Purple colours 8° dip or less, blue-green colours 9-18°, yellow-red 19°-40°. Steepest dipping mound flanks are observed in Balder Field.

high amplitude. Crosscutting seismic reflections can be found, in both crestal areas of mounds and also on flanks of mounds and appear to root from within Lista sequence (Sensu Huuse et al. 2007). Calibration of seismic observations with cored section is required in order to ascribe reflected morphologies as injected sandstones (discussed in Chapter 7). Figure 6.10 depicts quasi-wing and crestal discontinuity features.

Two Mounding styles are apparent, steep angular sided and rounded mounds. Chalk rafts are seen to locate within Lista and Sele sequence mounds. Internally seismic reflections vary between mixed to discontinuous seismic facies.

#### 6.3.3.2 Grane

Top Lista seismic surface is a semi-continuous to discontinuous seismic reflection and is described in Figure 6.8 showing extract value seismic attribute. Amplitude reflection strength decreases eastwards over Grane Field. This is due to extract value attribute sampling surrounding reflections even though a 0ms window is applied, because Lista surface is increasingly discontinuous. The mounded structure of the Grane Field area is shown by dip angle attribute. Minor crosscuts through Lista surface are observed but are not as high amplitude as in Balder Field. A single, rounded elongate mound is identified that does not appear to thin or thicken North or South and is approximately 7.5 km in length.

#### 6.3.3.3 Ringhorne

Top Lista surface is semi-continuous to discontinuous seismic reflection and is described in Figure 6.8 showing extract value seismic attribute. Lista sequence within Ringhorne Field is less mounded than either Grane or Balder Fields (Figure 6.12). Cross cutting seismic geometries are not seen although evidence for fault offset between Lista and Sele is apparent.

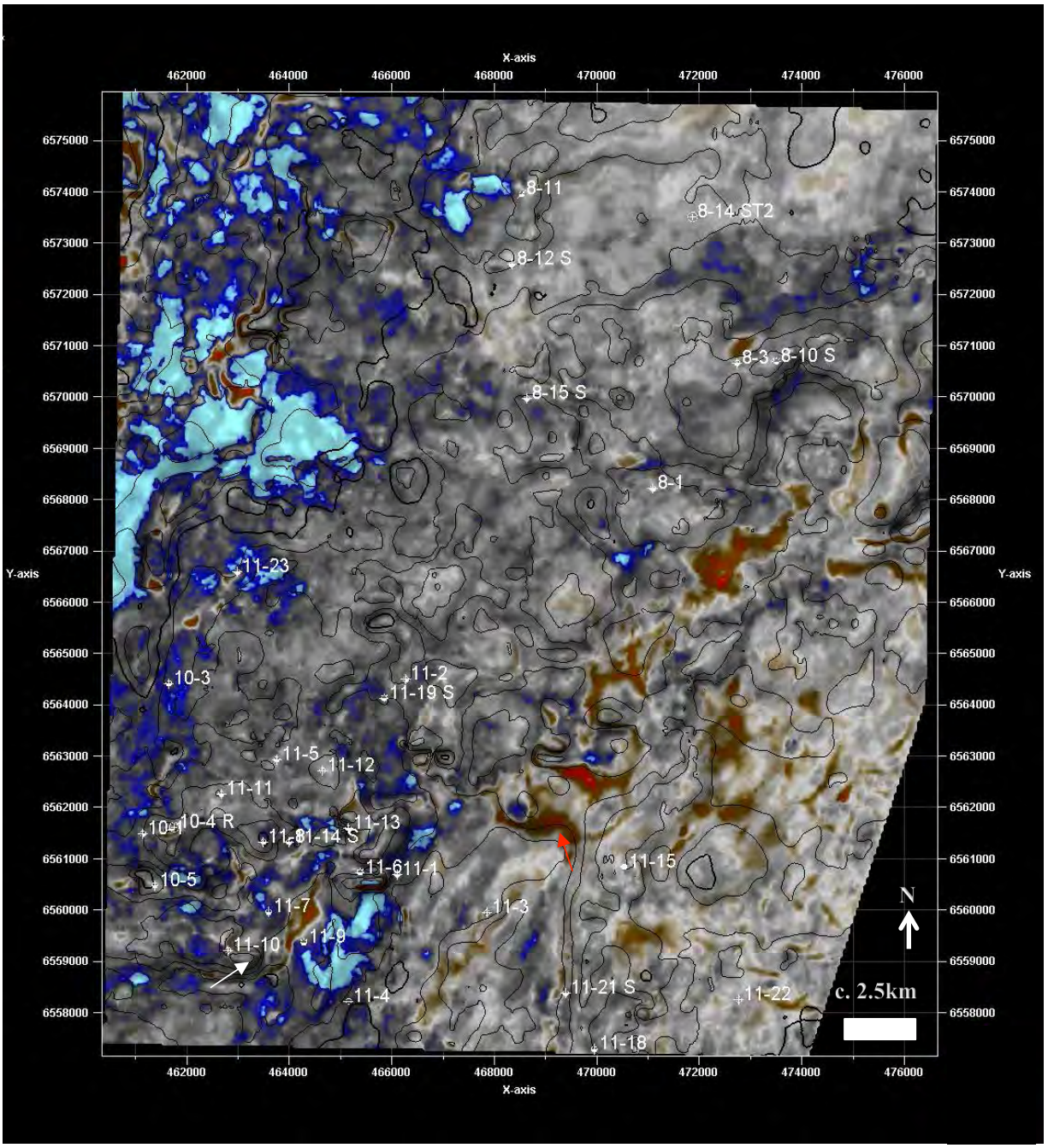


Figure 6.8: Lista sequence displaying extract value attribute with european polarity colour scaling, blue indicates decrease in acoustic impedence, red indicates increase in acoustic impedence. Lista sequence seismic horizon is a blue trough. White arrow points to linear breaks in Lista surface where crosscutting reflections cut through. Red arrow highlights decrease in amplitude continuity eastwards.

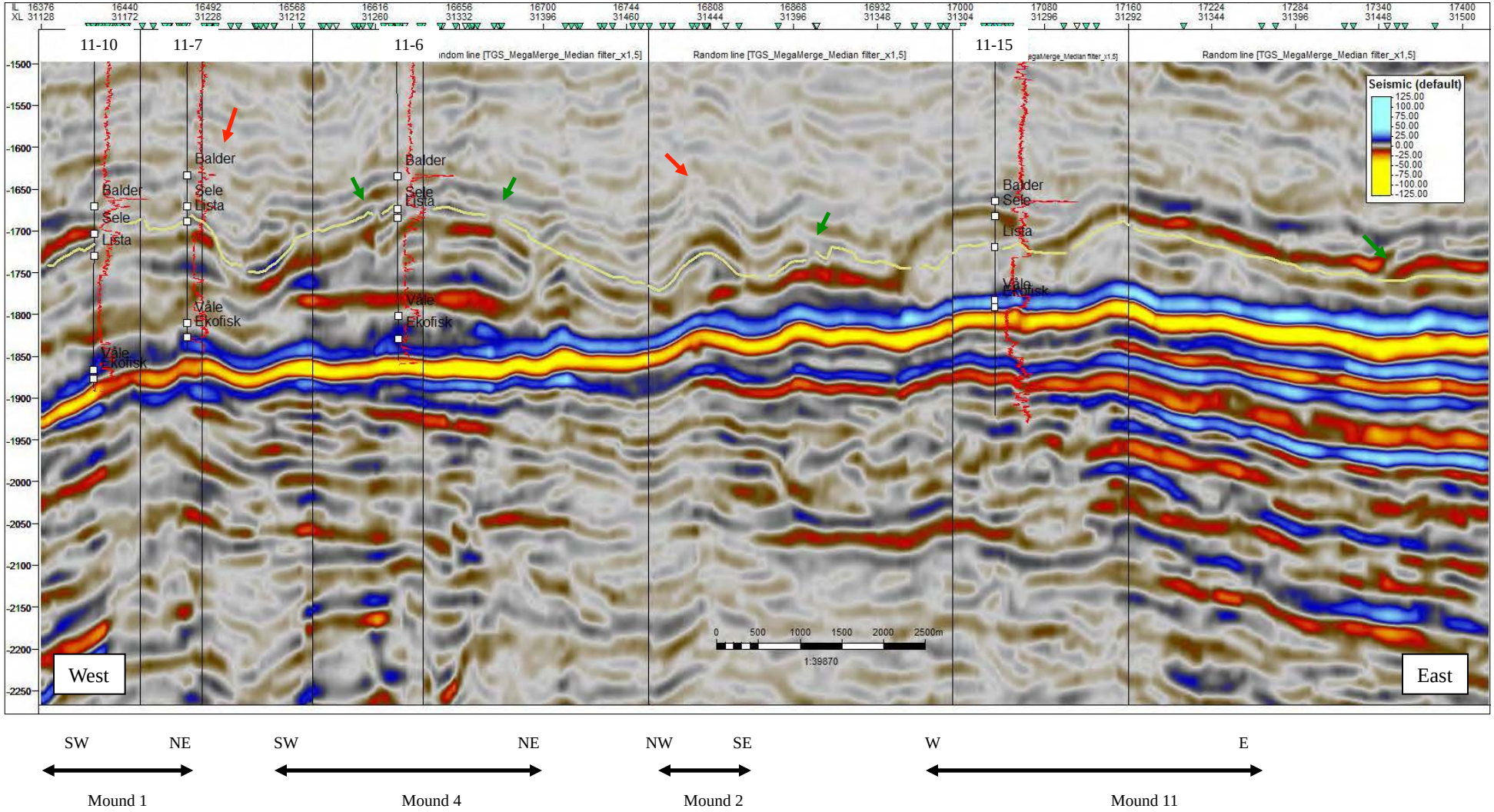


Figure 6.9: Composite seismic section from West (Balder Field) to East (Grane Field). Red Gamma-ray wireline logs displayed on 3d seismic (0-150 API). Yellow seismic horizon highlights Lista sequence pick with good correlation to wireline log stratigraphic interpretation. Green arrows point to discontinuities in Lista sequence, which locate on crests and flanks of mounds. Red arrows show discontinuities in Balder sequence, that locate on Lista sequence mounds in flank and crestal positions.

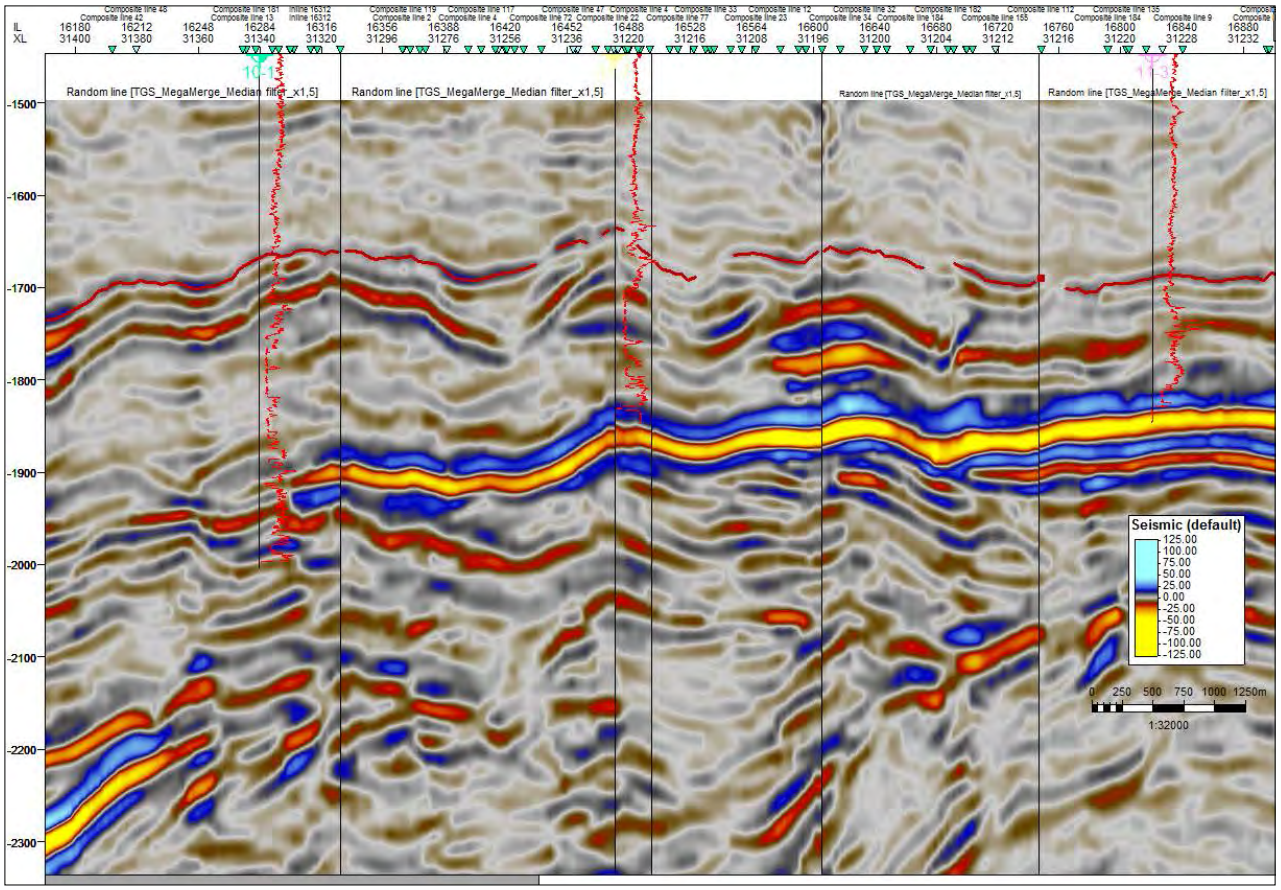


Figure 6.10 (a): Showing heavily mounded features at Lista sequence interval highlighted with a green arrow.

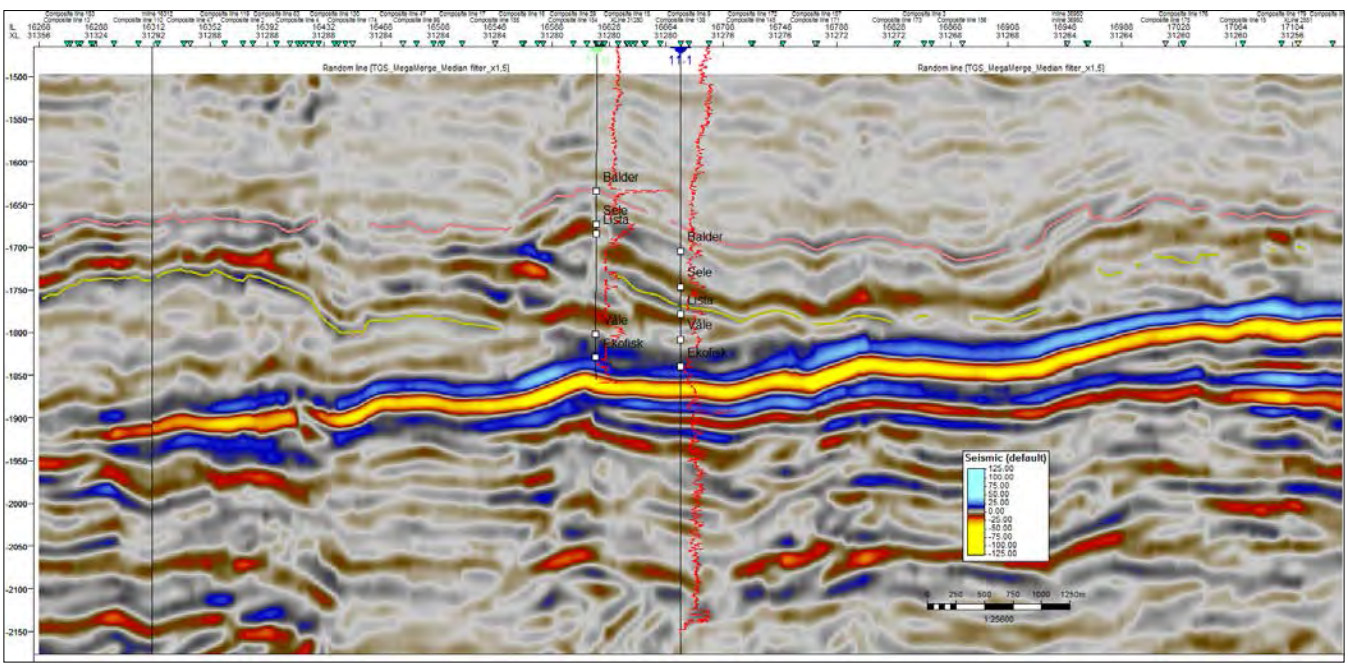


Figure 6.10 (b): Discontinous seismic reflections emanating from Lista sequence at Mound 4. Well 11-6 has intersected this mound and 3 block sandstones are observed.

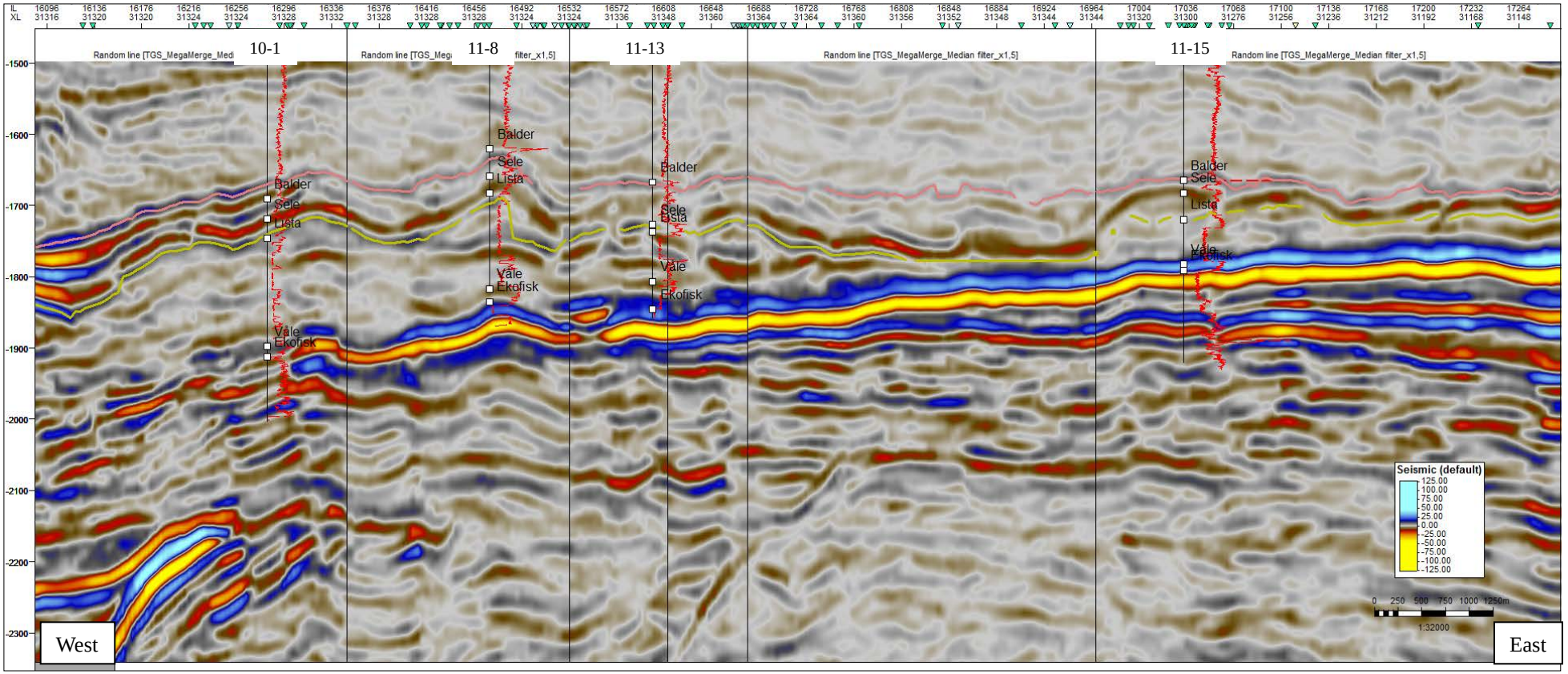


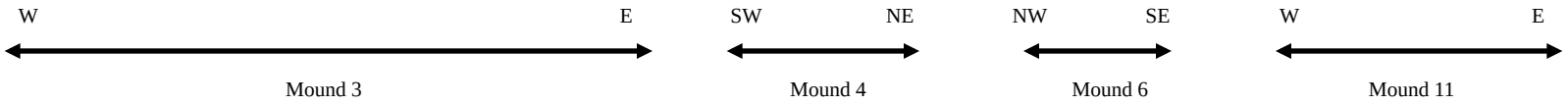


Figure 6.11: Composite seismic section from West (Balder Field) to East (Grane Field). Red Gamma-ray wireline logs displayed on 3d seismic (0-150 API). Yellow seismic horizon highlights Lista sequence pick with good correlation to wireline log stratigraphic interpretation. Red seismic surface indicates Top Balder seismic surface, a clear thickening of the Balder interval is observed between mounds.

### 6.3.4 Sele sequence

Sele seismic horizon is a continuous to semi-continuous reflection across the study area of moderate to high amplitude strength. Composed of a single seismic reflection that mirrors the underlying Lista seismic reflection, some partial thickening of this reflection is observed around flanks of underlying Lista mounds (Figure 6.10). The Sele sequence reflection is cross cut (similarly to Lista sequence) by high amplitude vertical or sub-vertical reflections. Similar to underlying Lista sequence the Sele seismic horizon is extensionally faulted in the West of the Balder Field.

### 6.3.5 Balder sequence

Top Balder seismic surface is continuous across the whole of the study area with a recogniseable dull, and low dip-angle reflection. Balder sequence is comprised of three reflections the lower two reflections onlap Sele sequence surface. Internal discontinuity is observed in this interval. Cross cutting seismic reflections are dull and curved and locate near to the base of the Balder sequence, commonly horizontal. An extra reflection is identified within lows flanking Lista and Sele sequence mounds (Figure 6.11). Mounding is not a characteristic of Balder sequence.

Figure 6.13 shows seismic facies observed at well locations through the study area. Continuous seismic reflections correlate with mudstone prone lithologies of Våle intervals whereas semi-continuous and discontinuous reflections are observed in Lista sequence.

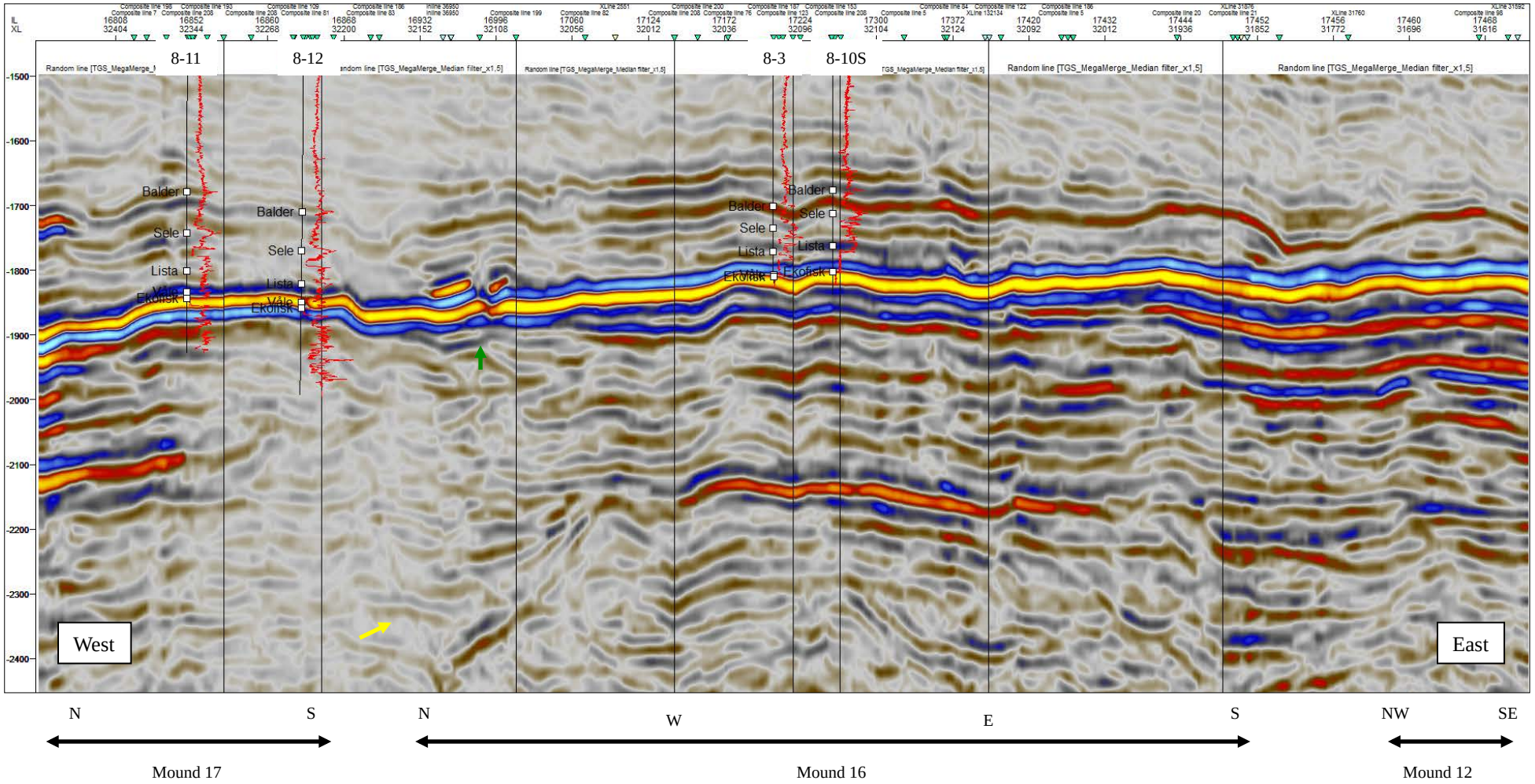


Figure 6.12: Composite seismic section from Northwest Ringhorne Field, Southeast to northern Grane Field. Red Gamma-ray wireline logs displayed on 3d seismic (0-150 API). Green arrows point to discontinuities at Lista and Ekofisk level which locate inside Mound 16. Yellow arrow points to a Mesozoic extensional fault, this fault plane defines the eastern margin of the deeper Jurassic hydrocarbon accumulation. Mound geometries at Ringhorne Field are broad with moderate to steep sides and are more flat topped than the Balder Field area.

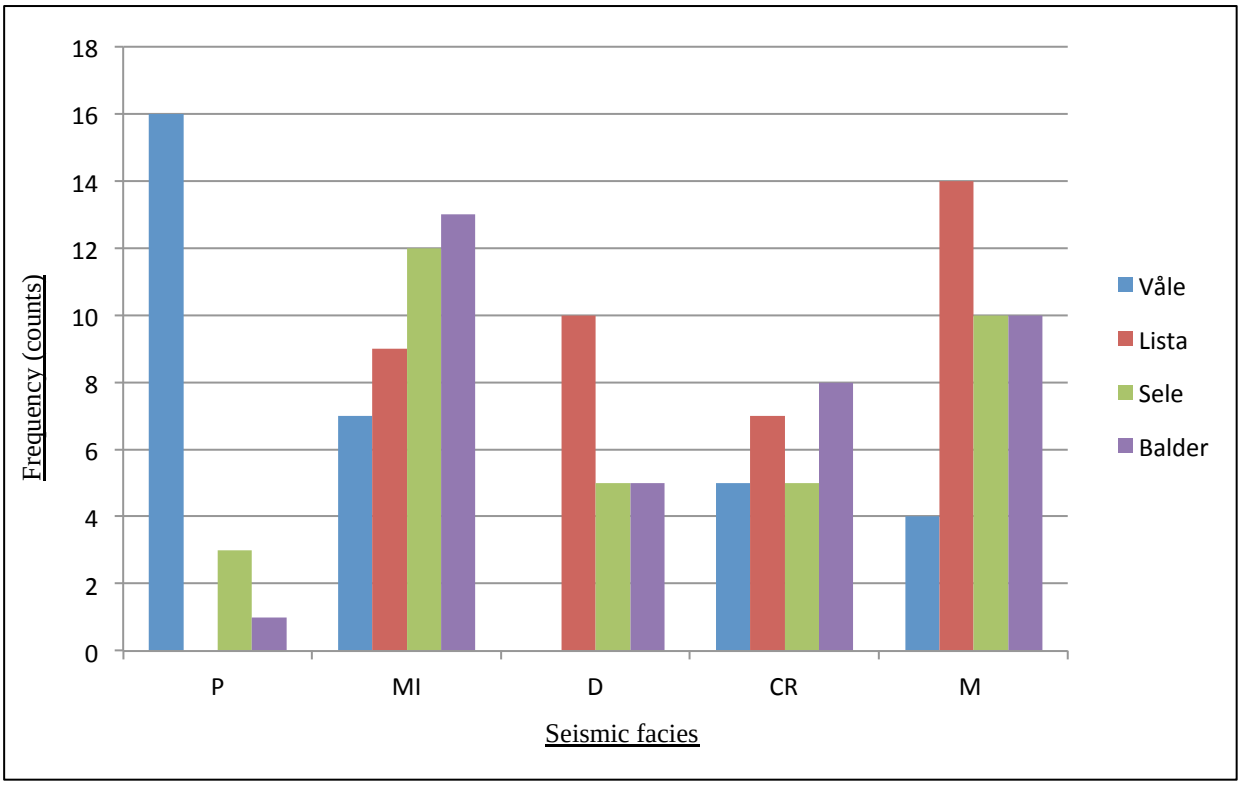


Figure 6.13: Bar chart showing frequency of seismic facies (x-axis) observed at well locations through out the study area, plotted against frequency (y-axis) of occurence. Våle sequence is dominated by continuous seismic reflections (P-S facies). Blocky sandstone wireline log responses are most common in Lista sequence and discontinous seismic reflections are more common in this sequence than any other. Semi-continous seismic reflections and cross-cutting seismic reflections are most are most common in Balder sequence. Mounded seismic facies are present in all sequences, but most commonly in sequences younger than Våle sequence.

### 6.3.6 Other seismic observations

Seismic V-shaped bright amplitude anomalies similar to features identified in Shoulders and Cartwright (2007) and Cartwright et al. (2008) are observed in Eocene mudstones above Balder Field and to the west of the Utsira high, shown in Figure 6.14. Polygonal faulting is observed in the overburden above the interval of interest, shown in Figure 6.14 and appendix 4 (Balder surface, Extract value amplitude extraction). Indications of vertical fluid escape are observed in 6.15. Seismic mapping and attribute extraction of Miocene aged reflections has not yielded any indication of extrudite features at palaeo-sea floor nor have pock marks been observed on the present day seafloor.

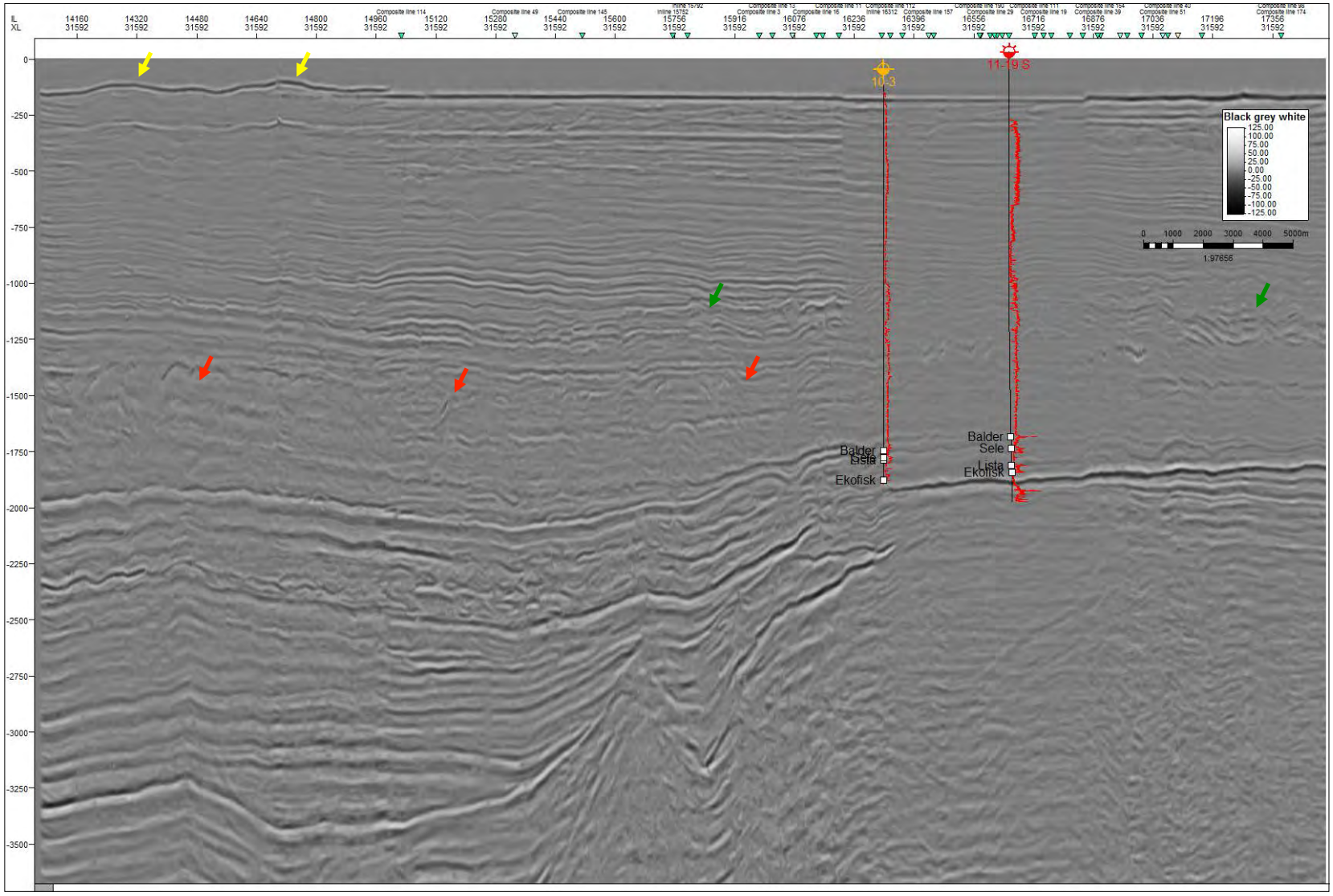


Figure 6.14: Inline 31592 TGS Mega Merge 3D seismic data. Red arrows point to conicol shaped V-injections within Lower Eocene Ypresian, Tay Formation. Green arrows highlight polygonal faulting within mudstone and sandstone lithologies of the Lower Eocene Tay Formation. Yellow arrows indicate velocity 'pull-up' effects, possible causes include vertical fluid migration and poor seismic imaging. It is unlikely that in-situ fluids (e.g. gas hydrates) would cause vertical striping over such a large vertical interval of 3D seismic data.

# Chapter 7: Synthesis

The focus of sections 7.1, 7.2, 7.3, and 7.4 is to correlate observations and interpretations from each dataset and from the three field areas, this is summarised in Appendix 6.

It is acknowledged that sandstone injection features observed in cored section are not directly observable on 3D seismic data. Direct correlation between cored section and seismic confirms an interpretation of injected sandstones (e.g. Jackson et al. 2011) and furthermore allows calibration of seismic data. Sandstone injections observed in cored section are not seismically resolvable as the maximum thickness of sandstone injection observed in cored section was 5m and the vertical resolution of seismic data is over 30m.

## 7.1 Ekofisk sequence

A Limestone platform underlies sediments of Paleocene and Eocene sediments. Limestone may have been eroded during deposition of sandstones of Våle sequence. Further interpretation of this interval is constrained by a lack of cored section, and poor vertical resolution observed on seismic data.

## 7.2 Lista sequence

Dominated by structureless (MS-CS facies) and blocky sandstones (BL-WL) often more than 100m thick, which display small scale loading structures near to the base of section and fluidization structures in upper parts of the sandstone column. Sandstone injections (DTS-CS) identified in cored section intrude into overlying mudstones in Ringhorne Field. Seismically resolvable crosscutting features emanate from the crest and flanks of mounds in Balder Field. Similar seismically observable crosscutting features are less common in Grane Field (western flank of Mound 11) and rare in Ringhorne Field (western flank of Mound 18). From TWT maps Mounding is more pronounced in Balder and Grane Fields where flank angles are commonly in excess of 20° compared to Ringhorne Field which has between 15-20° flank angles. Although these flank angles maybe inaccurate as maps have not been depth converted.

## 7.3 Sele sequence

Blocky sandstones (BL-WL) and interbedded (I-WL) wireline log responses are observed. Loading structures are observed within massive (MS-CS) and bedded sandstones (BS-CS). The internal seismic character of Sele sequence is unresolved (due to seismic imaging) and conforms to Lista sequence upper surface, throughout the study area. Sub-vertical cross cutting seismic facies are observed in Sele sequence in Balder and Grane Fields,

which likely root in Lista sequence.

## 7.4 Balder sequence

A heterogeneous interval, commonly consisting 2-20m thick basal sandstones fining upwards is characteristic of Balder sequence (BS-WL). Sandstone dykes (DTS-CS) and sills (SST-CS) less than 1m thicknesses are observed in cored section from Balder Field. Although uncalibrated by cored section, curved and flat lying seismically resolvable crosscutting reflections over Balder Field offer distinctly different geometries to those observed in Lista and Sele sequences. If calibrated, a vertical transition from vertical and sub-vertical geometries at Lista and Sele sequences, upwards into flat-lying and curved geometries in Balder sequence would suggest sill intrusion at shallower burial than sandstone dyke injections at Lista and Sele sequence levels. Present day, Balder sequence is 300m vertically thick, in the west of the Balder Field (well 10-5). Applying a basic decompaction trend to Balder sequence mudstones (Hansen, 1996) would place Lista sequence approximately 600m from mudline after immediately after deposition of Balder sequence. Depths of this order would favour dyke propagation at Lista sequence and and sill formation in Balder sequence (Jolly and Lonergan 2002).

## 7.5 Overpressure and trigger mechanisms causing sandstone injection

### 7.5.1 Balder Field

Wild and Briedis (2010) proposed that overpressure and trigger mechanisms were caused by catastrophic vertical release of fluid from within the Utsira High (Figure 7.1). In order to test this hypothesis 0.5kg of core was collected from wells 8-10 S (1814m) and 11-19 S (1960m) and cuttings material from well 11-15 (Lista sequence). Initial work (20 gram samples) suggested that heavy minerals Zircon and Garnet were present although in low concentrations. Larger sample sizes were therefore obtained with an aim to collect sufficient heavy minerals to justify U-Pb zircon dating. If heavy mineral signatures correlated with the observations of Morten (1993) a Tertiary aged source terrain (East Shetland Platform) could be applied and conversely, poor correlation could promulgate other provenance (e.g. Morton, 1992, Preston et al. 2002).

A toluene solution was used to remove heavy oil staining from sediments. Sandstones were crushed, sieved and heavy minerals extracted using bromoform solution. Sampled sections were almost devoid of heavy minerals restricting further work.

Kazerouni et al. 2011 describes heavy mineral segregation in injected sandstones from the Siri Canyon Danish North Sea. Caused by the non-uniform flow characteristics of fluidization. This opens the possibility that a placer band of heavy minerals was not intersected and only samples collected from depleted sections have so far been studied.

### 7.5.2 Another example of overpressure development

Conventional explanations (Chapter 2) of overpressure development maybe relevant causes for remobilization and injection in the study area (e.g. Lonergan et al. 2000). A lesser-described mechanism is the location of the Balder Field at the distal pinch-out of the Paleocene fairway, which may have created conditions for overpressure formation.

Extensional faulting is observed in the Lista, Sele and Balder sequences on the western margin of the Balder Field. Martinsen et al. (2005) suggested that differential subsidence of elevated Tertiary sediments on the Utsira High relative to sediments located west within the North Sea basin increased hydraulic head on sandstones located at the distal pinchout (Balder, Ringhorne and Grane Fields). No description of timings of subsidence are given, but elevation of sediments at the distal pinchout would act as a focus for dewatered fluid during early burial from a far larger catchment area than if a flat topography was observed.

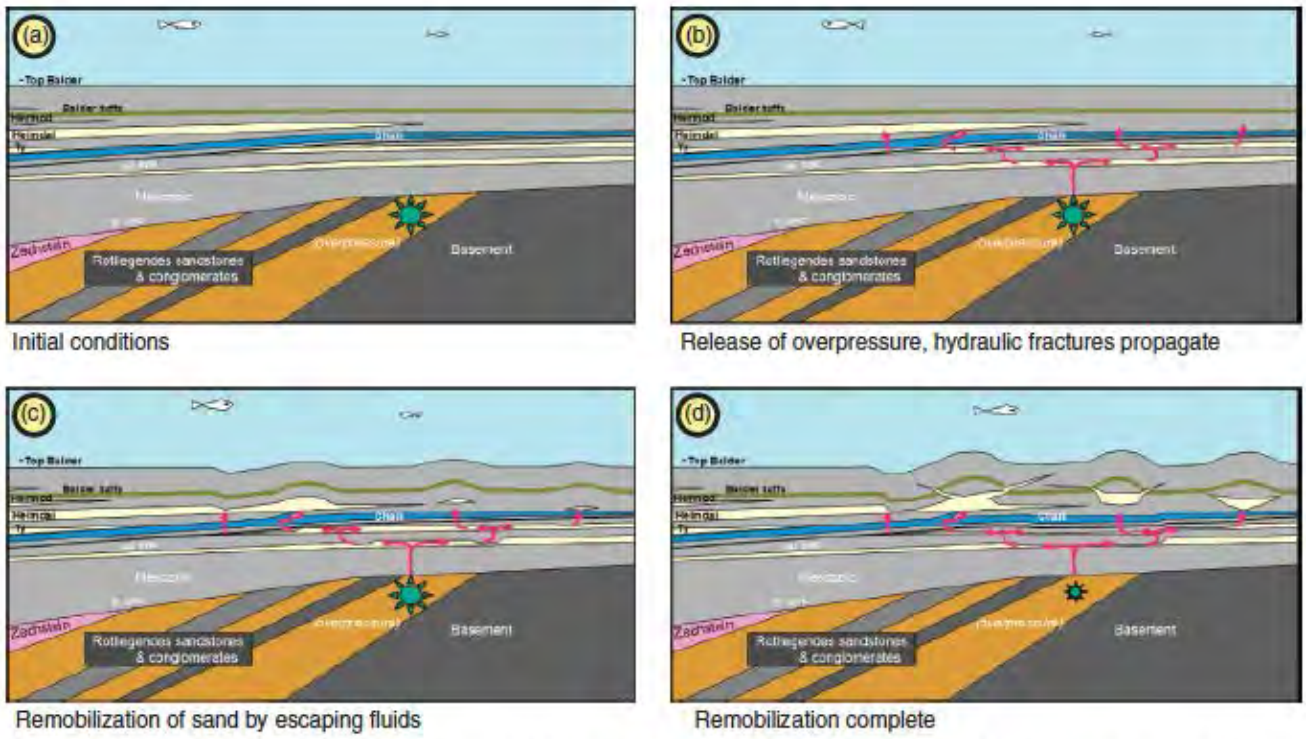


Figure 7.1: Model proposed by Wild and Briedis (2010) showing origin of overpressure development and effect on Paleocene and Eocene sediments.

## 7.6 Discussion and further work

Higher resolution 3D seismic data would add more clarity to geological understanding in this area. It is unclear if crosscutting seismic features (CR-S) are reflections of sandstone injectites as the present 3D seismic dataset is unable to resolve features below 30m. All of the injected sandstone identified in cored section is below 30m thickness. Higher resolution may provide more information on the vertical transition between CR-S facies observed in Lista and Sele sequences and CR-S facies observed in Balder sequence in the Balder Field. Currently seismic data indicates that Ringhorne Field is less affected by remobilization and injection than Balder Field – is this really true? Sandstone injections are observed in core (Well 8-10S) and Lista sequence sandstone is directly juxtaposed against Ekofisk Limestones. Therefore approximately 20-50m of Våle sequence mudstones are missing as deposition of this muddy interval is usually continuous across the study area.

A higher resolution biostratigraphic scheme would allow greater subdivision of the study interval. This is probably only beneficial in conjunction with higher resolution 3D seismic data as well log correlation within a stratigraphically complex interval is unreliable. Further division of Ta and Dvcs (Talling et al. 2012) may constrain presence of loading structures and allow understanding of whether each flow type has any lateral or vertical organisation. UV light, Thin section, X-ray diffraction and scanning electron microscopy could give an indication of mudstone content aiding either a turbulent or debritic division. In addition those techniques may help to apply post-depositional facies to massive sandstones, as fluidized sandstones have tighter grain packing after remobilization (Owen, 1987).
Data from production wells, of which there are approximately 60 wells, has not been included, further work could select and correlate cored sections from winged, crestal and crosscutting seismic reflections. Confirming, disproving or delineating to what extent seismic data correlates with cored section. In an area with so much data coverage it will be important

to selectively pick study data.

Other examples of further work may include, removal of statistical bias from core, wireline and seismic data summary graphs through the use of a bespoke facies scheme. Other further may focus upon heavy mineral analysis either from Balder Field or a known injected sandstone outcrop to understand heavy mineral distribution in injected sandstones.

## 7.7 Discussion, what is good enough evidence to suggest remobilization and injection?

In Chapter 1, 18 mounds were identified through seismic mapping. Mounds 8, 9 and 18 have been shown to contain injected sandstone in cored section. Figure 7.2 is a schematic graph showing the diagnostic capability of facies observed in this project. Cored section offers the only way to confidently identify remobilized and injected sandstones in the subsurface. A range of interpretations exist for wireline log facies and seismic data facies observed in this project.

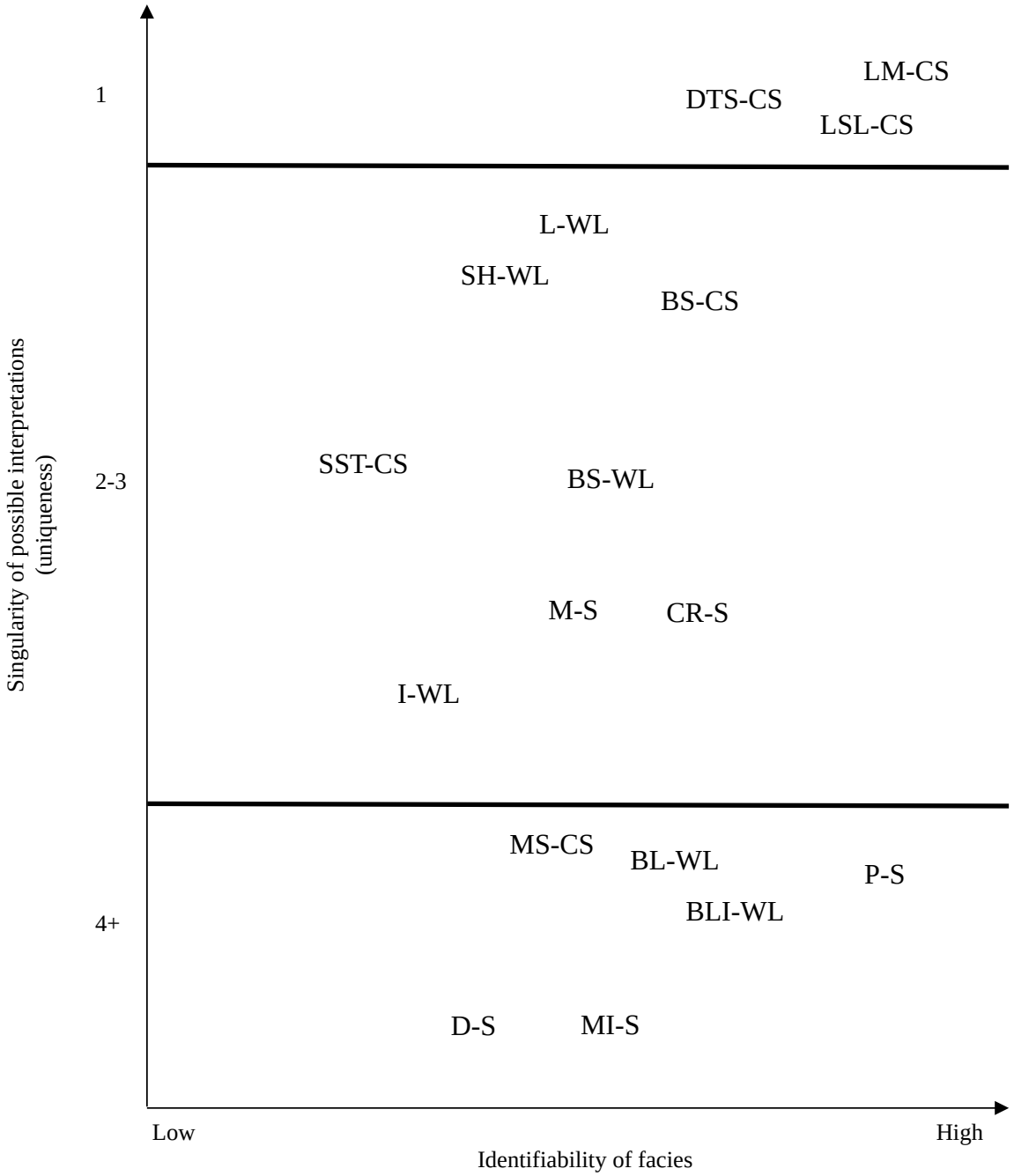


Figure 7.2: A schematic graph highlighting the uniqueness of possible interpretation based on observed facies.

## 7.8 Conclusions regarding subsurface datasets

Cored section data offers the only independent method to identify remobilized and injected sediments in the subsurface. Loading structures are common in gravity flows and may make no impact to connectivity within a reservoir interval. Whereas, injected sandstones may dramatically change reservoir characteristics.

Wireline logs describe lithology and composition of sediments. Single interpretation of depositional setting or depositional process is not possible due to the non-uniqueness of a range of depositional environments when displayed using wireline logs.

Three dimension seismic data uncalibrated by cored section cannot independently identify remobilised and injected sediments, due to resolution issues.

Direct integration of injected sandstones in cored section and seismic data may improve confidence in seismic data as an identification tool.

## 7.9 Conclusions regarding the Balder Field area

Loading and post-depositional fluidization structures are identified in Lista sequence, but sandstone injections are more commonly observed in Sele and Balder sequences in cored section, through-out the study area. Steeper flank angles observed from seismic data suggest a tentative interpretation that remobilization and injection has affected Balder Field to a greater degree than Grane Field and crosscutting seismic reflections are more common. From seismic data Ringhorne Field displays the least effects of remobilization and injection in this area.

## References

Anderton, R. 1995. Clastic facies models and facies analysis. Geological Society, London, Special Publications 1985, V. 18, p31-47

Allen, J. R. L. 1982. Sedimentary structures: their character and physical basis. Developments in sedimentology, vol. 30A. Amsterdam: B. Elsevier.

Alvarez, W., Stanley, E., O'Conner, D. and Chan, M. 1998. Synsedimentary deformation in the Jurassic of southeastern Utah – a case of impact shaking? Geology, 26, p.579-582

Ahmadi, Z.M., Sawyers, M., Kenyon-Roberts, S., Stanworth, C.W., Kugler, K.A., Kristensen J. and Fugelli, E.M.G. 2003, Paleocene, in Evans D., Graham C., Armour A., Bathurst P., (eds), The millennium atlas: Petroleum geology of the Central and northern North Sea: The Geological Society (London) pp 235-259

Amy, L. A., Talling, P. J., Peakall, J., Wynn, R. B. and Arzola Thynne, R. G. 2005 Bed geometry used to test recognition criteria of turbidites and (sandy) debrites. Sed. Geol., 79, 163–174.

Andresen, K., Clausen, O.R. & Huuse, M. 2009. A giant (5.3*107 m3) middle Miocene (c. 15 Ma) sediment mound (M1) above the Siri Canyon, Norwegian–Danish Basin: Origin and significance. Marine and Petroleum Geology, 27,

Baas, J.H. 2004 Conditions for formation of massive turbidite sandstones by primary depositional processes. Sed. Geol., 166, 293–310.

Beaubouef, R.T., 2004. Deep-water leveed-channel complexes of the Cerro Torro Formation, Upper Cretaceous, southern Chile. American Association of Petroleum Geologists 88 (11), 1471–1500.

Bergslien D., 2002 Balder and Jotun-two sides of the same coin? A comparison of two tertiary oil fields in the Norwegian North Sea: Petroleum Geoscience, v. 8, pp349-363

Bouma, A.H. 1962. Sedimentology of some Flysch deposits: A graphic approach to facies interpretation, Amsterdam: Elsevier, pp 168.

Bouma, A.H. 2004. Key controls on the characteristics of turbidite systems. In Lomas S A and Joeseph P (eds) 2004. Confined turbidite systems. Geological Society, London, Special publications, 222, p9-22.

Braccini, E., De Boer, W., Hurst, A., Huuse, M., Vigoritto, M., & Templeton, G. 2008. Sand injectites. Oilfield Review. 20 p34-49

Briedis, N. A., Bergslien D., Hjellbakk A, Hill R. E. and Moir G. J. 2007. Recognition criteria, significance to field performance, and reservoir modeling of sand injections in the Balder field, North Sea, in Hurst A., Cartwright J., (eds) Sand injectites: Implications for hydrocarbon exploration and production: AAPG Memoir 87, p.91-102.

Brown, A. 2006. Interpretation of Three-Dimensional Seismic Data, sixth ed. (AAPG Memoir 42).

Carstens, H. 1985. Early diagenetic cone-in-cone-structures in pyrite concretions. Journal of Sedimentary Petrology. Volume 55. Pg 105-108

Lonergan, L. and Cartwright, J.A. 1999. Polygonal Faults and Their Influence on Deep-Water Sandstone Reservoir Geometries, Alba Field United Kingdom Central North Sea. AAPG Bulletin, V. 83, No.3. p410-432.

Cartwright, J.A. and Dewhurst, D.N. 1998, Layer-bound compaction faults in fine-grained sediments: Geological Society of America Bulletin. V. 110, p. 1242-1257

Cartwright, J., James, D., Huuse, M., Vettel, W. & Hurst, A. 2008. The mechanics of saucer-shaped sandstone intrusions. Journal of Structural Geology, 30, 854-867.

Cartwright, J. 2010. Regionally extensive emplacement of sandstone intrusions: a brief review. Basin research, 22, 502-561.

Catuneau, O. 2006. Principles of Sequence Stratigraphy. Elsevier, 375 pp

Catuneau, O., Bhattacharya, J.P., and 22 others. 2010. Sequence stratigraphy: common ground after three decades of development. First break, v.28, p.41-54

Coward, M.P., Dewey, J.F., Hempton, M. and Holroyd, J. 2003. Tectonic evolution. P.17-33. In The Millenium Atlas: Petroleum geology of the Central and northern North Sea. in Evans D., Graham C., Armour A., Bathurst P., (eds). The Geological Society of London.

Cronin, B.T. and Kidd. R.B. 1998. Heterogeneity and lithotype distribution in ancient deep-sea canyons: Point Lobos deep-sea canyon as a reservoir analogue. Sedimentary Geology 115. Pp315-349

Davies, R.J., Posamentier, H.W., Wood, L.J. and Cartwright, J.A. (eds) 2007. Seismic Geomorphology: Applications to Hydrocarbon Exploration and Production. Geological Society, London, Special Publications, 277

Davies, R.J., Huuse, M., Hirst,P., Cartwright, J. and Yang, Y. 2006. Giant clastic intrusions primed by silica diagenesis. Geology 2006: 34 pp 917-920

Deegan. C.E., and Scull, B.J., 1977, A standard lithostratigraphic nomenclature for the Mesozoic of the Central and northern North Sea, in Finstad K G., and Selley R C., Coordinators, Mesozoic; Northern North Sea Symposium 1997 Proceedings: Norwegian Petroleum Society, p 24

de Boer, W., Rawlinson, P.B., and Hurst, A. 2007. Successful Exploration of a Sand Injectite Complex: Hamsun Prospect, Norway Block 24/9. In: Hurst, A., Cartwright, J. (Eds.), Sand Injectites: Implications for Hydrocarbon Exploration and Production: American Association of Petroleum Geologists Memoir, Tulsa, p.65–68.

den Hartog Jager, D., Giles, M.R. and Griffiths, G.R. (1993) Evolution of Paleogene

submarine fans in space and time. In: Petroleum Geology of Northwest Europe: Proceedings of the 4th Conference (Ed. by J.R. Parker), pp. 59-71.Geological Society, London.

Dewhurst, D.N., Yang, Y. and Aplin, C. 1999. Permeability and fluid flow in natural mudstones. Geological Society, London, Special Publications, v.158, p.23-43

Diggs, T.N., 2007. An outcrop study of clastic-injection structures in the Carboniferous 1808
Tesnus Formation, Marathon basin, Trans-Pecos Texas. In: Hurst, A., Cartwright, J. 1809
(Eds.), Sand Injectites: Implications for Hydrocarbon Exploration and Production: 1810
American Association of Petroleum Geologists Memoir, Tulsa, pp. 209–219.

Dixon, R.J., Schofield, K., Anderton, R., Reynolds, A.D., Alexander ,R.W.S., Williams, M.C. and Davies K G., 1995. Sandstone diapirism and clastic intrusion in the Tertiary submarine fans of the Bruce-Beryl embayment, Quadrant 9, UKCS, in Hartley A J., and Prosser D J., (eds) Characterization of deep marine clastic systems: Geological Society of London, Special Publications, 94, p.77-94

DiFelice, R., 1995. Hydrodynamics of liquid fluidization. Chemical Engineering Science 1804
50, 1213–1245.

Dimitrieva, E., Jackson, C.A.L., Huuse, M. and McCarthy, A. 2012. Palaeocene deep-water depositional systems in the North Sea Basin: a 3D seismic and well data case study, offshore Norway. Petroleum Geoscience, Vol. 18, 2012, pp 97-114

Duranti, D., Hurst, A., Hanson R., Bell, C., and McLeod, M., 2000. Reservoir characterization of a remobilized sand-rich turbidite reservoir-The Alba field. In: Petroleum Geology of Northwest Europe , Proceedings of the 4th Conference (ed.) J.R. Parker, Geological Society of London, pp161-171

Duranti D., Hurst A., Bell C., Groves S., and Hanson R., 2002, Injected and remobilized sands from the Alba field (Eocene, UKCS): Core and and wireline log characteristics: Petroleum Geoscience, V. 8 pp99-107.

Duranti, D. and Hurst, A. 2004. Fluidisation and injection in the deep-water sandstones of the Eocene Alba Formation (UK North Sea). Sedimentology, v.51, p.503-529

Eggenhuisen, J.T., McCaffrey, W.D., Haughton, P.D.W., Butler, R.W.H., Moore, I., Jarvie, A. and Hakes, W.G. 2010. Reconstructing large-scale remobilization of deep-water deposits and its impact on sand-body architecture from cored wells: The Lower Cretaceous Britannia Sandstone Formation, UK North Sea. Marine and Petroleum Geology, 27, p.1595-1615

Emery, D. and Myers, K. J. (eds) 1996. Sequence Stratigraphy. v + 297 pp. Oxford: Blackwell Science. ISBN 0 632 03706 7.

Embry A F 1990. Depositional sequences – theoretical considerations, boundary recognition and relationships to other genetic. In: A. Mørk (editor), Sequence stratigraphy Field Workshop, Svalbard 1990. Continental Shelf Institute (IKU), Trondheim, pp 1-26.

Embry, A.F. and Johannessen, E.P. 1992. T-R sequence stratigraphy, facies analysis and reservoir distribution in the uppermost Triassic-Lower Jurassic succession, western Sverdrup

basin, Arctic Canada. In T.O. Vorren, E. Bergsager, Ø.A. Dahl-Stamnes, E Holter, B. Johansen, e. Lie and T.B Lund (eds), Arctic Geology and Petroleum Geology. Norwegian Petroleum Society (NPF), Special Publication 2. Elsevier, Amsterdam, pp. 121-146.

Faleide, J.I., Kyrkjebø, R., Kjennerud T., Gabrielsen R H., Jordt H., Fanavoll S., and Bjerke MD., 2002. Tectonic impact on sedimentary processes during Cenozoic evolution of the northern North Sea and surrounding areas. In: Dore A G., Cartwright J A., Stoker M S., Turner J P. & White N. (eds) Exhumation of the North Atlantic Margin: Timing, mechanisms and implications for Petroleum Exploration. Geological Society, London, Special Publications, 196, 235-269.

Felix, M. and Peakall, J. (2006) Transformation of debris flows into turbidity currents: mechanisms inferred from laboratory experiments, Sedimentology, **53**, pp.107-123.

Felix, M., Leszczynski, S., Slaczka, A., Uchman, A., Amy, L. and Peakall, J. 2009. Field expressions of the transformation of debris flows into turbidity currents, with examples from the Polish Carpathians and the French Maritime Alps, Marine and Petroleum Geology, 26, p.2011-2020

Flint, S.S., Hodgson, D.M., et al. 2011. Depositional architecture and sequence stratigraphy of the Karoo basin floor to shelf edge succession, Laingsburg depocentre, South Africa. Marine and Petroleum Geology, 28, 658–674.

Fitzsimmons R., Veiberg D., & Kråkenes T., 2005 Characterization of the Heimdal Sandstones within Alveim, Quads 24 and 25, Norwegian North Sea. In Doré A G., And Vining B A., (eds) Petroleum Geology: North-West Europe and Global Perspectives-Proceedings of the 6th Petroleum Geology Conference, published by Geological Society, London pp123-131.

Fretwell, P.N., Gordon Canning, W., Hegre, J., Labourdette, R. & Sweatman, M. 2007. A new approach to 3-D geological modeling of complex sand injectite reservoirs: the Alba Field, United Kingdon Central North Sea. In: Hurst, A. & Cartwright J. (eds) Sand Injectites: mplications for Hydrocarbon Exploration and Production. American Association of Petroleum Geologists Memoirs, 87, 119–127.

Frey-Martínez, J., Cartwright, J., Hall, B., Huuse, M., 2007. Clastic intrusion at the base of deep-water sands: A trap-forming mechanism in the eastern Mediterranean. In: Hurst, A., Cartwright, J. (Eds.), Sand Injectites: Implications for Hydrocarbon exploration and Production: American Association of Petroleum Geologists Memoir, Tulsa, pp. 49–63.

Gay, A. and Berndt, C. 2007. Cessation/reactivation of polygonal faulting and effects on fluid flow in the Vøring Basin, Norwegian Margin. Journal of the Geological Society, London, Vol. 164, 2007 pp.129-141.

Gabrielsen, R.H., Kyrkjebø, R., Faleide, J.I., Fjeldskaar, W. and Kjennerud, T. 2001. The Cretaceous post-rift basin configuration of the northern North Sea. Petroleum Geoscience, 7, p. 137-154

Galloway, W.E. 1989. Genetic sequence stratigraphic sequences in basin analysis I: Architecture and genesis of flooding-surface bounded depositional

units. American Association of Petroleum Geologists Bulletin, 73, 125–142.

Galloway, W.E., Garber, J.L., Liu, X. & Sloan, B.J. 1993. Sequence stratigraphic and depositional framework of the Cenozoic fill, Central and Northern North Sea Basin. In: Parker, J.R. (ed.) Petroleum Geologyof Northwest Europe: Proceedings of the 4th Conference. GeologicalSociety, London, 33–43.

Gamberi, F. 2010. Subsurface sediment remobilization as an indicator of regional-scale defluidization within the upper Tortonian Marnoso-arenacea formation (Apenninic foredeep, northern Italy). Basin Research, 22, p.562-577

Ghibaudo, G. 1992. Subaqueous Sediment Gravity Flows: Practical Criteria for their Field Description and Classification. Sedimentology, v.39, p.423-454.

Goldsmith, P.J., Hudson, G. and Van Veen, P. 2003. Triassic. In: Evans, D., Graham, C., Armour, A. and Bathurst, P (eds.), The Millennium Atlas: petroleum geology of the central and northern North Sea, p. 105-127.

Glennie, K.W. 1990a. Outline of North Sea History & Structural framework. In Glennie, K.W. (ed). Introduction to to the Petroleum Geology of the North Sea. Blackwell Scientific Publications.

Haaland, H.J., Furnes, H., Martinsen, O.J. 2000. Paleogene tuffaceous intervals, Grane Field (Block 25/11), Norwegian North Sea: their depositional, petrographical, geochemical character and regional implications. Marine and Petroleum Geology, 17, p.101-118

Hadler-Jacobsen, F., Gardner, M.H. and Borer, J.M. 2007. Seismic stratigraphic and geomorphic analysis along the West African continental margin. Seismic Geomorphology: Applications to Hydrocarbon Exploration and Production. Geological Society, London, Special Publications, 277

Haq, B.U., Hardenbol, J. and Vail, P.R. 1988. Mesozoic and Cenozoic chronostratigraphy and cycles of relative sea-level change. In: Sea-level Changes – An integrated Approach. Wilgus, C.K. and six others (eds). Special publication of the Society of Economic Petrologists and Mineralogists, No.42, p.71-108

Hamberg, L., Jepsen, A.M., Borch, N.T., Dam, G., Engkilde, M.K., Svendsen, J.B., 2007. Mounded Structures of Injected Sandstones in Deep-marine Paleocene Reservoirs, Cecile Field, Denmark. In: Hurst, A., Cartwright, J. (Eds.), Sand Injectites: Implications for Hydrocarbon Exploration and Production: American Association of Petroleum Geologists Memoir, Tulsa, pp. 69–79.

Hanslien, S. 1987. Balder. Geology of Norwegian Oil and Gas Fields. Graham & Trotman, London, pp 193-201

Hansen, S. 1996. A compaction trend for Cretaceous and Tertiary shales on the Norwegian Shelf based on sonic transit times: Petroleum Geoscience, V. 2, pp159-166.

Haughton, P.D.W., Barker, S.P. and McCaffrey, W.D. 2003. 'Linked' debrites in sand-rich

turbidite systems – origin and significance. Sedimentology, 50, p.459-482

Hempton, M., Marshall, J., Sadler, S., Hogg, N., Charles, R. & Harvey, C. 2005. Turbidite reservoirs of the Sele Formation, Central North Sea: geological challenges for improving production. In: Parker, J.R. (ed.) Petroleum Geology of Northwest Europe and Global Perspectives – Proceedings of the 6th Petroleum Geology Conference. Geological Society, London, 449–459.

Hillier, R. D. and Cosgrove, J.W. 2002. Core and seismic observations of overpressure-related deformation within Eocene sediments of the Outer Moray Firth, UKCS. Petroleum Geoscience, Vol. 8 2002, pp. 141-149

Hiscott, R.N. and Pickering, K.T. 1984. Reflected turbidity currents on an Ordovician basin floor, Canadian Appalachians. Nature, 311, pp.143-145

Hubbard, S.M., Romans, B.W., Graham, S.A., 2007. An outcrop example of large-scale conglomeratic intrusions sourced from deep-water channel deposits, Cerro Toro Formation, Magallanes basin, southern Chile. In: Hurst, A., Cartwright, J. (Eds.), Sand Injectites: Implications for Hydrocarbon Exploration and Production: American Association of Petroleum Geologists Memoir, Tulsa, pp. 199–207.

Hurst S., Lovell M A., Morton A., 1990. Geological Applications of Wireline Logs. Geol Soc Spec Pub 48

Hurst, A., Cartwright, J. and Duranti, D. 2003. Fluidization structures produced by upward injection of sand through a sealing lithology. Subsurface sediment mobilization: Introduction: Geological Society [London] Special Publication

Hurst, A., Cartwright, J.A., Duranti, D., Huuse, M. and Nelson, M. 2005. Sand injectites: an emerging global play in deep-water clastic environments. In: Doré, A.G. & Vining, B. (eds) Petroleum Geology of NW Europe: Proceedings of the 6th Conference, Geological Society, London, p.133-144

Hurst, A. and Cartwright, J. 2007. Relevance of Sand Injectites to Hydrocarbon Exploration and Production: In Hurst, A. and Cartwright, J. (eds). Sand injectites: Implications for hydrocarbon exploration and production: AAPG Memoir 87, p.1-19

Hurst, A., Scott, A. and Vigorito, M. 2011. Physical characteristics of sand injectites. Earth-Science Reviews, 106, p.215–246.

Hurst, A., Cartwright, J.A., Huuse, M. & Duranti, D. 2006. Extrusive sandstones (extrudites): a new class of stratigraphic trap? Geol. Soc., London, Spec. Publ., 254, 289-300.

Husmo, T., Hamar, G.P., Høiland, O., Johannesen, E.P., Rømuld, A., Spencer, A.M. and Titterton, R. 2003. Lower and Middle Jurassic. 129-155. in The Millenium Atlas: Petroleum geology of the central and northern North Sea. in Evans D., Graham C., Armour A., Bathurst P., (eds),

Hustoft, S., Bunz, S. and Mienert, J. 2010. Three-dimensional seismic analysis of the morphology and spatial distribution of chimneys beneath the Nyegga pockmark field,

offshore mid-Norway. Basin Research, 22, p.465-480

Huuse, M. 2002. Cenozoic uplift and denudation of southern Norway: insights from the North Sea basin. Geological Society, London, Special publications, vol.196, p.209-233

Huuse, M. and Mickelson, M. 2004. Eocene sandstone intrusions in the Tampen Spur area (Norwegian North Sea Quad 34) imaged by 3D seismic data. Marine and Petroleum Geology, vol.21, p.141–155

Huuse, M., Duranti, D., Steinsland, N., Guargena, C. G., Prat, P., Holm, K., Cartwright, J. A. & Hurst, A. 2004. Seismic characteristics of large-scale sandstone intrusions in the Paleogene of the South Viking Graben, UK and Norwegian North Sea. In: Davies R. J., Cartwright J., Stewart S. A, Underhill, J. R., Lappin M. (eds) 3D Seismic Technology: Application to the Exploration of Sedimentary Basins. Geological Society, London, Memoir, 29, 263-277.

Huuse, M., Cartwright, J., Gras, R. & Hurst, A. 2005. Km-scale sandstone intrusions in the Eocene of the Outer Moray Firth (UK North Sea): migration paths, reservoirs, and potential drilling hazards. In: Doré, A.G. & Vining, B. (eds) Petroleum Geology of NW Europe: Proceedings of the 6th Conference, Geological Society, London, 1577-1594

Huuse, M., Cartwright, J., Hurst, A. and Steinsland, N. 2007. Seismic Characterization of Large-scale Sandstone Intrusions. In: Hurst, A. & Cartwright, J. (ed.) Sand Injectites: Implications for Hydrocarbon Exploration and Production. AAPG Memoir, 87, p.21–35

Huuse, M., Jackson, C.A.L., Van Rensbergen, P., Davies, R.J., Flemings, P.B., Dixon, R.J. 2010. Subsurface sediment remobilization and fluid flow in sedimentary basins: an overview, Basin Research, 2010, Vol.22, p.342-360

Isaksen, D. and Tonstad, K. 1989. A revised Cretaceous and Tertiary lithostratigraphic nomenclature for the Norwegian North Sea. Bulletin of Norwegian Petroleum Directorate, No. 5.

Ilstad, T., De Blasio, F.V., Elverhøi, A., Harbitz, C.B., Engvik, L., Longva, O. and Marr, J.G. 2004. On the frontal dynamics and morphology of submarine debris flows. Marine Geology, 213, p.481-497

Jackson, C.A.L. 2007. The geometry, distribution and development of clastic injectites in deep-marine depositional systems: examples from the Late Cretaceous Kyrre Formation, Maløy Slope, Norwegian Margin. In: Hurst, A. & Cartwright, J.A. (eds) Sand Injectites: Implications for Hydrocarbon Exploration and Production. American Association of Petroleum Geologists, Memoirs, 87, 37–48.

Jackson, C.A.L., Kane, K.E. and Larsen, E. 2010. Structural evolution of minibasins on the Utsira High, northern North Sea; implications for Jurassic sediment dispersal and reservoir distribution, Petroleum Geoscience, Vol.16, p.105-120

Jackson, C.A.L. and Somme, T.O. 2011. Borehole evidence for wing-like clastic intrusion complexes on the western Norwegian margin, Geological Society of London, Vol:168, p.1075-1078

Jackson, C.A.L., Mahlo, S. and Briggs, O. 2013. The Role of Polygonal Fault Mapping in De-Risking Deepwater Reservoir Presence: A 3-D Seismic Reflection Case Study from Offshore Norway. AAPG conference,

Joy, A.M. 1993. Comments on the pattern of post-rift subsidence in the Central and Northern North Sea Basin. In: Williams, G.D. & Dobb, A.(eds) Tectonics and Seismic Sequence Stratigraphy. Geological Society,London, Special Publications, 71, 123–140.

Johansson, M., Braakenburg, N.E., Stow, D.A.V. and Faugères, J.C. 1998. Deep-water massive sands: facies, processes and channel geometry in. the Numidian Flysch, Sicily. Sedimentary Geology, 115, p233-265.

Jenssen, A. I., Bergslien, D., Rye-Larsen, M. and Lindholm R. M. 1993. Origin of complex mound geometry of Paleocene submarine-fan sandstone reservoirs, Balder Field, Norway. Petroleum Geology of Northwest Europe: Proceedings of the 4th conference (edited by J. R. Parker). The Geological Society, London, p.135-143

Jennette, D.C., Garfield, T.R., Mohrig, D.C. and Cayley, G.T. 2000. The interaction of shelf accommodation, sediment supply and sea level in controlling the facies, architecture and sequence stacking patterns of the Tay and Forties/Sele basin- floor fans, central North Sea. In: Deep-Water Reservoirs of the World (Ed. by P.Weimer, R.M. Slatt, J. Coleman, N.C. Rosen, H. Nelson, A.H. Bouma, M.J. Styzen & D.T. Lawrence), GCSSEPM Found., 20th Annual conf., Houston p.402-421

Jolly, R.J.H. and Lonergan, L. 2002, Mechanism and controls on the formation of sand intrusions: Journal of the Geological Society (London) v. 159, pp 605-617

Jonk, R., Hurst A., Duranti D., Parnell J., Mazzini A., and Fallick A E., 2005, Origin and timing of sand injection, petroleum migration, and diagenesis in Tertiary reservoirs, South Viking Graben, North Sea. AAPG Bull., 89 (3) pp 329-357

Jonk, R., Cronin, B.T., Hurst, A., 2007. Variations in Sediment Extrusion in Basin-floor, Slope, and Delta-front Settings: Sand Volcanoes and Extruded Sand Sheets fromthe Namurian of County Clare, Ireland. In: Hurst, A., Cartwright, J. (Eds.), Sand Injectites: Implications for Hydrocarbon Exploration and Production: American Association of Petroleum Geologists Memoir, Tulsa, pp. 221–226.

Jonk, R. 2010. Sand-rich injectites in the context of short-lived and long-lived fluid flow. Basin Research 22, pp603-621.

Jones, S.M., White, N., Clarke, B.J., Rowley, E. and Gallagher, K. 2002. Present and past

influence of the Iceland Plume on sedimentation. in Dore, A.G., Cartwright, J.A., Stoker, M.S., Turner, J.P. and White, N. 2002. exhumation of the North Atlantic Margin: Timing, mechanisms and Implications for Petroleum Exploration. Geological Society, London, Special Publications, 196, 13-25.

Jordt, H., Thyberg, B.I. and Nøttvedt, A. 2000. Cenozoic evolution of central and northern North Sea with focus on differential vertical movements of the basin floor and surrounding clastic source areas. In Nøttvedt A et al. (eds). Dynamics of the Norwegian Margin. Geological Society, London, Special publications, 167, 219-243.

Kane, I.A. and Hodgson, D. 2010 Submarine channel levees: criteria for recognition of levee subenvironments: exhumed examples from The Rosario Fm (Baja, Mexico) and the Laingsburg Fm. (Karoo Basin). Mar. Petrol. Geol., 28, 807–823.

Kane, I.A. 2010, Development and flow structures of sand injectites: The Hind Sandstone Member injectite complex, Carboniferous, UK. Marine and Petroleum Geology 27 pp1200-1215

Kazerouni, A.M., Friis, H., Svendsen, J.B. and Weibel, R. 2011. Heavy mineral sorting in downwards injected Palaeocene sandstone, Siri Canyon, Danish North Sea, Sedimentary Geology, 236, p.279-285

Knox, R.W.O'B. and Holloway S. 1992. Paleogene of the Central and Northern North Sea. Lithostratigraphic nomenclature of the UK North Sea, Vol.1. Knox R W O'B., and Cordey W G., (eds). (Nottingham: British Geological Survey).

Kneller, B. 2003. The influence of flow parameters on turbidite slope and channel architecture. Marine and Petroleum Geology, 20, pp.901–910

Kneller, B. and McCaffrey, W. D. 2003 The interpretation of vertical sequences in turbidite beds: the influence of longitudinal flow structure. J. Sed. Res., 73, 706–713.

Kjeilen-Eilertsen, F., Veiberg, D., Larssen, B. and Eide, A. 2009. New play model revealed amongst beach ridges, lagoons and palm trees – Stord Basin, North Sea – Norway. Exploration Revived conference 17-18 March.

Kjennerud, T. and Gilmore, G.K. 2003. Integrated Palaeogene palaeobathymetry of the northern North Sea. Petroleum Geoscience, Vol. 9 pp125-132

Kilhams B., Hartley A., Huuse M., and Davis C., 2012. Characterizing the Paleocene turbidites of the North Sea: the Mey Sandstone Member, Lista Formation, UK Central Graben. Petroleum Geoscience, Vol. 18, pp. 337-354

Leeder, M.R. 2011. Sedimentology and sedimentary basins: from turbulence to tectonics, Second edition. Blackwell publishing.

Leon, R., Somoza,L., Medialdea, T., Hernandez-Molina, F. J., Vazquez, J.T., D|az-Del-Rio,V. and Gonzalez, F. J.(2010) Pockmarks, collapses and blind valleys in the Gulf of Cadiz. Geo-Mar. Lett.,30,231-247

Lomas, S.A. and Joseph, P. 2004. Confined turbidite systems. Geological Society of London, Special Publications, v.222, p.1-7

Lonergan L., Lee N., Johnson H D., Cartwright J A. and Jolly R J H. 2000. Remobilization and injection in deepwater depositional systems: Implications for reservoir architecture and prediction, in Weimer P., Slatt R M., Coleman J., Rosen N C., Nelson H., Bouma A H., Styzen M J., and Lawrence D T., (eds). Deep-water reservoirs of the world: Gulf Coast Section SEPM Foundation, 20th annual conference, Houston, p.515-532

Lonergan, L., Borlandelli, C., Taylor, A., Quine, M. & Flanagan, K. 2007. The Three-dimensional Geometry of Sandstone Injection Complexes in the Gryphon Field, United Kingdom North Sea. In: Hurst, A. & Cartwright, J. (eds) Sand Injectites: Implications for Hydrocarbon Exploration and Production. American Association of Petroleum Geologists Memoirs, 87, 103–112.

Løseth, H.L.,Wensaas, B., Arntsen, N., Hovland,M., 2003. Gas and fluid injection triggering shallow mudmobilization in the Hordaland Group, North Sea. In: Van Rensbergen, P., Hillis, R., Maltman, A., Morley, C. (Eds.), Subsurface sediment mobilization: Special Publications, vol. 216. Geological Society, London, pp. 139–157.

Lowe, D.R. 1982. Sediment gravity flows: II. Depositional models with special reference to the deposits of high-density turbidity currents. Journal of Sedimentary Petrology. 52, pp279-297.

Lowe, D.R. and LoPiccolo, R. D. 1974. The characteristics and origins of dish and pillar structures. J. Sedim. Petrol., 44, 484-501.

Lowe, D.R. 1975. Water escape structures in coarse-grained sediments. Sedimentology, 22, p.157–204

Lowe , D.R. 1976a Subaqueous liquefied and fluidised sediment flows and their deposits. Sedimentology, 23, 285–308.

Lundin, E.R. and Dore, A.G. 2005. Fixity of the Iceland "hotspot" on the Mid-Atlantic Ridge: Observational evidence, mechanisms, and implications for Atlantic volcanic margins. GSA Special Papers, Vol. 388, p.627-651

Lyngsie, S.B. and Thybo, H. 2007. A new tectonic model for the Laurentia-Avalonia-Baltica sutures in the North Sea: A case study along MONA LISA profile 3. Tectonophysics, 429, p.201-227

Mangerud, G., Dreyer, T., Søyseth, L., Martinsen, O.. and Ryseth, A. 1999. High-resolution biostratigraphy and sequence development of the Palaeocene succession, Grane Field, Norway. In: Underhill, J. R. (ed.) Development and Evolution of the Wessex Basin, Geological Society, London, Special Publications, 133, 167-184.

Martinsen, O. J., Lien, T. and Jackson C.A.L. 2005. Turbidite systems offshore Norway. In: Dore, A.G. and Vining, B.A. (eds) Petroleum Geology: North-West Europe and Global Perspectives—Proceedings of the 6th Petroleum Geology Conference, p.1147–1164

Maltman, A.J. and Bolton, A. 2003. How sediments become mobilized. In: Subsurface sediment Mobilization (Eds by P.Van Rensbergen, R.R. Hillis, A.J. Maltman & C.K. Morley). Geological Society, Special Publications, 216, p.9-20

Mayall, M., Jones, E. and Casey, M. 2006. Turbidite channel reservoirs-Key elements in facies prediction and effective development. Marine and Petroleum Geology 23 pp821-841

Mazzini, A., Duranti, D., Jonk, R., Parnell, J., Cronin, B.T., Hurst, A., Quine, M., 2003a. Palaeo-carbonate seep structures above an oil reservoir, Gryphon Field, Tertiary, North Sea. Geo-Marine Letters 23, 323–339.

Mazzini, A. 2009. Mud volcanism: Processes and implications. Marine and Petroleum Geology, 26, p.1677-1680

McArthur, A.D., Hartley, A.J., Jolley, D.W., Archer, S.G. and Lawrence, H.M. 2008. Late Jurassic Slumping in the "J Block" region of the UKCS Central Graben: Temporal and Spatial Relationship to Freshney Sandstone Turbidite Reservoirs. Search and Discovery Article #30166

McKenzie, D. 1978. Some remarks on the development of sedimentary basins. Earth Planet, Sci. Lett., 40, p.25-32

Middleton, G.V. and Hampton, M.A. 1973, Sediment gravity flows: Mechanics of flow and deposition, in Middleton G V., and Bouma A H., (eds) Turbidites and deep-water sedimentation-short course notes: Pacific Section SEPM, pp 1-38

Milton, N.J., Bertram, G.T. and Vann, I.R. 1990. Early Palaeogene tectonics and sedimentation in the Central North Sea. In Tectonic events responsible for Britain's oil and gas reserves. Hardman RFP., and Brooks J., (eds). Special Publications of the Geological Society London No. 55 pp 339-351.

Minisini, D. and Schwartz, H. 2007 An early Paleocene cold seep system in the Panoche and Tumey Hills, Central California (United States). In: Sand Injectites: Implications for hydrocarbon Exploration and Production (Ed. by A. Hurst & J.A. Cartwright), AAPGMem. 87, pp185-197.

Mitchum, R.M., Vail, P.R. and Thompson, S. 111. 1977. Seismic Stratigraphy and global changes of sea level, part 2: the depositional sequence as a basic unit for stratigraphic analysis. in Seismic Stratigraphy –Applications to Hydrocarbon Exploration. Paynton C E., (ed.). Memoir of the American Association of Petroleum Geologists, No. 26 pp 53-62

Moreau, J., Ghienne, J, F., and Hurst A., 2012. Kilometre-scale sand injectites in the intracratonic Murzuq Basin (South-west Libya): an igneous trigger? Sedimentology, Vol.59, issue 4, pp.1321-1344

Morton, A.C. 1992. Provenance of Brent Group sandstones: heavy mineral constraints. In: Morton A.C., Haszeldine R.S., Giles M.R. & Brown S. (eds) Geology of the Brent Group. Geological Society of London, Special Publication 61, p. 227-244

Morton, A.C., Hallsworth, C.R. & Wilkinson, G.C. 1993. Stratigraphic evolution

of sand provenance during Paleocene deposition in the North Sea area. In: Parker, J.R. (ed.) Petroleum Geology of Northwest Europe: Proceedings of the 4th Conference. Geological Society, London, 73–84.

Morley, C.K. 2003. Outcrop examples of mudstone intrusions from the Jerudong anticline, Brunei Darussalam and inferences for hydrocarbon reservoirs. In: Van Rensbergen, P., Hillis, R., Maltman, A., Morley, C. (Eds.), Subsurface sediment mobilization: Special Publications, vol. 216. Geological Society, London, pp. 381-394.

Moss, J.L. and Cartwright, J. 2010. 3D seismic expression of km-scale fluid escape pipes from offshore Namibia. Basin Research, 22, p.481-501

Mudge, D.C. and Copestake P. 1992a. A revised Lower Paleocene stratigraphy for the Outer Moray Firth, North Sea. Marine Petroleum Geology 9 pp53-69

Mudge, D.C. Copestake, P. 1992b, Lower Paleogene lithostratigraphy of the Northern North Sea: Marine and Petroleum Geology, v9 pp 287-301

Mudge, D.C., and Bujak, J.P., 1994. Eocene stratigraphy of the North Sea basin. Marine and Petroleum Geology, Vol. 11. pp 166-181

Mudge, D.C., and Bujak, J.P., 1996. Paleocene biostratigraphy and sequence stratigraphy of the UK central North Sea. Marine and Petroleum Geology, 13, pp.295-316

Mulder, T. and Alexander, A. 2001. The physical character of subaqueous sedimentary density flows and their deposits. Sedimentology, 48, 269–299.

Murchison, R.I. 1827. On the coal field of Bora in Sutherlandshire and some other stratified deposits in the North of Scotland. Geological Society of London, 2, p.293–326

Neal, J.E. 1996. A summary of Paleogene sequence stratigraphy in northwest Europe and the North Sea. In: Knox, R.W., Corfield, R.M. & Dunay R.E. (ed.) Correlation of the Early Paleogene in Northwest Europe. Geological Society, London, Special Publications, 101, 15–42.

Newman, M.St.J., Reeder, M.L., Woodruff, A.H.W. and Hatton, I.R. 1993. The Geology of the Gryphon Oil Field. Geological Society of London, Petroleum Geology Conference Series, v.4, p.123-133

Petrobank, Norwegian Petroleum Directorate (NPD) data repository, available at: http://www.npd.no

Norlex stratigraphic nomenclature, available at: http://www.nhm.uio.no/norlex/index.html

Nichols, R.J., Sparks, R.S.J. and Wilson, C.J.N. 1994. Experimental studies of the fluidization of layered sediments and the formation of fluid escape structures. Sedimentology 41, 233–253.

Nichols, R.J. 1995, The liquefaction and remobilization of sandy sediments, in Hartley, A.J., and Prosser, D.J., eds., Characterization of deep-marine clastic systems: Geological Society

[London] Special Publication 94, p. 63–76.

Obermeier, S. 1996. Use of liquefaction-induced features for paleoseismic analysis-An overview of how seismic liquefaction features can be distinguished from other features and how their regional response distribution and properties of source sediment can be used to infer the location and strength of Holocene paleo-earthquakes. Engineering Geology, v44, pp1-76

Osborne, M.J. and Swarbrick, R.E. 1997. Mechanisms for generating overpressure in sedimentary basins, a re-evaluation. AAPG Bulletin, v.81, pp1023-1041

Owen, G. 1987. Deformation processes in unconsolidated sands. In: Deformation of sediments and sedimentary rocks (Ed. Jones, M.E., and Preston, R.M.F.,), Geological Society of London, Special Publications, 29, p.11-24

Owen, G. 1996. Experimental soft-sediment deformation: structures form by the liquefaction of unconsolidated sands and some ancient examples. Sedimentology, 43, pp.279–293

Owen, G. 2003. Load structures: gravity-driven sediment mobilization in the shallow subsurface. In: Van Rensbergen, P., Hillis, R., Maltman, A., Morley, C. (Eds.), Subsurface sediment mobilization: Special Publications, vol. 216. Geological Society, London, pp.21–34

Parize, O., Beaudoin, B., Champanhet, J.M., Friés, G., Imbert, P., Labourdette, R., Paternoster, B., Rubino, J.L., Schneider, F., 2007b. A Methodical Approach to Clastic Injectites: From Field Analysis to Seismic Modeling–Examples of the Vocontian Aptian and Albian Injectites (Southeast France). In: Hurst, A., Cartwright, J. (Eds.), Sand Injectites: Implications for Hydrocarbon Exploration and Production: American Association of Petroleum Geologists Memoir, Tulsa, pp. 173–183.

Parnell, J. and Kelly, J., 2003. Remobilization of sand from consolidated sandstones: evidence from mixed bitumen-sand intrusions. Subsurface sediment mobilization: Introduction: Geological Society [London] Special Publication 216, 505-513

Peakall, J., McCaffrey W.D., Kneller, B.C., 2000. A process model for the evolution, morphology and architecture of sinuous submarine channels, Journal of Sedimentary Research, 70, pp.434-448

Petrel software manuals. 2012. Available at:
http://www.slb.com/services/software/geo/petrel.aspx

Pickering, K., Stow, D.A.V., Watson, M. and Hiscott, R. 1986. Deep-water Facies, Processes and Models: A Review and Classification Scheme for Modern and Ancient Sediments. Earth Science Reviews, 23, p.75-174

Pickering, K.T., Clark, J.D., Smith, R.D.A., Hiscott, R.N., Ricci Lucchi, F. and Kenyon, H.H. 1995. Architectural element analysis of turbidite systems, and selected topical problems for sand-prone deep-water systems. Atlas of Deep-water environments.

Posamentier, H.W. and Allen, G.P. 1999. Siliciclastic sequence stratigraphy: Concepts and Applications. Society of Economic Paleontologists and Mineralogists (SEPM), Concepts in Sedimentology and Paleontology #7.

Posamentier, H.W., Kolla, V., 2003. Seismic geomorphology and stratigraphy of depositional elements in deep-water settings. Journal of Sedimentary Research, 73, 367–388.

Posamentier, H.W. and Walker, R.G. 2006. Deep-water turbidites and submarine fans: Special Publication, Society for Sedimentary Geology, v.84, p.399-520

Posamentier, H.W., Davies, R.J., Cartwright, J.A. and Wood, L., 2007. Seismic geomorphology–an overview. In: Davies, R.J., Posamentier, H.W., Wood, L. & Cartwright, J.A. (eds) Seismic Geomorphology: Applications to Hydrocarbon Exploration and Production. geological Society, London, Special Publications, 277, 1–14.

Posamentier, H. W. and James, D. P. 2009. An Overview of Sequence-Stratigraphic Concepts: Uses and Abuses, in Sequence Stratigraphy and Facies Associations (eds H. W. Posamentier, C. P. Summerhayes, B. U. Haq and G. P. Allen), Blackwell Publishing Ltd., Oxford, UK.

Prelat, A., Hodgson, D.M., and Flint, S., 2009. Evolution, architecture and hierarchy of distributary deep-water deposits: a high-resolution outcrop investigation from the Permian Karoo Basin, South Africa. Sedimentology, 56, 2132–2154.

Prélat, A. and Hodgson, D.M. 2013. The full range of turbidite bed thickness patterns in submarine lobes: Controls and implications, Journal of the Geological Society, 170, p.209-214

Pringle, J.K., Westerman, A.R., Stanbrook, D.A., Tatum, D.I. and Gardiner, A.R. 2007. Sand volcanoes of the Carboniferous Ross Formation, County Clare, Western Ireland: 3D internal sedimentary structure and Formation. P.227-233

Rider, M.H. 1990. Gamma-ray log shape used as a facies indicator: critical analysis of an oversimplified methodology. Geological Society, London, Special Publications, vol. 48, p.27-37

Rider, M.H., 1996. The geological interpretation of Well Logs 2nd edition. Whittles publishing ISBN 1-870325-36-2

Reading, H.G., and Richards, M., 1994. Turbidite systems in deep-water basin margins classified by grain size and feeder system. American Association of Petroleum Geologists Bulletin, 78, pp792–822.

Rodrigues, N., Cobbold, P.R., Løseth, H., 2009. Physical modelling of sand injectites. Tectonophysics 474, 610–632.

Ross, J.A., Peakall, J., and Keevil, G.M., 2011. An integrated model of extrusive sand injectites in cohesionless sediments. Sedimentology, 58, 1693-1715.

Satur, N., Hurst, A., 2007. Sand-injection structures in deep-water sandstones from the Ty formation (Paleocene), Sleipner Øst Field, Norwegian North Sea. In: Hurst, A., Cartwright, J. (Eds.), Sand Injectites: Implications for Hydrocarbon Exploration and Production: American Association of Petroleum Geologists Memoir, Tulsa, pp. 113–117.

Sarg, J.F. and Skjold, L.J. 1982, Stratigraphic traps in Paleocene sands in the Balder area, Halbouty ed,. The deliberate search for the subtle trap: AAPG Memoir 32, pp 197-206

Scott, A.S.J., Vigorito, M., Hurst, A., 2009. The Process of Sand Injection: Internal Structures and Relationships with Host Strata (Yellowbank Creek Injectite Complex, California, U.S.A.). Journal of Sedimentary Research 79, 1–18.

Shanmugan, G. 1996b. High density currents: Are they sandy debris flows? Journal of sedimentary Research., 66 (1) pp 2-10

Shanmugan, G. Miola R J., 1995. Reinterpretation of depositional processes in a classic flysch sequence (Pennsylvanian Jackfork Group), Ouachita Mountians, Arkansas and Oklahoma: Reply AAPG Bull., 81 (3) pp 476-491

Shanmugan, G. 2000. 50 years of the turbidite paradigm (1950s-1990s): deep-water processes and facies models. Marine and Petroleum Geology, 17, p.285-342

Sherry, T. J., Rowe, C.D., Kirkpatrick, J.D. and Brodsky, E.E. 2012. Emplacement and dewatering of the world's largest exposed sand injectite complex. Geochemistry, Geophysics, Geosystems, 13, 1, p.1-17

Shoulders, S., Cartwright, J. and Huuse, M. 2007. Large-scale conical sandstone intrusions and polygonal faults in Tranche 6 of the Faroe-Shetland Basin. Marine and Petroleum Geology, 24, 173-188.

Sinclair, H.D. and Tomasso, M. 2002. Depositional evolution of confined turbidite basins. Journal of Sedimentary Research, 72, 451–456.

Sinclair, H. D. and Cowie, P. A. 2003 Basin-floor topography and the scaling of turbidites. J. Geol., 111, 277–299.

Slatt, R.M., Jordan, D.W., D'Agostino, A.E. and Gillespie, R.H. 1992. Outcrop gamma-ray logging to improve understanding of subsurface well log correlations. Geological Society, London, Special Publications, v.65, p.3-19

Skjold, L. J. 1980. Paleocene sands of the Balder Area. The Sedimentation of the North Sea Reservoir Rocks. Norwegian Petroleum Society, Article V11.

Sohn, Y.K. 1997 On traction-carpet sedimentation. J. Sed. Res., 67, 502–509.

Sohn, Y.K., Choe, M.Y. and Jo, H.R. 2002. Transition from debris flow to hyperconcentrated flow in a submarine channel (the Cretaceous Cerro Torro Formation, southern Chile). Terra Nova, 14 405-415

Stow, D.A.V. (1985). Deep-sea clastics: where are we and where are we going? In: P.J.Brenchley and B.P.J.Williams (eds.), Sedimentology: recent developments and applied aspects, Geological Society, London, Special Publications, 18, p.67-93

Stow, D.A.V. and Johansson, M. 2000. Deep-water massive sands: nature, origin and

hydrocarbon implications. Marine and Petroleum Geology, 17, p.145-174

Stow, D.A.V. and Piper, D.J.W. 1984b Deep-water fine-grained sediments: facies models. In: Fine Grained Sediments: Deep-Water Processes and Facies (Eds D.A.V. Stow and D.J.W. Piper), Geol. Soc. Spec. Publ. 15, 611–646.

Stow, D.A.V. 2007. Sedimentary rocks in the Field, a colour guide. Manson publishing. P.320

Stuevold, L.M., Faerseth, R.B., Arnesen, L., Cartwright, J. and Moller, N. 2003. Polygonal faults in the Ormen Lange Field, Møre Basin, offshore Mid Norway. Subsurface sediment mobilization: Geological Society [London] Special Publication

Surlyk, F., Gjelberg, J.,Noe-Nygaard,N., 2007. The Upper Jurassic Hareelv Formation of East Greenland:A giant sedimentary injection complex. In:Hurst,A., Cartwright, J.A. (Eds.), Sand Injectites: Implications for Hydrocarbon Exploration and Production: American Association of Petroleum Geologists Memoir, Tulsa, p. 141–149.

Svendsen, J.B., Hansen, H.J., Staermose, T. & Engkilde, M.K. 2010. Sand remobilization and injection above an active salt diapir: the Tyr sand of the Nini Field, Eastern North Sea. Basin Research, 22, p.548–561.

Szarawarska, E., Huuse, M., Hurst, A., de Boer, W., Lu, L., Molyneux, S. & Rawlinson, P. 2010. 3D seismic characterisation of large-scale sandstone intrusions in the lower Palaeogene of the North Sea: completely injected vs in situ remobilized sandbodies. Basin Research, 22, p.517–532

Talling, P.J., Sumner, E.J., Malgesini, G. and Masson, D.G. 2012b Subaqueous sediment density flows: Depositional processes and deposit types. Sedimentology, 59, p.1937–2003. doi:10.1111/j.1365-3091.2012.01353.x.

Talling, P.J., Malgesini, G., and Felletti, F., 2013. Can liquefied debris flows deposit clean sand over large areas of sea floor? Field evidence from the Marnoso-arenacea Formation, Italian Apennines. Sedimentology, 60, pp720-762

Talling, P.J., 2001. On the frequency distribution of turbidite thickness. Sedimentology, 48, 1297–1329.

Taylor, B.J., 1982. Sedimentary dykes, pipes and related structures in the Mesozoic sediments of south-eastern Alexander Island. British Antarctic Survey Bulletin 51, p.1–42

Templeton, G., King, P. and Reeder, M. 2002. Leadon Field – Description of Frigg reservoir sand injection structures. EAGE 64th Conference & Exhibition – Florence, Italy, 27-30th May 2002.

Templeton, G., Konings, S., Wilkie, C., Benton, P., Marcas, G., McInally, A. and Ings, R. 2009. Gryphon Field Development-Past, Present and Future. SPE 124751, p.1-15

Timbrell, G. 1993. Sandstone architecture of the Balder Formation depositional system, UK quadrant 9 and adjacent areas. In: Petroleum Geology of Northwest Europe: Proceedings of

the 4th Conference (Ed. by J.R. Parker), Geol. Soc., 1, p.107-121.

Tonkin, N.S., McIlroy, D., Meyer, R., and Moore-Turpin, A., 2010. Bioturbation influence on reservoir quality: A case study from Cretaceous Ben Nevis Formation, Jeanne d'Arc Basin, offshore Newfoundland, Canada. AAPG Bulletin, V.94, No.7, pp1059-1078

Underhill, J.R. and Partington, M.A. 1993. Jurassic thermal doming and deflation in the North Sea: implications of the sequence stratigraphic evidence, vol. 4, p.337-345

Van Rensbergen, P., Hillis, R.R., Maltman, A.J., and Morley, C.K., eds., 2003, Subsurface sediment mobilization: Introduction: Geological Society [London] Special Publication 216, p. 1–8.

Vail, P.R., Mitchum, R.M., Jr and Thompson, S. III 1977. Seismic stratigraphy and global changes of sea-level, part 3: relative changes of sea-level from coastal onlap. In: Payton, C.E. (ed.) Seismic stratigraphy – Applications to Hydrocarbon Exploration. AAPG Memoir 26, p.63-81

Van Wagoner, J.C., Posamentier, H.W., Mitchum, R.M., Vail, P.R., Sarg, J.F., Loutit, T.S. and Hardenbol, J. 1988. An overview of sequence stratigraphy and key definitions. In: Wilgus, C.K., Hastings, B.S., Kendal, C.G.St.C., Posamentier, H.W., Ross, C.A. and Van Wagoner, J.C. (eds). Sea-level changes – An integrated Approach. Society of Economic Paleontologists and Mineralogists (SEPM), Special Publication, 42, p.39-45

Vetel, W. and Cartwright, J. 2010. Emplacement mechanics of sandstone intrusions: insights from the Panoche Giant Injection Complex, California. Basin Research, 22, p.783-807

Vigorito, M.,Hurst, A., Cartwright, J. & Scott, A. 2008. Regional-scale subsurface crustal ediment remobilization: geometry and architecture. J.Geol.Soc.Lond.,Spec.Publ., 65(3), 609-612.

Walker, R G., 1978. Deep-water sandstone facies and ancient submarine fans: models for exploration for stratigraphic traps. AAPG Bulletin, 62, pp.932-966

Wyn, R.B., Talling, P.J., Masson, D.G., leBas, T.P., Cronin, B.T. and Stevenson, C.J. 2012. The influence of subtle gradient changes on deep-water gravity flows: A case study from the Moroccan Turbidite System. SEPM, Special Publication, 99, p.371-383

Wild, J. and Briedis, N. 2010. Structural and stratigraphic relationships of the Palaeocene mounds of the Utsira High. Basin Research, 22, p.533–547

Zanella, E. and Coward, M.P. 2003. Structural framework. P.45-59 in The Millenium Atlas: Petroleum geology of the central and northern North Sea. in Evans D., Graham C., Armour A., Bathurst P., (eds),

Zanella, E., Coward, M.P. and McGrandle, A. 2003. Crustal structure. 35-45

Ziegler, W.H., Doery, R. and Scott, J. 1986. Tectonic habitat of Norwegian oil and gas. In Habitat of Hydrocarbons on the Norwegian Continental Shelf. Norwegian Petroleum

Society. Graham and Trotman, p.3-19

Ziegler, P.A. 1990. Tectonic and palaeogeographic development of the North Sea rift system. 1-36 in Tectonic Evolution of the North Sea Rifts. Blundell D J., and Gibbs A D., (eds). Oxford: Clarendon Press.

# Appendix 1 – Examples of remobilized and injected sediments

## Appendix 1a: Characteristics of subsurface dataset responses

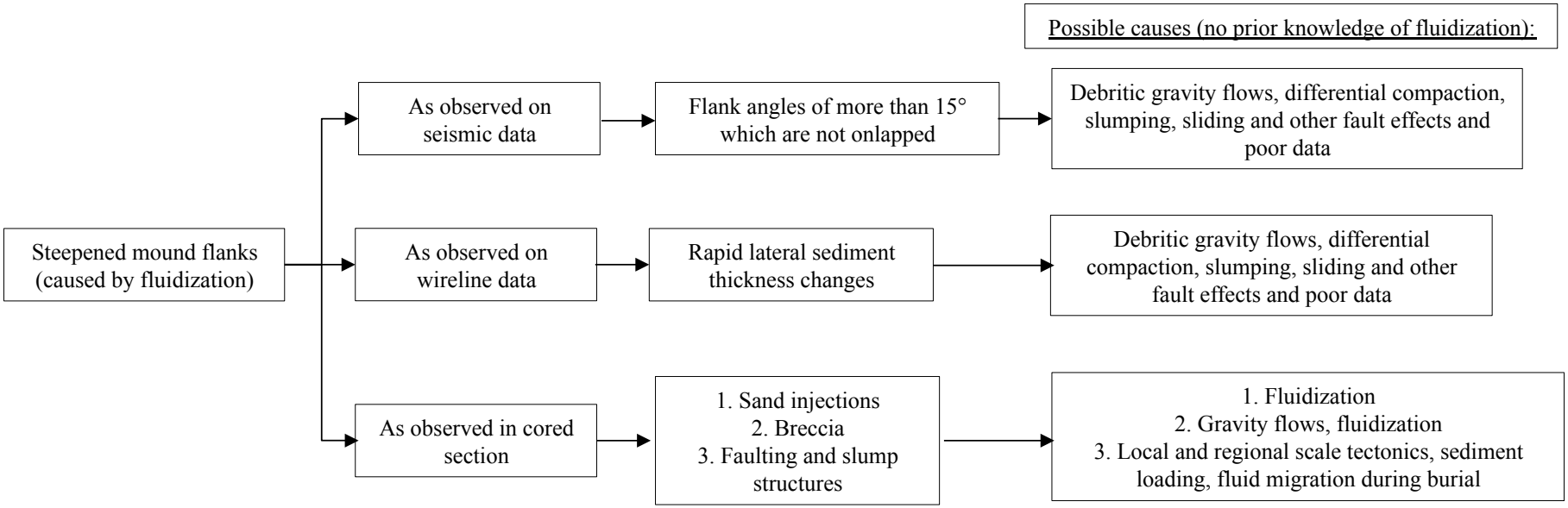


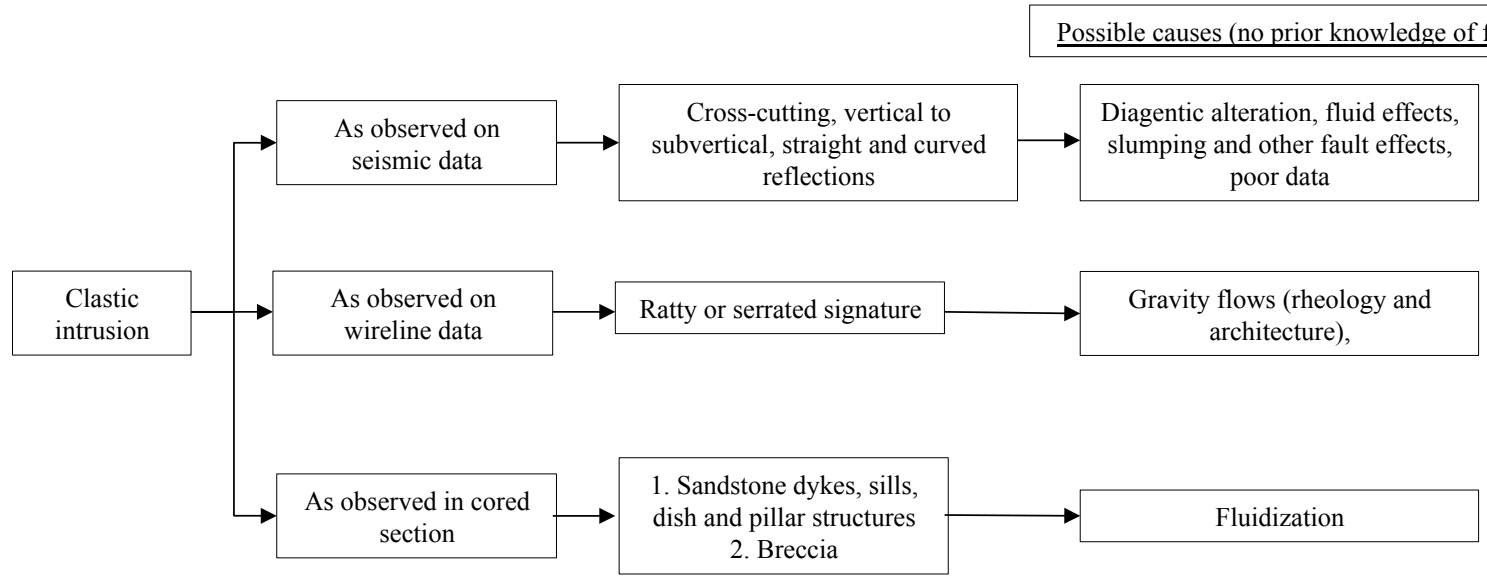


**Appendix 1a: Characteristics of subsurface responses, reservoir geometry**

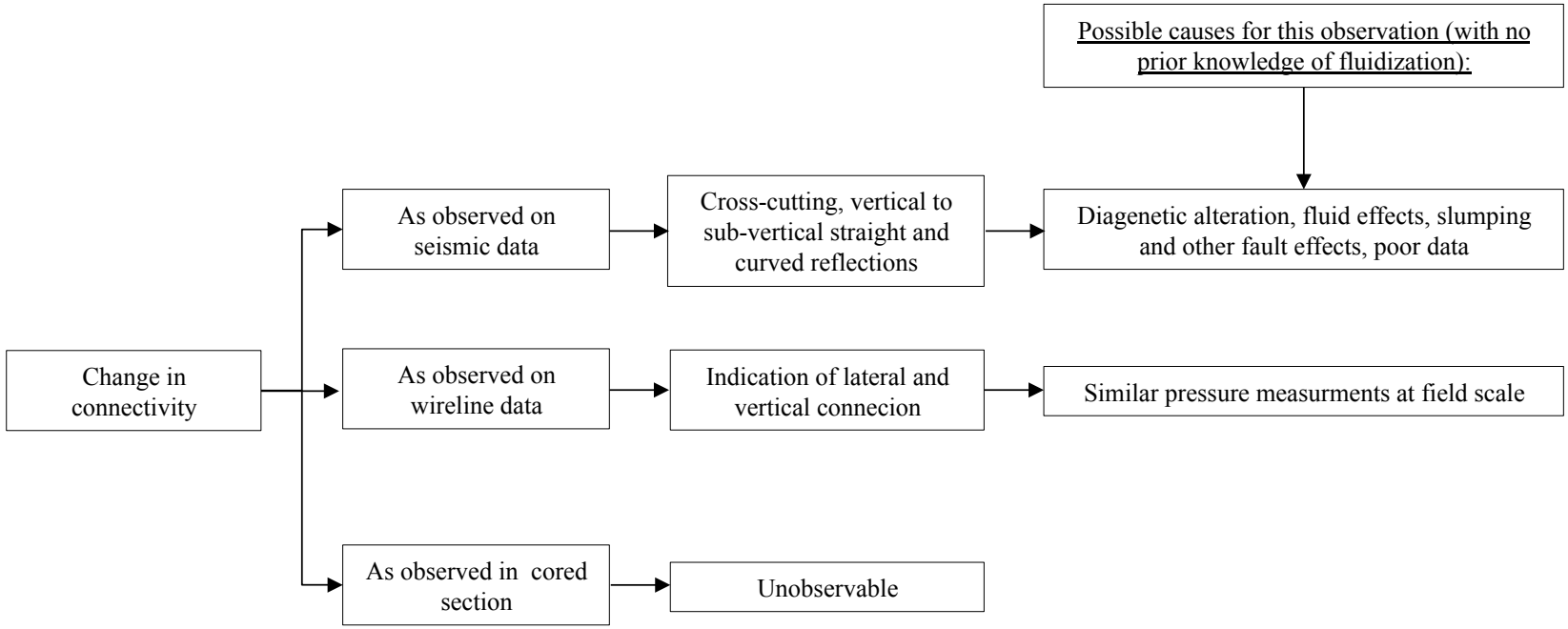


**Appendix 1a: Characteristics of subsurface responses, reservoir connectivity**

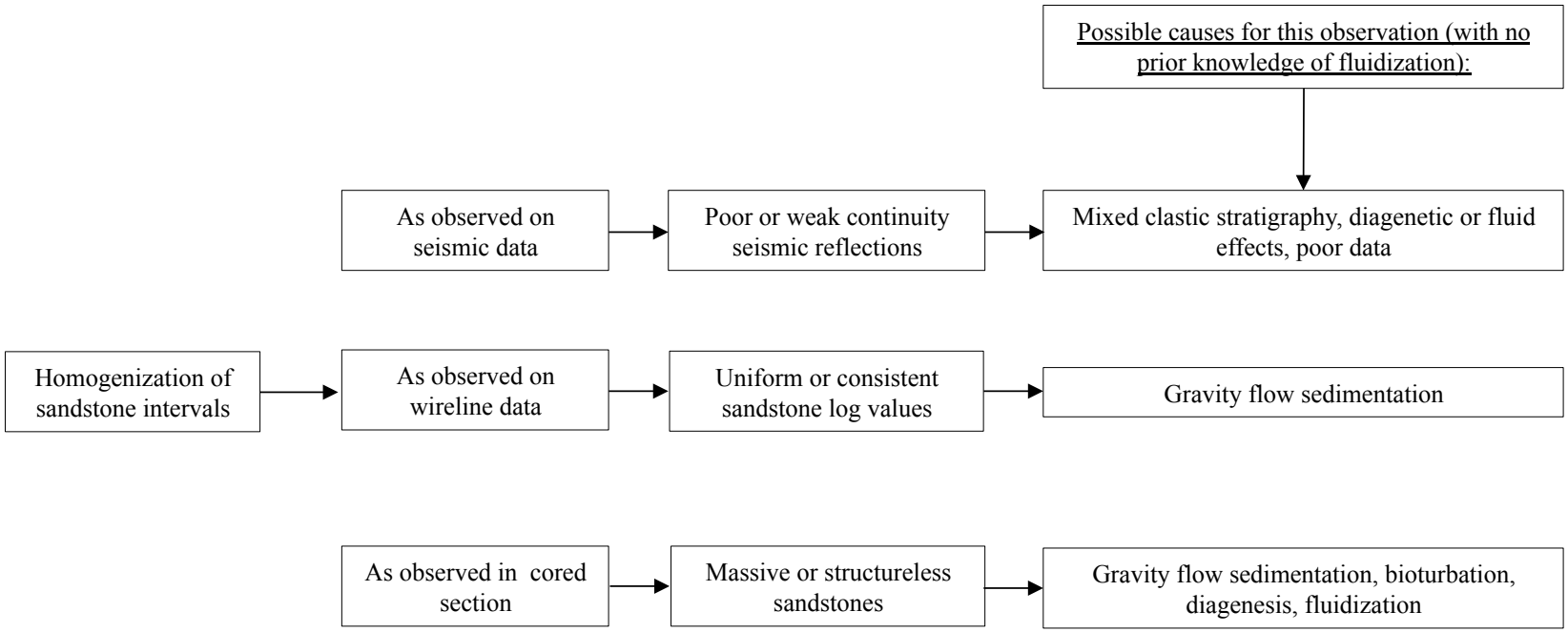


**Appendix 1a: Characteristics of subsurface responses, reservoir properties**

# Appendix 2 – Sequence stratigraphy

Appendix 2a: Sequence boundary depths

Appendix 2b: Biostratigraphic raw data

| | NPD Lithostratigraphic top | | | | | | | | | Sequence pick | | | |
|---|---|---|---|---|---|---|---|---|---|---|---|---|---|
| Well | Ekofisk Fm | Ty Mbr | Våle Fm | Heimdal Mbr | Lista Fm | Hermod Mbr | Sele Fm | Balder Fm | | Våle sequence | Lista sequence | Sele sequence | Balder sequence |
| 25/8-1 | 1846.00 | | 1841.00 | 1777.00 | 1767.00 | 1754.00 | 1736.00 | 1665.00 | | 1830.88 | 1764.94 | 1743.20 | 1697.47 |
| 25/8-3 | 1841.00 | | | 1783.00 | 1770.00 | 1753.00 | 1733.00 | 1667.00 | | 1838.36 | 1780.38 | 1740.82 | 1703.35 |
| 25/8-14 ST2 | | | | | | | | | | 2361.58 | 2275.09 | 2195.11 | 2102.96 |
| 25/8-11 | 1876.00 | | 1872.00 | | 1824.00 | 1765.00 | 1743.00 | 1678.00 | | 1863.59 | 1823.34 | 1747.45 | 1678.69 |
| 25/8-12 S | | | 1880.00 | | 1839.00 | 1785.00 | 1766.00 | 1699.00 | | 1871.40 | 1836.77 | 1771.18 | 1700.12 |
| 25/8-4 | 1841.00 | | 1836.00 | 1743.00 | 1710.00 | | | 1670.00 | | 1835.15 | 1760.12 | 1715.1 | 1675.61 |
| 25/8-10 S | 1827.00 | | | 1761.00 | 1741.00 | 1725.00 | 1708.00 | 1645.00 | | | 1770.1 | 1716.15 | 1677.60 |
| 25/8-15 S | | | | | 3822.00 | | 3347.00 | 3086.00 | | 4356.29 | 3674.14 | 3385.67 | 3164.42 |
| | | | | | | | | | | | | | |
| 25/10-1 | | | | | | 1730.00 | 1717.00 | 1682.00 | | | | 1716.39 | 1682.84 |
| 25/10-3 | 1911.00 | | | 1841.00 | 1841.00 | 1808.00 | 1769.00 | 1711.00 | | 1888.2 | 180.27 | 1771.06 | 1731.11 |
| 25/10-4 R | | | | 1760.00 | 1747.00 | | 1720.00 | 1682.00 | | 1900.50 | 1742.45 | 1717.86 | 1678.33 |
| 25/10-5 | 1991.00 | | | 1906.00 | 1859.00 | 1831.00 | 1820.00 | 1743.00 | | 1956.9 | 1895.12 | 1823.45 | 1780.08 |
| | | | | | | | | | | | | | |
| 25/11-1 | 1895.00 | 1868.00 | | | 1821.00 | 1794.00 | 1778.00 | 1698.00 | | 1853.99 | 1820.18 | 1780.90 | 1729.00 |
| 25/11-2 | | | | | | 1780.00 | 1765.00 | 1699.00 | | | | 1766.61 | 1699.30 |
| 25/11-3 | 1852.00 | 1824.00 | 1817.00 | 1782.00 | 1757.00 | | 1747.00 | 1711.00 | | 1796.85 | 1759.08 | 1744.86 | 1711.00 |
| 25/11-4 | 1874.00 | | | | 1820.00 | 1792.00 | 1776.00 | 1695.00 | | 1856.45 | 1818.46 | 1776.68 | 1730.68 |
| 25/11-5 | | | | 1798.00 | 1773.00 | 1731.00 | 1724.00 | 1661.00 | | 1899.30 | 1771.50 | 1720.40 | 1671.05 |
| 25/11-6 | 1903.00 | 1877.00 | 1864.00 | 1718.00 | 1702.00 | | 1688.00 | 1646.00 | | 1866.59 | 1700.90 | 1689.40 | 1647.00 |
| 25/11-7 | 1921.00 | | 1918.00 | 1751.00 | 1716.00 | | 1711.00 | 1667.00 | | 1895.2 | 1734.18 | 1713.15 | 1670.20 |
| 25/11-8 | 1925.00 | | 1915.00 | 1722.00 | 1712.00 | | 1699.00 | 1655.00 | | | 1719.06 | 1693.20 | 1650.23 |
| 25/11-9 | 1887.00 | | 1882.00 | 1855.00 | 1825.00 | 1782.00 | 1768.00 | 1670.00 | | 1876.29 | 1822.60 | 1769.68 | 1677.30 |
| 25/11-10 | 1968.00 | | 1958.00 | 1780.00 | 1760.00 | | 1725.00 | 1682.00 | | 1941.45 | 1759.00 | 1728.50 | 1693.00 |
| 25/11-11 | 1940.00 | | 1910.00 | 1754.00 | 1738.00 | | 1714.00 | 1655.00 | | 1916.2 | 1736.6 | 1716.00 | 1656.20 |
| 25/11-12 | 1904.00 | | 1890.00 | 1785.00 | 1751.00 | | 1731.00 | 1675.00 | | 1888.00 | 1743.20 | 1727.60 | 1681.6 |
| 25/11-13 | 1908.00 | 1875.00 | 1862.00 | 1858.00 | 1820.00 | 1769.00 | 1744.00 | 1678.00 | | 1852.4 | 1760.00 | 1745.60 | 1678.60 |
| 25/11-14 S | | | | 1903.00 | 1859.00 | | 1834.00 | 1762.00 | | | 1825.00 | 1817.70 | 1765.60 |
| 25/11-15 | 1818.00 | | 1807.00 | 1734.00 | 1678.00 | | 1674.00 | 1660.00 | | 1804.30 | 1721.50 | 1674.80 | 1858.80 |
| 25/11-16 | 1897.00 | | 1885.00 | 1767.00 | 1739.00 | | 1733.00 | 1698.00 | | 1883.30 | 1752.80 | 1733.80 | 1697.10 |
| 25/11-18 | 1834.00 | | 1807.00 | 1742.00 | 1695.00 | | 1690.00 | 1674.00 | | 1805.70 | 1736.80 | 1689.70 | 1651.16 |
| 25/11-19 S | 2045.00 | | 2030.00 | | 1996.00 | 1891.00 | 1865.00 | 1792.00 | | 2031.5 | 1886.6 | 1868.7 | 1793.7 |
| 25/11-21 S | | | | 1838.00 | 1757.00 | | 1745.00 | 1736.00 | | 1889.8 | 1767.85 | 1738.4 | 1724.8 |
| 25/11-22 | 1774.00 | | 1769.00 | | 1692.00 | | 1686.00 | 1677.00 | | 1758.1 | 1679.8 | 1686.4 | 1677.1 |
| 25/11-23 | 1971.00 | 1944.00 | | 1899.00 | 1866.00 | 1796.00 | 1782.00 | 1699.00 | | 1925.6 | 1889.1 | 1784.00 | 1701.2 |

**Appendix 2a: NPD lithostratigraphic depths (left) included here to highlight difference with chronostratigraphically defined sequences (right)**

| Depth (MD) | Statement | Assemblage | Data source | Series | Stage |
|---|---|---|---|---|---|
| 1470 | Common | P. cornatum | swc | | Middle Eocene |
| 1500 | Common | G. bartonensis | | | Middle Eocene |
| 1520 | | R. borussica | | | Middle Eocene |
| 1550 | | S. spectabilis | | | Middle Eocene |
| 1610 | | R. ampiectins | | | Middle Eocene |
| 1625 | | D. ficusoides | | | Middle Eocene |
| 1633 | Common | P. germinatum | swc | | Middle Eocene |
| 1665 | | D. pachyderum | swc | | Middle Eocene |
| 1672 | | E. ursuiae | swc | | Middle Eocene |
| 1695 | | Cosinodiscus | swc | | Middle Eocene |
| 1695 | | G. ordinatum | | | Early Eocene |
| 1753 | | A. margarita | core | | Late Palaeocene |
| 1743 | | S. spectabilis | core | | Late Palaeocene |
| 1789 | | A. senenensis | core | | Late Palaeocene |
| 1795 | | Spiniferites | core | | Late Palaeocene |
| 1851 | | A. senenensis | | | Early Palaeocene |
| 1925 | | H. bugersis? | swc | | Late Cretaceous |

**Biostratigraphic data for well 25/11-16 located outside seismic coverage, South of Balder Field**

| Depth (MD) | Statement | Assemblage | Data source | Series | Stage |
|---|---|---|---|---|---|
| 1440 | Presence | Heteraulacacysta porosa | | | Late Middle Eocene |
| 1450 | Presence | Areospheridium diktyoplokus | | | Late Middle Eocene |
| 1470 | | Areospheridium fenestratum | | | Late Middle Eocene |
| 1480 | Presence | Karrerulina conversa | | | Late Middle Eocene |
| 1540 | | Subbotina eocaena | | | Eocene |
| 1620 | | D. nudum | | | Eocene |
| 1600 | | Eatonicytsa ursulae | | | Eocene |
| 1600 | | Systematophora placacantha | | | Eocene |
| 1667 | | A. aubertae | | | Eocene |
| 1667 | | Cyclamina amplectens | | | Eocene |
| 1677 | | M. oxycona | | | Paleocene |
| 1687 | | Coscinodiscus | | | Paleocene |
| 1721.5 | | R. jarvisi | core | | Paleocene |
| 1796.3 | | S. spectabilis | core | | Paleocene |
| 1804 | | Gyroidina | core | | Paleocene |

**Biostratigraphic data for well 25/11-18 South of Grane Field located in Mound 11**

| Depth (MD) | Statement | Assemblage | Data source | Series | Stage |
|---|---|---|---|---|---|
| 1480 | | A. arcuatum | swc | | Eocene |
| 1485 | | A. diktyopiokus | swc | | Eocene |
| 1500 | Common | A. aubertae | | | Eocene |
| 1500 | | A. arcuatum | swc | | Eocene |
| 1520 | Influx | agglutinating foraminiferids | | | Eocene |
| 1525 | Minor influx | P. comatum | swc | | Eocene |
| 1551 | | S. spectabilis | swc | | Eocene |
| 1561 | Consistent | R. aff. Ampiectens | | | Eocene |
| 1561 | Common | P. geminatum? | swc | | Eocene |
| 1567 | Common | R. aff. Ampiectens | swc | | Eocene |
| 1571 | Re-apperance | S. spectabilis | | | Eocene |
| 1571 | Common | Dracodinium | | | Eocene |
| 1571 | | D. pachydermum | swc | | Eocene |
| 1580 | Influx | E. ursuiae | swc | | Eocene |
| 1585 | | Red stained agglutinants | swc | | Eocene |
| 1590 | Influx | I. hiatus | swc | | Late Paleocene Early Eocene |
| 1590 | | Caryapoifenites app. | swc | | Late Paleocene Early Eocene |
| 1590 | | D. oebisfeldensis | swc | | Late Paleocene Early Eocene |
| 1590 | | G. ordinata | swc | | Late Paleocene Early Eocene |
| 1630.16 | | Hemiaulus sp. 1 | core | | Late Paleocene Early Eocene |
| 1640 | | Coscinodiscus sp.1 | core | | Late Paleocene Early Eocene |
| 1643.50 | | Prasinophyta | core | | Late Paleocene Early Eocene |
| 1647.45 | Abundant | C. wardenensis | core | | Late Paleocene |
| 1649.20 | | Coscinodiscus sp. 7 | core | | Late Paleocene |
| 1650.55 | | A. augustus | core | | Late Paleocene |
| 1650.55 | | A. quin ? | core | | Late Paleocene |
| 1654.15 | | S. spectabilis | core | | Late Paleocene |
| 1657.15 | | A. margarita | core | | Late Paleocene |
| 1667.90 | | A. senonensis 'robusta' | core | | Late Paleocene |
| 1688.80 | Abundant | A. senonensis 'robusta' | core | | Late Paleocene |
| 1721.50 | Abundant | P. pyrophorum | core | | Late Paleocene |
| 1730.50 | Influx | L? viborgense Cenodiscus sp. | | | Late Paleocene |
| 1737.80 | Common | P. cf. Australinum | | | Late Paleocene |
| 1737.80 | | G. pseudobulloides | | | Late Paleocene |
| 1738 | Common | N. perfectus | | | Late Paleocene |
| 1738 | Common | C. edentulus | core | | Late Paleocene |
| 1741 | Abundant | A. reticulata | core | | Late Paleocene |
| 1743 | | R. rugosa | | | Late Paleocene |
| 1743 | | A. cymbiformis | | | Late Paleocene |
| 1743 | | G. obliquum | | | Late Paleocene |

## Biostratigraphic data for well 25/11-17 located outside seismic coverage, South of Balder Field

| Depth (MD) | Statement | Assemblage | Data source | Series |
|---|---|---|---|---|
| 1520 | | S. spectabilis | | Middle Eocence |
| 1525 | Influx | P. geminatum | | Middle Eocence |
| 1545 | Abundant | P. geminatum | | Middle Eocence |
| 1570 | | R. aff. Ampiectens | | Middle Eocence |
| 1585 | | E. ursulae | | Early-Middle Eocene |
| 1585 | Common | D. pechyderum | | Early-Middle Eocene |
| 1585 | Common | W. articulats | | Early-Middle Eocene |
| 1590 | Common | R. ampiectens | | Early-Middle Eocene |
| 1603 | | S. spectabilis | SWC | Early-Middle Eocene |
| 1610 | | E. ursulae | | Early-Middle Eocene |
| 1622 | | H. tenuispinosum | SWC | Early Eocene |
| 1627 | | A. senonensis | SWC | Early Eocene |
| 1650 | | S. navarroana | SWC | Early Eocene |
| 1668.40 | | A. senonensis | | Early Eocene |
| 1674.30 | | Coscinodiscus sp. 1 | Core | Early Eocene |
| 1678 | Influx | D. oebisfeldensis | Core | Late Paleocene |
| 1713 | | S. spectabilis | SWC | Late Paleocene |
| 1719 | | A. margarita | | Late Paleocene |
| 1719 | | A. senonensis | SWC | Late Paleocene |
| 1746 | | A. senonensis | Core | Late Paleocene |
| 1762 | Abundant | P. pyrophorum | | Late Paleocene |
| 1762 | | P. cf. australinum | Core | Late Paleocene |
| 1830.50 | | Cenodiscus spp. | Core | Late Paleocene |
| 1836 | Influx | P. cf. australinum | Core | Late Paleocene |
| 1837 | | P. compressa | SWC | Late Paleocene |
| 1837 | | M. pseudobulloides | SWC | Late Paleocene |
| 1837 | Common | N. perfectus | SWC | Late Paleocene |
| 1840 | | A. reticulata | SWC | Late Paleocene |
| 1842 | Abundant | M. pseudobulloides | SWC | Early Paleocene |
| 1842 | V.Common | P. dimorphosus | SWC | Early Paleocene |
| 1850 | | A. cymbiformis | SWC | Cretaceous |
| 1860 | | Heterohelix spp. | SWC | Cretaceous |
| 1870 | | R. levis | SWC | Cretaceous |
| 1875 | | G. havanensis | SWC | Cretaceous |
| 1890 | Common | W. barnesae | | Cretaceous |
| 1890 | Common | H. trabeculatus | | Cretaceous |
| 1890 | | S. granulata polonica | | Cretaceous |
| 1890 | | P. capitosa | | Cretaceous |

**Biostratigraphic data for well 25/8-4 located outside seismic coverage, East of Ringhorne Field**

# Appendix 3 – Cored section data

Appendix 3a:  Cored section logging sheets

Appendix 3b:  Cored section lithofacies observed

**SIMON MORRIS** **BIRKBECK COLLEGE**

**WELL: 25\11-23**

**Balder sequence**

**COUNTRY: Norway**

DATE: Autumn 2007 | SCALE: 1:25

AUTHOR: S.Morris | SHEET: 7 of 7

DRILLERS DEPTH METRES | CORE | OIL STAIN | SAMPLE | AGE | GAMMA RAY | GRAIN SIZE AND SEDIMENTARY STRUCTURES | LITHOLOGY | BIOTURBATION | TRENDS | FACIES | COLOUR | DESCRIPTION

CORE: CORE NUMBER; NO RECOVERY; SAMPLE REMOVED; RUBBLE

OIL STAIN: GOOD; MODERATE; POOR; TAR

SAMPLE: T = Thin section; S = SEM; X = XRD; C = Core piece

GRAIN SIZE AND SEDIMENTARY STRUCTURES: 32mm; 16mm; 8mm; 4mm; 2mm; 1mm; 500µm; 250µm; 125µm; 63µm; 20µm; Pebble; Granule; Sand; v. crs.; crs.; m.; f.; v.f.; Silty; Clay; Anhydrite / Coal

BIOTURBATION: 25; 50; 75

1731

1732

1733

1734

1735

1736

Core number 1

Balder sequence

LM

BLU-GRY

DTS

Injectite identified by discordant upper and lower surfaces

LM

BLU-GRY

Planar bedded\laminated Mudstone throughout

DTS

DTS

**SIMON MORRIS** **BIRKBECK COLLEGE**

**WELL: 25\11-23**

**Balder sequence**

**COUNTRY: Norway**

DATE: Autumn 2007 | SCALE: 1:25

AUTHOR: S.Morris | SHEET: 6 of 7

DRILLERS DEPTH METRES | CORE | OIL STAIN | SAMPLE | AGE | GAMMA RAY | GRAIN SIZE AND SEDIMENTARY STRUCTURES | LITHOLOGY | BIOTURBATION | TRENDS | FACIES | COLOUR | DESCRIPTION

CORE: CORE NUMBER; NO RECOVERY; SAMPLE REMOVED; RUBBLE

OIL STAIN: GOOD; MODERATE; POOR; TAR

SAMPLE: T = Thin section; S = SEM; X = XRD; C = Core piece

GRAIN SIZE AND SEDIMENTARY STRUCTURES: 32mm; 16mm; 8mm; 4mm; 2mm; 1mm; 500µm; 250µm; 125µm; 63µm; 20µm; Pebble; Granule; Sand; v. crs.; crs.; m.; f.; v.f.; Silty; Clay; Anhydrite / Coal

BIOTURBATION: 25; 50; 75

1736

1737

1738

1739

1740

1741

GY

Planar bedded\laminated

GY

GY

LM

Core number 1

Balder sequence

**SIMON MORRIS** **BIRKBECK COLLEGE**

**WELL: 25\11-23**

**Balder sequence**

**COUNTRY: Norway**

DATE: Autumn 2007 | SCALE: 1:25

AUTHOR: S.Morris | SHEET: 5 of 7

DRILLERS DEPTH METRES | CORE | OIL STAIN | SAMPLE | AGE | GAMMA RAY | GRAIN SIZE AND SEDIMENTARY STRUCTURES | LITHOLOGY | BIOTURBATION | TRENDS | FACIES | COLOUR | DESCRIPTION

CORE: CORE NUMBER; NO RECOVERY; SAMPLE REMOVED; RUBBLE

OIL STAIN: GOOD; MODERATE; POOR; TAR

SAMPLE: T = Thin section; S = SEM; X = XRD; C = Core piece

GRAIN SIZE AND SEDIMENTARY STRUCTURES: 32mm; 16mm; 8mm; 4mm; 2mm; 1mm; 500µm; 250µm; 125µm; 63µm; 20µm; Pebble; Granule; Sand; v. crs.; crs.; m.; f.; v.f.; Silty; Clay; Anhydrite / Coal

BIOTURBATION: 25; 50; 75

1741
1742
1743
1744
1745
1746

LM

Poorly defined cross-bedding

MS

LM

DTS

DTS

LM

MS

**SIMON MORRIS** **BIRKBECK COLLEGE**

**WELL: 25\11-23**

**Balder sequence**

**COUNTRY: Norway**

DATE: Autumn 2007 | SCALE: 1:25

AUTHOR: S.Morris | SHEET: 4 of 7

DRILLERS DEPTH METRES | CORE | OIL STAIN | SAMPLE | AGE | GAMMA RAY | GRAIN SIZE AND SEDIMENTARY STRUCTURES | LITHOLOGY | BIOTURBATION | TRENDS | FACIES | COLOUR | DESCRIPTION

CORE: CORE NUMBER; NO RECOVERY; SAMPLE REMOVED; RUBBLE

OIL STAIN: GOOD; MODERATE; POOR; TAR

SAMPLE: T = Thin section; S = SEM; X = XRD; C = Core piece

GRAIN SIZE AND SEDIMENTARY STRUCTURES: 32mm; 16mm; 8mm; 4mm; 2mm; 1mm; 500µm; 250µm; 125µm; 63µm; 20µm; Pebble; Granule; Sand; v. crs.; crs.; m.; f.; v.f.; Silty; Clay; Anhydrite / Coal

BIOTURBATION: 25; 50; 75

1746

1747

1748

1749

1750

1751

Core number 2

Balder sequence

DTS

LM

BS

DTS

LSL

BS

m

m

m

Minor injected sands

Probably concordant upper contact

Dish structures

**SIMON MORRIS** **BIRKBECK COLLEGE**

**WELL: 25\11-23**

**Balder sequence**

**COUNTRY: Norway**

DATE: Autumn 2007 | SCALE: 1:25

AUTHOR: S.Morris | SHEET: 3 of 7

DRILLERS DEPTH METRES | CORE | OIL STAIN | SAMPLE | AGE | GAMMA RAY | GRAIN SIZE AND SEDIMENTARY STRUCTURES | LITHOLOGY | BIOTURBATION | TRENDS | FACIES | COLOUR | DESCRIPTION

CORE: CORE NUMBER; NO RECOVERY; SAMPLE REMOVED; RUBBLE

OIL STAIN: GOOD; MODERATE; POOR; TAR

SAMPLE: T = Thin section; S = SEM; X = XRD; C = Core piece

GRAIN SIZE AND SEDIMENTARY STRUCTURES: 32mm; 16mm; 8mm; 4mm; 2mm; 1mm; 500µm; 250µm; 125µm; 63µm; 20µm; Pebble; Granule; Sand; v. crs.; crs.; m.; f.; v.f.; Silty; Clay; Anhydrite / Coal

BIOTURBATION: 25; 50; 75

1751

1752

1753

1754

1755

1756

Core number 2

Balder sequence

BS/MS?

Very difficult to differentiate internal structures due to high, tar-like oil stain

**SIMON MORRIS** **BIRKBECK COLLEGE**

**WELL: 25\11-23**

**Balder sequence**

**COUNTRY: Norway**

DATE: Autumn 2007 | SCALE: 1:25

AUTHOR: S.Morris | SHEET: 2 of 7

DRILLERS DEPTH METRES | CORE | OIL STAIN | SAMPLE | AGE | GAMMA RAY | GRAIN SIZE AND SEDIMENTARY STRUCTURES | LITHOLOGY | BIOTURBATION | TRENDS | FACIES | COLOUR | DESCRIPTION

CORE: CORE NUMBER; NO RECOVERY; SAMPLE REMOVED; RUBBLE

OIL STAIN: GOOD; MODERATE; POOR; TAR

SAMPLE: T = Thin section; S = SEM; X = XRD; C = Core piece

GAMMA RAY: GR; 0 GAPI 100

GRAIN SIZE AND SEDIMENTARY STRUCTURES: 32mm; 16mm; 8mm; 4mm; 2mm; 1mm; 500µm; 250µm; 125µm; 63µm; 20µm; Pebble; Granule; Sand; v. crs.; crs.; m.; f.; v.f.; Silty; Clay; Anhydrite / Coal

BIOTURBATION: 25 50 75

1755.5
1756
1757
1758
1759
1760
1760.5

Core Number 2

Balder sequence

MS?

Intermittent M'stone clasts around 1-5cm diameter

Core is oil stained, therefore colour of rock unclear- less oil stain than sheet 3 of 7.

Loading structures

BS/MS

**SIMON MORRIS** **BIRKBECK COLLEGE**

**WELL: 25\11-23**

**Balder sequence**

**COUNTRY: Norway**

DATE: Autumn 2007 | SCALE: 1:25

AUTHOR: S.Morris | SHEET: 1 of 7

DRILLERS DEPTH METRES | CORE | OIL STAIN | SAMPLE | AGE | GAMMA RAY | GRAIN SIZE AND SEDIMENTARY STRUCTURES | LITHOLOGY | BIOTURBATION | TRENDS | FACIES | COLOUR | DESCRIPTION

CORE: CORE NUMBER; NO RECOVERY; SAMPLE REMOVED; RUBBLE

OIL STAIN: GOOD; MODERATE; POOR; TAR

SAMPLE: T = Thin section; S = SEM; X = XRD; C = Core piece

GAMMA RAY: GR; 0 GAPI 100

GRAIN SIZE: 32mm 16mm 8mm 4mm 2mm 1mm 600µm 250µm 125µm 63µm 20µm; Pebble; Granule; Sand: v. crs. crs. m. f. v.f.; Silty; Clay; Anhydrite / Coal

BIOTURBATION: 25 50 75

1760.5
1761
1762
1763
1764
1765
1765.5

Core Number 2

Balder sequence

| FACIES | DESCRIPTION |
|---|---|
| BS | |
| MS | Massive sandstones with small scale loading structures |
| LSL | Calcite cemented siltstone concretion |
| | Planar lamination |
| MS/DTS? | Mudstone Rip-up clast (in excess of 10cm, note Gamma-ray increase) |
| DTS | Upturned laminae |
| LSL | Calcite cemented siltstone concretion |
| | Pebble horizons |
| DTS | |
| LSL | Occasional grey tuff beds |
| | Planar lamination |
| | Discordant upper and lower contacts mudstone Brecciation |
| SST | |
| | Compressional and extensional faults |
| LM | Convolute bedding |
| DTS | |
| | Sharp contact to *In situ* claystone and sandstone beds |
| LM | |

**SIMON MORRIS** **BIRKBECK COLLEGE** **WELL: 25\11-16**

**Lista sequence** **COUNTRY: Norway**

DATE: Autumn 2007 | SCALE: 1:25

AUTHOR: S.Morris | SHEET: 5 of 5

DRILLERS DEPTH METRES | CORE | OIL STAIN | SAMPLE | AGE | GAMMA RAY | GRAIN SIZE AND SEDIMENTARY STRUCTURES | LITHOLOGY | BIOTURBATION | TRENDS | FACIES | COLOUR | DESCRIPTION

CORE: CORE NUMBER; NO RECOVERY; SAMPLE REMOVED; RUBBLE

OIL STAIN: GOOD; MODERATE; POOR; TAR

SAMPLE: T = Thin section; S = SEM; X = XRD; C = Core piece

GRAIN SIZE AND SEDIMENTARY STRUCTURES: 32mm; 16mm; 8mm; 4mm; 2mm; 1mm; 500µm; 250µm; 125µm; 63µm; 20µm; Pebble; Granule; Sand; v. crs.; crs.; m.; f.; v.f.; Silty; Clay; Anhydrite / Coal

BIOTURBATION: 25; 50; 75

1767

1768

1769

1770

1771

1772

Core number 6

Lista sequence

BS

MS

MS

MS

Low angle cross strat

Dish structures, heavy oil stain obscuring cores

Low angle cross strat

Dish structures, heavy oil stain obscuring cores

Low angle cross strat

**SIMON MORRIS** **BIRKBECK COLLEGE** **WELL: 25\11-16**

**Lista sequence** **COUNTRY: Norway**

DATE: Autumn 2007 | SCALE: 1:25

AUTHOR: S.Morris | SHEET: 4 of 5

DRILLERS DEPTH METRES | CORE | OIL STAIN | SAMPLE | AGE | GAMMA RAY | GRAIN SIZE AND SEDIMENTARY STRUCTURES | LITHOLOGY | BIOTURBATION | TRENDS | FACIES | COLOUR | DESCRIPTION

CORE: CORE NUMBER; NO RECOVERY; SAMPLE REMOVED; RUBBLE

OIL STAIN: GOOD; MODERATE; POOR; TAR

SAMPLE: T = Thin section; S = SEM; X = XRD; C = Core piece

GRAIN SIZE AND SEDIMENTARY STRUCTURES: 32mm; 16mm; 8mm; 4mm; 2mm; 1mm; 500µm; 250µm; 125µm; 63µm; 20µm; Pebble; Granule; Sand; v. crs.; crs.; m.; f.; v.f.; Silty; Clay; Anhydrite / Coal

BIOTURBATION: 25; 50; 75

1772

1773

1774

1775

1776

1777

Core number 6

Lista sequence

MS

MS

BS

Low-angle cross strat to planar bedded

Heavily oil stained

Low-angle cross strat to planar bedded

**SIMON MORRIS** **BIRKBECK COLLEGE** **WELL: 25\11-16**

**Lista sequence** **COUNTRY: Norway**

DATE: Autumn 2007 | SCALE: 1:25

AUTHOR: S.Morris | SHEET: 3 of 5

DRILLERS DEPTH METRES | CORE | OIL STAIN | SAMPLE | AGE | GAMMA RAY | GRAIN SIZE AND SEDIMENTARY STRUCTURES | LITHOLOGY | BIOTURBATION | TRENDS | FACIES | COLOUR | DESCRIPTION

CORE NUMBER; NO RECOVERY; SAMPLE REMOVED; RUBBLE; GOOD; MODERATE; POOR; TAR; T = Thin section; S = SEM; X = XRD; C = Core piece

32mm 16mm 8mm 4mm 2mm 1mm 500µm 250µm 125µm 63µm 20µm

Pebble; Granule; Sand: v. crs. crs. m. f. v.f.; Silty; Clay; Anhydrite / Coal

25 50 75

1777

1778

1779

1780

1781

1782

Core number 6

Lista sequence

BS

BS/MS

BS

Heavily oil stained

High angle cross strat

Heavily oil stained
making confident facies
identification difficult

Heavily oil stained

**SIMON MORRIS** **BIRKBECK COLLEGE**

**WELL: 25\11-16**

**Lista sequence**

**COUNTRY: Norway**

DATE: Autumn 2007 | SCALE: 1:25

AUTHOR: S.Morris | SHEET: 2 of 5

DRILLERS DEPTH METRES | CORE | OIL STAIN | SAMPLE | AGE | GAMMA RAY | GRAIN SIZE AND SEDIMENTARY STRUCTURES | LITHOLOGY | BIOTURBATION | TRENDS | FACIES | COLOUR | DESCRIPTION

CORE: CORE NUMBER; NO RECOVERY; SAMPLE REMOVED; RUBBLE

OIL STAIN: GOOD; MODERATE; POOR; TAR

SAMPLE: T = Thin section; S = SEM; X = XRD; C = Core piece

GRAIN SIZE: 32mm 16mm 8mm 4mm 2mm 1mm 500µm 250µm 125µm 63µm 20µm

Pebble; Granule; Sand: v. crs. crs. m. f. v.f.; Silty; Clay; Anhydrite / Coal

BIOTURBATION: 25 50 75

1782

1783

1784

1785

1786

1787

Core number 7

Core number 8

Lista sequence

BS

BS

LM

GRN M'Stone

Minor Silt\Clay horizons

Heavily oil stained sandstones very difficult to define textures or sedimentary structures

Planar laminated green mudstones often dark green to very dark green and heavily bioturbated with Zoophycos burrows

**SIMON MORRIS** **BIRKBECK COLLEGE** **WELL: 25\11-16**

**Lista sequence** **COUNTRY: Norway**

DATE: Autumn 2007 | SCALE: 1:25

AUTHOR: S.Morris | SHEET: 1 of 5

DRILLERS DEPTH METRES | CORE | OIL STAIN | SAMPLE | AGE | GAMMA RAY | GRAIN SIZE AND SEDIMENTARY STRUCTURES | LITHOLOGY | BIOTURBATION | TRENDS | FACIES | COLOUR | DESCRIPTION

CORE NUMBER; NO RECOVERY; SAMPLE REMOVED; RUBBLE; GOOD; MODERATE; POOR; TAR; T = Thin section; S = SEM; X = XRD; C = Core piece

32mm 16mm 8mm 4mm 2mm 1mm 500µm 250µm 125µm 63µm 20µm

Pebble; Granule; Sand: v. crs. crs. m. f. v.f.; Silty; Clay; Anhydrite / Coal

25 50 75

1787
1788
1789
1790
1791
1792

Core number 8

Lista sequence

LM
Green mudstones

MS
LT. GY

LM

MS
LT. GY

MS
LT. GY

LSL

LM
GRN M'stone

Planar laminated Mudstone

Sharp contacts

Loading

Inverse-Normal grading

Mud rip-up clasts

Sharp contact to mudstone

Minor sandstones and siltstones

Planar laminated mudstones

**SIMON MORRIS** **BIRKBECK COLLEGE**

**WELL: 25\11-15**

**Lista sequence**

**COUNTRY: Norway**

DATE: Autumn 2007 | SCALE: 1:50

AUTHOR: S.Morris | SHEET: 2 of 2

DRILLERS DEPTH METRES | CORE (CORE NUMBER; NO RECOVERY; SAMPLE REMOVED; RUBBLE) | OIL STAIN (GOOD; MODERATE; POOR; TAR) | SAMPLE (T = Thin section; S = SEM; X = XRD; C = Core piece) | AGE | GAMMA RAY (GR; 0–140) | GRAIN SIZE AND SEDIMENTARY STRUCTURES (32mm; 16mm; 8mm; 4mm; 2mm; 1mm; 500µm; 250µm; 125µm; 63µm; 20µm; Pebble; Granule; Sand: v. crs., crs., m., f., v.f.; Silty; Clay; Anhydrite / Coal) | LITHOLOGY | BIOTURBATION (25; 50; 75) | TRENDS | FACIES | COLOUR | DESCRIPTION

1718
1722
1726
1730
1734
1738
1742
1746
1750
1754
1758

LM

MS

BS/MS

Lista sequence

Planar laminated\bedded

Discordant upper bedding surface-fluid escape?

Remobilization?

Large scale dish structures

Fluid escape structures

Low-angle cross strat-
Planar bedding throughout

**SIMON MORRIS** **BIRKBECK COLLEGE**

**WELL: 25\11-15**

**Lista sequence**

**COUNTRY: Norway**

DATE: Autumn 2007 | SCALE: 1:50

AUTHOR: S.Morris | SHEET: 1 of 2

DRILLERS DEPTH METRES | CORE | OIL STAIN | SAMPLE | AGE | GAMMA RAY | GRAIN SIZE AND SEDIMENTARY STRUCTURES | LITHOLOGY | BIOTURBATION | TRENDS | FACIES | COLOUR | DESCRIPTION

CORE: CORE NUMBER; NO RECOVERY; SAMPLE REMOVED; RUBBLE

OIL STAIN: GOOD; MODERATE; POOR; TAR

SAMPLE: T = Thin section; S = SEM; X = XRD; C = Core piece

GRAIN SIZE: 32mm 16mm 8mm 4mm 2mm 1mm 500µm 250µm 125µm 63µm 20µm; Pebble; Granule; Sand: v. crs. crs. m. f. v.f.; Silty; Clay; Anhydrite / Coal

BIOTURBATION: 25 50 75

1758

Core number 5

1762

1766

1770

1774

Core number 6

1778

1782

1786

1790

1794

Core number 7

1798

Lista sequence

| FACIES | COLOUR | DESCRIPTION |
|---|---|---|
| MS | BRN | Planar Lamination |
| MS | BRN | Massive sandstones |
| MS | | Mudstone rip-up clasts |
| MS | BRN | Massive sandtones |
| MS | | Large scale dish structures |
| MS/BS | BRN | Low angle cross-stratification |
| MS/BS | | Fluid escape structures |
| MS/BS | | HM/SM |
| BS | LT. GRY | Planar Lamination |
| BS | | Planar Lamination |

**SIMON MORRIS** **BIRKBECK COLLEGE** **WELL: 25\10-5**

**FORMATION: Above Balder FM** **COUNTRY: Norway**

DATE: Autumn 2007 | SCALE: 1:25

AUTHOR: S.Morris | SHEET: 2 of 2

DRILLERS DEPTH METRES | CORE | OIL STAIN | SAMPLE | AGE | GAMMA RAY | GRAIN SIZE AND SEDIMENTARY STRUCTURES | LITHOLOGY | BIOTURBATION | TRENDS | FACIES | COLOUR | DESCRIPTION | INTERPRETATION

CORE: CORE NUMBER; NO RECOVERY; SAMPLE REMOVED; RUBBLE

OIL STAIN: GOOD; MODERATE; POOR; TAR

SAMPLE: T = Thin section; S = SEM; X = XRD; C = Core piece

GRAIN SIZE AND SEDIMENTARY STRUCTURES: 32mm; 16mm; 8mm; 4mm; 2mm; 1mm; 500µm; 250µm; 125µm; 63µm; 20µm; Pebble; Granule; Sand; v. crs.; crs.; m.; f.; v.f.; Silty; Clay; Anhydrite / Coal

BIOTURBATION: 25; 50; 75

1738

1739

1740

1741

1742

1743

Core number 1

Lower Horda Claystone/Sandstone Formation

m

m

m

GRN

SSM

D.GRY

Mud Rip-up clasts

Small loading structures

Normally graded planar bedded sandstone

Brecciated M’stone

**SIMON MORRIS** **BIRKBECK COLLEGE** **WELL: 25\10-5**

**Balder sequence** **COUNTRY: Norway**

DATE: Autumn 2007 | SCALE: 1:25

AUTHOR: S.Morris | SHEET: 1 of 2

DRILLERS DEPTH METRES | CORE | OIL STAIN | SAMPLE | AGE | GAMMA RAY | GRAIN SIZE AND SEDIMENTARY STRUCTURES | LITHOLOGY | BIOTURBATION | TRENDS | FACIES | COLOUR | DESCRIPTION

CORE: CORE NUMBER; NO RECOVERY; SAMPLE REMOVED; RUBBLE

OIL STAIN: GOOD; MODERATE; POOR; TAR

SAMPLE: T = Thin section; S = SEM; X = XRD; C = Core piece

GRAIN SIZE: 32mm 16mm 8mm 4mm 2mm 1mm 500µm 250µm 125µm 63µm 20µm

Pebble; Granule; Sand: v. crs. crs. m. f. v.f.; Silty; Clay; Anhydrite / Coal

BIOTURBATION: 25 50 75

1783

1784

1785

1786

1787

1788

Core number 4

Balder sequence

SSM

GRY-GRN

L.GRN

D.GRN

Mud Rip-up clasts in Siltstone

Low angle cross strat

Planar bedded sandstones

Convolute bedding within M’stone

Planar bedded M’stone

**SIMON MORRIS** **BIRKBECK COLLEGE** **WELL: 25\8-11**

**Sele sequence** **COUNTRY: Norway**

DATE: Autumn 2007 | SCALE: 1:25

AUTHOR: S.Morris | SHEET: 5 of 5

DRILLERS DEPTH METRES | CORE | OIL STAIN | SAMPLE | AGE | GAMMA RAY | GRAIN SIZE AND SEDIMENTARY STRUCTURES | LITHOLOGY | BIOTURBATION | TRENDS | FACIES | COLOUR | DESCRIPTION

CORE: CORE NUMBER; NO RECOVERY; SAMPLE REMOVED; RUBBLE

OIL STAIN: GOOD; MODERATE; POOR; TAR

SAMPLE: T = Thin section; S = SEM; X = XRD; C = Core piece

GRAIN SIZE: 32mm 16mm 8mm 4mm 2mm 1mm 500µm 250µm 125µm 63µm 20µm; Pebble; Granule; Sand: v. crs. crs. m. f. v.f.; Silty; Clay; Anhydrite / Coal

BIOTURBATION: 25 50 75

1765

D. Gy

Planar bedded\laminated grey M'stone

LM

1766

1767

D. BRN

Loading structures

1768

Weak planar bedding

Angular 3-10cm Mud Rip-up clasts

BS

1769

D. Gy

Planar bedded\laminated grey M'stone

LM

1770

Core Number 6

Sele sequence

**SIMON MORRIS** **BIRKBECK COLLEGE** **WELL: 25\8-11**

**Sele sequence** **COUNTRY: Norway**

DATE: Autumn 2007 | SCALE: 1:25

AUTHOR: S.Morris | SHEET: 4 of 5

DRILLERS DEPTH METRES | CORE | OIL STAIN | SAMPLE | AGE | GAMMA RAY | GRAIN SIZE AND SEDIMENTARY STRUCTURES | LITHOLOGY | BIOTURBATION | TRENDS | FACIES | COLOUR | DESCRIPTION

CORE: CORE NUMBER; NO RECOVERY; SAMPLE REMOVED; RUBBLE

OIL STAIN: GOOD; MODERATE; POOR; TAR

SAMPLE: T = Thin section; S = SEM; X = XRD; C = Core piece

GRAIN SIZE AND SEDIMENTARY STRUCTURES: 32mm; 16mm; 8mm; 4mm; 2mm; 1mm; 500µm; 250µm; 125µm; 63µm; 20µm; Pebble; Granule; Sand; v. crs.; crs.; m.; f.; v.f.; Silty; Clay; Anhydrite / Coal

BIOTURBATION: 25; 50; 75

1770

1771

1772

1773

1774

1775

Core Number 6

Sele sequence

D. Gy

D. BRN

D. Gy

Planar bedded\laminated grey M'stone

D. Gy

D. Gy

LM

LT. Gy

Weak planar bedding

BS

**SIMON MORRIS** **BIRKBECK COLLEGE** **WELL: 25\8-11**

**Sele sequence** **COUNTRY: Norway**

DATE: Autumn 2007 | SCALE: 1:25

AUTHOR: S.Morris | SHEET: 3 of 5

| DRILLERS DEPTH METRES | CORE | OIL STAIN | SAMPLE | AGE | GAMMA RAY | GRAIN SIZE AND SEDIMENTARY STRUCTURES | LITHOLOGY | BIOTURBATION | TRENDS | FACIES | COLOUR | DESCRIPTION |
|---|---|---|---|---|---|---|---|---|---|---|---|---|
| | CORE NUMBER; NO RECOVERY; SAMPLE REMOVED; RUBBLE | GOOD; MODERATE; POOR; TAR | T = Thin section; S = SEM; X = XRD; C = Core piece | | | 32mm 16mm 8mm 4mm 2mm 1mm 500µm 250µm 125µm 63µm 20µm; Pebble; Granule; Sand: v. crs. crs. m. f. v.f.; Silty; Clay; Anhydrite / Coal | | 25 50 75 | | | | |
| 1775 | | | | | | | | | | | LT. Gy | |
| 1776 | | | | | | | | | | | LT. Gy | Core is progressively poorly preserved, from 1778-75m |
| 1777 | | | | | | | | | | | LT. BRN | |
| 1778 | | | | | | | | | | | BRN | |
| 1779 | | | | | | | | | | | D. BRN | Weak indications of dish and pipe structures<br>Weak planar bedding |
| 1780 | Core number 6 | | | Hermod Sandstone Formation | | | | | | MS | | |

**SIMON MORRIS** **BIRKBECK COLLEGE** **WELL: 25\8-11**

**Sele sequence** **COUNTRY: Norway**

DATE: Autumn 2007 | SCALE: 1:25

AUTHOR: S.Morris | SHEET: 2 of 5

DRILLERS DEPTH METRES | CORE | OIL STAIN | SAMPLE | AGE | GAMMA RAY | GRAIN SIZE AND SEDIMENTARY STRUCTURES | LITHOLOGY | BIOTURBATION | TRENDS | FACIES | COLOUR | DESCRIPTION

CORE: CORE NUMBER; NO RECOVERY; SAMPLE REMOVED; RUBBLE

OIL STAIN: GOOD; MODERATE; POOR; TAR

SAMPLE: T = Thin section; S = SEM; X = XRD; C = Core piece

GRAIN SIZE AND SEDIMENTARY STRUCTURES: 32mm, 16mm, 8mm, 4mm, 2mm, 1mm, 500µm, 250µm, 125µm, 63µm, 20µm; Pebble, Granule, Sand (v. crs., crs., m., f., v.f.), Silty, Clay, Anhydrite / Coal

BIOTURBATION: 25 50 75

1780

1781

1782

1783

1784

1785

Core number 6

Sele sequence

LT. Gy

LT. Gy

LT. Gy

LT. Gy

MS

Structureless grey Sandstones

Small scale loading?

**SIMON MORRIS** **BIRKBECK COLLEGE**

**WELL: 25\8-11**

**Sele sequence**

**COUNTRY: Norway**

DATE: Autumn 2007 | SCALE: 1:25

AUTHOR: S.Morris | SHEET: 1 of 5

DRILLERS DEPTH METRES | CORE | OIL STAIN | SAMPLE | AGE | GAMMA RAY | GRAIN SIZE AND SEDIMENTARY STRUCTURES | LITHOLOGY | BIOTURBATION | TRENDS | FACIES | COLOUR | DESCRIPTION

CORE: CORE NUMBER; NO RECOVERY; SAMPLE REMOVED; RUBBLE

OIL STAIN: GOOD; MODERATE; POOR; TAR

SAMPLE: T = Thin section; S = SEM; X = XRD; C = Core piece

GRAIN SIZE AND SEDIMENTARY STRUCTURES: 32mm; 16mm; 8mm; 4mm; 2mm; 1mm; 500µm; 250µm; 125µm; 63µm; 20µm; Pebble; Granule; Sand; v. crs.; crs.; m.; f.; v.f.; Silty; Clay; Anhydrite / Coal

BIOTURBATION: 25; 50; 75

1785

1786

1787

1788

1789

1790

Core number 6

Sele sequence

BS/MS — LT. Gy — Weak planar bedding

Structureless grey Sandstones

MS — LT. Gy

BS/MS — LT. Gy — Weak planar bedding

LT. Gy

**SIMON MORRIS** **BIRKBECK COLLEGE**

**WELL: 25\8-10ST2**

**Lista sequence**

**COUNTRY: Norway**

DATE: Autumn 2007 | SCALE: 1:25

AUTHOR: S.Morris | SHEET: 3 of 3

DRILLERS DEPTH METRES | CORE | OIL STAIN | SAMPLE | AGE | GAMMA RAY | GRAIN SIZE AND SEDIMENTARY STRUCTURES | LITHOLOGY | BIOTURBATION | TRENDS | FACIES | COLOUR | DESCRIPTION

CORE: CORE NUMBER; NO RECOVERY; SAMPLE REMOVED; RUBBLE

OIL STAIN: GOOD; MODERATE; POOR; TAR

SAMPLE: T = Thin section; S = SEM; X = XRD; C = Core piece

GRAIN SIZE AND SEDIMENTARY STRUCTURES: 32mm; 16mm; 8mm; 4mm; 2mm; 1mm; 500µm; 250µm; 125µm; 63µm; 20µm; Pebble; Granule; Sand; v. crs.; crs.; m.; f.; v.f.; Silty; Clay; Anhydrite / Coal

BIOTURBATION: 25; 50; 75

1761

1762

1763

1764

1765

1766

Core number 1

Lista sequence

BS

LSL

LM

GRN

Planar bedded sandstones

High angle cross strat

Minor pebble bed

Planar bedded M’stone

**SIMON MORRIS** **BIRKBECK COLLEGE** **WELL: 25\8-10ST2**

**Lista sequence** **COUNTRY: Norway**

DATE: Autumn 2007 | SCALE: 1:25

AUTHOR: S.Morris | SHEET: 2 of 3

DRILLERS DEPTH METRES | CORE | OIL STAIN | SAMPLE | AGE | GAMMA RAY | GRAIN SIZE AND SEDIMENTARY STRUCTURES | LITHOLOGY | BIOTURBATION | TRENDS | FACIES | COLOUR | DESCRIPTION

CORE: CORE NUMBER; NO RECOVERY; SAMPLE REMOVED; RUBBLE

OIL STAIN: GOOD; MODERATE; POOR; TAR

SAMPLE: T = Thin section; S = SEM; X = XRD; C = Core piece

GRAIN SIZE AND SEDIMENTARY STRUCTURES: 32mm; 16mm; 8mm; 4mm; 2mm; 1mm; 500µm; 250µm; 125µm; 63µm; 20µm; Pebble; Granule; Sand; v. crs.; crs.; m.; f.; v.f.; Silty; Clay; Anhydrite / Coal

BIOTURBATION: 25; 50; 75

1776

1777

1778

1779

1780

1781

Core number 1

Lista sequence

LM

BS

LM

BS

LM

GRN

GRN

GRN

YEL-BRN obscured by oil stain

Planar laminated GRN M'stone

High angle cross strat

Sharp contact between M'stone and S'stone

Dish structures

Weak planar bedding

Planar laminated GRN M'stone

**SIMON MORRIS** **BIRKBECK COLLEGE**

**WELL: 25\8-10ST2**

**Lista sequence**

**COUNTRY: Norway**

DATE: Autumn 2007 | SCALE: 1:25

AUTHOR: S.Morris | SHEET: 1 of 3

DRILLERS DEPTH METRES | CORE | OIL STAIN | SAMPLE | AGE | GAMMA RAY | GRAIN SIZE AND SEDIMENTARY STRUCTURES | LITHOLOGY | BIOTURBATION | TRENDS | FACIES | COLOUR | DESCRIPTION

CORE: CORE NUMBER; NO RECOVERY; SAMPLE REMOVED; RUBBLE

OIL STAIN: GOOD; MODERATE; POOR; TAR

SAMPLE: T = Thin section; S = SEM; X = XRD; C = Core piece

GRAIN SIZE AND SEDIMENTARY STRUCTURES: 32mm; 16mm; 8mm; 4mm; 2mm; 1mm; 500µm; 250µm; 125µm; 63µm; 20µm; Pebble; Granule; Sand; v. crs.; crs.; m.; f.; v.f.; Silty; Clay; Anhydrite / Coal

BIOTURBATION: 25; 50; 75

1781

1782

1783

1784

1785

1786

Core number 1

Lista sequence

MS

BS

YEL-BRN

Structureless sandstones

Weak planar bedding

**SIMON MORRIS** **BIRKBECK COLLEGE**

**WELL: 25\8-10s**

**Sele sequence**

**COUNTRY: Norway**

DATE: Autumn 2007 | SCALE: 1:25

AUTHOR: S.Morris | SHEET: 2 of 2

DRILLERS DEPTH METRES | CORE | OIL STAIN | SAMPLE | AGE | GAMMA RAY | GRAIN SIZE AND SEDIMENTARY STRUCTURES | LITHOLOGY | BIOTURBATION | TRENDS | FACIES | COLOUR | DESCRIPTION

CORE: CORE NUMBER; NO RECOVERY; SAMPLE REMOVED; RUBBLE

OIL STAIN: GOOD; MODERATE; POOR; TAR

SAMPLE: T = Thin section; S = SEM; X = XRD; C = Core piece

GRAIN SIZE AND SEDIMENTARY STRUCTURES: 32mm, 16mm, 8mm, 4mm, 2mm, 1mm, 500µm, 250µm, 125µm, 63µm, 20µm; Pebble, Granule, Sand (v. crs., crs., m., f., v.f.), Silty, Clay, Anhydrite / Coal

BIOTURBATION: 25, 50, 75

1729

1730

1731

1732

1733

1734

Core number 1

Sele sequence

DFS\HDS

MS

IJ

HM

MS-RM?

Planar bedding

Mud rip-up clasts

Inverse-normal grading, with pebble beds

minor sandstone injectite

15cm (length) ptygmatically folded minor sandstones

minor sandstone injectite

Discordant upper contact

Weak indications of dish structures

Discordant upper contact

Weak indications of dish structures

**SIMON MORRIS** **BIRKBECK COLLEGE** **WELL: 25\8-10s**

**Sele sequence** **COUNTRY: Norway**

DATE: Autumn 2007 | SCALE: 1:25

AUTHOR: S.Morris | SHEET: 1 of 2

DRILLERS DEPTH METRES | CORE | OIL STAIN | SAMPLE | AGE | GAMMA RAY | GRAIN SIZE AND SEDIMENTARY STRUCTURES | LITHOLOGY | BIOTURBATION | TRENDS | FACIES | COLOUR | DESCRIPTION

CORE: CORE NUMBER; NO RECOVERY; SAMPLE REMOVED; RUBBLE

OIL STAIN: GOOD; MODERATE; POOR; TAR

SAMPLE: T = Thin section; S = SEM; X = XRD; C = Core piece

GRAIN SIZE AND SEDIMENTARY STRUCTURES: 32mm; 16mm; 8mm; 4mm; 2mm; 1mm; 500µm; 250µm; 125µm; 63µm; 20µm; Pebble; Granule; Sand; v. crs.; crs.; m.; f.; v.f.; Silty; Clay; Anhydrite / Coal

BIOTURBATION: 25; 50; 75

1734

1735

1736

1737

1738

1738.5

Core number 1

Hemod Sandstone Formation

DTS

LM

LSL/BS

BS

GRN M'stone, YEL-BRN sandstone heavily oil stained

Localised sandstone injections-discordant upper and lower contacts

Dish structures within injections

Climbing ripple lamination

Inverse to normal grading

Planar bedded M'stone

Mud rip-up clasts

Extensional and compressional micro-faulting

**SIMON MORRIS** **BIRKBECK COLLEGE**

**WELL: 25\8-4**

**Lista sequence**

**COUNTRY: Norway**

DATE: Autumn 2007 | SCALE: 1:25

AUTHOR: S.Morris | SHEET: 10 of 10

DRILLERS DEPTH METRES | CORE | OIL STAIN | SAMPLE | AGE | GAMMA RAY | GRAIN SIZE AND SEDIMENTARY STRUCTURES | LITHOLOGY | BIOTURBATION | TRENDS | FACIES | COLOUR | DESCRIPTION

CORE: CORE NUMBER; NO RECOVERY; SAMPLE REMOVED; RUBBLE

OIL STAIN: GOOD; MODERATE; POOR; TAR

SAMPLE: T = Thin section; S = SEM; X = XRD; C = Core piece

GRAIN SIZE: 32mm, 16mm, 8mm, 4mm, 2mm, 1mm, 500µm, 250µm, 125µm, 63µm, 20µm; Pebble, Granule, Sand (v. crs., crs., m., f., v.f.), Silty, Clay, Anhydrite / Coal

BIOTURBATION: 25 50 75

1779

1780

1781

1782

1783

1784

Core number 7

Lista sequence

LM

BS

LT. GY

MS

LT. GY

Weak planar bedding

Large scale dewatering struictures

Structureless sandstones

**SIMON MORRIS** **BIRKBECK COLLEGE**

**WELL: 25\8-4**

**Lista sequence**

**COUNTRY: Norway**

DATE: Autumn 2007 | SCALE: 1:25

AUTHOR: S.Morris | SHEET: 9 of 10

DRILLERS DEPTH METRES | CORE | OIL STAIN | SAMPLE | AGE | GAMMA RAY | GRAIN SIZE AND SEDIMENTARY STRUCTURES | LITHOLOGY | BIOTURBATION | TRENDS | FACIES | COLOUR | DESCRIPTION

CORE: CORE NUMBER; NO RECOVERY; SAMPLE REMOVED; RUBBLE

OIL STAIN: GOOD; MODERATE; POOR; TAR

SAMPLE: T = Thin section; S = SEM; X = XRD; C = Core piece

GRAIN SIZE AND SEDIMENTARY STRUCTURES: 32mm; 16mm; 8mm; 4mm; 2mm; 1mm; 500µm; 250µm; 125µm; 63µm; 20µm; Pebble; Granule; Sand; v. crs.; crs.; m.; f.; v.f.; Silty; Clay; Anhydrite / Coal

BIOTURBATION: 25; 50; 75

1784

1785

1786

1787

1788

1789

Core number 7

Lista sequence

| FACIES | COLOUR | DESCRIPTION |
|---|---|---|
| MS | LT. GY | Massive structureless sandstones |
| MS | LT. GY | |
| MS | LT. GY | Massive structureless sandstones |
| MS | LT. GY | |

**SIMON MORRIS** **BIRKBECK COLLEGE**

**WELL: 25\8-4**

**Lista sequence**

**COUNTRY: Norway**

DATE: Autumn 2007 | SCALE: 1:25

AUTHOR: S.Morris | SHEET: 8 of 10

DRILLERS DEPTH METRES | CORE | OIL STAIN | SAMPLE | AGE | GAMMA RAY | GRAIN SIZE AND SEDIMENTARY STRUCTURES | LITHOLOGY | BIOTURBATION | TRENDS | FACIES | COLOUR | DESCRIPTION

CORE NUMBER; NO RECOVERY; SAMPLE REMOVED; RUBBLE; GOOD; MODERATE; POOR; TAR; T = Thin section; S = SEM; X = XRD; C = Core piece

32mm 16mm 8mm 4mm 2mm 1mm 500µm 250µm 125µm 63µm 20µm

Pebble; Granule; Sand: v. crs., crs., m., f., v.f.; Silty; Clay; Anhydrite / Coal

25 50 75

1789
1790
1791
1792
1793
1794

Core number 7

Lista sequecne

LT. GY

MS

Massive structureless sandstones

Loading structures

LT. GY

MS

LT. GY

Massive structureless sandstones

**SIMON MORRIS** **BIRKBECK COLLEGE** **WELL: 25\8-4**

**Lista sequence** **COUNTRY: Norway**

DATE: Autumn 2007 | SCALE: 1:25

AUTHOR: S.Morris | SHEET: 7 of 10

CORE: CORE NUMBER; NO RECOVERY; SAMPLE REMOVED; RUBBLE

OIL STAIN: GOOD; MODERATE; POOR; TAR

SAMPLE: T = Thin section; S = SEM; X = XRD; C = Core piece

GRAIN SIZE AND SEDIMENTARY STRUCTURES: 32mm; 16mm; 8mm; 4mm; 2mm; 1mm; 500µm; 250µm; 125µm; 63µm; 20µm; Pebble; Granule; Sand; v. crs.; crs.; m.; f.; v.f.; Silty; Clay; Anhydrite / Coal

BIOTURBATION: 25; 50; 75

| DRILLERS DEPTH METRES | AGE | GAMMA RAY | LITHOLOGY | TRENDS | FACIES | COLOUR | DESCRIPTION |
|---|---|---|---|---|---|---|---|
| 1794 | | | | | | | |
| 1795 | | | | | MS | LT. GY | Massive structureless sandstones |
| 1796 | | | | | MS | | |
| 1797 | | | | | MS | LT. GY | Massive structureless sandstones |
| 1798 | | | | | | | Low-angle cross strat<br>Weak planar bedding |
| 1799 | | | | | BS | LT. GY | |

Core number 8

Lista sequence

**SIMON MORRIS** **BIRKBECK COLLEGE**

**WELL: 25\8-4**

**Lista sequence**

**COUNTRY: Norway**

DATE: Autumn 2007 | SCALE: 1:25

AUTHOR: S.morris | SHEET: 6 of 10

DRILLERS DEPTH METRES | CORE | OIL STAIN | SAMPLE | AGE | GAMMA RAY | GRAIN SIZE AND SEDIMENTARY STRUCTURES | LITHOLOGY | BIOTURBATION | TRENDS | FACIES | COLOUR | DESCRIPTION

CORE: CORE NUMBER; NO RECOVERY; SAMPLE REMOVED; RUBBLE

OIL STAIN: GOOD; MODERATE; POOR; TAR

SAMPLE: T = Thin section; S = SEM; X = XRD; C = Core piece

GRAIN SIZE AND SEDIMENTARY STRUCTURES: 32mm; 16mm; 8mm; 4mm; 2mm; 1mm; 500µm; 250µm; 125µm; 63µm; 20µm; Pebble; Granule; Sand; v. crs.; crs.; m.; f.; v.f.; Silty; Clay; Anhydrite / Coal

BIOTURBATION: 25; 50; 75

1799
1800
1801
1802
1803
1804

Core number 8

Lista sequence

FACIES: BS; MS; BS; MS; BS

COLOUR: LT. GY; LT. GY; LT. GY; LT. GY

DESCRIPTION:

Structureless sandstones

Weak planar bedding

**SIMON MORRIS** **BIRKBECK COLLEGE** **WELL: 25\8-4**

**Lista sequence** **COUNTRY: Norway**

DATE: Autumn 2007 | SCALE: 1:25

AUTHOR: S.Morris | SHEET: 5 of 10

DRILLERS DEPTH METRES | CORE | OIL STAIN | SAMPLE | AGE | GAMMA RAY | GRAIN SIZE AND SEDIMENTARY STRUCTURES | LITHOLOGY | BIOTURBATION | TRENDS | FACIES | COLOUR | DESCRIPTION

CORE: CORE NUMBER; NO RECOVERY; SAMPLE REMOVED; RUBBLE

OIL STAIN: GOOD; MODERATE; POOR; TAR

SAMPLE: T = Thin section; S = SEM; X = XRD; C = Core piece

GRAIN SIZE AND SEDIMENTARY STRUCTURES: 32mm; 16mm; 8mm; 4mm; 2mm; 1mm; 500µm; 250µm; 125µm; 63µm; 20µm; Pebble; Granule; Sand; v. crs.; crs.; m.; f.; v.f.; Silty; Clay; Anhydrite / Coal

BIOTURBATION: 25; 50; 75

1804

1805

1806

1807

1808

1809

Core number 8

Heimdal sandstone Member

FACIES: BS; MS; BS

COLOUR: LT. GY; LT. GY; LT. GY; LT. GY

DESCRIPTION:

Loadins and dish sturtcures

Low-angle cross strat

Planar bedding

Weak planar bedding

**SIMON MORRIS** **BIRKBECK COLLEGE** **WELL: 25\8-4**

**Lista sequence** **COUNTRY: Norway**

DATE: Autumn 2007 | SCALE: 1:25

AUTHOR: S.Morris | SHEET: 4 of 10

| DRILLERS DEPTH METRES | CORE | OIL STAIN | SAMPLE | AGE | GAMMA RAY | GRAIN SIZE AND SEDIMENTARY STRUCTURES | LITHOLOGY | BIOTURBATION | TRENDS | FACIES | COLOUR | DESCRIPTION |
|---|---|---|---|---|---|---|---|---|---|---|---|---|

CORE: CORE NUMBER; NO RECOVERY; SAMPLE REMOVED; RUBBLE

OIL STAIN: GOOD; MODERATE; POOR; TAR

SAMPLE: T = Thin section; S = SEM; X = XRD; C = Core piece

GRAIN SIZE AND SEDIMENTARY STRUCTURES: 32mm; 16mm; 8mm; 4mm; 2mm; 1mm; 500µm; 250µm; 125µm; 63µm; 20µm; Pebble; Granule; Sand; v. crs.; crs.; m.; f.; v.f.; Silty; Clay; Anhydrite / Coal

BIOTURBATION: 25; 50; 75

1809

1810

1811

1812

1813

1814

Core number 8

Core number 9

Lista sequence

LT GY

MS

Structureless sands

LT GY

MS

LT GY

**SIMON MORRIS** **BIRKBECK COLLEGE** **WELL: 25\8-4**

**Lista sequence** **COUNTRY: Norway**

DATE: Autumn 2007 | SCALE: 1:25

AUTHOR: S.Morris | SHEET: 3 of 10

| DRILLERS DEPTH METRES | CORE | OIL STAIN | SAMPLE | AGE | GAMMA RAY | GRAIN SIZE AND SEDIMENTARY STRUCTURES | LITHOLOGY | BIOTURBATION | TRENDS | FACIES | COLOUR | DESCRIPTION |
|---|---|---|---|---|---|---|---|---|---|---|---|---|
| 1814 | CORE NUMBER; NO RECOVERY; SAMPLE REMOVED; RUBBLE | GOOD; MODERATE; POOR; TAR | T = Thin section; S = SEM; X = XRD; C = Core piece | | | 32mm 16mm 8mm 4mm 2mm 1mm 500µm 250µm 125µm 63µm 20µm; Pebble; Granule; Sand: v. crs. crs. m. f. v.f.; Silty; Clay; Anhydrite / Coal | | 25 50 75 | | BS | LT. GY | Weak planar bedding |
| 1815 | | | | | | | | | | BS | LT. GY | Weak planar bedding |
| 1816 | | | | | | | | | | MS | | |
| 1817 | | | | | | | | | | BS | LT. GY | |
| 1818 | | | | | | | | | | BS | LT. GY | Weak planar bedding |
| 1819 | Core number 9 | | Lista sequence | | | | | | | | | |

**SIMON MORRIS** **BIRKBECK COLLEGE** **WELL: 25\8-4**

**Lista sequence** **COUNTRY: Norway**

DATE: Autumn 2007 | SCALE: 1:25

AUTHOR: S.Morris | SHEET: 2 of 10

| DRILLERS DEPTH METRES | CORE | OIL STAIN | SAMPLE | AGE | GAMMA RAY | GRAIN SIZE AND SEDIMENTARY STRUCTURES | LITHOLOGY | BIOTURBATION | TRENDS | FACIES | COLOUR | DESCRIPTION |
|---|---|---|---|---|---|---|---|---|---|---|---|---|
| | CORE NUMBER; NO RECOVERY; SAMPLE REMOVED; RUBBLE | GOOD; MODERATE; POOR; TAR | T = Thin section; S = SEM; X = XRD; C = Core piece | | | 32mm 16mm 8mm 4mm 2mm 1mm 500µm 250µm 125µm 63µm 20µm; Pebble; Granule; Sand: v. crs. crs. m. f. v.f.; Silty; Clay; Anhydrite / Coal | | 25 50 75 | | | | |
| 1819 | | | | | | | | | | | | Crystalline texture- cementation effect? |
| | | | | | | | | | | | LT. GY | |
| | | | | | | | | | | BS | | |
| 1820 | | | | | | | | | | | | |
| | | | | | | | | | | MS | | Massive homogenous sandstone |
| | | | | | | | | | | | LT. GY | |
| 1821 | | | | | | | | | | | | |
| | | | | | | | | | | | | Weak planar bedding |
| 1822 | | | | | | | | | | | | |
| | | | | | | | | | | | LT. GY | High textural & mineralogical maturity |
| 1823 | | | | | | | | | | | | |
| | | | | | | | | | | | LT. GY | |
| | | | | | | | | | | BS | | |
| 1824 | Core number 9 | | | Lista sequence | | | | | | | | |

**SIMON MORRIS** **BIRKBECK COLLEGE**

**WELL: 25\8-4**

**Lista sequence**

**COUNTRY: Norway**

DATE: Autumn 2007 | SCALE: 1:25

AUTHOR: S.Morris | SHEET: 1 of 10

DRILLERS DEPTH METRES | CORE | OIL STAIN | SAMPLE | AGE | GAMMA RAY | GRAIN SIZE AND SEDIMENTARY STRUCTURES | LITHOLOGY | BIOTURBATION | TRENDS | FACIES | COLOUR | DESCRIPTION

CORE: CORE NUMBER; NO RECOVERY; SAMPLE REMOVED; RUBBLE

OIL STAIN: GOOD; MODERATE; POOR; TAR

SAMPLE: T = Thin section; S = SEM; X = XRD; C = Core piece

GRAIN SIZE AND SEDIMENTARY STRUCTURES: 32mm; 16mm; 8mm; 4mm; 2mm; 1mm; 500µm; 250µm; 125µm; 63µm; 20µm; Pebble; Granule; Sand; v. crs.; crs.; m.; f.; v.f.; Silty; Clay; Anhydrite / Coal

BIOTURBATION: 25; 50; 75

1824

1825

1826

1827

1828

1829

Core number 9

Lista sequence

MS

LT. GY

LT. GY

LT. GY

Weak planar bedding

LT. GY

Weak planar bedding

| Depth MD (m) | Facies 1 | Facies 2 |
|---|---|---|
| 1729 | | |
| 1729.5 | BS | |
| 1729.80 | MS | |
| 1729.90 | LM | SST |
| 1730 | MS | |
| 1730.85 | MS | |
| 1732.15 | LM | SST |
| 1732.25 | SST | LSD |
| 1733 | LM | DTS/SST |
| 1734.20 | DTS | |
| 1735.35 | LM | DTS |
| 1735.50 | BS | |
| 1735.80 | LM | |
| 1736 | LSL | |
| 1736.20 | BS | |
| 1736.50 | LM | |
| 1737 | MS | |
| 1737.20 | LM | |
| 1737.35 | BS | |
| 1737.40 | LSL | |
| 1738.5 | LM | |
| | | |
| 1761 | | |
| 1761.30 | LSL | |
| 1762 | BS | SDS |
| 1763 | BS | |
| 1763.4 | BS | |
| 1764.1 | MS | SDS |
| 1764.2 | LM | |
| 1764.4 | MS | SDS |
| 1764.6 | LM | |
| 1765 | LSL | |
| 1766 | LM | |
| | | |
| 1776 | | |
| 1777.3 | LM | |
| 1777.6 | BS | |
| 1778 | LM | |
| 1779.5 | MS | SDS |
| 1781 | LM | |
| 1783.5 | MS | SDS |
| 1785 | MS | SDS |

Well: 8-10S

| Depth MD (m) | Facies 2 | Facies 2 |
|---|---|---|
| 1767.8 | | |
| 1769.5 | MS | SDS |
| | | |
| 1769.8 | | |
| 1770.1 | BS | SDS |
| | | |
| 1770.4 | | |
| 1773.5 | MS | SDS |
| | | |
| 1774 | | |
| 1774.5 | BS | |
| | | |
| 1776 | | |
| 1777 | BS | |
| 1777.5 | MS | |
| | | |
| 1778 | | |
| 1779.9 | MS | |
| 1780 | BS | |
| | | |
| 1781.10 | | |
| 1782 | MS | |
| 1783 | BS | |
| | | |
| 1783.5 | | |
| 1784 | BS | |
| 1787 | LM | |

Well: 11-16

| Depth MD (m) | Facies 1 | Facies 2 |
|---|---|---|
| 1739 | | |
| 1739.8 | MS | MCB |
| | | |
| 1740.1 | | |
| 1741 | MS | |
| 1743 | LM | |
| | | |
| 1785 | | |
| 1786 | LSL | |
| 1786.2 | BS | |
| 1786.5 | BS | |
| 1787.3 | BS | |
| 1788 | LM | |

Well: 10-5

| Depth MD (m) | Facies 1 | Facies 2 |
|---|---|---|
| 1765 | | |
| 1765.8 | LM | |
| 1767 | BS | |
| 1768 | BS | |
| 1768.8 | MS | |
| 1774.5 | LM | |
| 1775.5 | BS | |
| 1778 | MS | LSD |
| 1779 | BS | |
| 1781 | MS | SDS |
| 1785 | MS | LSD |
| 1788 | MS | |
| 1789.5 | MS | |

Well: 8-11

| Depth MD (m) | Facies 1 | Facies 2 |
|---|---|---|
| 1718 | | |
| 1732 | LM | |
| 1740 | MS | LSD |
| 1742 | MS | SDS |
| 1758 | MS | SDS |
| 1762 | BS | |
| 1767 | MS | MCB |
| 1774 | MS | SDS |
| 1785 | MS | LSD |
| | | |
| 1786 | | |
| 1789 | BS | |
| 1795 | MS | SDS |
| 1798 | MS | SDS |

Well: 11-15

| Depth MD (m) | Facies 1 | Facies 2 |
|---|---|---|
| 1734 | | |
| 1734.5 | LM | |
| 1734.8 | DTS | |
| 1735 | LM | |
| 1735.5 | LM | |
| 1735.6 | DTS | |
| 1735.7 | LM | |
| 1736.1 | DTS | SST |
| 1738.1 | LM | |
| 1738.2 | DTS | |
| 1739.1 | LM | |
| 1739.15 | SST | |
| 1740.5 | SST | |
| 1741 | LM | |
| 1741.1 | DTS | |
| 1743.2 | LM | |
| 1743.4 | DTS | |
| 1744.4 | LM | |
| 1744.55 | DTS | |
| 1744.65 | LM | |
| 1744.75 | SST | |
| 1745.5 | LM | |
| 1746 | DTS | |
| 1746.1 | SST | |
| 1747.4 | LM | |
| 1747.55 | DTS | |
| 1749 | LM | DTS |
| 1749.7 | BS | |
| 1750.2 | LM | |
| 1751 | BS | |
| 1755.5 | MS | SDS |
| | | |
| 1756 | | |
| 1760.1 | MS | MCB |
| 1762 | BS | |
| 1762.3 | LSL | |
| 1763.2 | DTS | MCB |
| 1763.5 | LSL | |
| 1764 | DTS | |
| 1764.2 | DTS | |
| 1764.6 | LM | |
| 1765 | DTS | |
| 1765.3 | LM | |
| 1765.4 | DTS | |
| 1765.5 | LM | |

Well: 11-23

| Depth MD (m) | Facies 1 | Facies 2 |
|---|---|---|
| 1779 | | |
| 1780.25 | DTS | |
| 1780.5 | LM | DTS |
| 1781 | DTS | |
| 1781.4 | MS | SDS |
| 1783 | MS | SDS |
| | | |
| 1783.2 | | |
| 1783.4 | MS | |
| | | |
| 1783.45 | | |
| 1783.55 | MS | |
| | | |
| 1783.60 | | |
| 1784 | MS | |
| 1785 | MS | SDS |
| | | |
| 1785.2 | | |
| 1786 | MS | SDS |
| | | |
| 1786.7 | | |
| 1788 | MS | SDS |
| | | |
| 1788.1 | | |
| 1789 | MS | SDS |
| 1791.8 | MS | SDS |
| | | |
| 1791.9 | | |
| 1792.9 | MS | |
| | | |
| 1794.6 | | |
| 1795.8 | MS | SDS |
| | | |
| 1795.9 | | |
| 1796.2 | MS | SDS |
| | | |
| 1796.8 | | |
| 1797.2 | MS | SDS |
| | | |
| 1797.7 | | |
| 1801.8 | MS | |
| | | |
| 1802.4 | | |
| 1812 | MS | SDS |
| | | |
| 1812.5 | | |
| 1814.6 | MS | SDS |
| | | |
| 1814.7 | | |
| 1819 | MS | |
| 1819.5 | MS | |
| 1824 | MS | SDS |
| 1829 | MS | |

Well: 8-4

| Depth MD (m) | Facies 1 | Facies 2 |
|---|---|---|
| 1869 | | |
| 1871.1 | LM | |
| 1871.65 | DTS | MCB |
| 1873.05 | LM | LSL |
| 1873.85 | DTS | MCB |
| 1874.5 | LM | |
| 1874.55 | SST | |
| 1876.75 | LM | |
| 1877.0 | DTS | |
| 1877.2 | LM | |
| 1877.3 | DTS | |
| 1877.65 | LM | |
| 1878.3 | DTS | |
| 1879.7 | LM | |
| 1879.75 | SST | |
| 1879.90 | LM | |
| 1879.95 | SST | |
| 1880 | LM | |
| 1880.15 | SST | |
| 1883.90 | LSL | |
| 1884.10 | BS | |
| 1886 | LM | |
| 1889.35 | LM | LSL |
| | | |
| 1889.40 | | |
| 1891.20 | DTS | |
| 1896 | LM | LSL |
| 1901.5 | DTS | |
| | | |
| 1902 | | |
| 1904 | MS | SDS |
| | | |
| 1905.3 | | |
| 1905.7 | MS | LSD |
| | | |
| 1906 | | |
| 1908.5 | MS | LSD |
| | | |
| 1908.6 | | |
| 1915 | MS | LSD |
| | | |
| 1915.30 | | |
| 1921.5 | MS | |
| 1926.5 | MS | SDS |
| | | |
| 1930 | | |
| 1931 | BS | SDS |

Well: 11-19S

## Appendix 3b: Cored section lithofacies observed

# Appendix 4 – Wireline log section data

Appendix 4a:  Wireline log facies for all wells

Appendix 4b:  Wireline log facies observed

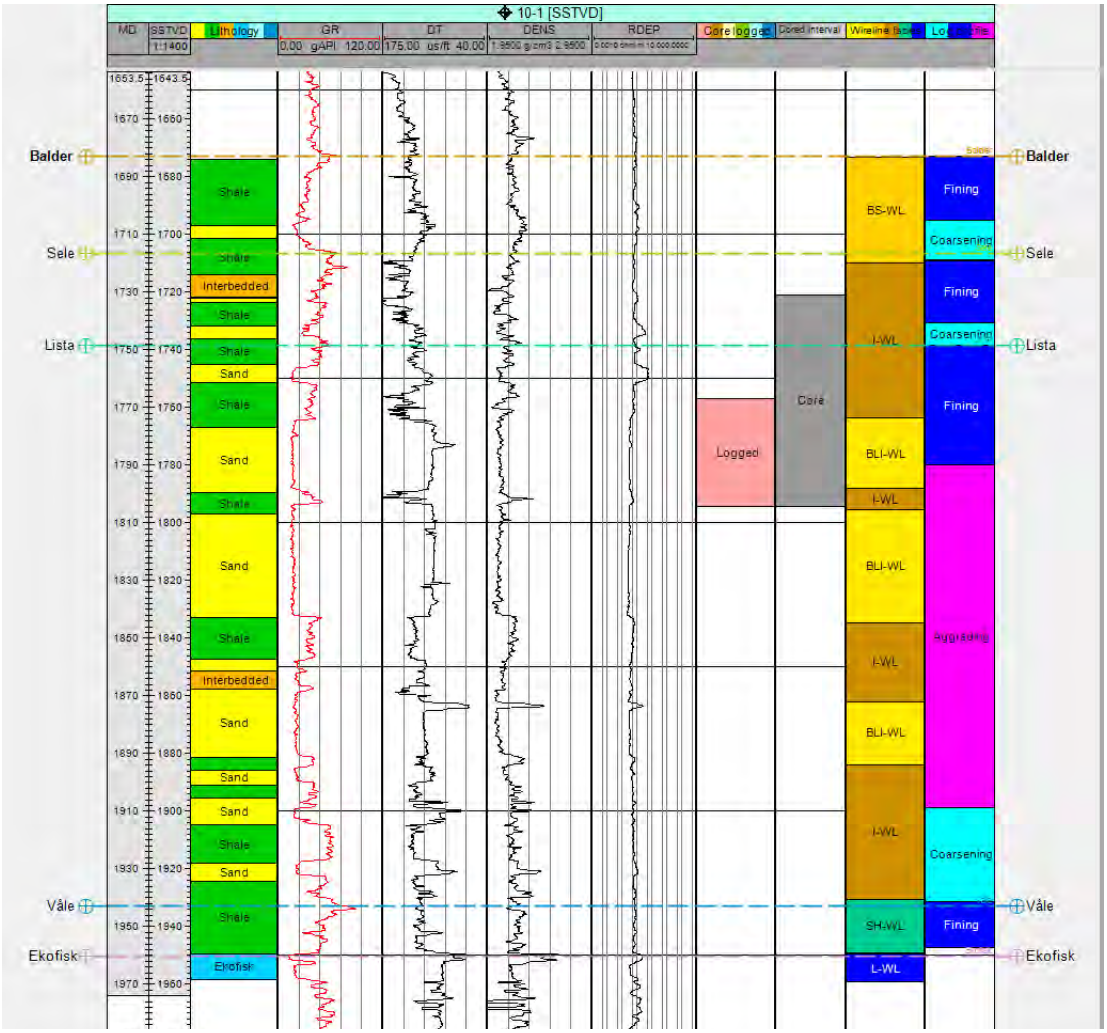
10-1 [SSTVD]
MD
SSTVD
1:1400
Lithology
GR
0.00 gAPI 120.00
DT
175.00 us/ft 40.00
DENS
1.9500 g/cm3 2.9500
RDEP
Core logged
Cored interval
Wireline facies
Lo
file
1653.5
1643.5
1670
1660
1690
1680
1710
1700
1730
1720
1750
1740
1770
1760
1790
1780
1810
1800
1830
1820
1850
1840
1870
1860
1890
1880
1910
1900
1930
1920
1950
1940
1970
1960
Balder
Sele
Lista
Våle
Ekofisk
Shale
Interbedded
Sand
Ekofisk
Logged
Core
BS-WL
I-WL
BLI-WL
SH-WL
L-WL
Fining
Coarsening
Aggrading
Balder
Sele
Lista
Våle
Ekofisk

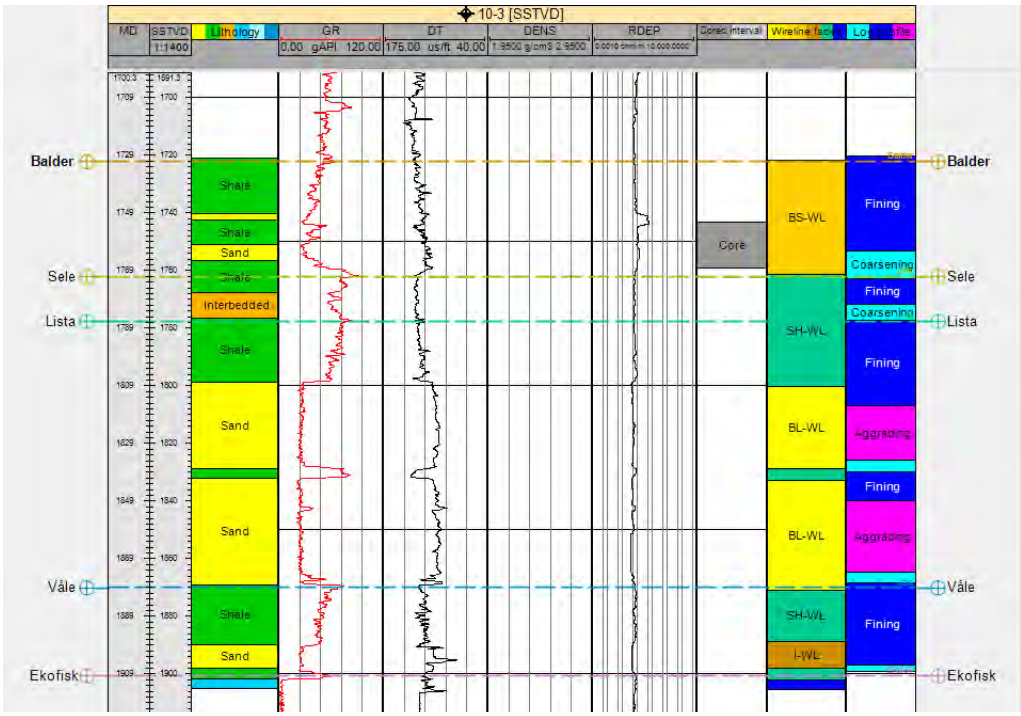
10-3 [SSTVD]
MD
SSTVD
1:1400
Lithology
GR
0.00 gAPI 120.00
DT
175.00 us/ft 40.00
DENS
1.9500 g/cm3 2.9500
RDEP
Coreq interval
Wireline facies
Balder
Sele
Lista
Våle
Ekofisk
Shale
Sand
Interbedded
Core
BS-WL
SH-WL
BL-WL
I-WL
Fining
Coarsening
Aggrading

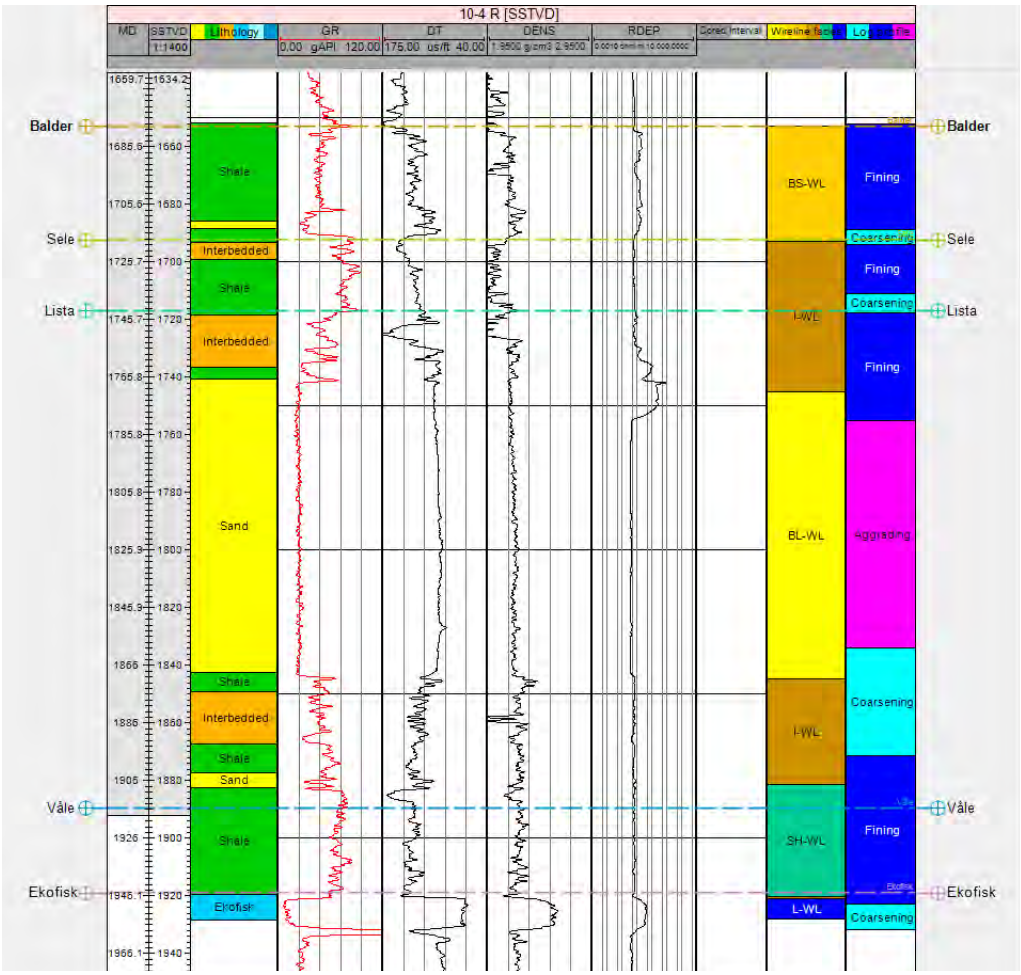
10-4 R [SSTVD]
MD
SSTVD
1:1400
Lithology
GR
0.00 gAPI 120.00
DT
175.00 us/ft 40.00
DENS
RDEP
Wireline facies
Balder
Sele
Lista
Våle
Ekofisk
Shale
Interbedded
Sand
Ekofisk
BS-WL
I-WL
BL-WL
SH-WL
L-WL
Fining
Coarsening
aggrading

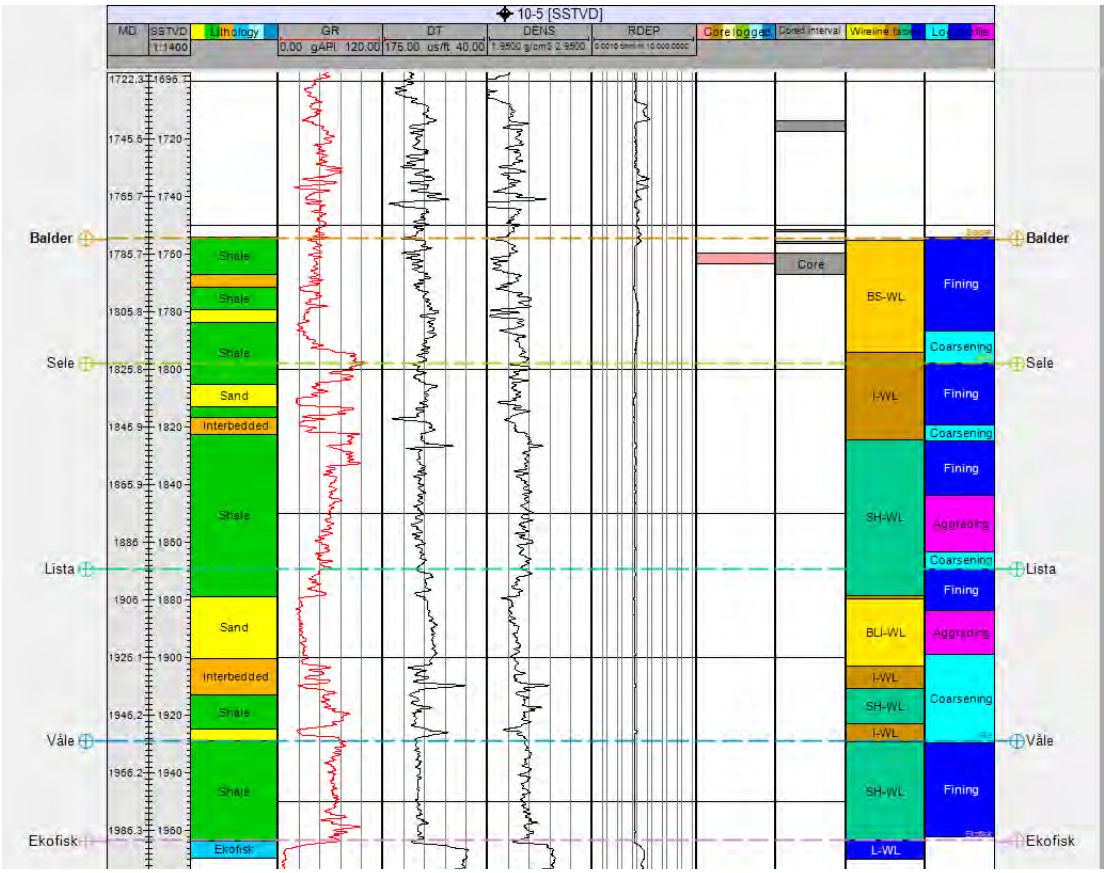
10-5 [SSTVD]
MD
SSTVD
1:1400
Lithology
GR
0.00 gAPI 120.00
DT
175.00 us/ft 40.00
DENS
1.9500 g/cm3 2.9500
RDEP
Core logged
Cored interval
Wireline fac
1722.3
1696.7
1745.6
1720
1765.7
1740
1785.7
1760
1805.8
1780
1825.8
1800
1846.9
1820
1865.9
1840
1886
1860
1906
1880
1926.1
1900
1946.2
1920
1966.2
1940
1986.3
1960
Balder
Sele
Lista
Våle
Ekofisk
Shale
Shale
Shale
Sand
Interbedded
Shale
Sand
Interbedded
Shale
Shale
Ekofisk
Core
BS-WL
I-WL
SH-WL
BLI-WL
I-WL
SH-WL
I-WL
SH-WL
L-WL
Fining
Coarsening
Fining
Coarsening
Fining
Aggrading
Coarsening
Fining
Aggrading
Coarsening
Fining
Balder
Sele
Lista
Våle
Ekofisk

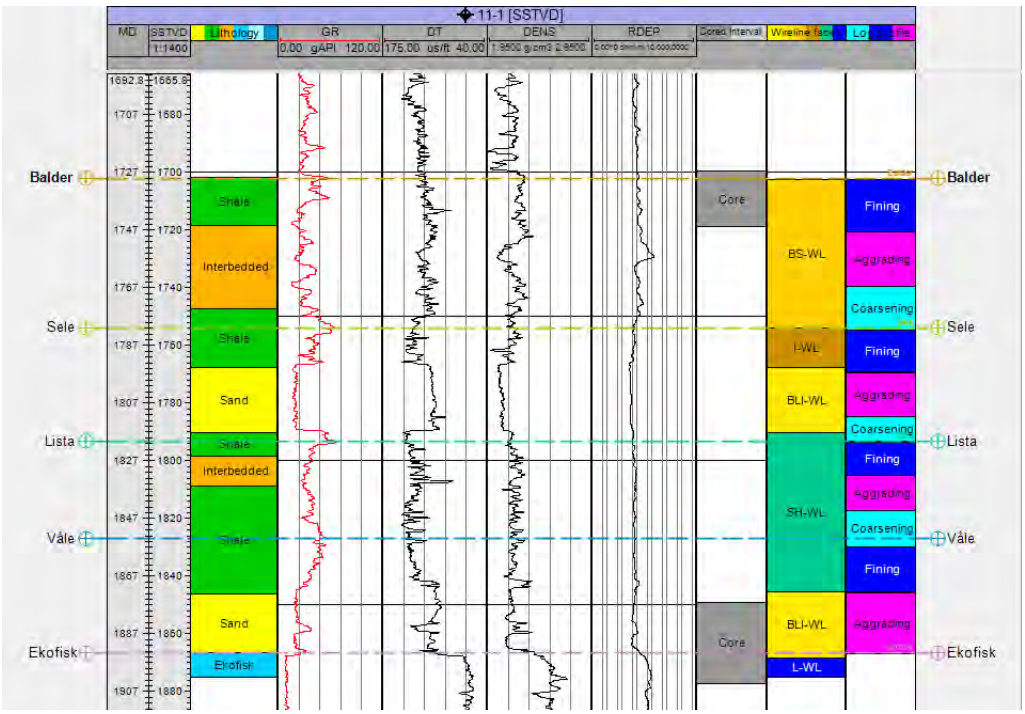
11-1 [SSTVD]
MD
SSTVD
1:1400
Lithology
GR
0.00 gAPI 120.00
DT
175.00 us/ft 40.00
DENS
RDEP
Cored Interval
Wireline facies
1692.8
1665.8
1707
1680
1727
1700
1747
1720
1767
1740
1787
1760
1807
1780
1827
1800
1847
1820
1867
1840
1887
1860
1907
1880
Balder
Sele
Lista
Våle
Ekofisk
Shale
Interbedded
Shale
Sand
Shale
Interbedded
Shale
Sand
Ekofisk
Core
Core
BS-WL
I-WL
BLI-WL
SH-WL
BLI-WL
L-WL
Fining
Aggrading
Coarsening
Fining
Aggrading
Coarsening
Fining
Aggrading
Coarsening
Fining
Aggrading
Balder
Sele
Lista
Våle
Ekofisk

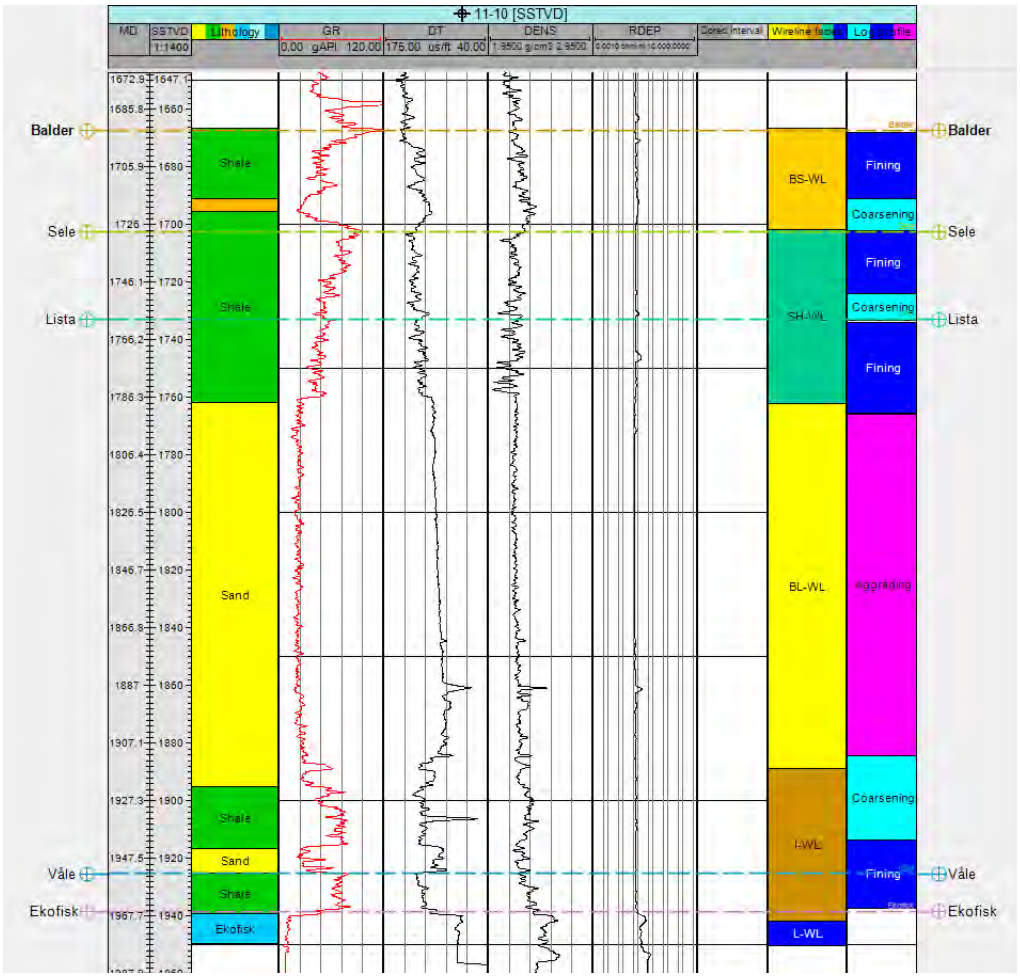
11-10 [SSTVD]
MD
SSTVD
1:1400
Lithology
GR
0.00 gAPI 120.00
DT
175.00 us/ft 40.00
DENS
1.9500 g/cm3 2.9500
RDEP
Cored Interval
Wireline fa
Balder
Sele
Lista
Våle
Ekofisk
Shale
Sand
Shale
Sand
Shale
Ekofisk
BS-WL
SH-WL
BL-WL
I-WL
L-WL
Fining
Coarsening
Fining
Coarsening
Fining
aggrading
Coarsening
Fining

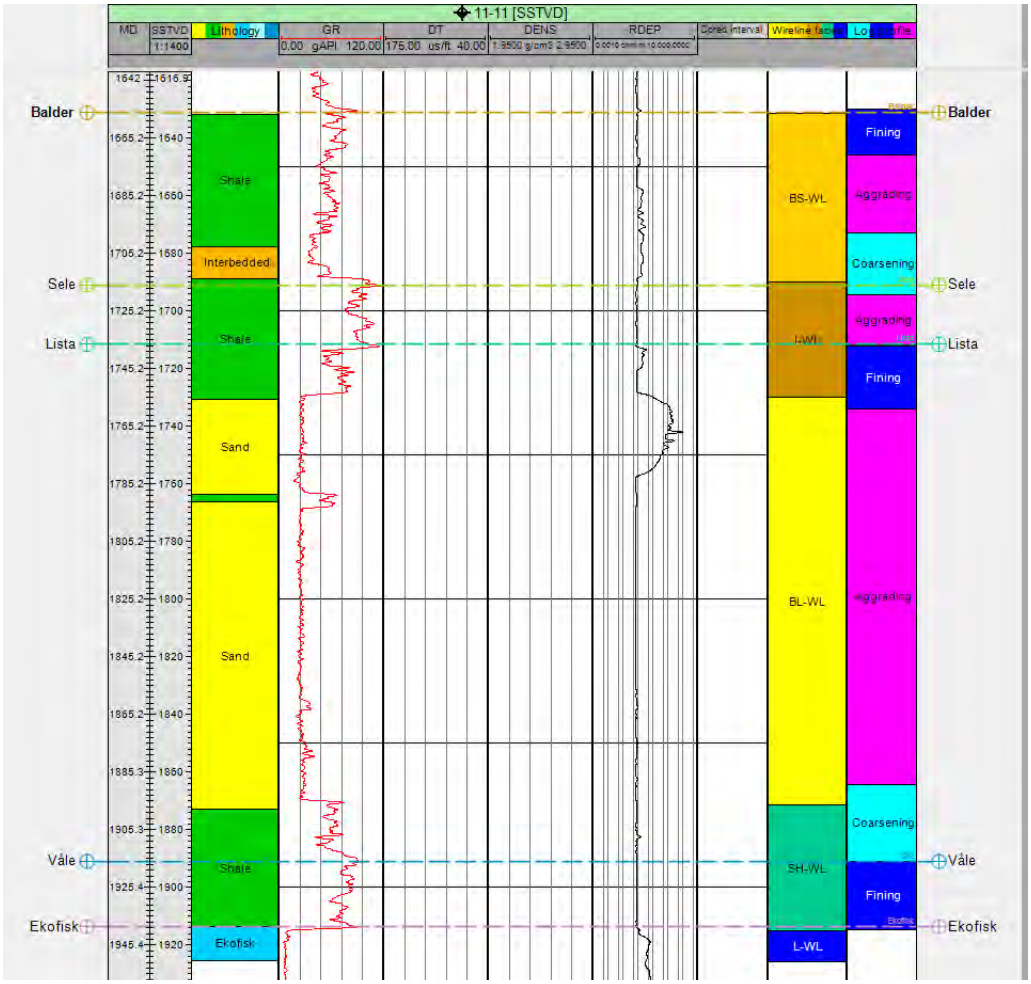
11-11 [SSTVD]
MD
SSTVD
1:1400
Lithology
GR
0.00 gAPI 120.00
DT
175.00 us/ft 40.00
DENS
1.9500 g/cm3 2.9500
RDEP
Cored Interval
Wireline facies
Log profile
Balder
Sele
Lista
Våle
Ekofisk
Shale
Interbedded
Shale
Sand
Sand
Shale
Ekofisk
BS-WL
I-WL
BL-WL
SH-WL
L-WL
Fining
Aggrading
Coarsening
Aggrading
Fining
Aggrading
Coarsening
Fining

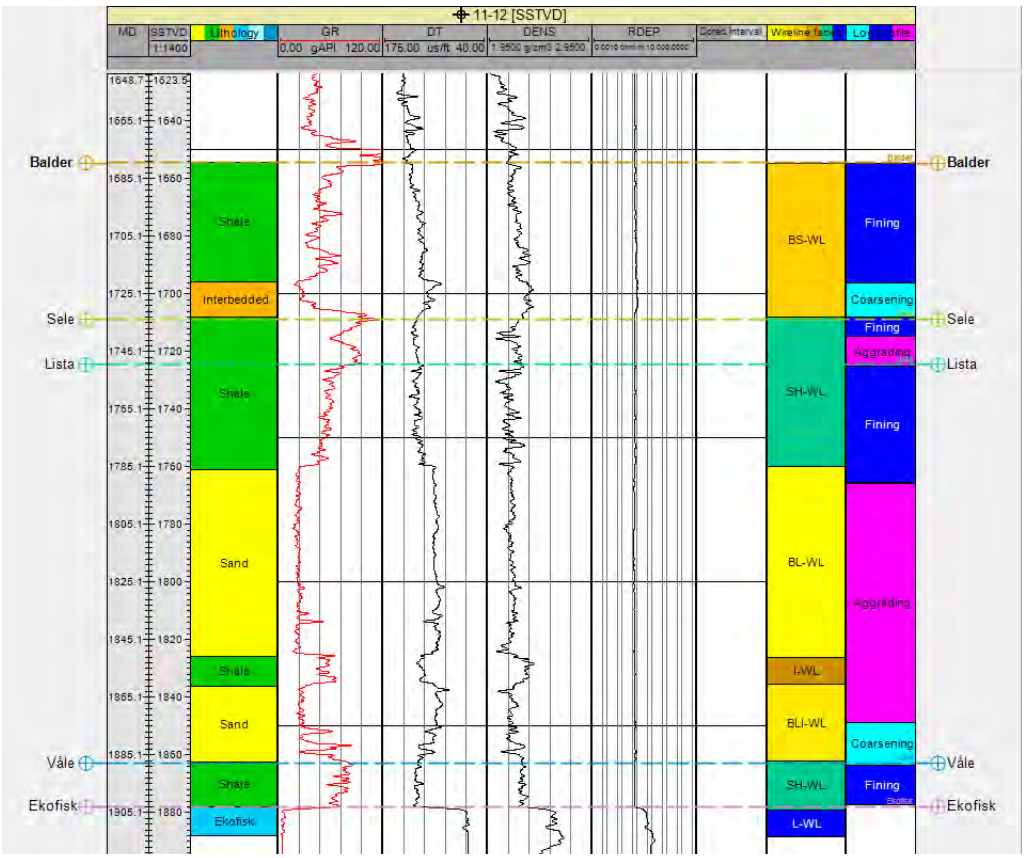
11-12 [SSTVD]
MD
SSTVD
1:1400
Lithology
GR
0.00 gAPI 120.00
DT
175.00 us/ft 40.00
DENS
RDEP
Cored Interval
Wireline facies
Balder
Sele
Lista
Våle
Ekofisk
Shale
Interbedded
Shale
Sand
Shale
Sand
Shale
Ekofisk
BS-WL
SH-WL
BL-WL
I-WL
BLI-WL
SH-WL
L-WL
Fining
Coarsening
Fining
Aggrading
Fining
Aggrading
Coarsening
Fining

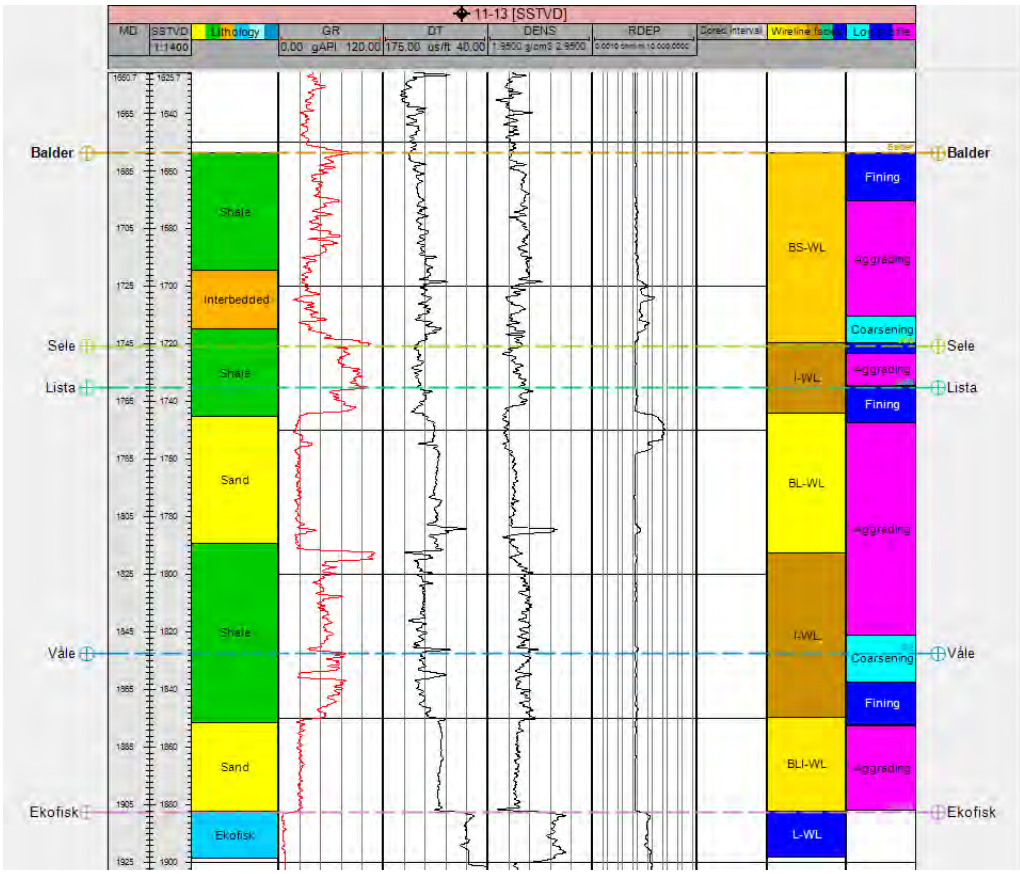
11-13 [SSTVD]
MD
SSTVD
1:1400
Lithology
GR
0.00 gAPI 120.00
DT
175.00 us/ft 40.00
DENS
1.9500 g/cm3 2.9500
RDEP
Correl. Interval
Wireline facies
Balder
Sele
Lista
Våle
Ekofisk
Shale
Interbedded
Shale
Sand
Shale
Sand
Ekofisk
BS-WL
I-WL
BL-WL
I-WL
BLI-WL
L-WL
Fining
Aggrading
Coarsening
Aggrading
Fining
Aggrading
Coarsening
Fining
Aggrading

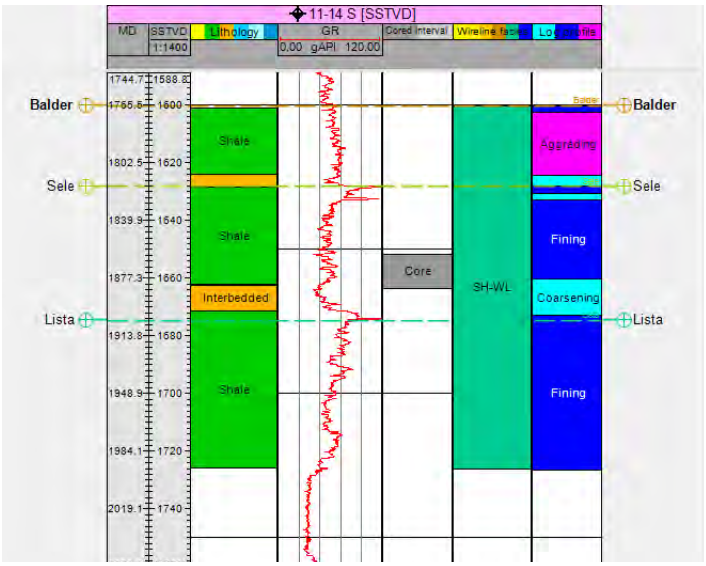
11-14 S [SSTVD]
MD
SSTVD
1:1400
Lithology
GR
0.00 gAPI 120.00
Cored interval
Wireline facies
Log profile
Balder
Sele
Lista
1744.7
1588.9
1765.6
1600
1802.5
1620
1839.9
1640
1877.3
1660
1913.8
1680
1948.9
1700
1984.1
1720
2019.1
1740
Shale
Shale
Interbedded
Shale
Core
SH-WL
Aggrading
Fining
Coarsening
Fining
Balder
Sele
Lista

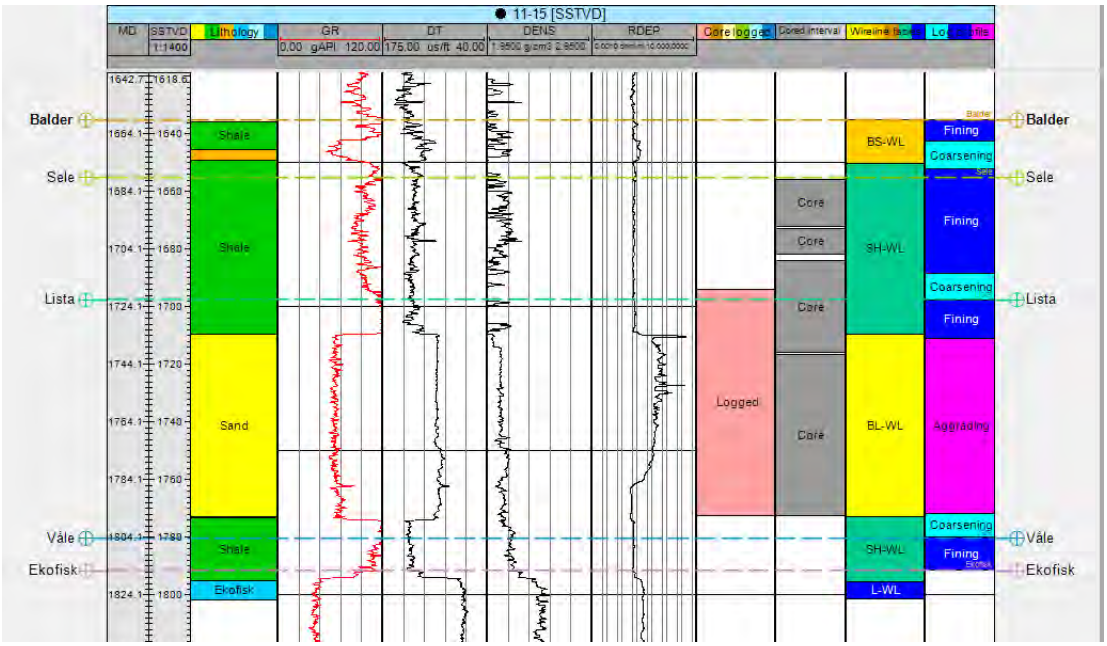
11-15 [SSTVD]
MD
SSTVD
1:1400
Lithology
GR
0.00 gAPI 120.00
DT
175.00 us/ft 40.00
DENS
1.9500 g/cm3 2.8500
RDEP
Core logged
Cored interval
Wireline fa...
Lo... Infe...
1642.7
1618.6
1664.1
1640
1684.1
1660
1704.1
1680
1724.1
1700
1744.1
1720
1764.1
1740
1784.1
1760
1804.1
1780
1824.1
1800
Balder
Sele
Lista
Våle
Ekofisk
Shale
Shale
Sand
Shale
Ekofisk
Logged
Core
Core
Core
Core
BS-WL
SH-WL
BL-WL
SH-WL
L-WL
Fining
Coarsening
Fining
Coarsening
Fining
Aggrading
Coarsening
Fining
Balder
Sele
Lista
Våle
Ekofisk

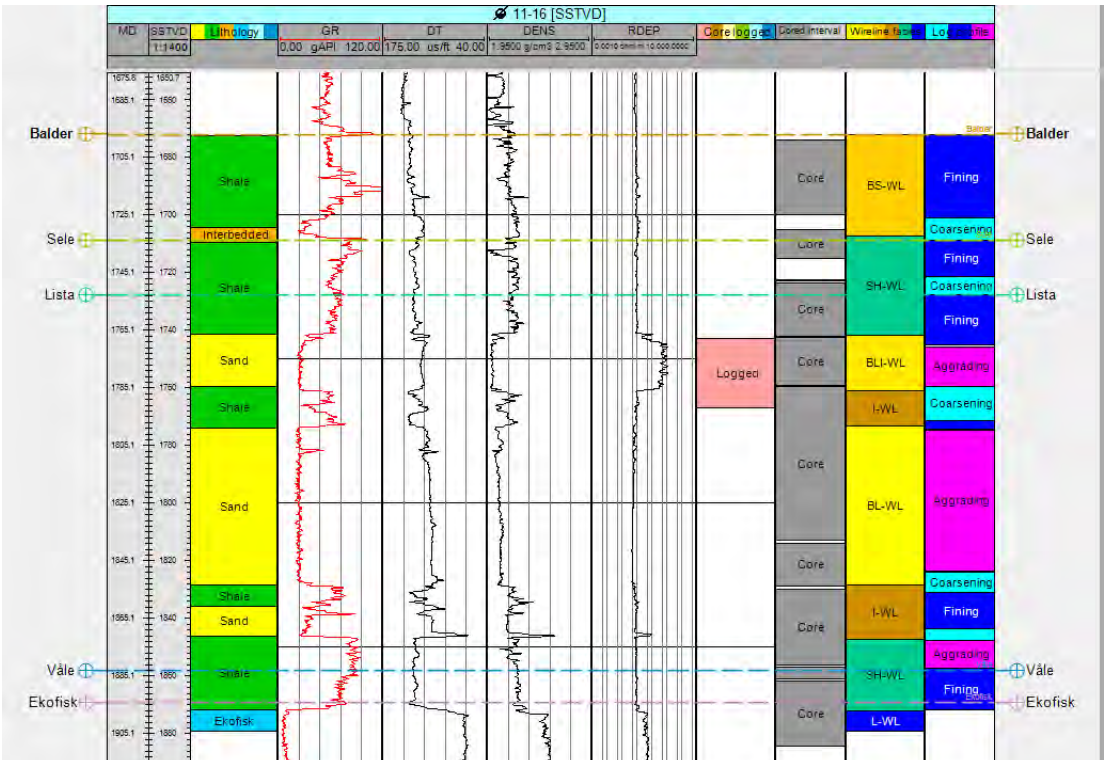
11-16 [SSTVD]
MD
SSTVD
1:1400
Lithology
GR
0.00 gAPI 120.00
DT
175.00 us/ft 40.00
DENS
1.9500 g/cm3 2.9500
RDEP
Core logged
Cored interval
Wireline facies
Balder
Sele
Lista
Våle
Ekofisk
Shale
Interbedded
Shale
Sand
Shale
Sand
Shale
Sand
Shale
Ekofisk
Logged
Core
BS-WL
SH-WL
BLI-WL
I-WL
BL-WL
I-WL
SH-WL
L-WL
Fining
Coarsening
Fining
Coarsening
Fining
Aggrading
Coarsening
Aggrading
Coarsening
Fining
Aggrading
Fining

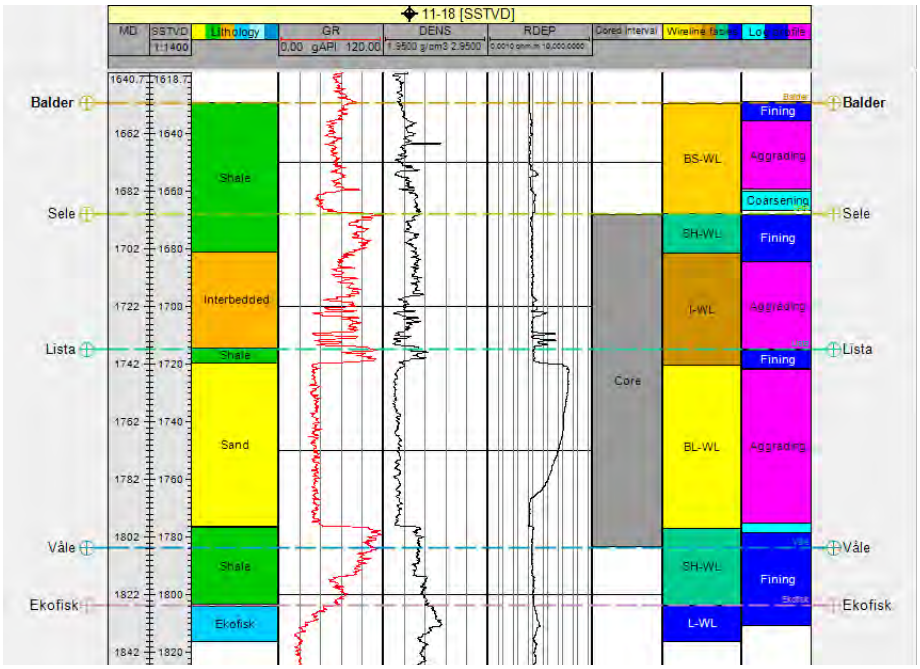
11-18 [SSTVD]
MD
SSTVD
1:1400
Lithology
GR
0.00 gAPI 120.00
DENS
1.9500 g/cm3 2.9500
RDEP
Cored Interval
Wireline fac
Balder
Sele
Lista
Våle
Ekofisk
Shale
Interbedded
Shale
Sand
Shale
Ekofisk
Core
BS-WL
SH-WL
I-WL
BL-WL
SH-WL
L-WL
Fining
Aggrading
Coarsening
Fining
Aggrading
Fining
Aggrading
Fining

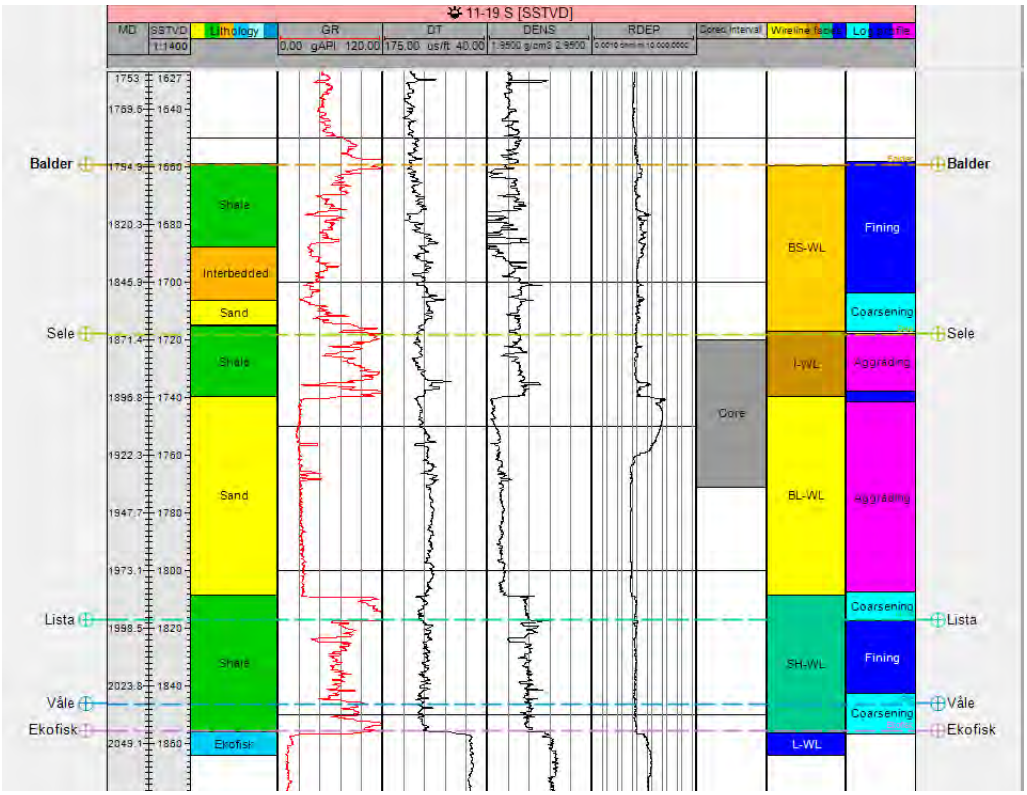
11-19 S [SSTVD]
MD
SSTVD
1:1400
Lithology
GR
0.00 gAPI 120.00
DT
175.00 us/ft 40.00
DENS
1.9500 g/cm3 2.9500
RDEP
Coreд Interval
Wireline Test
Log Facies
1753
1627
1768.6
1640
1794.9
1660
1820.3
1680
1845.9
1700
1871.4
1720
1896.8
1740
1922.3
1760
1947.7
1780
1973.1
1800
1998.5
1820
2023.8
1840
2049.1
1860
Balder
Sele
Lista
Våle
Ekofisk
Shale
Interbedded
Sand
Shale
Sand
Shale
Ekofisk
Core
BS-WL
I-WL
BL-WL
SH-WL
L-WL
Fining
Coarsening
Aggrading
Aggrading
Coarsening
Fining
Coarsening
Balder
Sele
Lista
Våle
Ekofisk

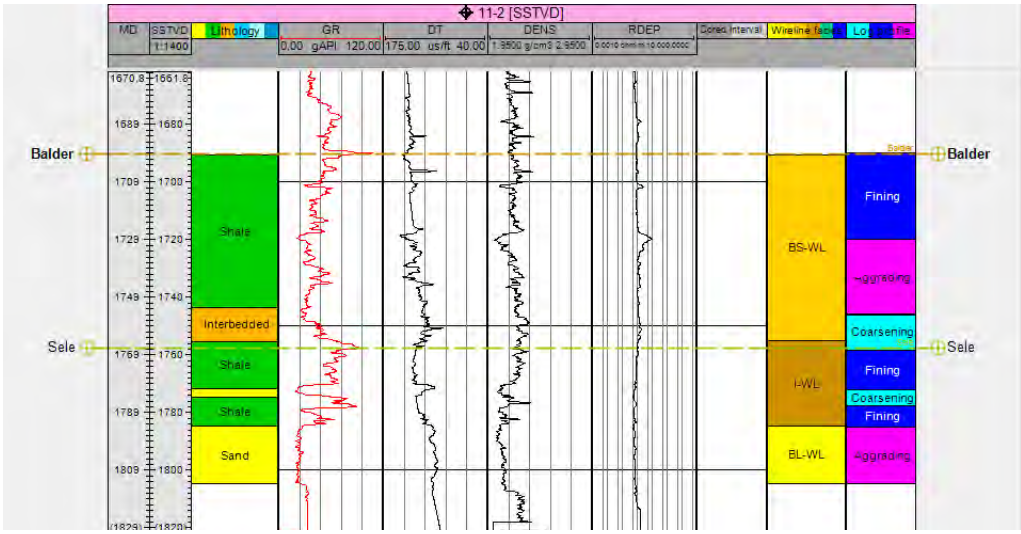
11-2 [SSTVD]
MD
SSTVD
1:1400
Lithology
GR
0.00 gAPI 120.00
DT
175.00 us/ft 40.00
DENS
1.9500 g/cm3 2.9500
RDEP
Zones
Wireline facies
Log profile
1670.8
1661.8
1689
1680
1709
1700
1729
1720
1749
1740
1769
1760
1789
1780
1809
1800
Balder
Sele
Shale
Interbedded
Shale
Shale
Sand
BS-WL
I-WL
BL-WL
Balder
Fining
Aggrading
Coarsening
Fining
Coarsening
Fining
Aggrading
Balder
Sele

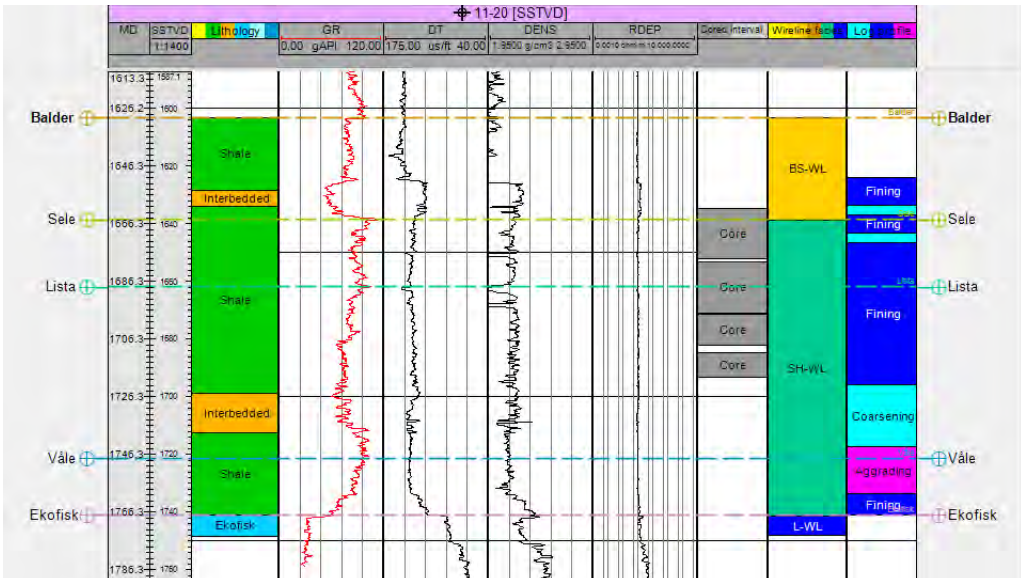
11-20 [SSTVD]
MD
SSTVD
1:1400
Lithology
GR
0.00 gAPI 120.00
DT
175.00 us/ft 40.00
DENS
1.9500 g/cm3 2.9500
RDEP
Cored Interval
Wireline facies
Balder
Sele
Lista
Våle
Ekofisk
Shale
Interbedded
Shale
Interbedded
Shale
Ekofisk
Core
Core
Core
Core
BS-WL
SH-WL
L-WL
Fining
Fining
Fining
Coarsening
Aggrading
Fining

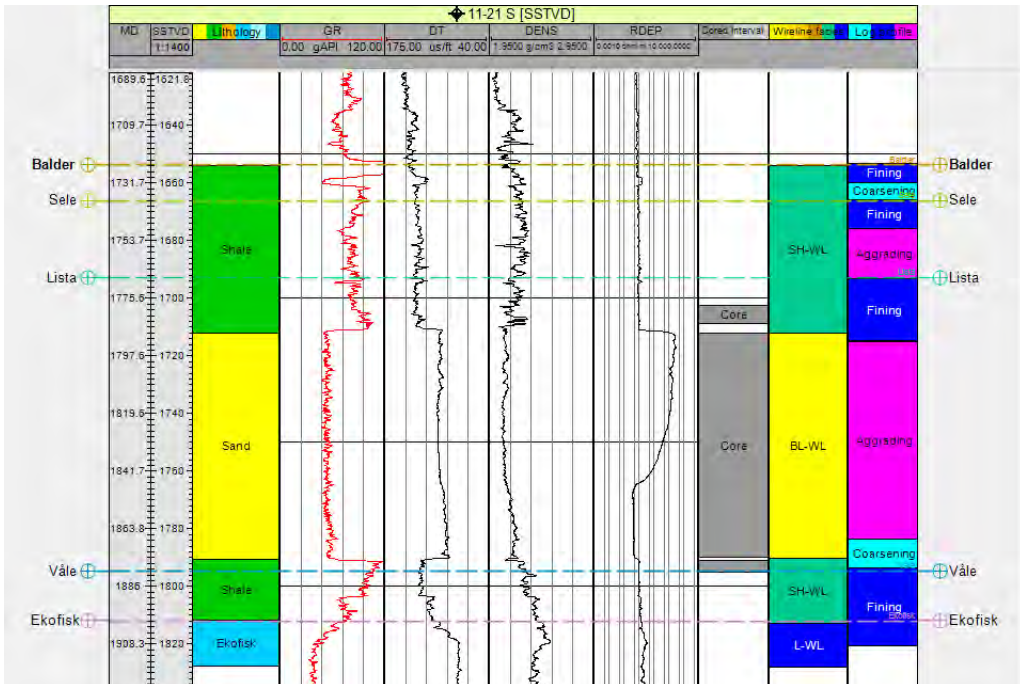
11-21 S [SSTVD]
MD
SSTVD
1:1400
Lithology
GR
0.00 gAPI 120.00
DT
175.00 us/ft 40.00
DENS
1.9500 g/cm3 2.9500
RDEP
Cored Interval
Wireline fac
Balder
Sele
Lista
Våle
Ekofisk
Shale
Sand
Shale
Ekofisk
Core
Core
SH-WL
BL-WL
SH-WL
L-WL
Fining
Coarsening
Fining
Aggrading
Fining
Aggrading
Coarsening
Fining

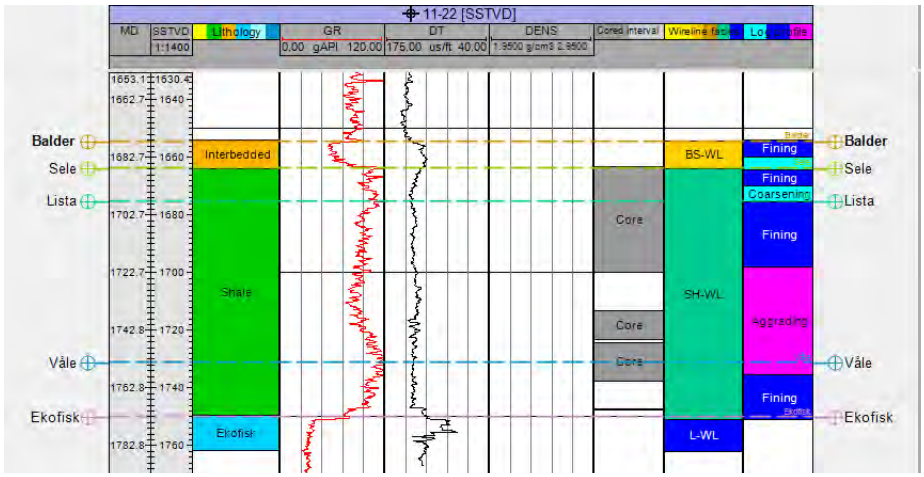
11-22 [SSTVD]
MD
SSTVD
1:1400
Lithology
GR
0.00 gAPI 120.00
DT
175.00 us/ft 40.00
DENS
1.9500 g/cm3 2.9500
Cored Interval
Wireline facies
Log facies
1653.1
1630.4
1662.7
1640
1682.7
1660
1702.7
1680
1722.7
1700
1742.8
1720
1762.8
1740
1782.8
1760
Balder
Sele
Lista
Våle
Ekofisk
Interbedded
Shale
Ekofisk
Core
Core
Core
BS-WL
SH-WL
L-WL
Fining
Fining
Coarsening
Fining
Aggrading
Fining
Balder
Sele
Lista
Våle
Ekofisk

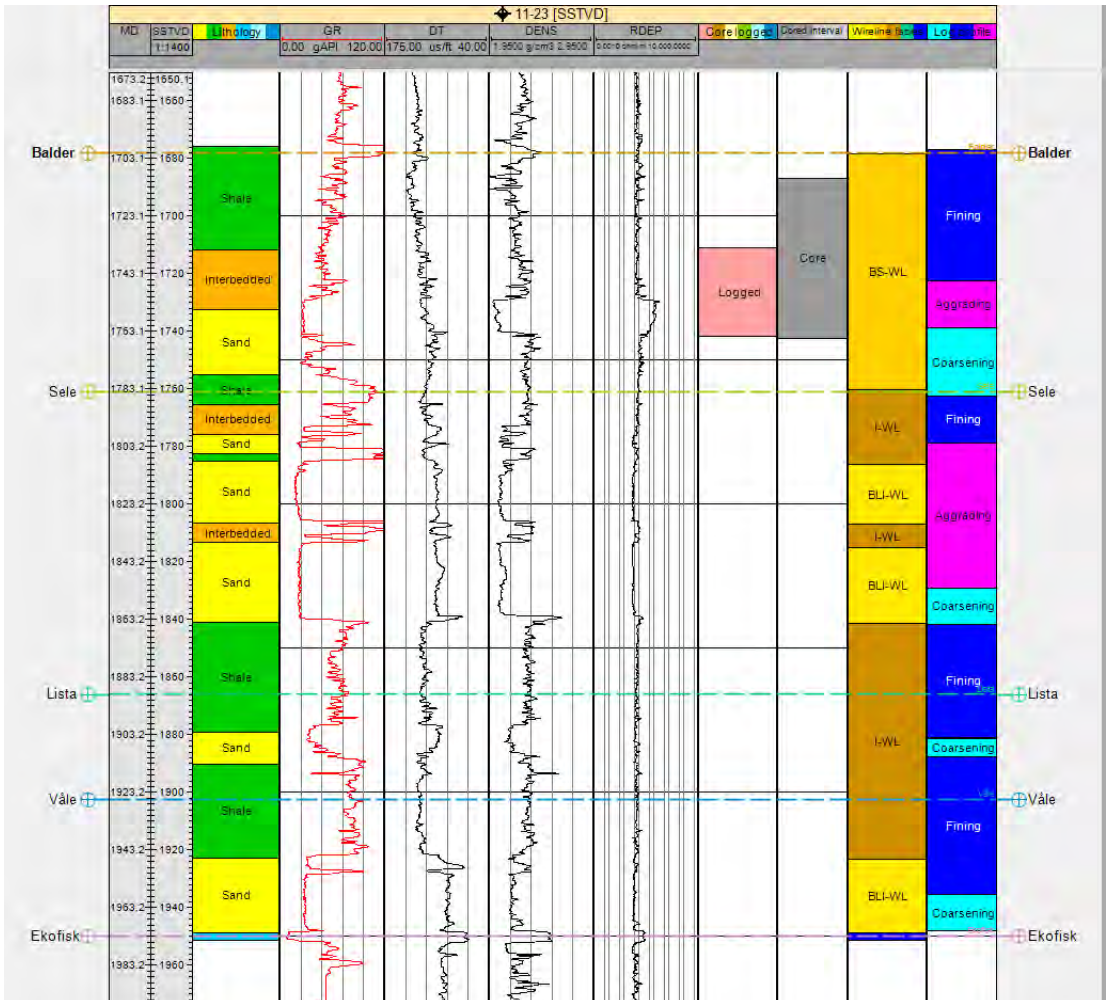
11-23 [SSTVD]
MD
SSTVD
1:1400
Lithology
GR
0.00 gAPI 120.00
DT
175.00 us/ft 40.00
DENS
1.9500 g/cm3 2.9500
RDEP
Core logged
Cored interval
Wireline facies
Balder
Sele
Lista
Våle
Ekofisk
Shale
Interbedded
Sand
Logged
Core
BS-WL
I-WL
BLI-WL
Fining
Aggrading
Coarsening

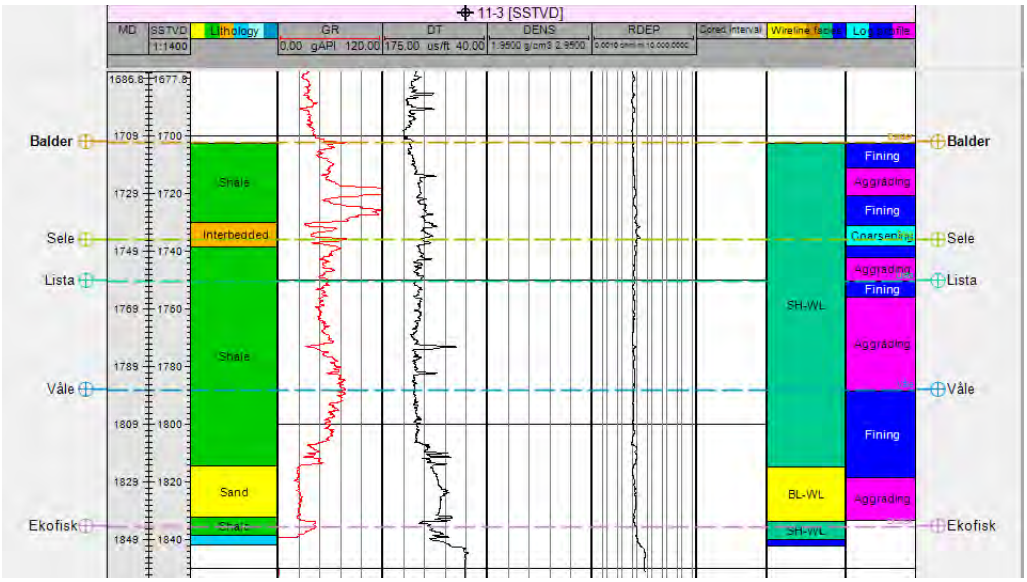
11-3 [SSTVD]
MD
SSTVD
1:1400
Lithology
GR
0.00 gAPI 120.00
DT
175.00 us/ft 40.00
DENS
1.9500 g/cm3 2.9500
RDEP
Cored Interval
Wireline facies
1686.8
1677.8
1709
1700
1729
1720
1749
1740
1769
1760
1789
1780
1809
1800
1829
1820
1849
1840
Balder
Sele
Lista
Våle
Ekofisk
Shale
Interbedded
Shale
Sand
Shale
SH-WL
BL-WL
SH-WL
Fining
Aggrading
Fining
Coarsening
Aggrading
Fining
Aggrading
Fining
Aggrading
Balder
Sele
Lista
Våle
Ekofisk

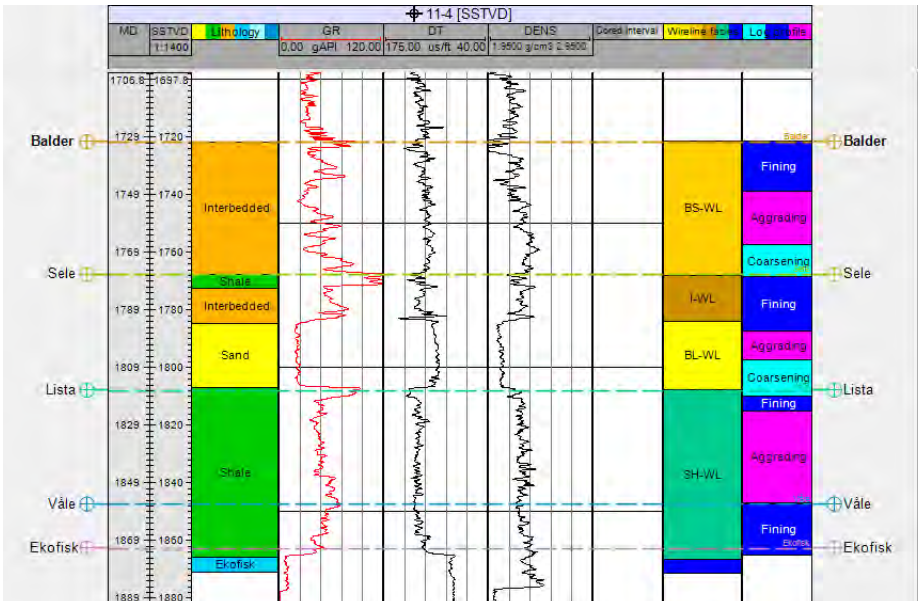
11-4 [SSTVD]
MD
SSTVD
1:1400
Lithology
GR
0.00 gAPI 120.00
DT
175.00 us/ft 40.00
DENS
1.9500 g/cm3 2.9500
Cored Interval
Wireline fields
Balder
Sele
Lista
Våle
Ekofisk
Interbedded
Shale
Interbedded
Sand
Shale
Ekofisk
BS-WL
I-WL
BL-WL
SH-WL
Fining
Aggrading
Coarsening
Fining
Aggrading
Coarsening
Fining
Aggrading
Fining

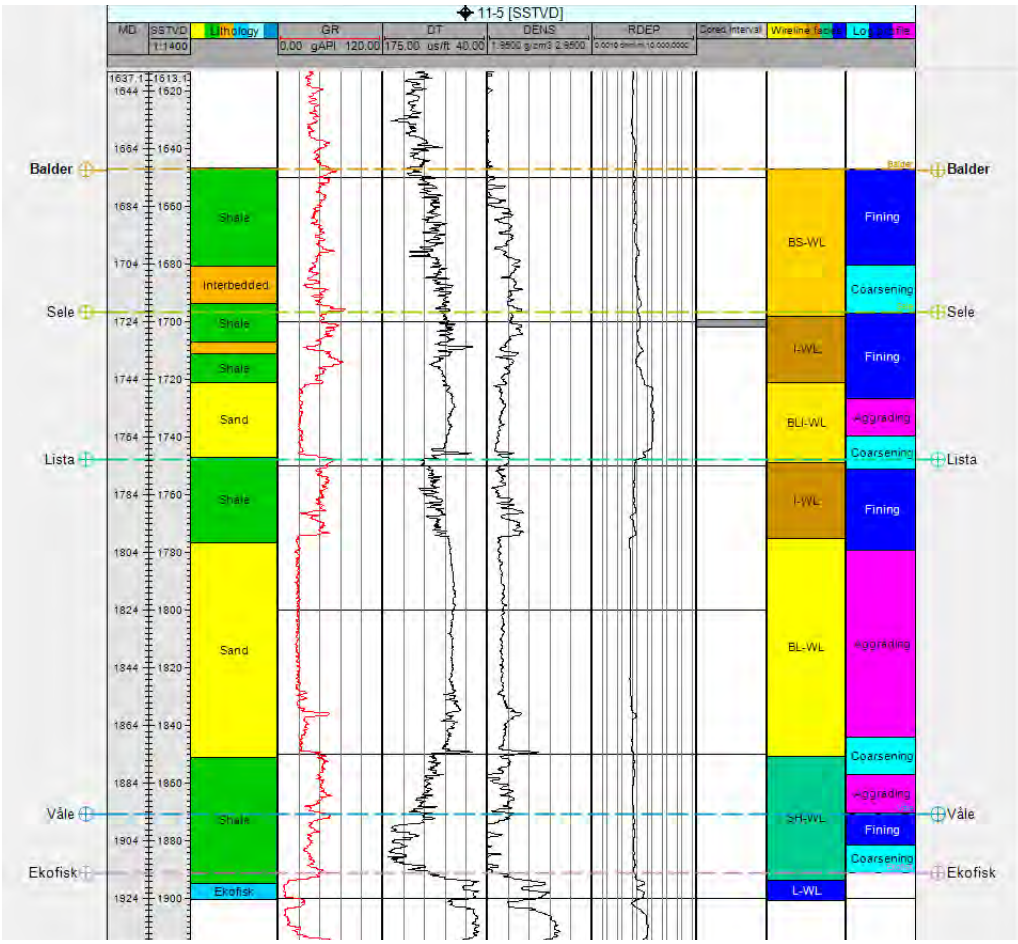
11-5 [SSTVD]
MD
SSTVD
1:1400
Lithology
GR
0.00 gAPI 120.00
DT
175.00 us/ft 40.00
DENS
1.9500 g/cm3 2.9500
RDEP
Cored Interval
Wireline facies
Balder
Sele
Lista
Våle
Ekofisk
Shale
Interbedded
Sand
Ekofisk
BS-WL
I-WL
BLI-WL
I-WL
BL-WL
SH-WL
L-WL
Fining
Coarsening
Aggrading
Fining
Aggrading
Coarsening
Fining
Aggrading
Coarsening
Fining
Coarsening

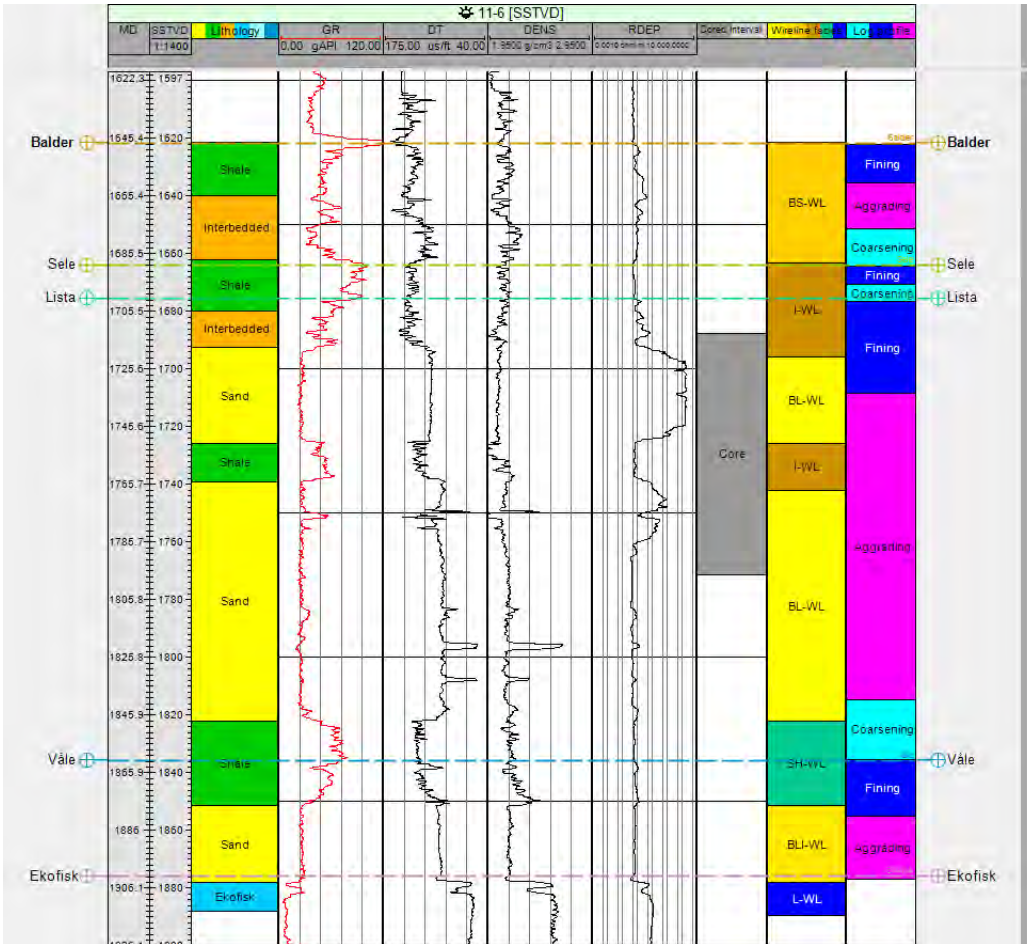
11-6 [SSTVD]
MD
SSTVD
1:1400
Lithology
GR
0.00 gAPI 120.00
DT
175.00 us/ft 40.00
DENS
1.9800 g/cm3 2.9500
RDEP
Coreg Interval
Wireline facies
Balder
Sele
Lista
Våle
Ekofisk
Shale
Interbedded
Shale
Interbedded
Sand
Shale
Sand
Shale
Sand
Ekofisk
Core
BS-WL
I-WL
BL-WL
I-WL
BL-WL
SH-WL
BLI-WL
L-WL
Fining
Aggrading
Coarsening
Fining
Coarsening
Fining
Aggrading
Coarsening
Fining
Aggrading
Balder
Sele
Lista
Våle
Ekofisk

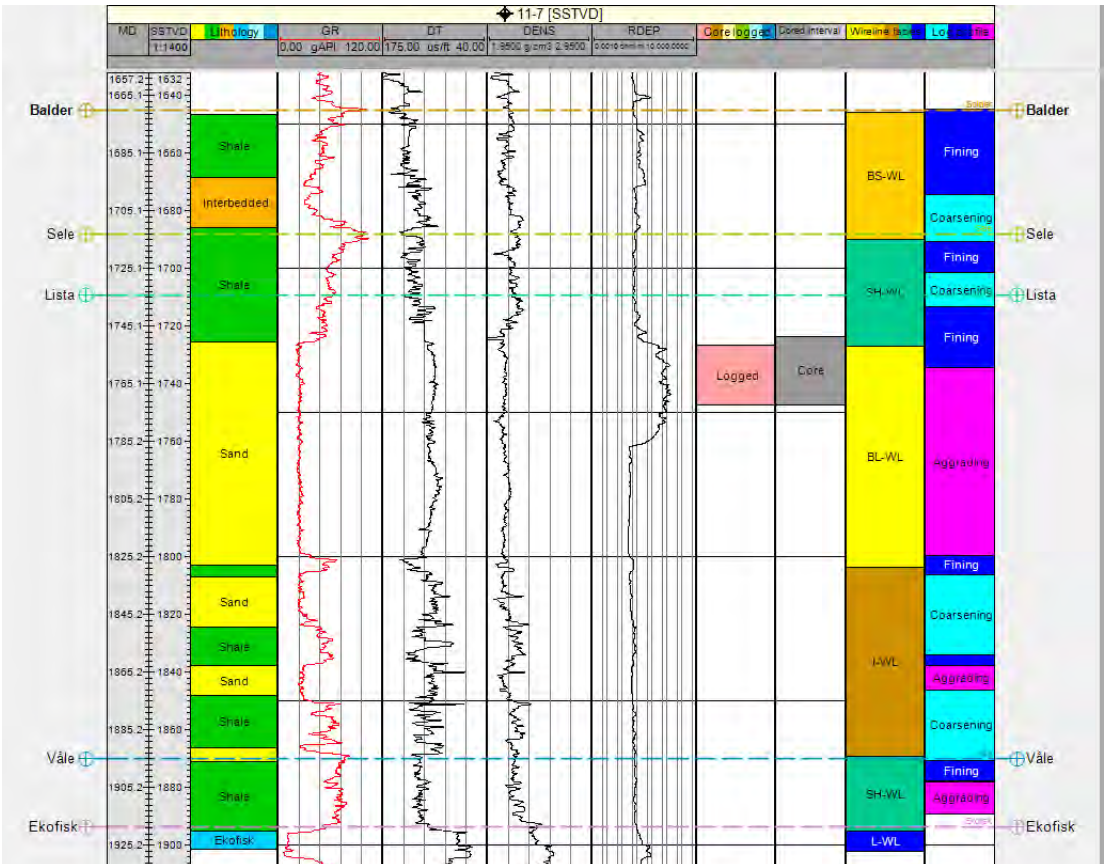
11-7 [SSTVD]
MD
SSTVD
1:1400
Lithology
GR
0.00 gAPI 120.00
DT
175.00 us/ft 40.00
DENS
1.9500 g/cm3 2.9500
RDEP
Core logged
Cored interval
Wireline tasks
Balder
Sele
Lista
Våle
Ekofisk
Shale
Interbedded
Sand
Ekofisk
Logged
Core
BS-WL
SH-WL
BL-WL
I-WL
SH-WL
L-WL
Fining
Coarsening
Aggrading

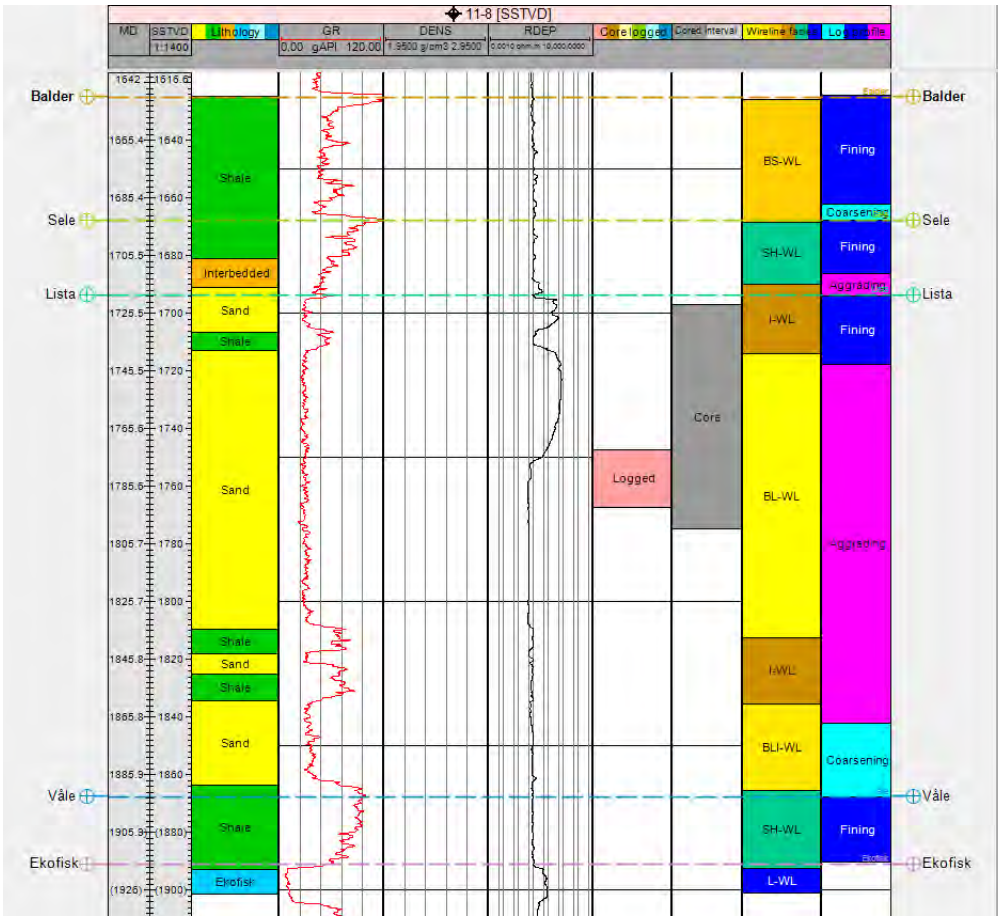
11-8 [SSTVD]
MD
SSTVD
1:1400
Lithology
GR
0.00 gAPI 120.00
DENS
1.9500 g/cm3 2.9500
RDEP
Core logged
Cored interval
Wireline fac
Balder
Sele
Lista
Våle
Ekofisk
Shale
Interbedded
Sand
Shale
Sand
Shale
Sand
Shale
Sand
Shale
Ekofisk
Logged
Core
BS-WL
SH-WL
I-WL
BL-WL
I-WL
BLI-WL
SH-WL
L-WL
Fining
Coarsening
Fining
Aggrading
Fining
Aggrading
Coarsening
Fining

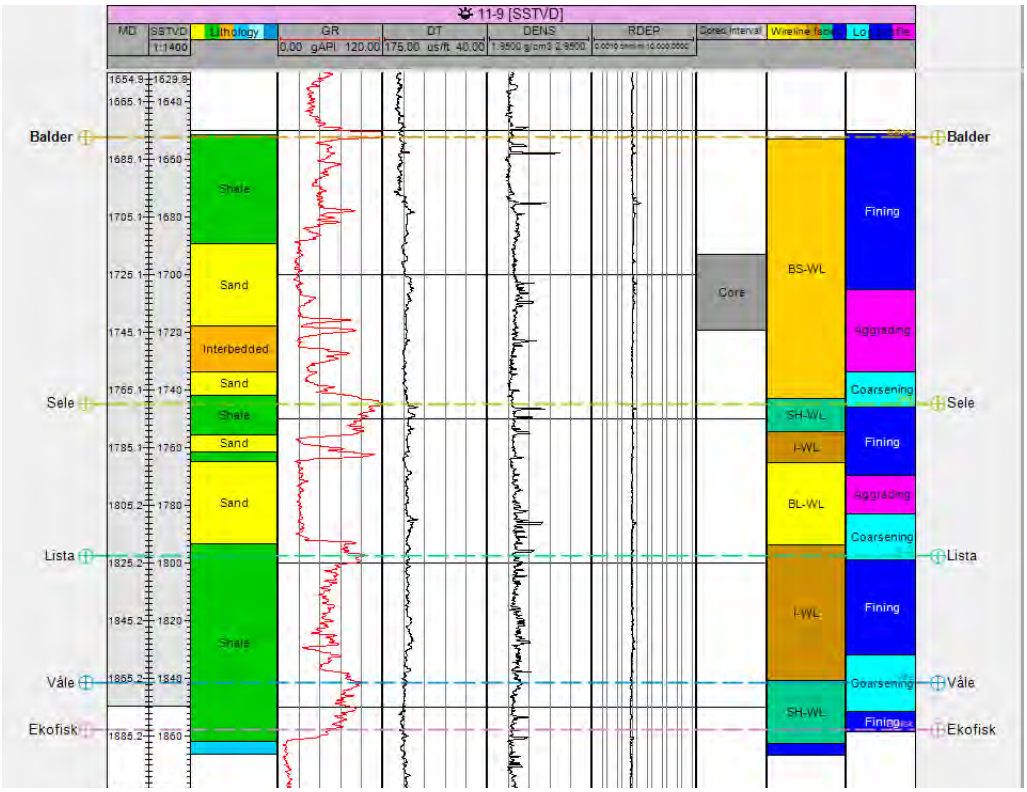
11-9 [SSTVD]
MD
SSTVD
1:1400
Lithology
GR
0.00 gAPI 120.00
DT
175.00 us/ft 40.00
DENS
1.9500 g/cm3 2.9500
RDEP
Core Interval
Wireline facies
Balder
Sele
Lista
Våle
Ekofisk
Shale
Sand
Interbedded
Sand
Shale
Sand
Sand
Shale
Core
BS-WL
SH-WL
I-WL
BL-WL
I-WL
SH-WL
Fining
Aggrading
Coarsening
Fining
Aggrading
Coarsening
Fining
Coarsening
Fining

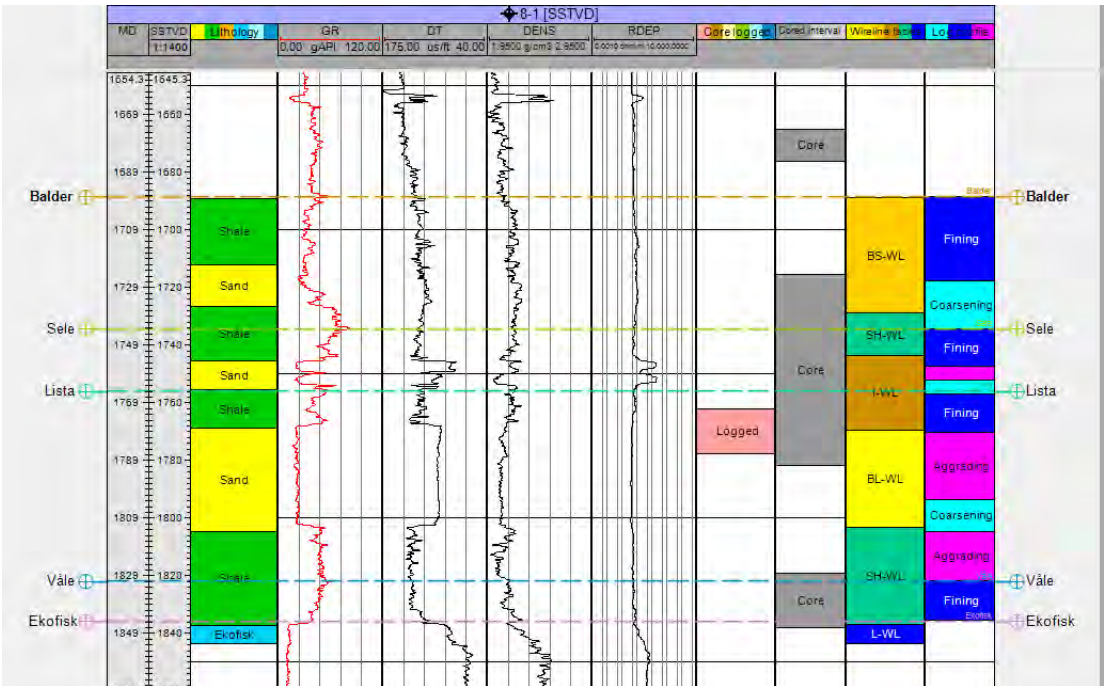
8-1 [SSTVD]
MD
SSTVD
1:1400
Lithology
GR
0.00 gAPI 120.00
DT
175.00 us/ft 40.00
DENS
1.9500 g/cm3 2.9500
RDEP
Core logged
Cored interval
Wireline fa
Balder
Sele
Lista
Våle
Ekofisk
Shale
Sand
Shale
Sand
Shale
Sand
Shale
Ekofisk
Core
Core
Logged
Core
BS-WL
SH-WL
I-WL
BL-WL
SH-WL
L-WL
Fining
Coarsening
Fining
Fining
Aggrading
Coarsening
Aggrading
Fining

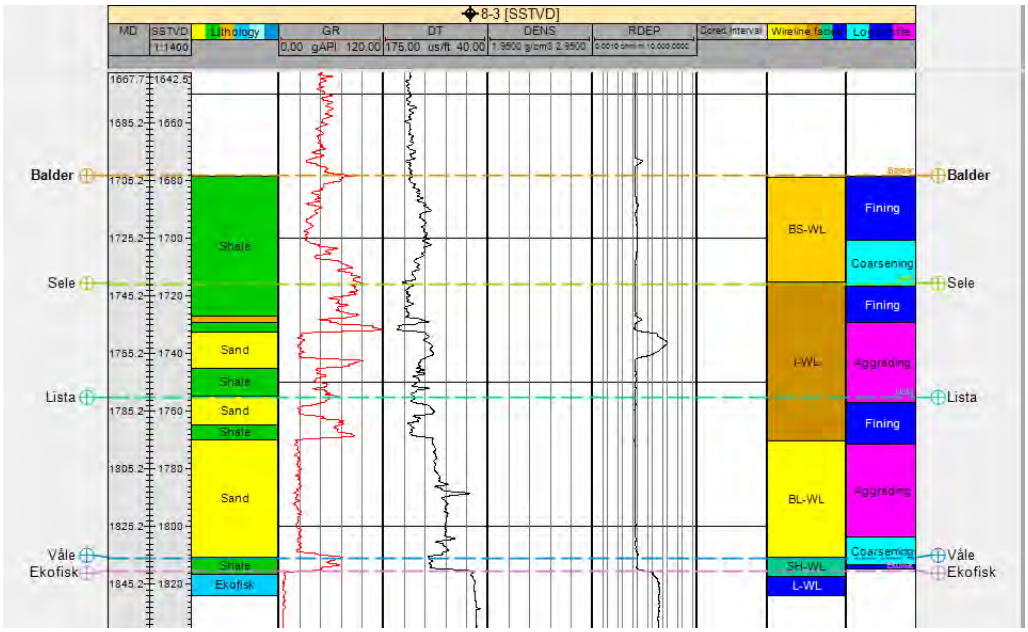
8-3 [SSTVD]
MD
SSTVD
1:1400
Lithology
GR
0.00 gAPI 120.00
DT
175.00 us/ft 40.00
DENS
1.9500 g/cm3 2.9500
RDEP
Cored Interval
Wireline facies
Balder
Sele
Lista
Våle
Ekofisk
Shale
Sand
Shale
Sand
Shale
Sand
Shale
Ekofisk
BS-WL
I-WL
BL-WL
SH-WL
L-WL
Fining
Coarsening
Fining
Aggrading
Fining
Aggrading
Coarsening

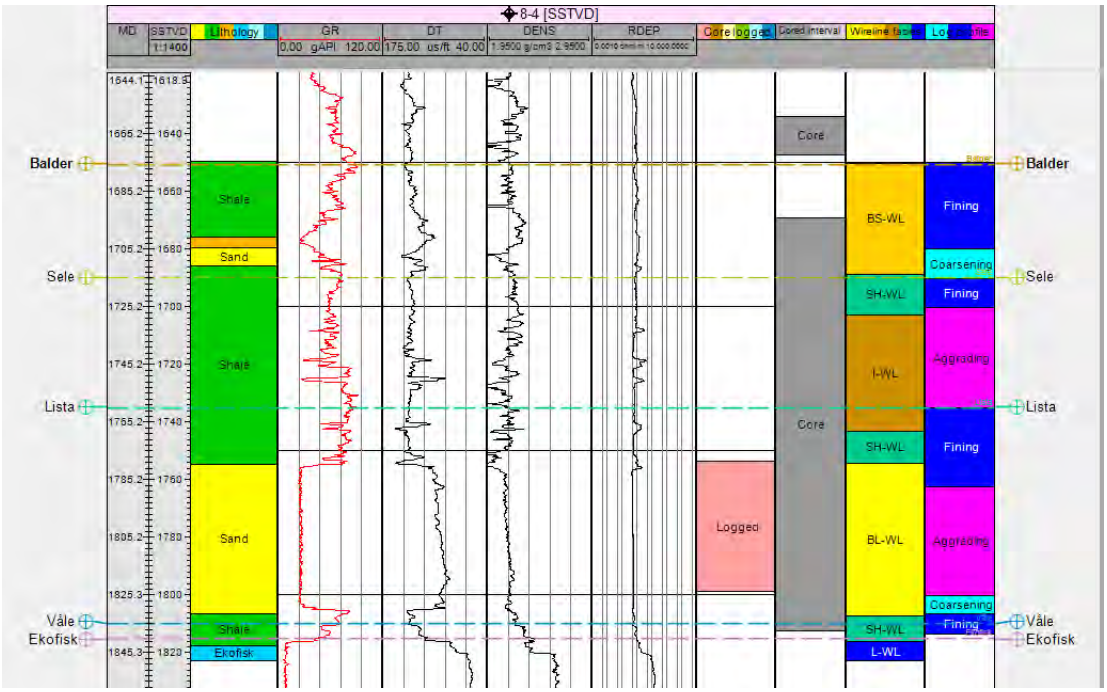
8-4 [SSTVD]
MD
SSTVD
1:1400
Lithology
GR
0.00 gAPI 120.00
DT
175.00 us/ft 40.00
DENS
1.9500 g/cm3 2.9500
RDEP
Core logged
Cored interval
Wireline facies
Log facies
1644.1
1618.9
1665.2
1640
1685.2
1660
1705.2
1680
1725.2
1700
1745.2
1720
1765.2
1740
1785.2
1760
1805.2
1780
1825.3
1800
1845.3
1820
Balder
Sele
Lista
Våle
Ekofisk
Shale
Sand
Shale
Sand
Shale
Ekofisk
Core
Logged
Core
BS-WL
SH-WL
I-WL
SH-WL
BL-WL
SH-WL
L-WL
Fining
Coarsening
Fining
Aggrading
Fining
Aggrading
Coarsening
Fining
Balder
Sele
Lista
Våle
Ekofisk

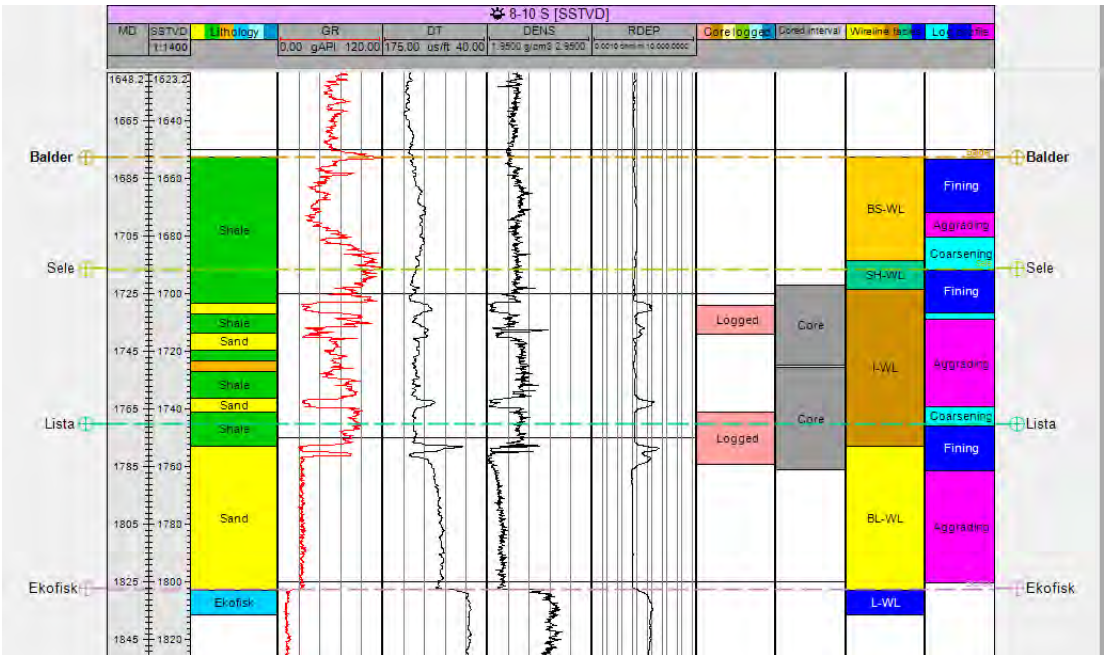
8-10 S [SSTVD]
MD
SSTVD
1:1400
Lithology
GR
0.00 gAPI 120.00
DT
175.00 us/ft 40.00
DENS
1.9500 g/cm3 2.9500
RDEP
Core logged
Cored interval
Wireline fa
Balder
Sele
Lista
Ekofisk
Shale
Sand
Ekofisk
Logged
Core
BS-WL
SH-WL
I-WL
BL-WL
L-WL
Fining
Aggrading
Coarsening

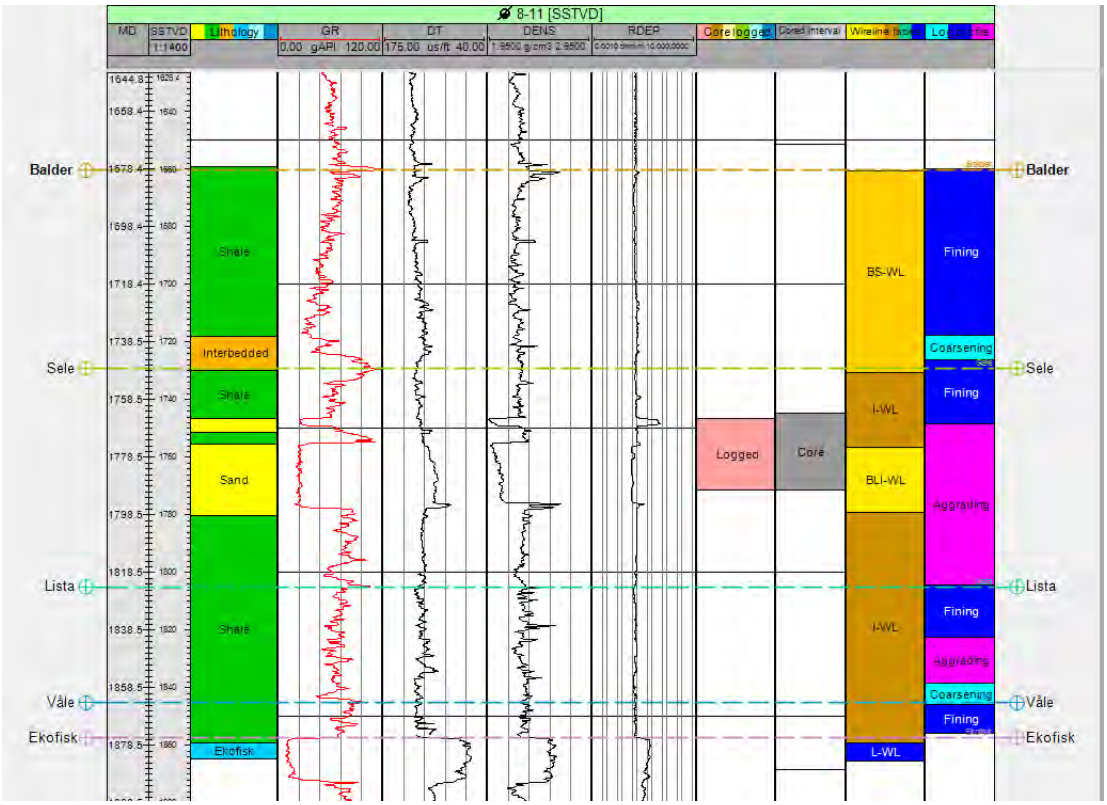
8-11 [SSTVD]
MD
SSTVD
1:1400
Lithology
GR
0.00 gAPI 120.00
DT
175.00 us/ft 40.00
DENS
RDEP
Core logged
Cored interval
Wireline facies
Log facies
Balder
Sele
Lista
Våle
Ekofisk
Shale
Interbedded
Shale
Sand
Shale
Ekofisk
Logged
Core
BS-WL
I-WL
BLI-WL
I-WL
L-WL
Fining
Coarsening
Fining
Aggrading
Fining
Aggrading
Coarsening
Fining

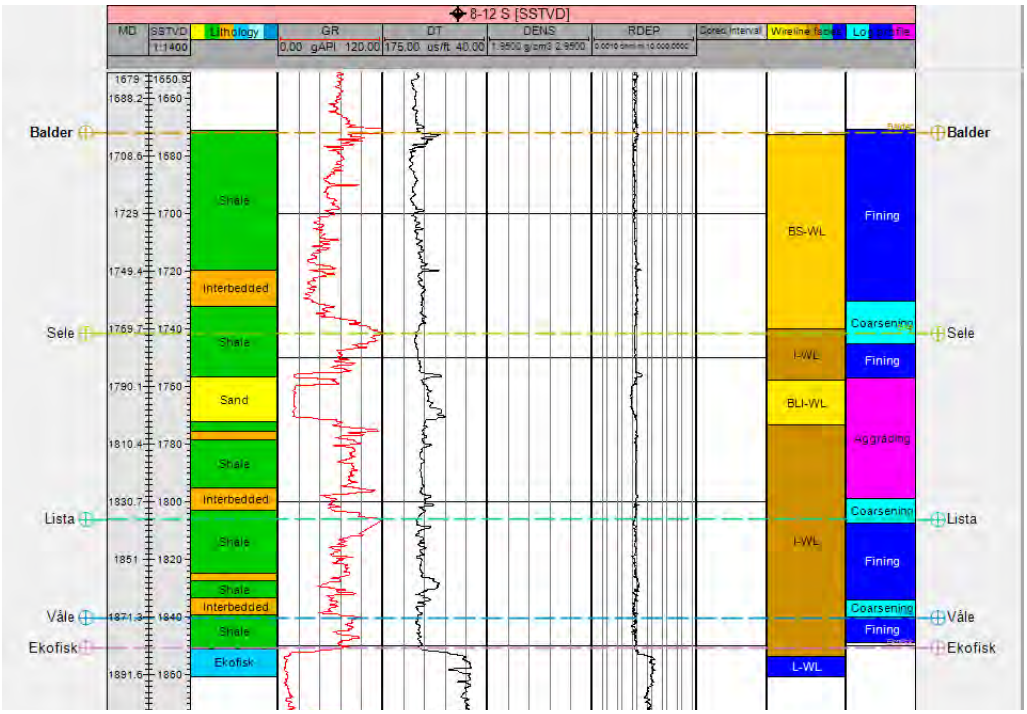
8-12 S [SSTVD]
MD
SSTVD
1:1400
Lithology
GR
0.00 gAPI 120.00
DT
175.00 us/ft 40.00
DENS
1.9500 g/cm3 2.9500
RDEP
Coreg Interval
Wireline facies
Balder
Sele
Lista
Våle
Ekofisk
Shale
Interbedded
Shale
Sand
Shale
Interbedded
Shale
Shale
Interbedded
Shale
Ekofisk
BS-WL
I-WL
BLI-WL
I-WL
L-WL
Fining
Coarsening
Fining
Aggrading
Coarsening
Fining
Coarsening
Fining
Balder
Sele
Lista
Våle
Ekofisk

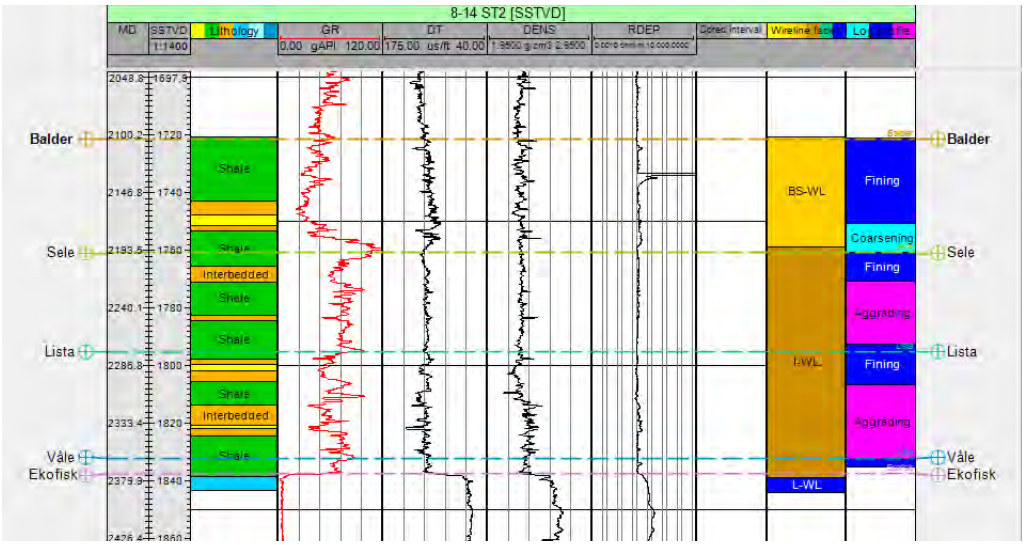
8-14 ST2 [SSTVD]
MD
SSTVD
1:1400
Lithology
GR
0.00 gAPI 120.00
DT
175.00 us/ft 40.00
DENS
1.9500 g/cm3 2.9500
RDEP
Coreg Interval
Wireline facies
Lo
Balder
Sele
Lista
Våle
Ekofisk
Shale
Interbedded
BS-WL
I-WL
L-WL
Fining
Coarsening
Aggrading

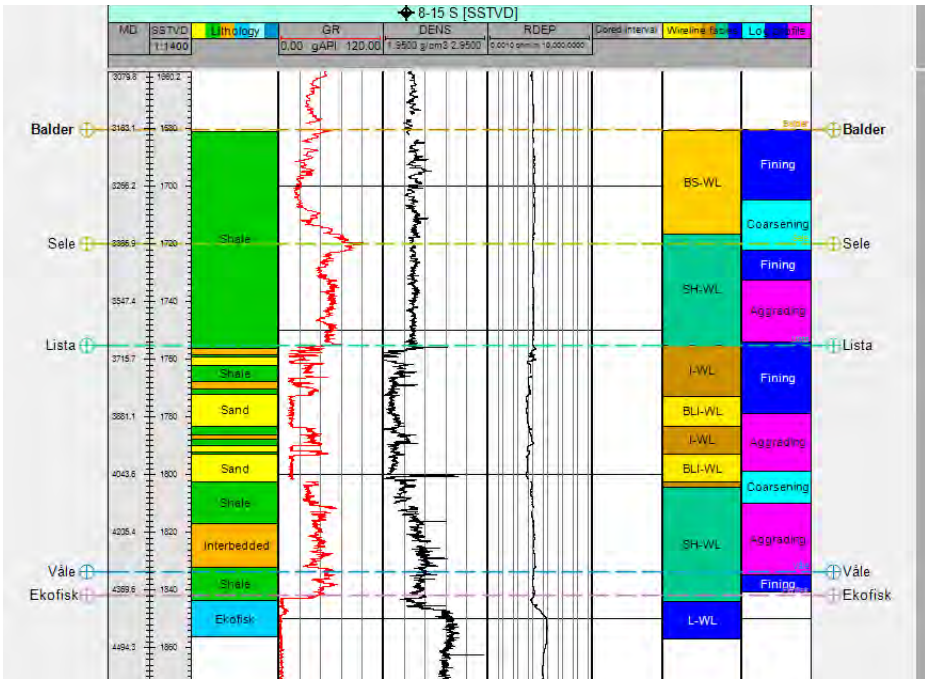
8-15 S [SSTVD]
MD
SSTVD
1:1400
Lithology
GR
0.00 gAPI 120.00
DENS
1.9500 g/cm3 2.9500
RDEP
Cored Interval
Wireline fa
Balder
Sele
Lista
Våle
Ekofisk
Shale
Sand
Shale
Sand
Shale
Interbedded
Shale
Ekofisk
BS-WL
SH-WL
I-WL
BLI-WL
I-WL
BLI-WL
SH-WL
L-WL
Fining
Coarsening
Fining
Aggrading
Fining
Aggrading
Coarsening
Aggrading
Fining
Balder
Sele
Lista
Våle
Ekofisk

| | **Våle** | **Lista** | **Sele** | **Balder** |
|---|---|---|---|---|
| **Well** | Wireline | Wireline | Wireline | Wireline |
| **25/8-1** | SH | BL / I | SH | BS |
| **25/8-3** | SH | BL / I | I | BS |
| **25/8-14 ST2** | I | I | I | BS |
| **25/8-11** | I | I | BLI / I | BS |
| **25/8-12 S** | I | I | I | BS |
| **25/8-4** | SH | BL / SH | I / SH | BS |
| **25/8-10 S** | | BL | I | BS |
| **25/8-15 S** | SH | BLI / I | SH | BS |
| | | | | |
| **25/10-1** | SH | BLI / I | I | BS |
| **25/10-3** | SH | BL / SH | SH | BS |
| **25/10-4** | SH | BL / I | I | BS |
| **25/10-5** | I | BLI / I | I | BS |
| | | | | |
| **25/11-1** | BLI / SH | SH | BLI / I | BS |
| **25/11-2** | | | BL / I | BS |
| **25/11-3** | BL / SH | SH | SH | SH |
| **25/11-4** | SH | SH | BL / I | BS |
| **25/11-5** | SH | BL / I | BLI / I | BS |
| **25/11-6** | BLI / SH | BL / I | I | BS |
| **25/11-7** | SH | BL / I | SH | BS |
| **25/11-8** | SH | BL / I | SH | BS |
| **25/11-9** | SH | I | BL / I | BS |
| **25/11-10** | I | BL / I | SH | BS |
| **25/11-11** | SH | BL / I | I | BS |
| **25/11-12?** | SH | BL / I | SH | BS |
| **25/11-13** | BL / I | BL / I | SH | BS |
| **25/11-14 S** | | | | |
| **25/11-15** | SH | BL | SH | BS |
| **25/11-16** | SH | BL | SH | BS |
| **25/11-18** | SH | BL | I | BS |
| **25/11-19 S** | SH | SH | BL / I | BS |
| **25/11-21 A** | SH | BL | SH | SH |
| **25/11-22** | SH | SH | SH | BS |
| **25/11-23** | BLI / I | I | BLI / I | BS |

**Appendix 4a: Most commonly occurring wireline log facies for all wells**

# Appendix 5 – Seismic data

Appendix 5a: Seismic surfaces

Appendix 5b: Seismic facies observed

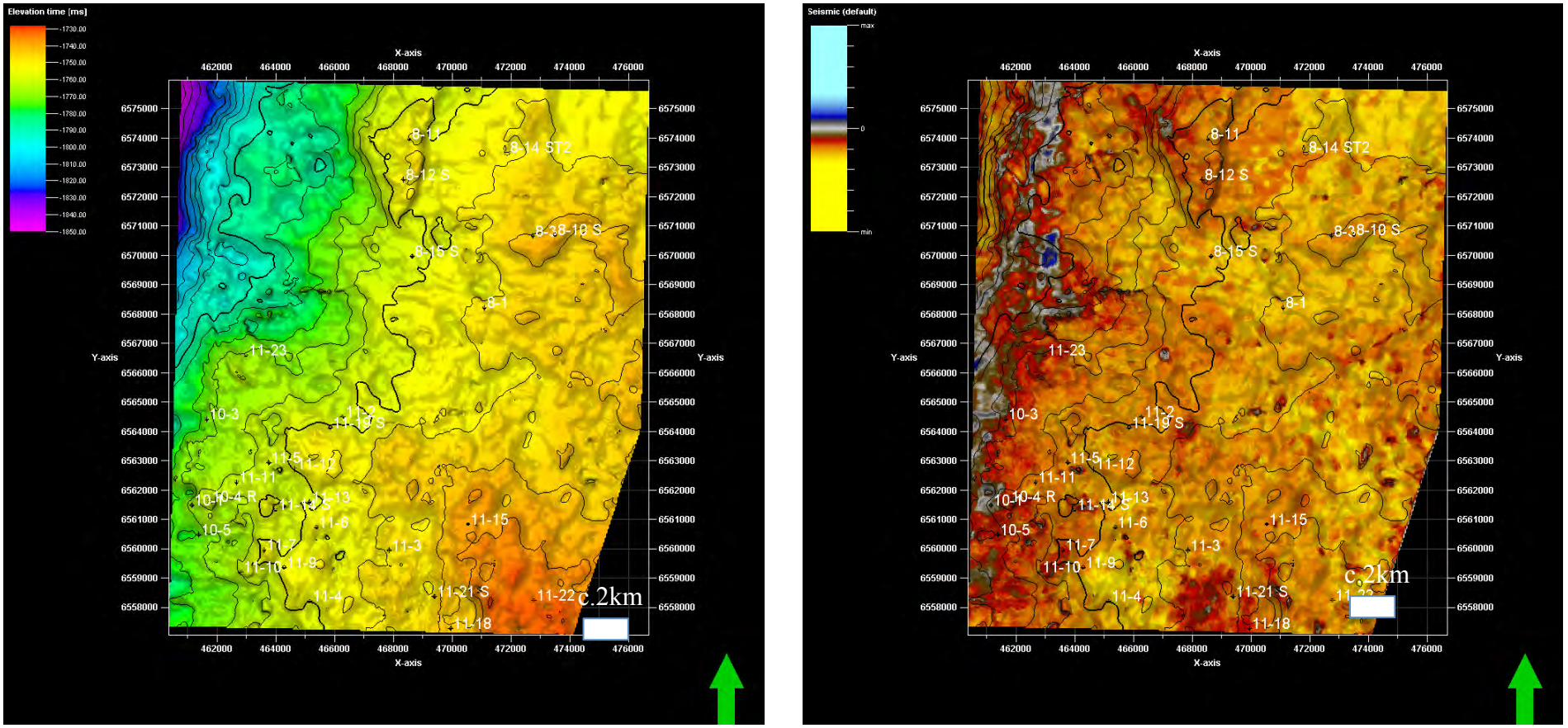


Appendix 5a: Ekofisk surface displayed in TWT (left), contour interval of 25ms. Extract value amplitude attribute (right), contour interval of 25ms, vertical exaggeration x10

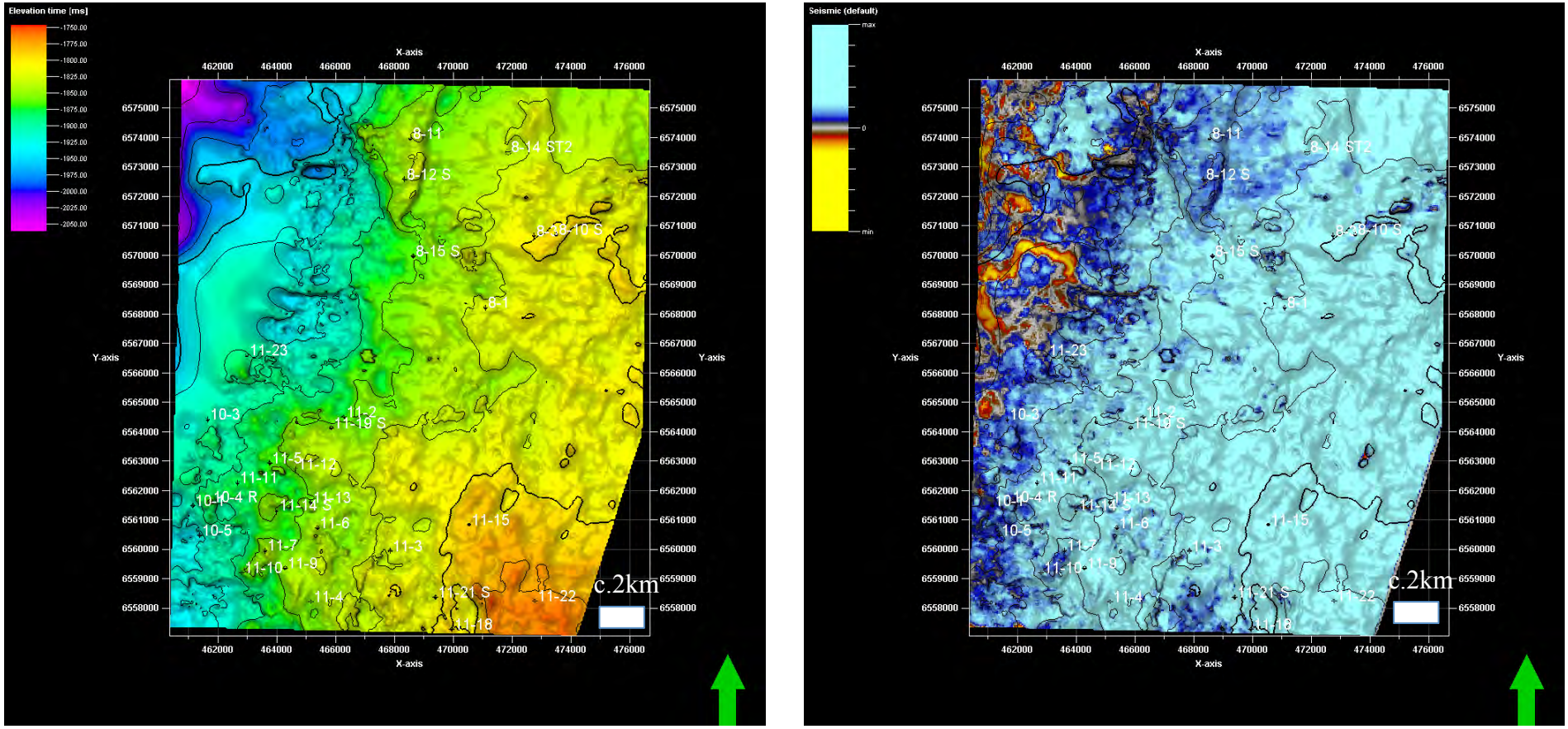


Appendix 5a: Vale surface displayed in TWT (left), contour interval of 25ms. Extract value amplitude attribute (right), contour interval of 25ms, vertical exaggeration x10

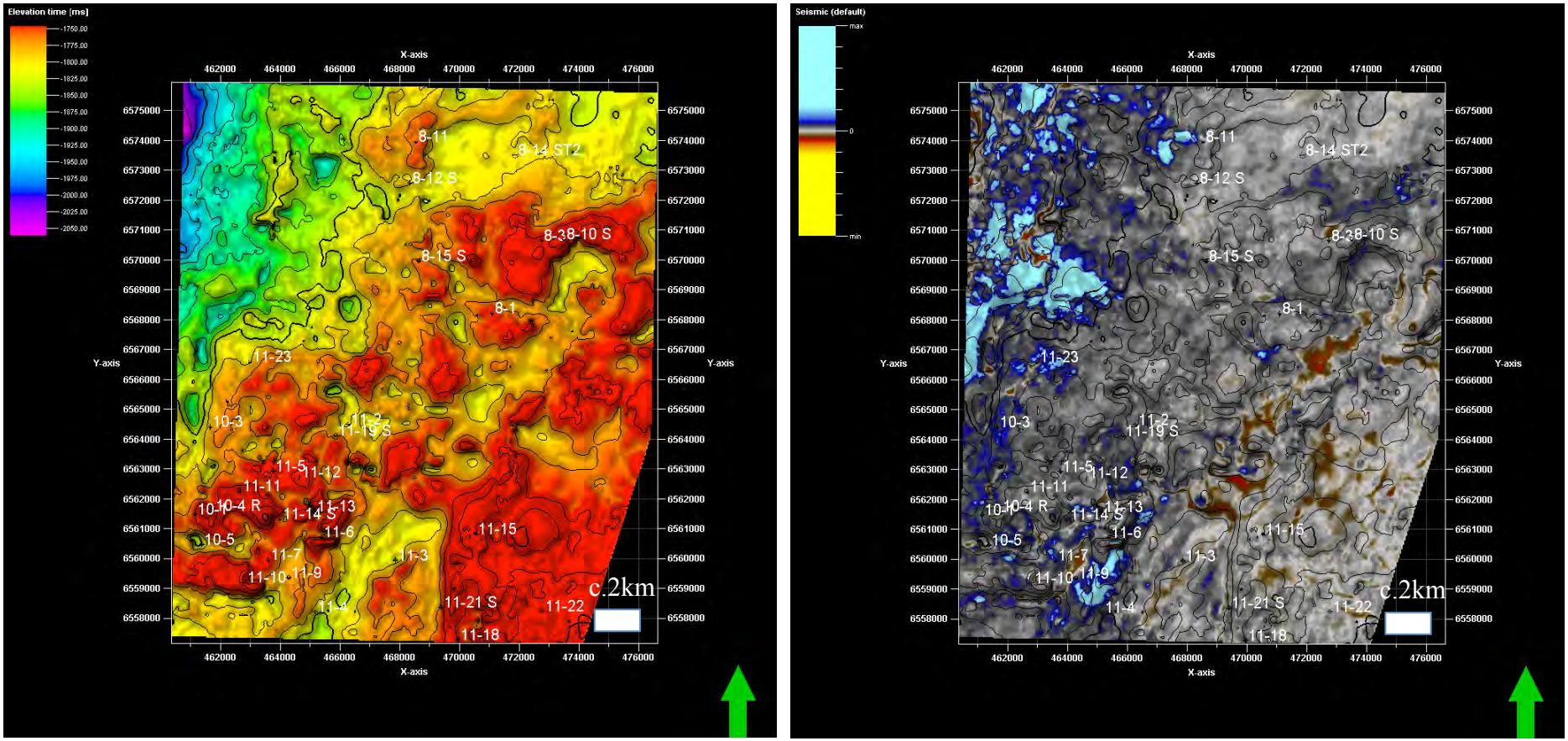


Appendix 5a: Lista surface displayed in TWT (left), contour interval of 25ms. Extract value amplitude attribute (right), contour interval of 25ms, vertical exaggeration x10

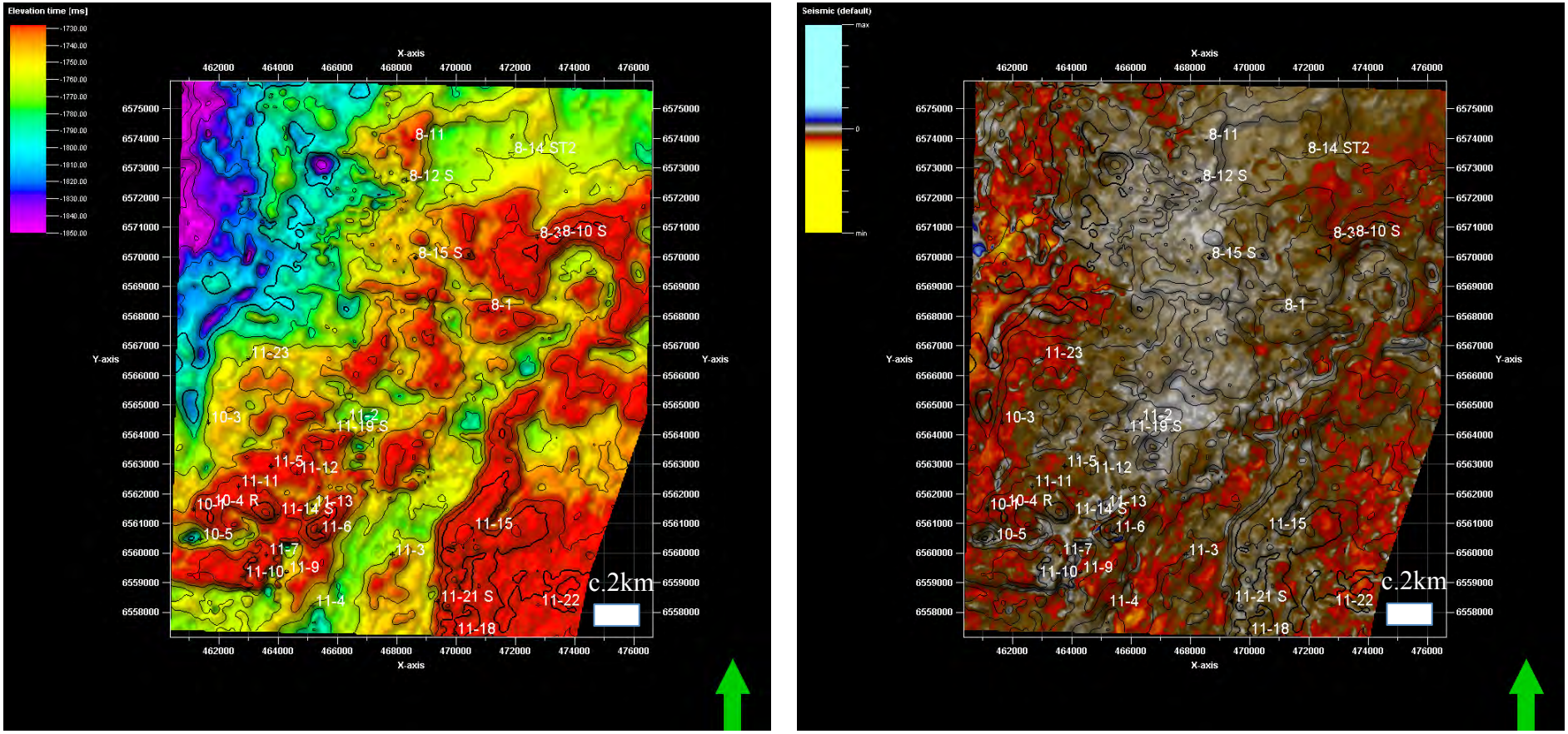


Appendix 5a: Sele surface displayed in TWT (left), contour interval of 25ms. Extract value amplitude attribute (right), contour interval of 25ms, vertical exaggeration x10

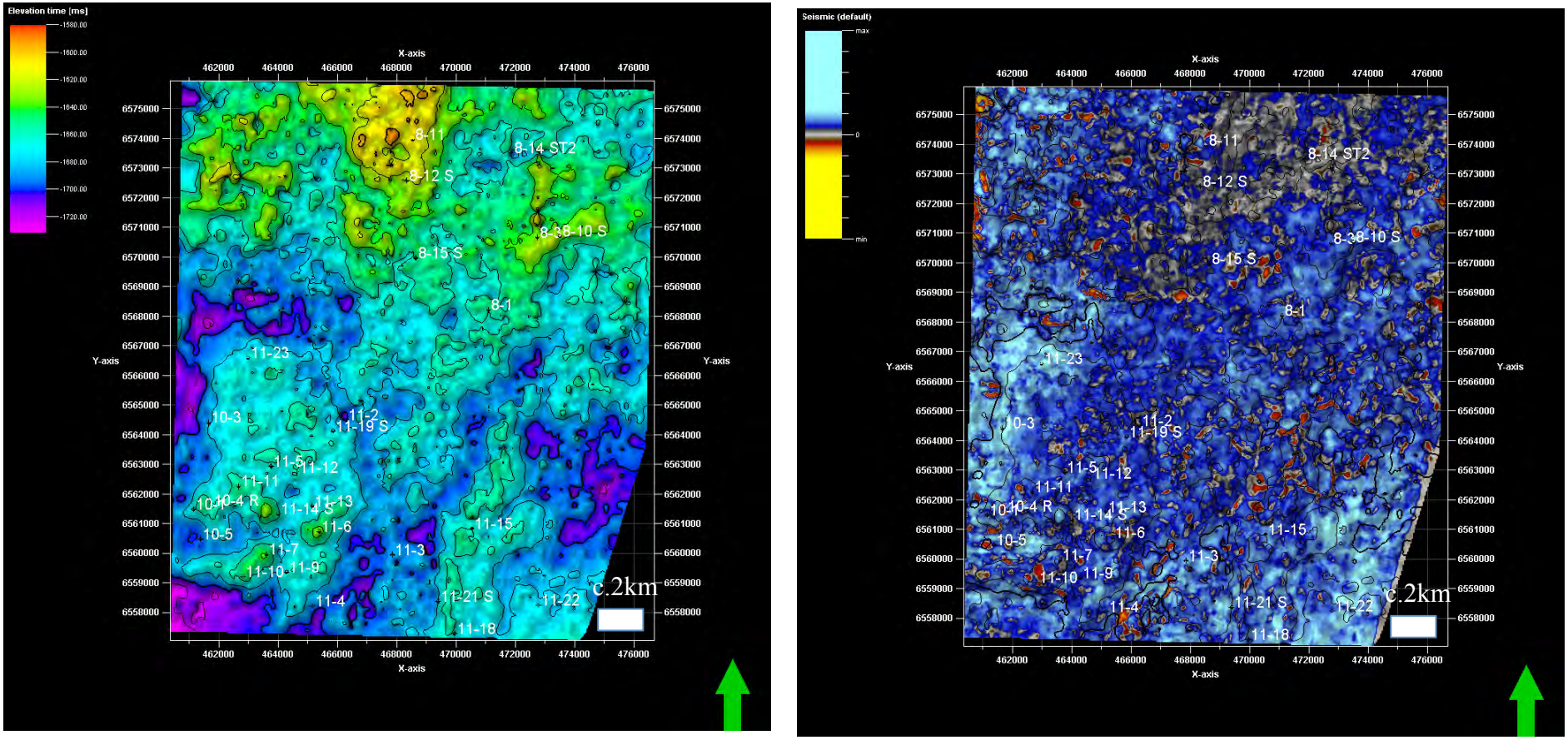


Appendix 5a: Balder surface displayed in TWT (left), contour interval of 25ms. Extract value amplitude attribute (right), contour interval of 25ms, vertical exaggeration x10

| | **Våle** | **Lista** | **Sele** | **Balder** |
|---|---|---|---|---|
| **Well** | Seismic | Seismic | Seismic | Seismic |
| **25/8-1** | P | MI | MI | MI |
| **25/8-3** | P | MI | P | MI |
| **25/8-14 ST2** | p | MI | MI | D |
| **25/8-11** | P | MI | MI | M |
| **25/8-12 S** | MI | D | MI | D |
| **25/8-4** | | | | |
| **25/8-10 S** | P | MI | P | MI |
| **25/8-15 S** | | | | |
| | | | | |
| **25/10-1** | M | M | M | M |
| **25/10-3** | MI | MI | MI | MI |
| **25/10-4** | M | M | M | M / CR |
| **25/10-5** | MI | D | MI | MI |
| | | | | |
| **25/11-1** | MI / CR | MI | P | MI |
| **25/11-2** | P | D / M /CR | D | D |
| **25/11-3** | MI / CR | D / M /CR | D / CR | MI / CR |
| **25/11-4** | P | M | M | MI |
| **25/11-5** | P | D | MI | MI |
| **25/11-6** | CR / M | CR / M | CR / M | CR / M |
| **25/11-7** | CR / M | CR / M | CR / M | CR / M |
| **25/11-8** | M | M | M | M |
| **25/11-9** | P | M / CR | M / CR | CR / D |
| **25/11-10** | M | D | D | CR / D |
| **25/11-11** | MI | D | MI | CR / MI |
| **25/11-12?** | P | D | MI | MI |
| **25/11-13** | MI / CR | CR / M | D / CR | M / CR |
| **25/11-14 S** | | | | |
| **25/11-15** | P | D / M | MI | M |
| **25/11-16** | | | | |
| **25/11-18** | P | D / M | D / M | M |
| **25/11-19 S** | P | MI / CR | MI | MI |
| **25/11-21 A** | P | M | M | MI |
| **25/11-22** | P | MI | MI | P |
| **25/11-23** | P | M | M | M |

**Appendix 5b: Most commonly occurring seismic facies for all wells**

# Appendix 6 – Synthesis

Appendix 6a:  Synthesis of facies observations

| | | | Våle | | Lista | | | Sele | | Balder | |
|---|---|---|---|---|---|---|---|---|---|---|---|
| **Mound** | **Field area** | **Wells present** | **Wireline logs** | **Seismic** | **Cored section** | **Wireline logs** | **Seismic comments are also relevant for Sele sequence** | **Cored section** | **Well bore** | **Cored section** | **Seismic** |
| **Mound 1** | Balder Field | 11-10, 11-7 well 11-9 (eastern flank) | Mudstone dominated interval | Discontinuity observed in west of mound. Doming is also observed. | No core cut in 11-10 & 11-9. Well 11-7 core is rubble | Dominated by blocky sandstones. Interbedded facies also exist. | Steeply dipping at eastern margin. Well 11-7 drilled directly through a crestal intrusion complex. Probably well 11-9 drilled through winged intrusion emanating from Mound 4. Well 11-10 may also have penetrated a intrusion complex although poorly seismically imaged. | No core cut. | Mudstone dominated interval wells 11-10 and 11-7. Blocky sandstones are observed in well 11-9. | No core cut in 11-10, 11-7. Core is cut in 11-9 but is not logged. | Balder Sequence thickens into eastern flank of Mound 1. |
| **Mound 2** | East Balder Field | 11-3 | Twenty metre thick block sandstone observed, surrounded above and below by mudstones. | Continous to semi-continous onlapping reflections. Indication of seismic discontinuity. | No core cut. | Mudstone dominated interval. | Low relief mound, lista sequence 1-2 seismic reflections. Well 11-3 drilled on flank possible injections although unclear. | No core cut. | Mudstone dominated interval. | No core cut. | Balder sequence thickens into 'low' between Mound 4 and Mound 11. Occasional cross cut are seen and whilst internal reflectors are wavy, seismic reflections are continous |
| **Mound 3** | Balder Field | 10-1, 10-4R, 11-11, 11-8, 11-14S | Mudstone dominated interval | Two seismic discontinuities observed in centre of mound and Eastern flank. | No core cut in 10-4R and 11-11 and 11-14S, rubble observed in 10-1 and 11-8. | Interbedded sandstones with a lesser portion of blocky sandstones for wells 10-1 and 10-4R. Wells 11-11 and 11-8 both are dominated by blocky sandstones. | U-shaped feature with 3 mound crests. Wells 10-1 and 10-4 penetrated western crest with clear cross-cutting, injection features. Well 11-11 low relief, well tested centre of central mound. Well 11-8 tested crest of eastern mound. Wing injections emanate from southern flank | Core present but not logged in well 10-1 and 11-14S. No core cut in 10-4R, 11-11, 11-8 | Mudstone dominated interval with minor sandstone interbeds. | No core cut in 10-1, 10-4R, 11-11, 11-8 and 11-14S. | Winged intrusions emanate from Mound 4 into Balder sequence. Balder sequence mimics underlying Sele and Lista surfaces. |
| **Mound 4** | Balder Field | 11-6, 11-1 (eastern flank), 11-13 (western flank) | Sandstones in excess of 20m is observed in both 11-6 and 11-13, which is directly juxtaposed against Limestones. | Seismic discontinuity observed at Våle/Ekofisk interval on North-eastern flank of mound. | No core cut in 11-1 and 11-13, Rubble only observed in 11-6 | Blocky sandstones are the dominate wireline log facies in well 11-6 in the centre of the mound. An equal division between blocky sandstones and mudstones in seen in well 11-13 and mudstones are seen 11-1, both located on the flanks of this mound. | Highly mounded feature well 11-6 tested crest of structure of which appears as a crestal intrusion complex. A northern wing is observed tested by well 11-13 | No core cut in 11-6, 11-1 and 11-13. | Mudstone dominated interval although 15m thick blocky sandstones are observed in well 11-1. | No core cut in 11-6 and 11-13. Core cut in 11-1 but not logged. | Numerous cross-cutting intrusion features that are low-angle and curved. Seismic reflections onlap onto mound Mound 4 in the East and Mound 3 in the West. |
| **Mound 5** | Balder Field | 11-5 | Mudstone dominated interval | Seismic discontinuity observed at Våle/Ekofisk interval on southern flank of this mound. | No core cut in 11-5 | An equal division between blocky sandstones and mudstones is observed. | Low relief structure no evidence of injection. Tested by well 11-5 near to crest of structure | Four metre core cut in Sele sequence not logged. | Blocky sandstones (18m thick) and mudstones are observed | No core cut in 11-5 | Semi-continous equal package thickness Balder sequece onlaps onto Lista and Sele Mounding eastward. |
| **Mound 6** | East Balder Field | Undrilled | Undrilled | Seismic discontinuty perhaps elongate observed in throughout (North-South) of the mound approximately 2 km in length. | Undrilled | Undrilled | Undrilled structure evidence of 2 wing features in the centre and north of the mound. | Undrilled | Undrilled | Undrilled | Curved and flat lying reflections thicknen into flanks in all directions from Mound 5. |
| **Mound 7** | Balder Field | Undrilled | Undrilled | No evidence of seismic discontinuity. High amplitude reflections. | Undrilled | Undrilled | Low relief structure no evidence of injection. Undrilled. | Undrilled | Undrilled | Undrilled | Equal thickness Balder sequence curves downwards into flank between Mound 7 and Mound 9 although thickening is not seen. |
| **Mound 8** | North-East Balder Field | 11-23 (northern flank) | Sandstone in excess of 20m is observed, directly juxtaposed against Limestones. | No evidence of seismic discontinuity. High amplitude reflections. | No core cut in 11-23 | Mudstone dominated interval. | Low relief structure, although plausible flank well 11-35 has interesected a wing feature at Lista sequence level | No core cut. | Interbedded and blocky sandstones are observed. | Sandstone dykes and sill of less than 1m thick and interbedd in siltstones and mudstone facies. | Blader sequence of equal thickness, seismic reflection are semi-continous. |
| **Mound 9** | Balder Field | 11-12, 11-19S (northern flank), 11-2 (northern flank) | Mudstone dominated interval | Two dome like monds observed at Ekofisk and Våle surfaces. No indications of similar features at Lista sequence. A 500m wide 'pop-up' structure is observed in the South of the mound. | No core cut in 1-12, 11-19S and 11-2 | An equal division between blocky sandstones and mudstones is observed in well 11-12. Mudstones are observed in 11-19S | Low relief mound, well 11-12 drilled in southern crestal zone although no evidence of intrusion. Weak indications of near vertical intrusion near to well 11-19s, steep flank dipping East. | No core cut in 11-12 and 11-2, in well 11-19S Massive sandstone facies is observed at the base of the core section to contain small and large scale loading and post-depositional (dish) structures). Fourteen sandstone injections intrude overlying mudstones facies, both dykes and sills are observed | Mudstones are observed in well 11-12. Well 11-19S is dominated by over 60m blocky sandstones. Blocky sandstones are also observed in 11-2. | No core cut in 11-12, 11-19S and 11-2. | Balder sequence is faulted across the crest of Mound 9. No observable thickening is seen. |

## Appendix 6a: Synthesis of facies observations

| | | | Våle | | Lista | | | Sele | | Balder | |
|---|---|---|---|---|---|---|---|---|---|---|---|
| **Mound** | **Field area** | **Wells present** | **Wireline logs** | **Seismic** | **Cored section** | **Wireline logs** | **Seismic comments are also relevant for Sele sequence** | **Cored section** | **Well bore** | **Cored section** | **Seismic** |
| **Mound 10** | North-East Balder Field | Undrilled | Undrilled | Two linear breaks in Ekofisk surface are oberved in the centre of this mound. Although no evidence of 'pop-up' features | Undrilled | Undrilled | Low relief, undrilled structure with indications of vertical intrusion. Discontinous amplitude are observed beneath Lista sequence. | Undrilled | Undrilled | Undrilled | Minor thicken East and West is observed on Flanks of Mound 10. Minor thining over crest of structure. |
| **Mound 11** | Grane Field | 11-15, 11-21S, 11-18 | Mudstone dominated interval | No evidence of seismic discontinuity. High amplitude reflections. | Core from well 11-21S and 11-18 has not been logged. Well 11-15 contains Massive sandstone facies with basal small scale loading structures. Overlain by larger scale loading, with weak indication of pipe structures. | Dominated by blocky sandstones. Mudstone facies also exist. | Moderate to high relief this 9km long elongate structure has 3 potential wing sturctures emanating from the western flank. Well 11-15 tested the crest of the strutcure, but well 11-21S most likely tested a wing intrusion. | Core cut in 11-15 and 11-18 but not logged. No core cut in 11-21S. | Mudstone dominated interval is observed in wells 11-15 and 11-21S. Well 11-18 contains interbedded wireline log facies. | No core cut in 11-15, 11-21 and 11-18. | Winged intrusions from Lista and Sele sequences pass laterally into Balder sequence. Thickening of Balder sequence is observed west of Mound 11. Numerous cross-cuts and observed at Balder sequence level. |
| **Mound 12** | North Grane Field | Undrilled | Undrilled | No evidence of seismic discontinuity. High amplitude reflections. | Undrilled | Undrilled | Moderate to low relief mound 12 is a continuation of the Grane Mound 11 structure. No evidence for intrusion. | Undrilled | Undrilled | Undrilled | Balder sequence thickens into flanks of Mound 12, west between Mound 13 and Mound 11. |
| **Mound 13** | North-East Balder Field | 8-1 | Mudstone dominated interval | Indications on northern flank of discontinuity at Våle/ Ekofisk level. | Rubble is only preserved in well 8-1. | An equal division between blocky sandstones and mudstones is observed. | Mound 13 is a prominent mound with relatively braod low relief flank. Tested by well 8-1 in a crestal position, Perhaps weak indications of winged intrusion. | Core cut in 8-1 but not logged. | Interbedded wireline log facies are observed. | Core is cut but not logged. | Parrallel seismic reflections over the crest of Mound 13 pass laterally into thickening of Balder sequence into mound flanks. Low lying flat and curved intrusions are seen to exend from Lista sequence into Balder sequence. |
| **Mound 14** | North Balder Field | Undrilled | Undrilled | A very clear 'pop-up' structure locates beneath Mound 14. Approximately 600m in width this structre is the most easily observed feature of this type in the area. | Undrilled | Undrilled | Broad low relief structure with no evidence of intrusion although a clear 'pop-up' or seismic discontinuity feature is observed beneath. | Undrilled | Undrilled | Undrilled | Semi-continous reflections are cross-cut by winged intrusion from the western flank of Mound 14. Minor thickening west is observed. |
| **Mound 15** | West Ringhorne Field | 8-15 (north-western flank) | Mudstone dominated interval | Mound 15 locates directly above a discontinuity in Ekofisk/Våle surface. | No core cut | Interval dominated by mudstones and interbedded facies. | Low relief feature, no evidence of intrusion features | No core cut. | Mudstone dominated wireline log facies. | No core cut. | Semi continous seismic reflections are seen to extend over the crest of Mound 15 eastwards. No observable thickening is seen. |
| **Mound 16** | Ringhorne Field | Undrilled | Undrilled | No evidence of seismic discontinuity. High amplitude reflections. | Undrilled | Undrilled | Moderate relief structure with weak indications of winged intrusion from easttern flank of structure. | Undrilled | Undrilled | Undrilled | Minor thicken East and West is observed on Flanks of Mound 16. Minor thining over crest of structure. |
| **Mound 17** | West Ringhorne Field | 8-11, 8-12S (south flank) | Mudstone dominated interval | No evidence of seismic discontinuity. High amplitude reflections. | No core cut | Mudstone dominated interval. | Seismic data is of poor quality and indications of a multiple seismic reflection. Horst block at deeper Jurassic and Cretaceous level has been tested by well 8-11. Onlapping seismic reflections and high amplitude seismic events although no indication of amplitude anomaly. | Massive and bedded sandstone facies with small and large scale scale loading structures are observed in well 8-11. No core cut in 8-12S. | Around 10m blocky sandstones are observed in both 8-11 and 8-12S wells. Surrounded above and below by mudstones. | No core cut in well 8-11 and 8-12S. | Continous high amplitude seismic reflections are seen to onlap this Mesozoic Horst structure. |
| **Mound 18** | Ringhorne Field | 8-3, 8-10S | Mudstone dominated interval | Two seismic discontinuities at Ekofisk and Våle intervals locating directly beneath Mound 18. | No core cut in well 8-3. Massive and bedded sandstone facies contain small-scale loading structures. | Lista sequence blocky sandstones located directly above Limestones of Ekofisk sequence. Blocky sandstones also dominate well 8-3. | Mound 18 is approximately 6,5km in length but is not elongate. The mound is U-shape with limbs orientated in North-East, South-West direction. Directly south of well 8-3 Lista sequence thickens to over 6 seismic reflection rapidly thining east ward with indications of wing intrusions. A large (2km) wing intrusion emanates from the western flank of Mound 18 which appears to root from a crestal intrusion complex. | No core cut in 8-3. Bedded sandstones and siltstones are seen to underlie sill intrusions. | Interbedded wireline log facies are observed. | No core cut in 8-3 and 8-10S. | Minor thickening on Mound 18 flanks, semi-continous high amplitude reflections are observed. |

## Appendix 6a: Synthesis of facies observations